

Durham E-Theses

*Exploring the Structure of Scattering Amplitudes in
Quantum Field Theory: Scattering Equations,
On-Shell Diagrams and Ambitwistor String Models in
Gauge Theory and Gravity*

FARROW, JOSEPH,ALEXANDER

How to cite:

FARROW, JOSEPH,ALEXANDER (2022) *Exploring the Structure of Scattering Amplitudes in Quantum Field Theory: Scattering Equations, On-Shell Diagrams and Ambitwistor String Models in Gauge Theory and Gravity*, Durham theses, Durham University. Available at Durham E-Theses Online: <http://etheses.dur.ac.uk/14325/>

Use policy

The full-text may be used and/or reproduced, and given to third parties in any format or medium, without prior permission or charge, for personal research or study, educational, or not-for-profit purposes provided that:

- a full bibliographic reference is made to the original source
- a [link](#) is made to the metadata record in Durham E-Theses
- the full-text is not changed in any way

The full-text must not be sold in any format or medium without the formal permission of the copyright holders.

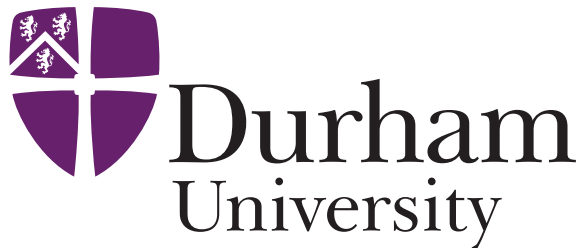
Please consult the [full Durham E-Theses policy](#) for further details.

Exploring the Structure of Scattering Amplitudes in Quantum Field Theory

*Scattering Equations, On-Shell Diagrams and
Ambitwistor String Models in Gauge Theory
and Gravity*

Joseph A. Farrow

A Thesis presented for the degree of
Doctor of Philosophy



Centre for Particle Theory
Department of Mathematical Sciences
Durham University
United Kingdom

February 2022

Exploring the Structure of Scattering Amplitudes in Quantum Field Theory

*Scattering Equations, On-Shell Diagrams and
Ambitwistor String Models in Gauge Theory and Gravity*

Joseph A. Farrow

Abstract: In this thesis I analyse the structure of scattering amplitudes in supersymmetric gauge and gravitational theories in four dimensional spacetime, starting with a detailed review of background material accessible to a non-expert. I then analyse the 4D scattering equations, developing the theory of how they can be used to express scattering amplitudes at tree level. I go on to explain how the equations can be solved numerically using a Monte Carlo algorithm, and introduce my MATHEMATICA package `treeamps4dJAF` which performs these calculations. Next I analyse the relation between the 4D scattering equations and on-shell diagrams in $\mathcal{N} = 4$ super Yang-Mills, which provides a new perspective on the tree level amplitudes of the theory. I apply a similar analysis to $\mathcal{N} = 8$ supergravity, developing the theory of on-shell diagrams to derive new Grassmannian integral formulae for the amplitudes of the theory. In both theories I derive a new worldsheet expression for the 4 point one loop amplitude supported on 4D scattering equations. Finally I use 4D ambitwistor string theory to analyse scattering amplitudes in $\mathcal{N} = 4$ conformal supergravity, deriving new worldsheet formulae for both plane wave and non-plane wave amplitudes supported on 4D scattering equations. I introduce a new prescription to calculate the derivatives of on-shell variables with respect to momenta, and I use this to show that certain non-plane wave amplitudes can be calculated as momentum derivatives of amplitudes with plane wave states.

Declaration

The work in this thesis is based on research carried out in the Department of Mathematical Sciences at Durham University. Chapter 2 provides a review of standard material; the results in this chapter are not my original research. Chapters 3 and 4 are based on my work from [1]. Chapter 5 is based on joint work in collaboration with Arthur Lipstein from [2], and on Appendix C of [3] which was completed in collaboration with Yvonne Geyer, Arthur Lipstein, Ricardo Monteiro, and Ricardo Stark-Muchão. Chapter 6 is also based on [2], and Chapter 7 is based on joint work in collaboration with Arthur Lipstein from [4]. No part of this thesis has been submitted elsewhere for any degree or qualification.

Copyright © 2022 Joseph A. Farrow.

“The copyright of this thesis rests with the author. No quotation from it should be published without the author’s prior written consent and information derived from it should be properly acknowledged.”

Preface and Acknowledgements

Before I start on the physics, I want to share a little of the humanity behind the equations.

My doctoral studies have spanned the last five and a half years years of my life, and have been a transformative experience for me in many ways. As expected, and as evidenced by this work, I've been on a journey of learning about mathematical physics and about what it means to be a researcher and a scientist. More fundamental than this for me however has been the accompanying journey of self-discovery; of learning how to sit alone with my work and with my thoughts and feelings, and how this has led to personal growth and to healing.

Throughout my studies I've had differing levels of difficulty with my health. During the first three and a half years I had increasing problems with anxiety and repetitive strain injury, which impacted on my studies and my daily life. I learnt and adapted, and through the adversity I kept up reasonably normal levels of functioning. Importantly this was enough to finish my research, and certainly a main part of these years of my life was a journey of discovery into mathematical physics and the world of academia.

At the end of my funded period of study the results I present in this work were already published in peer reviewed journals, which was a strong position for me to be in. I knew that what remained for me to finish my doctorate was to combine my papers together, review the literature and edit what was left until it became a complete piece of work. Knowing that my results were already certified gave me the

sense of safety I needed to face the depth of my suffering and disability, and it was at that time that the symptoms of my medical conditions came to a peak.

I became aware that my previous anxieties and repetitive strain injury were rooted in amnesia, post-traumatic stress disorder and related damage to my nerves and spine. These are serious conditions, and I found myself disabled around that time in many ways. Among other things I couldn't walk more than a few meters, couldn't interact with people under normal social circumstances, was unable to use a computer, and some months was unable even to focus my eyes on anything without causing migraines. The last two years then have been a different journey for me, of coming to terms with disability and of healing from trauma.

All these changes and restrictions that I slowly found happening to myself and my body have had a big impact on my life. I had accepted a postdoctoral research position starting after my funding finished which I had to turn down, and I've had to take most of the last two years away from working on research to manage my health. Spending that time on healing was both a great decision and the only possible decision, and though I'm not at full health now as I write, I'm making good progress towards a normal level of functionality.

So I've found the last few years of my life to be challenging in many ways, and with each challenge I've overcome I've grown a little stronger. I've had to learn how to be weak and vulnerable, how to reach out, how to listen. I've found that both healing and research have involved a deep process of introspection, teaching me to focus closely on myself and find out which parts are wholesome and beneficial, and which parts have been harmful and needed to change.

Integral to that process of personal growth has been the opportunity I've had to study for a PhD. It's given me the time I've needed to meet my demons and to start to learn a little about how to let them go in peace. As my studies draw to a close I'm able to carry so much more of my humanity out in the open than I could have when I started, and that's something that will always be with me and that I'll always be grateful for.

So writing my thesis is not something I could have done alone. I'm incredibly grateful for the support that I've had with typesetting, editing and proofreading from my friends Alastair Stewart, Calum Robson, Connor Armstrong and Clare Wallace. Crucial to the process also has been the support that I've had from my friends Will Monks and Joe Warriner in understanding the writing process and how to bring a project to completion.

Next I want to express my gratitude to my supervisor, Arthur Lipstein. Arthur has been a guide and a father figure to me in the worlds of academia and mathematical physics, and he's also been a great friend, supporting me through some of my darkest times during the last couple of years.

I also want to acknowledge those friends and colleagues who have supported me academically in my studies. I was fortunate enough during my degree to attend a number of different conferences and meet many different students and academics, so here are just a few of the people who helped me learn something relevant to this work. My thanks goes to my second supervisor Paul Heslop as well as Simon Badger, Jake Bourjaily, Daniele Dorigoni, Paolo Benincasa, Oliver Schlotterer, Ricardo Monteiro and Yvonne Geyer. I also want to thank Dan Rutter, Tim Whitbread, Themis Botsas, Philip Glass, Viet Tran, Ed Hughes, Giuseppe De Laurentis, Dan Martin and Teresa Abl, and well as Michael Enciso, Julio Parra-Martinez, Sebastian Mizera, Fei Teng, Giulio Salvatori and Ricardo Stark-Muchão.

Throughout the process of studying I've been incredibly lucky to have had friends and family around me who have supported me in many different ways, from chatting with me when I've been low to offering me their hospitality when I've needed somewhere to stay, and everything in between. Thank you Will Monks and Lilac Yosiphon, Jon Hasson and Zoe Schoenherr, Greg Evans and Beth Nelder, Paul and Kate Farrow, Joyce Farrow and Lizzy Farrow, Joyce Wang-Moncayo and family, Trishla Singh, James O'Neill and Karen Gonzalez, Yennifer Frasser, Marija Tomasevic, Jake Brooker, Matt Roberts, Tien Tran, Pepe Hipolito and Annie Moore, you've all contributed to me remaining sufficiently sane to work on my thesis in different and

wonderful ways.

Learning about and healing from the medical conditions that I have experienced over the last few years has taken a lot of my time, comparable to the number of hours needed to complete my doctoral thesis itself. In that regard I would like to thank Lisa Etherson, Jojo Maddison and Femke Nauschutz, who have all helped me with many hours of treatment and who have helped me to learn what I've needed to know about psychotherapy and physiotherapy to get through to the end of my studies.

Throughout my PhD studies I've found the spaces that I've spent time in to be an essential aspect of the learning process. I'd like to acknowledge how important the interdisciplinary and multicultural environment that I found in Ustinov College was to me during the $5\frac{1}{2}$ years of my doctoral studies, and especially how supportive the staff there have been to me during my illnesses. I also want to say how intellectually stimulating an environment I found both Durham University's mathematics department and high-energy physics groups to be, and to give my thanks to the staff from the department who've supported me along the way to navigate the administrative aspects of my medical conditions over the years.

Last but certainly not least, I have been fortunate enough to receive the financial support I needed to enable me to complete this work. I would like to thank the Engineering and Physical Sciences Research Council who funded the first $3\frac{1}{2}$ years of my studies under a PhD scholarship with grant number EP/L504762/1, and Ustinov College who funded my living expenses in the summer of 2019 under a Global Citizenship Programme Scholarship. I would also like to thank Zvi Bern, who funded my expenses for a research visit to UCLA in the summer of 2018. None of the work in this thesis was completed during the visit. I also want to thank my mother Penny Farrow for providing me with some financial support in 2020 and 2021.

The Tao that can be named is not the true Tao

— from *Tao Te Ching* by Lao Tse

*The most precious opportunity presents itself when we come to
the place where we think we can't handle whatever is happening*

— from *When Things Fall Apart* by Pema Chödrön

I dedicate this work to my father, Colin William Farrow.
I think you'd find most of what follows to be cryptic,
but I hope you'd be proud of me anyway.
I wouldn't be the man I am today without the twenty one
years that our paths overlapped.

Contents

Abstract	iii
List of Figures	xix
1 Introduction	1
1.1 Literature Review	1
1.2 Overview of this Thesis	6
2 Background Material	11
2.1 Scattering Amplitudes in Relativistic Quantum Field Theory	11
2.2 Specialising to 4 Dimensions of Spacetime	16
2.3 Supersymmetry, Superamplitudes and On-Shell Superspace	21
2.4 Super Yang-Mills Theory	25
2.5 Einstein Supergravity	29
2.6 Conformal Supergravity	32
2.7 Scattering Equations in general d and CHY Formalism for Tree-level Amplitudes	38
2.8 Refined 4D Scattering Equations	41
2.9 On-Shell Diagrams	44
2.10 Twistor Space	50
2.11 4D Ambitwistor String Theory	59

3	Analytical Properties of the 4D Scattering Equations	69
3.1	Calculating Amplitudes with the 4D Scattering Equations	70
3.2	Recovering the General d Scattering Equations for $d = 4$	74
3.3	Symmetries, Little Group Scaling and Grassmanians	76
3.4	Deleting Equations and Momentum Conservation	79
3.5	Permutations and Choice of Left Set	81
3.6	The Jacobian of the 4D Scattering Equations	83
4	Monte Carlo Numerical Methods for the 4D Scattering Equations	87
4.1	The 4D Scattering Equation as a Numerical System	87
4.2	Difficulties with CHY's Inverse Soft Algorithm	89
4.3	Monte Carlo Algorithm	92
4.4	Efficient Component Amplitude Extraction	97
4.5	Implementation in Mathematica with <code>treeamps4dJAF</code>	98
5	From 4D Scattering Equations to On-Shell Diagrams in $\mathcal{N} = 4$ Super Yang-Mills	101
5.1	Tree-level MHV	102
5.2	Tree-level NMHV	104
5.3	One-Loop	112
6	On-Shell Diagrams in $\mathcal{N} = 8$ Supergravity	121
6.1	Algorithm for Computing On-Shell Diagrams	122
6.2	Hodges Formula for Tree-level MHV	124
6.3	BGK Formula for Tree-level MHV	128
6.4	Tree-level NMHV	133

6.5	One-Loop	137
6.6	Bonus Relations in On-Shell Diagrams	141
6.7	Relations between spinors and minors	144
7	$\mathcal{N} = 4$ Conformal Supergravity Amplitudes in 4D Ambitwistor	
	String Theory	147
7.1	Plane Wave Graviton Multiplet Scattering	148
7.2	Derivation of Berkovits-Witten MHV Formula	152
7.3	Scattering Non-Plane Wave States	153
7.4	Non-Plane Wave Scalar Amplitudes	158
7.5	Non-Plane Wave Graviton Amplitudes	162
7.6	Momentum Derivatives	164
7.7	BRST Quantization	167
8	Conclusion	173
8.1	Summary of Results	173
8.2	Directions for Future Work	175
8.3	Concluding Remarks	180

List of Figures

2.1	Vertices and edges for on shell diagrams in $\mathcal{N} = 4$ super Yang-Mills and $\mathcal{N} = 8$ supergravity	45
2.2	Loop-level BCFW recursion for planar $\mathcal{N} = 4$ super Yang-Mills. The loop order of \mathcal{A}_L and \mathcal{A}_R must add up to l , and the total number of legs must add up to $n + 2$	46
2.3	Square move equivalence relation super Yang-Mills	46
2.4	Merger equivalence relations for $\mathcal{N} = 4$ super Yang-Mills	47
2.5	Tree-level BCFW recursion relations in $\mathcal{N} = 8$ supergravity	47
2.6	Definition of BCFW bridge decoration in $\mathcal{N} = 8$ supergravity	47
2.7	Merger equivalence relations in $\mathcal{N} = 8$ supergravity	48
4.1	Eulerian numbers of solutions to the 4D scattering equations	89
4.2	Convergent solutions at 6 points NMHV using CHY's inverse soft algorithm. Orange solid lines are solutions coming from 5 points $\overline{\text{MHV}}$ and blue dashed lines are from 5 points MHV.	91

-
- 4.3 Statistical summary of distribution of solutions to 4D scattering equations and timings of `NSolveMonteCarlo` algorithm. N_{runs} is the number of different set of numerical momenta used, $N_{\sigma} = (4n - 8) \binom{n-3}{k-2}$ N_{runs} is the number of solution points checked, γ_{σ} is the scaling parameter of the fitted Cauchy distribution and MAD_{σ} is the median absolute deviation. \bar{t} is the average time and STD_t is the standard deviation. Note that when N_{runs} is small solution point statistics may not be reliable even though N_{σ} is large, as they come from a small number of different choices of numerical momenta. 94
- 4.4 Histogram of timings for finding all solutions to the 4D scattering equations for 7559 sets of numerical momenta at 6 pts NMHV using `NSolveScatteringEquations4D`. The blue curve is `FrechetDistribution[3.7,1.6,-0.2]`, as a best fit by `MATHEMATICA`. 95
- 4.5 Histogram of 43776 solution points at 6 points NMHV taken from 7559 different random momenta. The blue dashed curve is `CauchyDistribution[0,0.447]`, and the red solid curve is an approximation with the uniform distribution $\mathcal{U}([-0.894, 0.894])$ 96
- 5.1 On-shell diagram for tree-level n -point MHV amplitude in $\mathcal{N} = 4$ super Yang-Mills in terms of $(n - 1)$ -point MHV amplitude . . . 103
- 5.2 On-shell diagrams contributing to the 6-point NMHV amplitude in $\mathcal{N} = 4$ super Yang-Mills 105
- 5.3 The 5+3 channel BCFW diagram contributing to the 6 point NMHV in $\mathcal{N} = 4$ super Yang-Mills. Edge variables are denoted as α_i . The label β is not an edge variable. 106
- 5.4 The 4+4 channel BCFW diagram contributing to the 6 point NMHV amplitude in $\mathcal{N} = 4$ super Yang-Mills. Edge variables are denoted as α_i . The labels β and γ are not edge variables. 108

5.5	Postnikov diagram for the 6 point NMHV amplitude in $\mathcal{N} = 4$ super Yang-Mills	109
5.6	Postnikov diagram for n -point \mathcal{N}^{k-2} MHV amplitude in $\mathcal{N} = 4$ super Yang-Mills	109
5.7	On-shell diagram for 1-loop four-point amplitude in $\mathcal{N}=4$ super Yang-Mills	113
5.8	On-shell diagram from which Figure 5.7 can be obtained by taking a forward limit and adding a decorated BCFW bridge.	113
5.9	The worldsheet configuration describing a 1-loop 4-point amplitude using the 4D scattering equations.	118
6.1	Relations between spinor bracket factors at each vertex of an on-shell diagram in $\mathcal{N} = 8$ supergravity	125
6.2	On-shell diagram contributing to tree-level n -point MHV tree amplitude in $\mathcal{N} = 8$ supergravity	126
6.3	Bonus-simplified on-shell diagram for 4-point amplitude	129
6.4	On-shell diagram showing how 4-point seed amplitude orientation is cut, and an inverse soft factor is inserted for $i \in \{5, \dots, n\}$	130
6.5	Decorated planar on-shell diagrams contributing to the 6 point NMHV amplitude in $\mathcal{N} = 8$ supergravity. The full amplitude can be obtained by summing over permutations of legs 1 to 4.	133
6.6	On-shell diagram for 1-loop four-point amplitude in $\mathcal{N}=8$ supergravity	138
6.7	On-shell diagram from which Figure 6.6 can be obtained by taking a forward limit and adding a decorated BCFW bridge.	139
6.8	BCFW recursion for tree-level MHV amplitudes in $\mathcal{N} = 8$ supergravity	142
6.9	The MHV bonus relations in $\mathcal{N} = 8$ supergravity can be used to eliminate one channel from the recursion in Figure 6.8, reducing the number of channels from $(n - 2)$ to $(n - 3)$	143

Chapter 1

Introduction

1.1 Literature Review

I start with a review of the relevant literature, to show where my research sits within the wider body of knowledge in the field ¹.

The development of new mathematical techniques for calculating scattering amplitudes has led to important advances in the range of accessible calculations, allowing for computations with more external states and higher loop order. In the 1980s the introduction of spinor helicity notation gave way to new simplified computations of four dimensional amplitudes which previously had seemed intractable, for example [5, 6, 7]. In recent years there have been many advances in the set of technical tools that exist for calculating perturbative scattering amplitudes. Key tree-level techniques include recursive methods for calculation of higher point amplitudes from lower point inputs, known as BCFW (Britto, Cachazo, Feng and Witten) recursion [8, 9], expression of n -point S -matrices in terms of a sum over the solution of algebraic scattering equations [10, 11], and the formulation of field theory amplitudes in terms of string worldsheet calculations, initially developed in twistor string theory [12, 13, 14], and more recently in ambitwistor string theory [15, 16]. Both

¹Note that this literature review is up to date only as of March 2019, due to an extended period of illness starting from that date

twistor string and ambitwistor string theory are string models whose spectra contain only field theory degrees of freedom, and hence their worldsheet S -matrices calculate scattering amplitudes in quantum field theory. In this work I focus on scattering amplitudes in gauge theory and gravity, of which two specific theories stand out. $\mathcal{N} = 4$ super-Yang-Mills and $\mathcal{N} = 8$ supergravity are believed to be the simplest quantum field theories in four dimensions, for a number of reasons. The planar scattering amplitudes of $\mathcal{N} = 4$ super Yang-Mills enjoy Yangian symmetry, which is a hallmark of integrability [17], and the loop amplitudes of $\mathcal{N} = 8$ supergravity exhibit unexpected UV cancellations which suggest that the theory may be perturbatively finite [18].

One of the first n -point amplitudes calculated in any theory was the Parke-Taylor form of the Yang-Mills tree-level MHV amplitude [7], which inspired a description in terms of 2D current algebra [19]. This idea was then generalised to $\mathcal{N} = 4$ super Yang-Mills amplitudes [12, 13], who proposed a worldsheet model for $\mathcal{N} = 4$ super Yang-Mills known as twistor string theory. The correlation function of worldsheet vertex operators in twistor string theory give rise to an elegant formula for tree-level amplitudes in terms of integrals over curves in twistor space [14]. The spectrum of the theory was also found to calculate $\mathcal{N} = 4$ conformal supergravity amplitudes [20] which can be seen as a mixed blessing, allowing for calculation of amplitudes with these states but making computations in pure $\mathcal{N} = 4$ super Yang-Mills at loop level more complex in this framework. Twistor string theory allows for the calculation of $\mathcal{N} = 4$ conformal supergravity amplitudes, but the Yang-Mills and conformal supergravity amplitudes decouple from one another only at tree-level, so the conformal supergravity states in the spectrum obstruct calculation of loop amplitudes in $\mathcal{N} = 4$ super Yang-Mills.

A similar worldsheet formula for $\mathcal{N} = 8$ supergravity was found in [21], following the discovery of a gravitational analogue of the Park-Taylor formula by Hodges [22]. Cachazo, He and Yuan extended the formula of [21] to a framework for calculating tree-level scattering of particles in arbitrary dimensions for a wide variety of non-

supersymmetric gauge and gravitational theories in terms of a unified set of scattering equations [11, 10, 23], which I will refer to as ‘general d scattering equations’ in this work. In the CHY framework, tree-level amplitudes for different theories of massless particles are supported on the solutions of these scattering equations, which were first discovered in the context of ordinary string theory in [24, 25]. Ambitwistor string theory is the worldsheet theory underlying CHY’s formulae, and was first constructed by Mason and Skinner [15]. Different worldsheet matter content in ambitwistor string theory corresponds to different spectra, allowing for CHY formulae for different quantum field theoretic amplitudes.

The power of the spinor helicity formalism in four dimensions along with the generality of the scattering equation formalism were combined to produce 4D ambitwistor string theory in [26, 27]. This model gives a worldsheet description for the tree-level S -matrices of Yang-Mills theories and Einstein gravity which are manifestly supersymmetric for any number of supersymmetries \mathcal{N} . They are supported on refined scattering equations which are graded by helicity degree, which I refer to as ‘4D scattering equations’ in this thesis. The formulae arising from 4D ambitwistor string theory are closely related to those arising from twistor string theory [19, 12, 13, 14, 21]. Amplitudes arising from 4D ambitwistor theory can be related to those of twistor string theory by integrating out the moduli of curves in twistor space from the twistor string representations [28].

Ambitwistor string models are critical in ten dimensions, and one-loop amplitudes in 10D ambitwistor string theories were first proposed in [29], with work also done in [29, 30, 31, 32]. In these original works the loop level scattering equations are written on the torus in terms of elliptic functions, but they can also be formulated in terms of rational off-shell scattering equations on the Riemann sphere [30, 33]. The 10D ambitwistor formulae have been further extended to two loops in [34], but finding a framework to calculate loop integrands for any theory in an intrinsically 4 dimensional setting using 4D ambitwistor string theory or the original twistor string has proven a difficult task.

Like the Berkovits-Witten twistor string, the 4D ambitwistor string for $\mathcal{N} = 4$ super Yang-Mills contains conformal supergravity in its spectrum, in particular a non-minimal model of $\mathcal{N} = 4$ conformal supergravity [35] which has a coupling between the Weyl tensor and scalar fields of the model, unlike in the original minimal conformal gravity [36]. Conformal supergravity has a number of undesirable features, most notably that it is not unitary. However there are still a number of reasons why it is interesting theoretically; it is renormalizable and can be made UV finite if coupled to $\mathcal{N} = 4$ super Yang-Mills [37, 38], and it is possible to obtain classical Einstein gravity with cosmological constant by imposing Neumann boundary conditions on conformal gravity [39, 40, 41]. This relationship between Einstein gravity and conformal gravity was used to find twistor string formulae for scattering amplitudes of Einstein supergravity in flat space [42, 43]. Conformal supergravity amplitudes were first studied in [20, 44, 45, 46, 47, 48], and more recently have been shown to arise from taking the double-copy of super-Yang-Mills with a new $(DF)^2$ gauge theory [49]. An ambitwistor string description of the $(DF)^2$ theory was subsequently found and used to deduce a CHY formula for conformal gravity amplitudes in general dimensions in [50]. Einstein gravity in de Sitter or anti de Sitter space in four dimensions was shown to have an embedding in conformal gravity in [39], providing motivation to study the amplitudes of conformal gravity and leading to proposals for worldsheet formulae for scattering amplitudes on these backgrounds in [51, 52]. These formulae suggest that amplitudes in anti de Sitter space should have some analogue of the double copy structure found in flat spacetime, as explored in [53, 54, 55].

Formulae supported on scattering equations have been successful in representing and calculating abstract theoretical properties of amplitudes such as soft limits [56, 57, 58, 59, 60], collinear limits [61] and relations between the S -matrices of different theories [23, 62]. Direct evaluation of amplitudes by solving the scattering equations is difficult, and some approaches solve the integrations by different methods [63, 64]. The equations have $(n - 3)!$ solutions at n points, and it is likely that finding all

of these solutions analytically for generic kinematics is not possible. Calculating amplitudes in this framework then becomes a primarily numerical problem, which has been addressed in the literature only for the general d equations.

On-shell diagrams were first proposed in [65], providing a diagrammatic framework to express BCFW recursion in planar $\mathcal{N} = 4$ super Yang-Mills at all loop orders. This allows the n -point l -loop integrand to be calculated recursively in terms less complex integrands, and ultimately to be built up out of 3-point vertices [8, 9, 66]. Unlike Feynman diagrams, on-shell diagrams do not contain virtual particles, and are named for the fact that all internal lines are on-shell. They were first developed in the context of planar $\mathcal{N} = 4$ super Yang-Mills [67] where they revealed an underlying Grassmannian structure, suggesting a geometric interpretation of the scattering amplitudes of the theory as the volume of an object known as the Amplituhedron [68]. On-shell diagrams can be extended to Yang-Mills theory with $\mathcal{N} < 4$ supersymmetries by introducing a physical orientation to the diagram representing the helicity of the superfield corresponding to each internal edge [69].

More recently, on-shell diagrams have been developed for tree-level amplitudes in $\mathcal{N} = 8$ supergravity, revealing new connections to planar $\mathcal{N} = 4$ super Yang-Mills [70, 71]. It is possible to compute $\mathcal{N} = 8$ supergravity amplitudes by decorating planar on-shell diagrams and summing over permutations of the external legs, giving rise to new Grassmannian integral formulae. Although it is possible to extend BCFW recursion to all loops in planar $\mathcal{N} = 4$ super Yang-Mills, and work has been done in Yang-Mills theory at one loop [3], it is not known how to generalize this to higher loops in Yang-Mills or other theories such as $\mathcal{N} = 8$ supergravity. Recent progress in this direction has been made using Q-cuts [32], which are intrinsically $d > 4$ dimensional and give rise to formulae closely related to those of 10D ambitwistor string theory. Current work exists relating worldsheet expressions from the twistor string to recursive formulae arising from BCFW [28, 72, 73], showing deep connections between the two approaches.

1.2 Overview of this Thesis

In this work I explore the structure of scattering amplitudes in quantum field theory, building upon recently developed techniques for calculating amplitudes. I develop a deeper understanding of the 4D scattering equations, on shell diagrams and 4D ambitwistor string theory, and how these computational methods can play a role in understanding the properties of scattering amplitudes in $\mathcal{N} = 4$ super Yang-Mills, $\mathcal{N} = 8$ supergravity and $\mathcal{N} = 4$ conformal supergravity. I start by giving a review of the background material necessary to understanding these computational methods and the scattering amplitudes of these theories in Chapter 2.

The 4D scattering equations have given rise to many different results in understanding scattering amplitudes, but prior to this work there has been no clear set of analytical and numerical results in the literature detailing how to use them to calculate amplitudes, and what subtleties must be addressed in this framework. I start this work by addressing these questions in Chapters 3 and 4, which are based on my work from [1]. I use these results to develop an understanding of the scattering amplitudes of $\mathcal{N} = 4$ super Yang-Mills, $\mathcal{N} = 8$ supergravity and $\mathcal{N} = 4$ conformal supergravity in Chapters 5, 6 and 7. In Chapter 3 I explain the analytical framework required for understanding the details of the 4D scattering equation formalism, and I provide details of how to find full sets of solutions for a given set of numerical momenta and MHV degree by Monte Carlo algorithm in Chapter 4.

To understand the problem of numerical solutions to the 4D scattering equations, it is helpful to first review numerical methods for the general d scattering equations. These equations can be reduced to a simplified polynomial form [74] which is tractable numerically in MATHEMATICA using `NSolve` up to 9 points on a standard laptop, and CHY provide an algorithm for finding individual solutions at higher points [11], but there are difficulties finding all solutions in this way. The 4D equations do not currently have an equivalent simplified polynomial form and depend on a larger set of variables than the general d equations, and as such `NSolve` cannot solve them

above 7 points. There exist published MATHEMATICA packages for evaluation of tree level amplitudes using BCFW[75, 76], but to date there have been no equivalent packages for calculating amplitudes using the scattering equations either analytically or numerically.[77] provide an algorithm for calculation of amplitudes in the CHY formalism numerically without directly solving the scattering equations, but no explicit implementation is given. Alongside my work from [1], and hence building on the material from Chapters 3 and 4 of this thesis, I developed the MATHEMATICA package `treeamps4dJAF`. `treeamps4dJAF` is included with the arXiv submission of [1], and can be used to calculate amplitudes analytically in the MHV sector and numerically for general N^k MHV at tree level using the 4D scattering equations. Previously available MATHEMATICA packages for calculating scattering amplitudes focused on Yang-Mills theory, and `treeamps4dJAF` provides the first explicit publicly available algorithms for calculating Einstein supergravity and $\mathcal{N} = 4$ conformal supergravity amplitudes at tree level.

On-shell diagrams are an alternative method to calculate scattering amplitudes, most notably in $\mathcal{N} = 4$ super Yang-Mills. The relationship between worldsheet formulae arising from twistor string theory and Grassmannian integral formulae coming from on-shell diagrams has been explored previously in [28, 78, 72, 73], and in Chapter 5 of this thesis I extend this analysis to understand how expressions supported on 4D scattering equations arising from 4D ambitwistor string theory can be related to those coming from on-shell diagrams. This shows how the seemingly disparate Grassmannian and worldsheet integral structures are related at tree-level, and provides a starting point to address the long-standing problem of finding a manifestly 4D worldsheet formula describing the integrands of scattering amplitudes in $\mathcal{N} = 4$ super Yang-Mills at loop level.

I start Chapter 5 by deriving Grassmannian integral formulae for tree-level MHV amplitudes in $\mathcal{N} = 4$ super Yang-Mills using on-shell diagrams, and map these to an expression supported on 4D scattering equations, based on my work from [2]. This calculation is particularly straightforward due to the fact that there is only

one solution to the 4D scattering equations in the MHV sector, which leads into the more complex analysis necessary to understand NMHV amplitudes in this setting. In the NMHV case it is necessary to specify a contour in the Grassmannian which will depend on the method used to compute the amplitudes, and for the 6-point NMHV amplitude I show that the three contributing on-shell diagrams correspond to residues of a single top form in the Grassmannian and can subsequently be encoded in a Grassmannian contour integral. This contour integral can then be mapped into an expression supported on 4D scattering equations using a global residue theorem. I then move to loop level, finding that on-shell diagrams can be used to obtain a new worldsheet formula for the 1-loop four point amplitude of $\mathcal{N} = 4$ super Yang-Mills, which is manifestly supersymmetric and supported on 1-loop scattering equations refined by MHV degree. Finally I go on to find the solution to the equations explicitly, solving the worldsheet integrals to give the standard form for the integrand in momentum space, based on my work from appendix C of [3]. This result is notable in that the worldsheet expression directly evaluates to the integrand with quadratic propagators in momentum space compared with the less standard linear propagators arising from previous approaches to 1 loop scattering equations [30], and lead to new worldsheet formulae for n -point 1-loop integrands with quadratic propagators in a variety of theories in [3].

In Chapter 6 of this thesis I extend the theory of on-shell diagrams in $\mathcal{N} = 8$ supergravity, also based on my work from [2]. Previous work on on-shell diagrams in $\mathcal{N} = 8$ supergravity calculated only 4 and 5 point amplitudes [70], and I give an expression for the full n -point MHV amplitude calculated in two different ways; the first giving the inherently non-planar Hodges matrix, and the second producing the BGK formula [79] as a sum over permutations of a planar sector of diagrams. The methods I develop to map worldsheet formulae to Grassmannian integrals in $\mathcal{N} = 4$ super Yang-Mills in Chapter 5 naturally extend $\mathcal{N} = 8$ supergravity, producing the Hodges matrix expression for the MHV amplitude as a Grassmannian integral. I then go on to study 6 points NMHV, where I find that the three decorated planar

on-shell diagrams from which the full amplitude can be derived do not correspond to residues of a single top form, as they do in $\mathcal{N} = 4$ super Yang-Mills. From it is not clear how to relate the Grassmannian contour integral expression for the amplitude obtained using on-shell diagrams to the worldsheet integral formula supported on 4D scattering equations using the global residue theorem, and new methods are necessary to show the correspondence, possibly using non-planar on-shell diagrams. Finally I use the fact that it is possible to describe the 1-loop 4-point amplitude of $\mathcal{N} = 8$ supergravity using a decorated on-shell diagram [70] to derive a worldsheet formula in this case, analogously to the calculation in $\mathcal{N} = 4$ super Yang-Mills in Chapter 5.

4D ambitwistor string theory provides the underlying mechanism to derive worldsheet expressions for scattering amplitudes supported on 4D scattering equations for a number of theories, notably super Yang-Mills and Einstein supergravity. This leaves a clear open problem, which is to find other theories whose tree-level S -matrices can be supported on 4D scattering equations. In Chapter 7 of this work I extend 4D ambitwistor string theory to calculate scattering amplitudes in $\mathcal{N} = 4$ conformal supergravity, giving concise supersymmetry covariant worldsheet expressions for the scattering of plane-wave graviton multiplets, based on my work from [4]. I find from this that a key feature of the amplitudes in this theory is that the number of negative helicity superfields is not in general equal to the Grassmann degree of the superamplitudes, as is the case for super Yang-Mills and Einstein supergravity. This means the MHV degree of the amplitude could be defined either as the number of negative helicity superfields scattered or as the Grassmann degree of the superamplitude, and I choose to define the MHV degree of the amplitude as the Grassmann degree as this definition better reflects the structure of the 4D scattering equations. For MHV amplitudes the worldsheet formula reduces to the one previously derived by Berkovits and Witten [20], and for general k the formula can be readily evaluated numerically using the methods I developed in Chapter 4. I use `treeamps4dJAF` to compare amplitudes calculated in this framework to results obtained from Feynman

diagrams and double copy techniques developed in [49] up to 8 points, checking cases in all MHV sectors.

Since the equations of motion for conformal gravity are fourth order in derivatives, they also admit non-plane wave solutions of the form $A \cdot x e^{ik \cdot x}$ for the graviton multiplets of the theory, which I explain in Chapter 2. Vertex operators for these non-plane wave states were previously proposed in twistor string theory [45] for $A^2 = 0$, and I find the analogous 4D ambitwistor vertex operators for these states in Chapter 7. These new vertex operators allow scattering of non-plane wave states with unrestricted A , and I find them to have a more compact and natural form than those of twistor string theory. Computing non-plane wave amplitudes using 4D ambitwistor string theory is computationally more complex than for plane wave modes, requiring the introduction of source terms in the path integral which leads to deformed scattering equations which I explain in detail. Using these results I find worldsheet formulae for the scattering amplitudes of non-plane states written in terms of derivatives with respect to the spinor degrees of freedom of the external states of the amplitude. Previous calculations of such amplitudes in [45] were restricted to 3 points, and with the methods developed in this thesis I develop some non-plane wave amplitudes at n -points. Finally I develop a prescription for taking momentum derivatives of spinor variables with respect to corresponding the off-shell momentum, which allows me to express the non-plane wave amplitudes as momentum derivatives of amplitudes with plane wave states.

In Chapter 8 I conclude the work of this thesis and provide possible directions for future research.

Chapter 2

Background Material

In this chapter I aim to provide a concise, comprehensive overview of the physical concepts and mathematical frameworks necessary to understand my results in the following chapters, and to make my notations and conventions clear to the reader. My intention is for this material to be accessible to a reader with some background in mathematics and physics, but who may not be familiar with the study of scattering amplitudes in quantum field theory.

2.1 Scattering Amplitudes in Relativistic Quantum Field Theory

Relativistic quantum field theory describes the interaction of particles as the quantized excitations of a field in a d dimensional space-time, combining quantum mechanical and special relativistic physics into a single consistent theoretical model. Quantum field theory is most widely studied in Minkowski spacetime, which I denote M^d generally or $M^d(\mathbb{R})$ or $M^d(\mathbb{C})$ depending on whether the coordinates are real or complex, and which I specialise to in this thesis. Spacetime manifolds are defined in terms of a metric tensor $g_{\mu\nu}$ which defines distances between points, and any coordinate transformations leaving the metric invariant are considered sym-

metries of the spacetime. The more symmetric a spacetime is the more tractable calculations will be in a given quantum field theory defined on that spacetime, and the maximum number of coordinate symmetries in a d -dimensional manifold is $\frac{d(d+1)}{2}$. Minkowski spacetime M^d has metric $(\eta_{\mu\nu}) = \text{diag}(-1, 1, \dots, 1)$ which is invariant under linear transforms which form Lorentz symmetry group $\text{SO}(d-1, 1)$ of rotations and boosts, as well as having translational symmetry in each of the d spacetime dimensions. Hence M^d is maximally symmetric with $\frac{d(d+1)}{2}$ symmetries, and the full spacetime symmetry group of M^d is known as the Poincaré group. Spacetime coordinate symmetries can be extended past this maximal limit in two ways by allowing for additional types of transformations; the first is known as supersymmetry which introduces extra Grassmann odd degrees of freedom to the manifold and is discussed in Section 2.3, and the second is conformal symmetry which allows for symmetries to be defined in terms of coordinate transformations which leave the metric invariant, and is discussed in Section 2.6.

Particle excitations of the fields each carry a spin $s' \in \frac{\mathbb{N}}{2}$ which is related to how their fields transform as representations of the Lorentz group, and states with integer spin are represented by Grassmann even fields and are called bosons, with half-integer spin particles represented by Grassmann odd fields and called fermions. Most calculations in this work will be for bosonic fields, with any fermionic calculations related to the bosonic amplitudes as a result of supersymmetry, as explained in Section 2.3. Another key property of any given state is its rest-mass m , and in this in this thesis I will consider only massless particles with $m = 0$.

Scattering amplitudes are among the most fundamental computable quantities in any quantum field theory, providing an important link between theory and experiment. They are the basic building blocks for the calculation of the scattering cross section, which is the main physical observable used to model the scattering processes which underlie particle collision experiments [80, 81]. The scattering process then is modelled in this setting by a collection of particles which start in the infinite past in non-interacting quantum states, interact with each other during finite times

and finish in non-interacting states in the infinite future. The scattering amplitude is the mathematical structure describing the interaction, and is a complex number describing the probability amplitude that a specified set of initial quantum states will interact to result in a given set of final state. As such the amplitude is a Lorentz invariant function of the quantum states at the beginning and the end of the process, most notably depending on the relativistic momenta of the particles as well as any coupling constants of interaction terms in the Lagrangian of the theory.

The quantum states at the beginning and end of the scattering process are well separated and as such are non-interacting, which means they solve the linearized equations of motion for the relevant quantum field. For a spin zero field $\phi(x)$, a spin one Yang-Mills field $A_\mu^a(x)$, and a spin two gravitational metric perturbation $h_{\mu\nu}(x)$, the standard linearized equations of motions after fixing any gauge symmetries are

$$\square\phi(x) = 0, \quad \square A_\mu^a(x) = 0 \quad \text{and} \quad \square h_{\mu\nu}(x) = 0, \quad (2.1.1)$$

with a basis for solutions with standard boundary conditions given by momentum eigenstates in the form of plane waves.

$$\phi(x) = \phi_0 e^{ik \cdot x}, \quad \square A_\mu^a(x) = \epsilon_\mu^a e^{ik \cdot x} \quad \text{and} \quad \square h_{\mu\nu}(x) = \epsilon_{\mu\nu} e^{ik \cdot x}. \quad (2.1.2)$$

Scattering amplitudes are often considered only for plane wave states such as these, but in this thesis I also consider states with more complex boundary conditions in conformal supergravity coming from 4th order linearized field equations, discussed in Section 2.6.

The quantum state of the particle before and after the interaction is then described by its momentum and polarisation structure, and the momenta k_i and polarisation ϵ_i of the i th particle will be the key variables that the scattering amplitude depends on. As the particles are massless these equations of motion enforce that $k_i^2 = 0$, and they are hence on-shell in the sense of Einstein's famous mass-shell relationship.

The polarisation vectors in equation (2.1.2) are defined only up to a choice of

gauge for any gauge symmetries of the theory, and are defined uniquely only after gauge fixing. For spin 1 particles the polarisation vectors the gauge symmetries and equations of motion of the theories [82, 83] remove two degrees of freedom and result in a total of $d - 2$ linearly independent polarisation vectors in d dimensions. This basis of polarisation vectors transforms in the fundamental representation of the little group, which is the subset of Lorentz transformations which leave the state's momentum vector invariant, and the little group for massless particles in d dimensions is $SO(d - 2)$. Spin 2 particles carry a rank 2 polarisation tensor, which can be written as a product of the polarisation vectors for spin 1 as described in Section 2.5.

Scattering amplitudes are defined in the S -matrix formalism where they can be considered as components of the scattering matrix or S -Matrix, which is an operator in the quantum field theory which evolves the initial quantum states before a collision to the final states afterwards. The S -matrix of a theory can be constrained by the axiom of unitarity, which requires that the probabilities for all possible outcomes of a given scattering process add up to 1. The outcomes of the process then form a consistent probability space, such that no information can be lost. In the S -matrix formalism unitarity requires $S^\dagger S = 1$ so that S is a unitary operator.

The probability of an initial set of quantum states $\langle \text{initial} |$ evolving to a final set of states $|\text{final}\rangle$ is then given in terms of the S -matrix by $|\langle \text{initial} | S | \text{final} \rangle|^2$. Any process involving n total states both incoming and outgoing can be calculated using a simple transformation from the process which takes n incoming particles $\langle 1, 2, \dots, n |$ to the vacuum $|0\rangle$ [80], so the interaction can always be considered as $|\langle 1, 2, \dots, n | S | 0 \rangle|^2$. To define the scattering amplitude from S it is necessary to subtract out the probability that the particles pass through one-another without interacting, and to accommodate for this S -Matrix can be split up into $S = \mathbb{1} + i\mathcal{T}$. The scattering amplitude is then defined as

$$\mathcal{A} := \langle 1, 2, \dots, n | \mathcal{T} | 0 \rangle. \quad (2.1.3)$$

The integer n counting the number of states in the process is referred to as the number of points of the amplitude, and for an n -point amplitude I define \mathcal{N} to be the set of all of the particle labels, so that $\mathcal{N} := \{1, \dots, n\}$. Amplitudes are often cyclically ordered, and in these cases I define any choice of labels which is greater than n by division modulo n , so that if $k \in \mathcal{N}$ then $n + k \sim k$.

The translational part of the Poincaré symmetry group of Minkowski spacetime results in overall conservation of momentum in the scattering process, $\sum_{i \in \mathcal{N}} k_i = 0$. Defining $P := \sum_{i \in \mathcal{N}} k_i$ this is encoded in the scattering amplitude with a Dirac delta function $\delta(P)$, and the amplitude can always be expanded as

$$\mathcal{A} = \delta^d(P) A(g; (p_1, \epsilon_1, q_1), (p_2, \epsilon_2, q_2), \dots, (p_n, \epsilon_n, q_n)), \quad (2.1.4)$$

where q_i denotes any additional quantum numbers defining particle state i . I use a simplified notation $\mathcal{A}(g; 1\dots n)$ to describe this functional dependence, with the particle label implying the information about the quantum states of each particle.

The classic approach to calculating scattering amplitudes is to relate $\langle 1, 2, \dots, n | \mathcal{T} | 0 \rangle$ to an correlation function of n field operators in the quantum field theory using the LSZ formula [80, 82], and to expand the path integral for that correlation function perturbatively to give the amplitude to different orders in the coupling constant g . This expansion can be expressed diagrammatically as a sum over all possible Feynman diagrams, which are graphs whose edges are called propagators and are calculated from the kinetic terms in the Lagrangian of the theory, and whose possible vertices are calculated from the interaction terms. The assumption of unitarity enforces bounds on the large momentum behaviour of the propagators and scattering amplitudes of the theory [84].

This approach has largely been superseded by newer techniques for calculating the amplitude, and in this thesis I will focus on computational frameworks known as on-shell diagrams, scattering equations and ambitwistor string theory. These techniques still rely on the perturbative expansion in terms of the coupling constant of the theory,

which can be written as

$$\mathcal{A}(g; 1 \dots n) = \mathcal{A}^{(0)}(1 \dots n) + g\mathcal{A}^{(1)}(1 \dots n) + g^2\mathcal{A}^{(2)}(1 \dots n) + O(g^3). \quad (2.1.5)$$

The zeroth order term in the perturbative expansion is known as the tree-level amplitude because the topology of Feynman diagrams at this order contains no closed loops. Higher order terms of degree L contain L closed loops, and each loop corresponds to an integral over off-shell momentum space. The Feynman diagram expansion shows that both tree-level amplitudes and the integrands of loop level amplitudes are rational functions, with the tree level amplitudes depending only on the on-shell momenta defining the scattering states, which the the loop amplitudes depend additionally on the off-shell loop momentum. In this thesis I consider mostly tree level amplitudes with some calculations at one loop, where the one-loop amplitude can be written as a loop integral as

$$\mathcal{A}^{(1)}(1 \dots n) = \int d^d\ell \mathcal{I}(\ell; 1 \dots n) \quad (2.1.6)$$

The loop integrals in scattering amplitudes above tree level diverge in general either in the UV or the IR regime and these divergences must be regulated. Dimensional regularisation is the most common way to regulate divergences at loop level which requires taking the dimension of the spacetime away from d by small amount and taking a limit back to d dimensions, although I will not make use of dimensional regularisation in this work.

2.2 Specialising to 4 Dimensions of Spacetime

While it is possible to calculate amplitudes in general dimensions, four dimensions of spacetime is the most physically relevant and nearly all calculations in this thesis will be for $d = 4$. The structure of scattering amplitudes is richer in four dimensions, allowing for more complex calculations at higher number of points and loop order,

although regulating loop integrals is generally done by taking the dimension of the spacetime slightly away from $d = 4$. This additional structure stems from the fact that the Lorentz group factorises in four dimensions into two copies of $SU(2)$, so that $SO(3,1) \simeq SL(2)_L \times SL(2)_R$. In this thesis I refer to the two copies as $SU(2)_L$ for left and $SU(2)_R$ for right to distinguish between them, and I use $\dot{\alpha}, \dot{\beta}, \dots$ for indices in $SU(2)_L$ and α, β, \dots for indices in $SU(2)_R$.

This splitting means that any representation of $SO(3,1)$ can be classified as a choice of representation for the left and right copies of $SU(2)$, which results in a more powerful framework than in general dimensions of spacetime because the representation theory of $SU(2)$ is particularly simple. Each representation of $SU(2)$ is defined by a choice of one natural number for the number of indices in the fundamental representation the representation carries, and then a general representation of $SO(3,1)$ can be written as a choice of two natural numbers. The fundamental representation of $SO(3,1)$ is then $(1,1)$ which corresponds to a spacetime vector, and the mapping in between vectors in $SO(3,1)$ and the two fundamental $SU(2)$ indices of $(1,1)$ is given by the 4D Pauli matrices, $\sigma_\mu^{\dot{\alpha}\alpha} = (\mathbb{1}^{\dot{\alpha}\alpha}, \sigma_i^{\dot{\alpha}\alpha})$ and $\bar{\sigma}_{\alpha\dot{\alpha}}^\mu = (\mathbb{1}_{\alpha\dot{\alpha}}, \sigma_i^{\alpha\dot{\alpha}})$ where σ_i are the standard 3D Pauli matrices. Hence any vector in $SO(3,1)$ can be written as a rank 2 tensor with one index in $SU(2)_L$ and one in $SU(2)_R$, so that

$$k^{\dot{\alpha}\alpha} := \sigma_\mu^{\dot{\alpha}\alpha} k^\mu, \quad \text{or} \quad k_{\alpha\dot{\alpha}} := \bar{\sigma}_{\alpha\dot{\alpha}}^\mu k^\mu. \quad (2.2.1)$$

Note that the indices are always ordered so that when they are upper the dotted index comes first, and when they are lower the undotted index comes first.

The Minkowski inner product of two vectors x and y is then given by $x \cdot y = x^{\dot{\alpha}\alpha} y_{\alpha\dot{\alpha}} = \text{Tr}(xy)$, and so the norm of a vector k is given by $k \cdot k = k^{\dot{\alpha}\alpha} k_{\alpha\dot{\alpha}} = \det(k^{\dot{\alpha}\alpha})$. Then any massless vector must satisfy $\det(k^{\dot{\alpha}\alpha}) = 0$, which implies that massless k can be written as the product of two Grassmann even spinors, one in the fundamental of $SU(2)_L$ and one in $SU(2)_R$. In this thesis I will refer to the spinors corresponding to the momentum vector for external state $i \in \mathcal{N}$ of an amplitude as $|i]^{\dot{\alpha}} \in SL(2)_L$, and $\langle i|^\alpha \in SL(2)_R$, where in $M^4(\mathbb{R})$ the two spinors are related by $|i] = \langle i|^\dagger$ with \dagger

the conjugate transpose. It will be important at some points to package the spinors up into two $2 \times n$ matrices, with the first index ranging over the spinor degrees of freedom and the second over the number of particles. In these cases, I will use the notation $\lambda = (\lambda_i^\alpha) = (\langle i |^\alpha)$, and $\tilde{\lambda} = (\tilde{\lambda}_i^\alpha) = (|i]^\alpha)$. Sometimes the spinors will not be specific to the external data a given particle, and then I will refer to them as $|\tilde{\lambda}]$ and $\langle \lambda |$, where the λ is now the variable name for the spinors and is not related to the external data of an amplitude.

The splitting of a massless 4-vector into two spinors can then be written as either

$$k_i = |i] \langle i| := (|i]^\alpha \langle i|^\alpha) \quad \text{or} \quad k_i = |i\rangle [i| := (|i\rangle_\alpha [i|^\alpha), \quad (2.2.2)$$

where in this notation $|i\rangle$ and $|i]$ are two component column vectors and $\langle i|$ and $[i|$ are two component row vectors, so that the tensor product in equation (2.2.2) matches the matrix multiplication. Massive vectors can also be represented in this formalism as a sum of two massless vectors. Any amplitude for massless particles written as a function of momentum vectors k_i must take into consideration the mass shell constraint $k_i^2 = 0$, but can be written as an unconstrained function of $|i]$ and $\langle i|$. Removing the need for quadratic on-shell constraints in the representation of the amplitude can simplify their algebraic expressions significantly.

The amplitude is Lorentz invariant and so it is necessary to construct Lorentz invariant functions of the spinor variables. There is an invariant rank 2 tensor in $SU(2)$ given by $\epsilon = \begin{pmatrix} 0 & 1 \\ -1 & 0 \end{pmatrix}$, which exists in $SU(2)_L$ as $(\epsilon^{\alpha\beta}) = (\epsilon_{\beta\alpha}) = \epsilon$, and in $SU(2)_R$ as $(\epsilon^{\dot{\beta}\dot{\alpha}}) = (\epsilon_{\dot{\alpha}\dot{\beta}}) = \epsilon$. These tensors can be used to map from the fundamental representations of $SU(2)_L$ and $SU(2)_R$ to their corresponding dual spaces, motivating the following definition for the dual spinors

$$\langle i| := (\epsilon |i])^T, \quad [i| := (\epsilon |i\rangle)^T. \quad (2.2.3)$$

Then $SU(2)$ invariant products are defined by matrix multiplication of the row vectors in the dual space with the column vectors in the fundamental representation,

so that

$$\begin{aligned}\langle ij \rangle &:= \langle i | j \rangle = \det(|i\rangle |j\rangle) = |i\rangle^1 |j\rangle^2 - |i\rangle^2 |j\rangle^1 \\ [ij] &:= [i | j] = \det(|i\rangle |j\rangle) = |i\rangle^1 |j\rangle^2 - |i\rangle^2 |j\rangle^1,\end{aligned}\tag{2.2.4}$$

noting that this is equivalent to the calculation of a two by two matrix. Lorentz invariant products of two null vectors can be constructed from the spinor brackets as

$$2k_i \cdot k_j = \langle ij \rangle [ji].\tag{2.2.5}$$

Relaxing the constraint that $|i] = \langle i|^\dagger$ reveals additional structure in the representation of scattering amplitudes, and allowing the two spinors to be independent of one another corresponds to complexifying the spacetime. The relationship for the Lorentz group then becomes $\text{SO}(3,1)^\mathbb{C} \simeq \text{SL}(2)_L \times \text{SL}(2)_R$, and I will work mostly with complexified momenta in this thesis.

The specialisation to four dimensions also simplifies the representation of polarisation vectors significantly, due to the particularly simple structure of the little group in 4D. The little group for null vectors in complexified 4D spacetime is $\text{GL}(1)$, which acts on the spinors as

$$(|i], \langle i|) \mapsto (\alpha_i |i], \frac{1}{\alpha_i} \langle i|) \quad \alpha \in \text{GL}(1),\tag{2.2.6}$$

leaving the vector $k_i = |i] \langle i|$ invariant. The representations of $\text{GL}(1)$ are specified by a single integer, which means that the helicity of a massless particle in 4D can be used to specify its polarisation structure, up to freedom of gauge choice. Spin one particles are restricted to a polarisation of either ϵ^+ or ϵ^- corresponding to positive or negative helicity, and spin two particles similarly have polarisation ϵ^{++} or ϵ^{--} . The forms of these polarisation vectors are given explicitly in terms of the spinor variables in [83], and depend on a reference spinor which encodes the gauge freedom. As a result of this the momentum and polarisation state of a spin one or spin two particle can be fully specified by a momentum and a choice of \pm , and hence the functional dependence of scattering amplitudes for these particles in 4D can be

written as

$$\mathcal{A} = \mathcal{A}(1^{h_1} 2^{h_2} 3^{h_3}, \dots, n^{h_n}), \quad (2.2.7)$$

which no longer depends on the polarisation vectors explicitly as in general dimensions of space-time. This is a significant simplification, reducing the dependence of the amplitude down from a polarisation vector constrained by gauge invariance for each particle down to a binary choice of helicity. This reduction in complexity is one of the main computational advantages in 4D compared to other dimensions of spacetime, and is used widely in theory and experiment and referred to as the spinor-helicity formalism, reviewed in [83, 85, 82] and first used in [6].

The simplicity of representing different massless amplitudes at n points in 4D by a binary choice of helicities is encoded in a further formalism, known as the MHV classification. For amplitudes with only one type of spin one or spin two particle it is standard to define the MHV degree k as the number of negative helicity particles where relevant. I also define a left set of particles L as the particles with negative helicity, and a right set R as the positive helicity particles, so that $L \sqcup R = \mathcal{N}$, $|L| = k$ and $|R| = n - k$. The tree-level amplitudes of a number of theories, including those of Yang-Mills and Einstein gravity as discussed in the next section, are zero for helicity configurations with all positive helicities ($k = 0$), and similarly for configurations with one positive helicity and all others negative ($k = 1$);

$$A^{(0)}(1^+ 2^+ 3^+ \dots n^+) = A^{(0)}(1^- 2^+ 3^+ \dots n^+) = 0, \quad (2.2.8)$$

as well as for $k = n - 1$ and $k = n$ by helicity conjugation.

The first non-zero amplitude is the amplitude with two negative helicity particles, and this is commonly referred to as the ‘maximal helicity violating’ or MHV amplitude, with the name coming from the idea that conservation of helicity results in the amplitudes in equation 2.2.8 being zero. The MHV classification then denotes all such amplitudes in terms of $k = |L|$ as $N^{(k-2)}$ MHV amplitudes.

Although amplitudes in the most common and physically relevant theories satisfy

equation (2.2.8), this is not always true and does not hold for example in conformal supergravity, as reviewed in Section 2.6 and discussed in detail in Chapter 7. It is still relevant to think of these amplitudes as fitting into the MHV classification, but now the ‘out-of-MHV’ amplitudes with $k = 0, 1, n - 1$ or n need not be equal to zero. An example of the computational power of this combination of techniques is illustrated by the 3 point amplitudes of Yang-Mills theory and Einstein gravity, which are completely fixed by Lorentz symmetry, translational invariance, little group scaling and unitarity bounds [86] to give

$$\begin{aligned}
 \mathcal{A}_{\text{YM}}(1^-2^-3^-) &= 0 & \mathcal{A}_{\text{YM}}(1^-2^-3^+) &= \delta^4(P) \frac{\langle 12 \rangle^4}{\langle 12 \rangle \langle 23 \rangle \langle 31 \rangle} \\
 \mathcal{M}_{\text{EG}}(1^-2^-3^-) &= 0 & \mathcal{M}_{\text{EG}}(1^-2^-3^+) &= \delta^4(P) \frac{\langle 12 \rangle^8}{\langle 12 \rangle^2 \langle 23 \rangle^2 \langle 31 \rangle^2}.
 \end{aligned}
 \tag{2.2.9}$$

2.3 Supersymmetry, Superamplitudes and On-Shell Superspace

The spacetime symmetries of a given quantum field theory can be augmented with an additional type of symmetry known as supersymmetry, which is a powerful tool in further constraining the structure of the scattering amplitudes of the theory. Supersymmetry groups bosonic and fermionic particles together into superpartners or supermultiplets, constraining the possible interactions between different kinds of fields and reducing the number of coupling constants. Supersymmetry was originally conceived purely as a theoretical endeavour [87], and it subsequently came to be believed that it would describe physics beyond the standard model [88], although it was not found at LHC energy scales as originally predicted, and its viability as a physical model in this setting is unclear [89]. In the study of scattering amplitudes the benefit of supersymmetry as a computational tool is clear however - the additional non-physical supersymmetries added to the theory make many more computations accessible, and a number of computational techniques which are now used to calculate scattering amplitudes relevant to standard model physics were first developed in

simpler supersymmetric models, whose scattering amplitudes do not model natural phenomena.

Each supersymmetry transformation of a given theory is parameterised by an anti-commuting Grassmann odd degree of freedom, and supersymmetry can be considered as acting on a spacetime which has Grassmann odd dimensions additional to the standard commuting degrees of freedom on the manifold to create a supermanifold. In four dimensions each supersymmetry added contributes four degrees of freedom to the manifold, so that with $\mathcal{N} \in \mathbb{N}$ supersymmetries $M^4(\mathbb{R})$ is extended to $M^{4|4 \times \mathcal{N}}(\mathbb{R})$. There is an $SU(\mathcal{N})$ symmetry under mixing different supersymmetries together which is known as the ‘ R -symmetry’ [83], and the new anticommuting coordinates on the supermanifold transform in the fundamental representation of $SU(2)_L \times SU(\mathcal{N})$ and $SU(2)_R \times SU(\mathcal{N})$ so that a point can be written as

$$(x, |\theta\rangle, |\bar{\theta}\rangle) \in M^{4|4 \times \mathcal{N}}(\mathbb{R}), \quad (2.3.1)$$

where $|\theta\rangle = (|\theta^I\rangle)$ and $|\bar{\theta}\rangle = (|\bar{\theta}^I\rangle)$. I use indices I, J, K, \dots to represent indices transforming in $SU(\mathcal{N})$.

The conserved charges $|\tilde{Q}\rangle$ and $|Q\rangle$ which generate each supersymmetry transformation are necessarily also Grassmann odd, and as such they anticommute with one-another and commute with the generators of the Poincaré group. The closure of the commutators of these generators produces a graded Lie algebra known as the super Poincaré algebra as the spacetime symmetry of the supersymmetric theory [90], which is given by

$$\left\{ |Q^I]^{\dot{\alpha}}, \langle Q_J|^\alpha \right\} = P^{\dot{\alpha}\alpha} \delta_J^I, \quad (2.3.2)$$

where P generates spacetime translations.

As supersymmetry transformations take linear combinations of bosonic and fermionic fields they can be considered as increasing or decreasing the helicity of the corresponding particle states by $\frac{1}{2}$. The states of different fields are then grouped together into a supermultiplet by the supersymmetry operations. As an example consider

$\mathcal{N} = 1$ super Yang-Mills theory, which is a theory of a gauge boson A_μ and a fermion ψ^α . The excitations of A_μ are a positive and a negative gluon, g^+ with helicity $+1$ and g^- with helicity -1 , and the excitations of ψ^α are ψ^+ with helicity $+\frac{1}{2}$ and ψ^- with helicity $-\frac{1}{2}$. The supersymmetry transformations combine these states together into the supermultiplets (g^+, ϕ^+) and (g^-, ϕ^-) , such that the multiplets are closed under action of the generators $[\tilde{Q}]$ and $\langle Q|$ of the supersymmetries.

Increasing the number of supersymmetries increases the number of different types of particles which can be related to one another, so for example $\mathcal{N} = 2$ allows for linear combinations of fields with spin differing by at most 1, and the gluon supermultiplets of $\mathcal{N} = 2$ super Yang-Mills theory are (g^+, ψ^+, ϕ) and $(g^-, \psi^-, \bar{\phi})$ where ϕ is a scalar field in the theory. Supermultiplets for a given \mathcal{N} can be constructed recursively from the multiplets for $\mathcal{N} - 1$, and contain a total of \mathcal{N} states.

This property of increasing and decreasing helicity introduces a bound on the number of supersymmetries \mathcal{N} for a given theory, and hence supersymmetry can be maximal or non-maximal. To see this, consider the negative helicity gluon in Yang-Mills theory. Increasing the helicity of this particle four times in steps of $+\frac{1}{2}$ using the generators of the supersymmetry gives a particle of helicity $+1$, which must be the positive helicity gluon. If we add an additional supersymmetry generator and increase one more time we get a spin $\frac{3}{2}$ particle, which is necessarily part of a gravitational theory, and so the theory is no longer Yang-Mills only. From this it can be that at the maximum number of super symmetries in Yang-Mills theory in 4D is $\mathcal{N} = 4$, and I discuss the $\mathcal{N} = 4$ Yang-Mills super multiplet in Section 2.4. Following a similar argument in Einstein gravity the maximum number of super symmetries in 4D is $\mathcal{N} = 8$, with supermultiplet discussed in Section 2.5. Maximal supersymmetry in conformal supergravity is $\mathcal{N} = 4$ and is discussed in Section 2.6. Increasing the helicities of a gravitational theory above 2 or below -2 produces higher-spin fields which have a number of undesirable physical properties, and so the maximal number of supersymmetries in four dimensions is generally considered to be 8. Note that setting $\mathcal{N} = 0$ recovers the original theory without supersymmetry.

One key way in which supersymmetry restricts the structure of scattering amplitudes in a given theory is described by the supersymmetric Ward identities [83], which enforce that certain linear combinations of amplitudes for different types of particles must add up to zero. This reduces the number of independent amplitudes that need to be calculated in the theory, and is a particularly powerful result which holds true for all values up the coupling constant, and hence all orders of perturbation theory. Supersymmetry also simplifies the structure of loop amplitudes in perturbation theory significantly, due to the fact that any internal loop degrees of freedom must now include a sum over states in the super multiplet of the theory, and cancellations arise due to a relative minus sign between fermionic and bosonic loops.

The supersymmetric Ward identities can be encoded by combining the component amplitudes for different particles together into a new structure called a superamplitude. The superamplitude can be considered as the amplitude for a process which scatters supermultiplets of the theory rather than scattering individual particles, and the amplitude for the individual particles is then referred to as a component amplitude. This is encoded in a formalism called ‘on-shell superspace’ which introduces Grassmann odd degrees of freedom $\eta_i = (\eta_i^I)$ which transform in the fundamental of $SU(\mathcal{N})$ for $i \in \mathcal{N}$, and superamplitudes are written as an expansion in the different η^I variables for each R -symmetry index as shown in sections 2.4, 2.5 and 2.6.

The supercharges corresponding to each external state the theory are then represented in terms of η as $|\tilde{q}_{iI}\rangle = |i\rangle \frac{\partial}{\partial \eta^I}$ and $|q_i^I\rangle = |i\rangle \eta_i^I$, and the $|q_i^I\rangle$ can be thought of as an additional Grassmann component to the momentum of each particle, referred to as the supermomentum of the particle. Physically the supermomentum encodes the The total supermomentum of all of the states combined is $|Q\rangle = \sum_{i \in \mathcal{N}} |q_i\rangle$, and the supersymmetric Ward identities enforce conservation of supermomentum so that the superamplitude always has a factor of $\delta^{2 \times \mathcal{N}}(Q)$. The superamplitude is then manifestly invariant under the $|Q\rangle$ supersymmetry transformations due to the $\delta^{2 \times \mathcal{N}}(Q)$, and can be shown to also be invariant under the $[\tilde{Q}]$ transformations [85]. This superspace formalism is chiral because $|Q\rangle$ and $[\tilde{Q}]$ are treated differently. The

mapping between this chiral superspace and the one where $[\tilde{Q}]$ is algebraic and $|Q\rangle$ acts as a derivative operator is given by a Grassmann Fourier transform from η to $\tilde{\eta}$ variables.

The MHV classification for amplitudes without supersymmetry is then generalised to superamplitudes by introducing the idea of an MHV sector. In super Yang-Mills theory the N^{k-2} MHV sector at n points is the set of component amplitudes related to the N^{k-2} MHV amplitude by supersymmetry, and in Einstein gravity it is the set of amplitudes related to the N^{k-2} MHV graviton amplitude. The N^{k-2} MHV superamplitude is a Grassmann function with a well-specified weight in η variables N_G , and amplitudes where N_G is not a multiple of \mathcal{N} are zero. As such it is natural to define the Grassmann degree $k_G := \frac{N_G}{\mathcal{N}}$ of the amplitude, and in super Yang-Mills and Einstein supergravity $k_G = k$. The relationship still holds in conformal supergravity but is more subtle in this case subtle, which I discuss in Section 2.6 and Chapter 7.

Component amplitudes for individual states can be extracted from the superamplitude by integrating against N_G relevant η variables specifying which particle is being scattered for each external state. A review of these techniques can be found in [85, 83], and the extension to non-maximal supersymmetry is discussed in detail in [91]. I illustrate this process with an example of extracting a component amplitude in $\mathcal{N} = 4$ super Yang-Mills theory in the next section.

2.4 Super Yang-Mills Theory

Yang-Mills theory describes the physics of a spin 1 vector boson A_μ with a gauge symmetry group $SU(N_c)$ whose quantized field excitations are referred to as gluons, and $N_c \in \mathbb{N}$ is referred to as the number of colours of the theory. Gauge theory is of fundamental importance to physics; in the standard model of particle physics it is used to model both the weak and strong nuclear forces. The Lagrangian of the

theory is widely used in many applications, and is given by

$$\mathcal{L} = -\frac{1}{4}F_{\mu\nu}F^{\mu\nu}, \quad (2.4.1)$$

where $F_{\mu\nu} = \partial_\mu A_\nu - \partial_\nu A_\mu - i\frac{g}{2}[A_\mu, A_\nu]$, g is the coupling constant of the theory and $A_\mu = A_\mu^a T^a$ where T^a are the generators of the adjoint representation of $SU(N_c)$. To calculate amplitudes in the Feynman diagram formalism would require finding interaction vertices from equation 2.4.1, but to use the methods developed in this thesis it will not be directly relevant. The equations of motion coming from this Lagrangian are

$$\partial^\mu F_{\mu\nu} + g[A^\mu, F_{\mu\nu}] = 0, \quad (2.4.2)$$

and the corresponding linearized equations in Lorenz gauge with plane wave solutions are given in (2.1.1).

Plane-wave gluon states in 4D Yang-Mills theory are then fully specified by a momentum and choice of helicity of the gauge boson, as well as an $SU(N_c)$ adjoint index for each particle. The dependence of an amplitude on the gauge group indices is referred to as its colour structure, and in any given amplitude the colour structure can be written as a sum over traces of the generators of the adjoint representation. This decouples the colour-dependent part of the amplitude from the dynamical structure depending on the momenta and helicities, and the remaining dynamical colour-independent functions are called colour ordered amplitudes. The colour ordered amplitudes are gauge invariant as well as Lorentz invariant, and as such can be more simple to work with than the full colour-dressed amplitude. At tree-level, the colour dressed amplitude can be written as

$$\mathcal{A}^{(0)}(1^{h_1, a_1} 2^{h_2, a_2} \dots n^{h_n, a_n}) = \sum_{\sigma \in S_{n-1}} \mathcal{A}^{(0)}(1^{h_1} \sigma(2^{h_2} \dots n^{h_n})) \text{Tr}(T^{a_1} T^{\sigma(a_2)} \dots T^{a_n}), \quad (2.4.3)$$

where S_{n-1} is the permutation group on $n - 1$ elements.

As the colour structure is completely specified for all amplitudes at tree level using only one trace over all n of the adjoint generators for each particle, the colour ordered

amplitude has mathematical structure under cyclic permutations \mathbb{Z}_n of the external data, and is cyclically symmetric in some cases as explained below. At higher loop levels it is necessary to consider more complex colour structures with multiple traces, and so in general there are many terms and the full colour ordered amplitude does not obey the cyclic structure that it does at tree level.

Considering the amplitude as a function of the rank of the gauge group N_c , these multiple trace terms are subleading in N_c compared to the single trace terms as N_c increases. It is then possible to take the limit as N_c goes to infinity and neglect these subleading terms, leaving a simplified subset of the terms from the full amplitude. This simplified object can be considered as the amplitude for a Yang-Mills theory in the ‘large- N limit’ [92, 82], where the theory is referred to as ‘planar Yang-Mills’. For this theory to be well-defined the coupling constant g must also be taken to infinity, keeping the combination $g' := g^2 N_c$ known as the ‘t Hooft coupling fixed. Colour ordered amplitudes in the large- N limit then have a cyclic structure for higher loop levels as well as at tree-level, and when discussing Yang-Mills amplitudes in this thesis I will consider only the calculation of colour ordered amplitudes in the large- N limit. I will denote Yang-Mills amplitudes as \mathcal{A} in this thesis.

In chapters 3 and 4 of this thesis I consider calculation of super Yang-Mills amplitudes with any number \mathcal{N} of supersymmetries, and in Chapter 5 I will focus on $\mathcal{N} = 4$ supersymmetry when considering Yang-Mills amplitudes. Maximal $\mathcal{N} = 4$ supersymmetry introduces additional properties for the superamplitude which make it easier to compute. The spectrum of the theory contains one gluon with two helicity states g^\pm , eight fermions ψ^{+I} and ψ^{-IJK} , and six scalars ϕ^{AB} . The maximal $\mathcal{N} = 4$ supersymmetry transformations link the negative and positive helicity gluons into the same multiplet and so there is only one supermultiplet in $\mathcal{N} = 4$ super Yang-Mills which can be written as a superfield in on shell super space as

$$\Phi = \Phi^+ = \Phi^- = g^- \eta_1 \eta_2 \eta_3 \eta_4 + \psi^{-IJK} \eta_I \eta_J \eta_K + \phi^{IJ} \eta_I \eta_J + \psi^{+I} \eta_I + g^+. \quad (2.4.4)$$

As a result of this the assignment of positive and negative helicities to the external

data of the superamplitude in the theory is arbitrary, and the superamplitudes are invariant under a \mathbb{Z}_n cyclic transformation of the particle labels. Yang-Mills theory is classically conformally invariant in four dimensional spacetime, and this symmetry extends to the quantum level for all values of the coupling constant exactly when $\mathcal{N} = 4$.

To completely specify an amplitude in super Yang-Mills theory at tree level, it is necessary to make a choice of number of supersymmetries \mathcal{N} , number of points n , left set of negative helicity superfields L and a cyclic ordering of the particles $\sigma \in S_n$, and I will always use cyclic ordering $\sigma = (1, 2, \dots, n)$ in this thesis. The tree-level superamplitude can then be written as

$$\mathcal{A}^{(n)}(\Phi_1^{h_1} \Phi_2^{h_2} \dots \Phi_n^{h_n}) = \mathcal{A}_{n,L,\mathcal{N}}^{(n)}, \quad (2.4.5)$$

where $k = k_G = |L|$, relating the MHV degree, Grassmann degree and number of negative helicity superfields.

With maximal $\mathcal{N} = 4$ supersymmetry the tree-level superamplitude is specified by a smaller set of choices due to the fact that $\Phi^+ = \Phi^-$. In this case it is necessary to specify simply a number of points and a Grassmann degree, and then the MHV degree is defined by the Grassmann degree so that $k := k_G$ and

$$\mathcal{A}^{(n)}(\Phi_1 \Phi_2 \dots \Phi_n) = \mathcal{A}_{n,k,\mathcal{N}=4}^{(n)}. \quad (2.4.6)$$

In general writing down n point formulae for scattering amplitudes is a complex task, but in Yang-Mills theory in the MHV sector the amplitude has a particularly simple form. The famous tree-level MHV Parke-Taylor amplitude is

$$\mathcal{A}_{n,\{i,j\},\mathcal{N}}^{(0)} = \delta^{4|2 \times \mathcal{N}}(P) \frac{\langle ij \rangle^{4-\mathcal{N}}}{\langle 12 \rangle \langle 23 \rangle \dots \langle n1 \rangle}, \quad (2.4.7)$$

where $L = \{i, j\}$, and the cyclic symmetry of the amplitude for $\mathcal{N} = 4$ is manifest. The expressions for a general N^k MHV amplitudes at tree-level in super Yang-Mills

theory are significantly more complex than the MHV amplitude, but are well known in the literature [93, 94].

Finally consider extracting the component amplitude $\mathcal{A}(g^-\psi^{-IJK}g^+\psi^{+L})$ from $\mathcal{A}_{4,2,\mathcal{N}=4}^{(0)}$ as an example to explain how component amplitudes are extracted from a superamplitude. Each component amplitude corresponds to a specific set of on-shell superspace variables η_i^I for each particle label i , and the relevant η_i^I for each state can be read off from the supermultiplet. Integrating the superamplitude against these Grassmann variables then relates the component amplitude to the superamplitude

$$\mathcal{A}^{(0)}(g^-\psi^{-IJK}g^+\psi^{+L}) = \int d\eta_1^1 d\eta_1^2 d\eta_1^3 d\eta_1^4 d\eta_2^I d\eta_2^J d\eta_2^K d\eta_4^L \mathcal{A}_{4,2,\mathcal{N}=4}^{(0)}. \quad (2.4.8)$$

2.5 Einstein Supergravity

The standard calculation of gravitational scattering amplitudes works from the Einstein-Hilbert Lagrangian, and I will refer to these amplitudes as Einstein gravity amplitudes. The Lagrangian is

$$\mathcal{L} = \frac{1}{\kappa} \sqrt{-g} R + \mathcal{L}_{\text{matter}}, \quad (2.5.1)$$

where R is the Ricci scalar, $\sqrt{-g}$ is a volume element on the space-time, $\kappa = 16\pi G_N$ is the coupling constant in terms of Newton's gravitational constant G_N , and $\mathcal{L}_{\text{matter}}$ describes any matter content considered. The Ricci scalar is a standard function of the metric $g_{\mu\nu}$, its inverse $g^{\mu\nu}$ and its derivatives $\partial_\sigma g^{\mu\nu}$ [95], and so the Einstein-Hilbert Lagrangian describes the self-interactions of a metric $g_{\mu\nu}$, which is a rank 2 symmetric tensor. The action corresponding to this Lagrangian is invariant under arbitrary parameterizations of the space-time manifold known as diffeomorphisms.

To calculate gravitational amplitudes in flat space, the metric is expanded as a perturbation around the Minkowski metric, so that

$$g_{\mu\nu} = \eta_{\mu\nu} + \kappa h_{\mu\nu}, \quad (2.5.2)$$

and the quantized field excitations of the perturbation $h_{\mu\nu}$ are spin 2 particles referred to as gravitons. The expansion of $\sqrt{-g}$ in orders of κ has infinitely many terms, and the interaction vertex structure of Einstein gravity in the Feynman diagram formalism is incredibly complex. Einstein gravity amplitudes in this thesis will be calculated using methods which do not refer to the Lagrangian, and so equation 2.5.1 will not be used directly.

The equations of motion of the Einstein-Hilbert Lagrangian in terms of the full metric $g_{\mu\nu}$ are the famous Einstein's field equations,

$$R_{\mu\nu} - \frac{1}{2}Rg_{\mu\nu} = T_{\mu\nu}, \quad (2.5.3)$$

where $R_{\mu\nu}$ is the Ricci tensor satisfying $R^\mu{}_\mu = R$, and $T_{\mu\nu}$ is the stress-energy tensor calculated from $\mathcal{L}_{\text{matter}}$. The linearized field equations for $h_{\mu\nu}$ in de Donder gauge [95] are given in equation 2.1.1, and so the states of the theory are plane waves, as in Yang-Mills theory, but with polarisation tensors of the form $\epsilon_{\mu\nu}$. The diffeomorphisms which leave both the perturbative form of the metric and the choice of gauge invariant constrain the form of these polarisation tensors, and are considered a gauge symmetry under which the amplitudes of the theory must be invariant. As with Yang-Mills theory there are only two different possible polarisation structures $\epsilon_{\mu\nu}^+$ and $\epsilon_{\mu\nu}^-$, and they can be decomposed in terms of the polarisation vectors of Yang-Mills theory as $\epsilon_{\mu\nu}^\pm = \epsilon_\mu^\pm \epsilon_\nu^\pm$ [83].

While there are many similarities between the structures of gauge theory and gravity amplitudes, there are also a number of notable differences. Importantly there is no notion of colour in gravity and hence no need for colour ordering. N^{k-2} MHV gravitational amplitudes do not have a cyclic structure as in Yang-Mills, and instead have an $S_k \times S_{n-k}$ permutation invariance under interchange of any two external states with the same helicity. In this thesis I will generally use \mathcal{M} to denote gravitational amplitudes.

Chapters 3 and 4 of this thesis consider calculation of Einstein supergravity amplitudes with any number \mathcal{N} of supersymmetries, and in Chapter 6 I will focus on

$\mathcal{N} = 8$ supergravity. As with Yang-Mills Theory, maximal $\mathcal{N} = 8$ supersymmetry introduces additional structure to superamplitude. The spectrum of the theory contains one graviton with two helicity states h^\pm , 16 gravitinos λ^{+I} and λ_I^- , 56 graviphotons A^{+IJ} and A_{IJ}^- , 112 spin $\frac{1}{2}$ fermions ψ^{+IJK} and ψ_{IJK}^- , and 70 scalars ϕ^{ABCD} . The $\mathcal{N} = 8$ supersymmetry transformations link the negative and positive helicity gravitons into the same multiplet, and so there is only one supermultiplet in $\mathcal{N} = 8$ supergravity which can be written as a superfield in on shell super space as

$$\Phi = \Phi^+ = \Phi^- = h^- \eta_1 \eta_2 \eta_3 \eta_4 \eta_5 \eta_6 \eta_7 \eta_8 + \dots + \psi^{+IJK} \eta_I \eta_J \eta_K + A^{+IJ} \eta_I \eta_J + \lambda^{+I} \eta_I + h^+. \quad (2.5.4)$$

As with $\mathcal{N} = 4$ super Yang-Mills, this means that the assignment of positive and negative helicities to the external data of the superamplitude in the theory is arbitrary, and hence $\mathcal{N} = 8$ supergravity amplitudes have a full S_n permutation symmetry under the exchange of any two external states.

Specifying an amplitude in Einstein supergravity requires the same information as in super Yang-Mills, and we have that

$$\mathcal{M}^{(n)}(\Phi_1^{h_1} \Phi_2^{h_2} \dots \Phi_n^{h_n}) = \mathcal{M}_{n,L,\mathcal{N}}^{(n)}, \quad (2.5.5)$$

with

$$\mathcal{M}^{(n)}(\Phi_1 \Phi_2 \dots \Phi_n) = \mathcal{M}_{n,k,\mathcal{N}=8}^{(n)}. \quad (2.5.6)$$

for maximal $\mathcal{N} = 8$ supersymmetry.

MHV amplitudes in supergravity can be written in a number of different ways, [79, 96], but perhaps the most concise and simple expression is written in terms of the MHV Hodges matrix \mathcal{H} [22]. The amplitude is

$$\mathcal{M}_{n,\{a,b\},\mathcal{N}}^{(0)} = \delta^{4|2 \times \mathcal{N}}(P) \langle ab \rangle^{8-\mathcal{N}} \frac{\det \mathcal{H}}{\langle ab \rangle \langle bc \rangle \langle ca \rangle}, \quad (2.5.7)$$

where c is any choice of particle label from $\mathcal{N} \setminus \{a, b\}$, and the amplitude can be shown to be independent of the choice of c . The MHV Hodges matrix \mathcal{H} is an

$(n - 3) \times (n - 3)$ matrix, defined as

$$\mathcal{H} := \begin{cases} \frac{[ij]}{\langle ij \rangle} & i \neq j, \\ \psi_{i,n}^{[a]|b)} & i = j, \end{cases}. \quad (2.5.8)$$

The diagonal elements are written in terms of the gravitational inverse soft factor $\psi_{i,n}^{[a]|b)}$, which is defined as

$$\psi_{j,n}^{[a]|b)} = \sum_{k \in \mathcal{N} \setminus \{j\}}^n \frac{[jk] \langle ka \rangle \langle kb \rangle}{\langle jk \rangle \langle ja \rangle \langle jb \rangle}, \quad (2.5.9)$$

and is also a building block for amplitudes in conformal supergravity. $|a\rangle$ and $|b\rangle$ in this formula can be taken to be particle labels, or any choice of external spinors, and $\psi_{i,n}^{ab}$ can be shown to be invariant under the choice of the spinors.

For the purposes of amplitudes written in terms of the 4D scattering equations, this expression for the MHV gravity amplitude can be considered the equivalent of the Parke-Taylor formula for supergravity. General N^k MHV amplitudes even at tree level in supergravity are much more complex than at MHV, and the possibility exists that more simple and beautiful expressions for these amplitudes can still be found, along with the hope that finding new forms could shed light on the structure of quantum gravitational physics.

2.6 Conformal Supergravity

Conformal gravity is a diffeomorphism invariant theory of a metric tensor field $g_{\mu\nu}$ similarly to Einstein gravity, but it differs from Einstein gravity in that it is additionally invariant under Weyl transformations of the metric $g_{\mu\nu} \mapsto e^{\Omega(x)} g_{\mu\nu}$ which enhance the Poincaré symmetry of the space-time to conformal symmetry. The addition of conformal symmetry results in a theory which is not unitary, and hence conformal gravity is not physical and cannot be used directly to model nature. Conformal symmetry however constrains the structure of the theory significantly, notably resulting in a gravitational theory with much better UV behaviour than

Einstein gravity. In this thesis I take the philosophy that studying conformally invariant gravitational amplitudes may help in developing techniques to study more physically relevant amplitudes in Einstein gravity.

Spacetime Lorentz and translational transformations preserve angles and lengths between points, for example rotationally symmetric objects are equivalent at different angles. Conformal transformations also preserve angles between points, but because they allow additionally for a scaling of the metric tensor of the space-time they no longer preserve lengths, and conformal symmetry is then a statement of the equivalence of objects at different length scales. Weyl invariance of a theory leaves the theory invariant under space-time scaling transformations $x \mapsto e^\alpha x$, and additionally conformal boost transformations K_μ which are constructed by inverting spacetime through the origin so that $x \mapsto \frac{x}{x^2}$, translating in the inverted space and inverting back [97]. The Poincaré group, scaling transformations and conformal boosts combine together to form the conformal group which in Minkowski space in d dimensions is $SO(d, 2)$. The introduction of these additional symmetries constrains the structure of the theory significantly and conformal field theory, the study of conformally invariant quantum field theories, is of fundamental importance in mathematical physics, with an introduction given in [97, 98].

While the Lagrangian of Einstein gravity is constructed from contractions of the Riemann tensor, the Lagrangian of conformal gravity is written in terms of the Weyl tensor $W_{\mu\nu\rho\sigma}$. The Weyl tensor is one of the irreducible components of the Riemann tensor when considered as a representation of the Lorentz group, and can be constructed from the Riemann tensor and the metric [95], and is the natural object to consider in constructing a conformal theory of gravity as it transforms covariantly under Weyl rescaling of the metric as $W_{\mu\nu\rho\sigma} \mapsto e^\Omega W_{\mu\nu\rho\sigma}$. The most simple Lagrangian for a theory of conformal gravity is then

$$\mathcal{L} = \sqrt{-g} \left(-\frac{1}{\mathfrak{K}^2} W_{\mu\nu\rho\sigma} W^{\mu\nu\rho\sigma} \right), \quad (2.6.1)$$

which is conformally invariant in four dimensions where the Weyl rescaling of the

volume element $\sqrt{-g} \mapsto e^{-\frac{d}{2}\Omega}\sqrt{-g}$ cancels with the conformal transformation of $W_{\mu\nu\rho\sigma}W^{\mu\nu\rho\sigma}$, so that $\sqrt{-g}W_{\mu\nu\rho\sigma}W^{\mu\nu\rho\sigma} \mapsto e^{\frac{\Omega}{2}(4-d)}\sqrt{-g}W_{\mu\nu\rho\sigma}W^{\mu\nu\rho\sigma}$. The coupling constant \mathfrak{K} is different from that of Einstein Gravity, having mass dimension 0 as required for conformal invariance.

The equations of motion coming from (2.6.1) are

$$(\nabla^\rho\nabla^\sigma + R^{\rho\sigma})W_{\rho\mu\nu\sigma} = 0, \quad (2.6.2)$$

and any solution to the vacuum Einstein's field equations also solves these conformal gravity equations [99]. In this thesis I will study scattering amplitudes in conformal gravity as perturbations $h_{\mu\nu}$ around Minkowski space-time, where the perturbative expansion is the same as that for Einstein gravity explained in the previous section except with coupling constant \mathfrak{K} . Expanding the equations in the coupling constant \mathfrak{K} , choosing an appropriate gauge and taking the linear terms gives the following linearized field equations for the graviton field in conformal gravity

$$\square^2 h_{\mu\nu} = 0. \quad (2.6.3)$$

The fact that these equations are fourth-order in derivatives leads to two main consequences for the theory. The first is that additional boundary conditions for scattering states in the theory can now be considered compared to Yang-Mills theory and Einstein gravity. Standard plane waves $e^{ik\cdot x}$ for $k^2 = 0$ are still scattering states in conformal gravity as they solve equation (2.6.3), but additionally to these states are the non-plane wave states

$$h_{\mu\nu} = \varepsilon_{\mu\nu} A \cdot x e^{ik\cdot x}, \quad (2.6.4)$$

where A is a vector. States for which $A \propto k$ solve the second order equations of motion $\square h_{\mu\nu} = 0$ and hence are equivalent to plane wave modes, and so non-plane wave states are defined for $A \sim A + \beta k$, for all $\beta \in \mathbb{R}$. There are both conceptual and mathematical difficulties in scattering these states, given that states in the S -matrix formalism are defined at $t \rightarrow \pm\infty$, and non-plane wave states grow linearly with t

in that limit. It is possible to circumvent these issues considering the amplitude as a distribution, which I discuss in Chapter 7.

A second consequence of the fourth order field equations of conformal gravity is that the propagators of the theory go as $\frac{1}{p^4}$, from which it can be seen that the theory is not unitary at the quantum level. To understand this, consider adding the Einstein-Hilbert Lagrangian as a mass deformation to the conformal gravity Lagrangian to give

$$\mathcal{L} = \left(-\frac{1}{\mathfrak{K}^2} W_{\mu\nu\rho\sigma} W^{\mu\nu\rho\sigma} - \frac{2}{\mathfrak{K}^2} m^2 R \right). \quad (2.6.5)$$

The Einstein-Hilbert Lagrangian has standard $\frac{1}{p^2}$ propagators, which resolves the $\frac{1}{p^4}$ propagators of the conformal theory to some massless and some massive graviton modes, all with standard propagators. The argument runs as follows; the linearized equation of motion is modified schematically from (2.6.3) to

$$\square \left(\square + m^2 \right) h_{\mu\nu} = 0, \quad (2.6.6)$$

which has propagator

$$\Delta(p) = \left(\frac{1}{p^2} \frac{1}{p^2 + m^2} \right) = \frac{1}{m^2} \left(\frac{1}{p^2} - \frac{1}{p^2 + m^2} \right). \quad (2.6.7)$$

The second equivalent expression under partial fractioning shows that the massless mode is physical with a standard $\frac{1}{p^2}$ propagator, but the massive mode is an unphysical ghost mode due to the minus sign in front of the $\frac{1}{p^2+m^2}$ propagator. Ghost modes are not compatible with unitarity, and conformal gravity is therefore non-unitary as the ghost mode remains in the $m \rightarrow 0$ limit, as explained in more detail in [35].

It is possible to modify the structure of conformal gravity by the addition of a complex scalar field, resulting in a class of models known as non-minimal conformal gravities. The Lagrangian of these theories is given by [35]

$$\mathcal{L} = \sqrt{-g} \left(f(\phi) W_{\mu\nu\rho\sigma}^+ W^{+\mu\nu\rho\sigma} + f(\bar{\phi}) W_{\mu\nu\rho\sigma}^- W^{-\mu\nu\rho\sigma} \right) + \mathcal{L}_{\phi^\pm, \text{int}}, \quad (2.6.8)$$

where $\mathcal{L}_{\phi^\pm, \text{int}}$ is given in [35] and contains the kinetic terms in ϕ as well as additional interaction terms in ϕ and g . $W_{\mu\nu\rho\sigma}^+$ is the self-dual and $W_{\mu\nu\rho\sigma}^-$ the anti self-dual

component of the Weyl tensor under Hodge duality in the spacetime, and a choice of complex analytic function f defines the theory. The theory can be naturally supersymmetrised to an $\mathcal{N} = 4$ super conformal field theory as explained in [35], with super-multiplet structure detailed below.

A specific non-minimal conformal supergravity was found to arise naturally in twistor string theory [20], for which $f(\phi) = \frac{1+\phi}{1-\phi}$. This model also arises naturally in 4D ambitwistor string theory, and will be the object of study of Chapter 7 of this work, and one additional benefit of studying non-minimal conformal supergravity is that plane wave amplitudes in the minimal theory are all equal to zero [43, 100]. To differentiate from other conformal supergravities the theory is named Berkovits-Witten conformal supergravity, and from now on when I refer to conformal supergravity in this work I always mean Berkovits-Witten non-minimal conformal supergravity.

The spectrum of the theory contains three different super-multiplets with their helicity conjugates. There are two types of graviton multiplets, one with plane wave boundary conditions and one with non-plane wave boundary conditions, and the scalar fields coupling to the Weyl tensor in the Lagrangian fit into these graviton multiplets. There are also plane wave gravitino multiplets in the theory [20], which I will not consider in this work.

The field content of the two different types of gravity multiplets is the same, with two graviton polarisation's h^\pm , eight gravitinos λ^{+I} and λ^{-IJK} , twelve graviphotons $A^{\pm IJ}$, eight spin $\frac{1}{2}$ fermions ψ_I^- and ψ^{+IJK} and two scalars, ϕ^+ and ϕ^- which are related to the complex scalar field from the Lagrangian by $\phi^- := \phi$ and $\phi^+ := \bar{\phi}$. The plane wave graviton multiplets can be written as superfields in on-shell superspace as

$$\begin{aligned}\Phi^- &= h^- \eta_1 \eta_2 \eta_3 \eta_4 + \lambda^{-IJK} \eta_I \eta_J \eta_K + A^{-IJ} \eta_I \eta_J + \psi^{-I} \eta_I + \phi^- \\ \Phi^+ &= \phi^+ \eta_1 \eta_2 \eta_3 \eta_4 + \psi^{+IJK} \eta_I \eta_J \eta_K + A^{+IJ} \eta_I \eta_J + \lambda^{+I} \eta_I + h^-, \end{aligned}\tag{2.6.9}$$

and the equivalent non-plane wave multiplets have the same Grassmann expansion

and are denoted Φ_x^\pm , with non-plane wave graviton states denoted h_x^\pm and scalars denoted ϕ_x^\pm .

The coupling between the Weyl tensor and the scalars in the Lagrangian results in a number of superamplitudes which are zero at tree level in super Yang-Mills and Einstein supergravity taking non-zero values in conformal supergravity, notably superamplitudes with all negative helicity superfields or with one negative helicity superfield. This means that the number of negative helicity superfields is not in general equal to the Grassmann degree of the superamplitude, and to fully specify a superamplitude, both a set of negative helicity superfields $\{\Phi^-\}$ and a Grassmann degree k_G must be given. Amplitudes for plane wave graviton multiplets in conformal supergravity at tree-level can then be written

$$\mathcal{M}^{(0)}(\Phi_1^{h_1}\Phi_2^{h_2}\dots\Phi_n^{h_n}) = \mathcal{M}_{n,\{\Phi^-\},k_G}^{(0)}. \quad (2.6.10)$$

The full set of three point super amplitudes for plane wave graviton multiplets up to helicity conjugation are given by

$$\mathcal{M}(- - -) = \delta^{4|8}(P), \quad \mathcal{M}(- - +) = 0, \quad (2.6.11)$$

with some component amplitudes for gravitons and scalars given by

$$\begin{aligned} \mathcal{M}(h^-h^-h^-) &= 0, & \mathcal{M}(h^-h^-h^+) &= 0 \\ \mathcal{M}(h^-h^-\phi^-) &= \langle 12 \rangle^4 \delta^4(P). \end{aligned} \quad (2.6.12)$$

The tree level super amplitude in $\mathcal{N} = 4$ conformal supergravity for $k_G = 2$ at n points is given by

$$\mathcal{M}_{n,\{\Phi^-\},k_G}^{(0)} = \delta^{4|8}(P) \prod_{i \in \Phi^+} \psi_{i,n}, \quad (2.6.13)$$

with the gravitational inverse soft factor $\psi_{i,n}$ defined in equation (2.5.9). Equation (2.6.13) is referred to as the Berkovits-Witten formula and was first calculated in twistor string theory in [20], and I give an alternative calculation of this amplitude in 4D ambitwistor string theory in Chapter 7. Some three point calculations

involving non-plane wave gravity multiplets are calculated in [45], and I extend these to n -point calculations in Chapter 7 of this thesis.

2.7 Scattering Equations in general d and CHY Formalism for Tree-level Amplitudes

The CHY (Cachazo-He-Yuan) formalism allows for compact expressions to be written down for the full n -point tree-level S -matrix in d -dimensions for many different theories [10]. Amplitudes in this formalism are written down as a sum over the solutions of the scattering equations,

$$\sum_{j \in \mathcal{N} \setminus \{i\}} \frac{k_i \cdot k_j}{s_i - s_j} = 0, \quad (2.7.1)$$

where k_i are a set of n -point null momenta obeying momentum conservation, and s_i are points on the Riemann sphere which I will refer to as worldsheet coordinates. In this thesis will refer to these equations as the ‘general d scattering equations’. They are parameterised by the d -dimensional momenta k_i for each particle, and are solved for the worldsheet coordinates s_i , and physically they are equivalent to the equations of electrostatics for n particles in 2D whose charges are vectors in Minkowski spacetime.

The equations have an $SL(2)$ symmetry arising from global conformal transformations on the worldsheet, which is found by acting with the Möbius transformation on all of the s_i

$$f : s_i \mapsto f(s_i) = \frac{as_i + b}{cs_i + d} \quad (2.7.2)$$

where $a, b, c, d \in \mathbb{C}$, with $ad - bc = 1$. This $SL(2)$ symmetry reduces the number of variables by three, and the equations are shown to have three linear dependencies, reducing the total number of independent equations for n down to $n - 3$. To solve the equations it is necessary to fix the $SL(2)$ symmetry, and a standard choice of gauge is $s_a = 0, s_b = 1$ and $s_c \rightarrow \infty$ for $a, b, c \in \mathcal{N}$.

For example for $n = 4$, fixing $s_1 = 0, s_2 = 1, s_3 \rightarrow \infty$ and choosing any one of the four equations produces an equivalent linear system for s_4 . The full solution is then

$$s = (1, 0, \infty, -\frac{k_1 \cdot k_4}{k_1 \cdot k_2}). \quad (2.7.3)$$

All solutions at 5 points are given in [101] as well as some analysis at 6 points for $d = 4$, but above this the system becomes much more complex to solve. In [11] an inductive argument is given to show that the equations have $(n - 3)!$ solutions at n points, hence showing that above $n = 5$ the question of finding all solutions becomes in principle a numerical problem, due to the Abel-Rufini theorem [102] which states that polynomial equations have no general solution in terms of radicals for degree 5 or higher.

In this general d formalism tree-level amplitudes can be expressed as integrals of a theory-specific integrand $f(s_i, k_i, \epsilon_i)$ over delta functions enforcing the scattering equations,

$$\mathcal{A}_n^{(0)} = \int \frac{d^n s}{\text{SL}(2)} \prod_{i \in \mathcal{N}} {}'\delta \left(\sum_{j \in \mathcal{N} \setminus \{i\}} \frac{k_i \cdot k_j}{s_i - s_j} \right) f(s_i, k_i, \epsilon_i). \quad (2.7.4)$$

As the equations have three linear dependencies, three delta functions must be removed and a corresponding Jacobian factor introduced. The notation for the delta functions is then defined so that

$$\prod_{i \in \mathcal{N}} {}'\delta \left(\sum_{j \in \mathcal{N} \setminus \{i\}} \frac{k_i \cdot k_j}{s_i - s_j} \right) := (s_a - s_b)(s_b - s_c)(s_c - s_a) \prod_{i \in \mathcal{N} \setminus \{a, b, c\}} \delta \left(\sum_{j \in \mathcal{N} \setminus \{i\}} \frac{k_i \cdot k_j}{s_i - s_j} \right), \quad (2.7.5)$$

where $a, b, c \in \mathcal{N}$. The integral is shown not to depend on the choice a, b and c in [11].

Any valid integrand f must be covariant under this $\text{SL}(2)$ symmetry additionally to its invariance under any other symmetries inherited from the corresponding amplitude. The number of integrations matches the number of delta functions, and hence the integral gives the instruction to sum the integrand times the relevant Jacobian

factor over the $(n-3)!$ solutions to the scattering equations. In this way, calculating tree-level scattering for massless particles in many theories can be reduced to solving a set of algebraic equations. Further details can be found in [11, 10].

The integrands of many different theories can be built up from matrices which depend on momenta k_i , polarisation vectors ϵ_i and worldsheet variables s_i , as shown in [10]. Perhaps the most important of these matrices is the following antisymmetric $2n \times 2n$ matrix Ψ , defined by

$$\Psi_{i,j} = \begin{cases} \frac{k_i \cdot k_j}{s_i - s_j} & i \neq j, \\ 0 & i = j, \end{cases} \quad \Psi_{i+n,j+n} = \begin{cases} \frac{\epsilon_i \cdot \epsilon_j}{s_i - s_j} & i \neq j, \\ 0 & i = j, \end{cases} \quad \Psi_{i+n,j} = \begin{cases} \frac{\epsilon_i \cdot k_j}{s_i - s_j} & i \neq j, \\ - \sum_{l \in \mathcal{N} \setminus \{i\}} \frac{\epsilon_i \cdot k_l}{s_i - s_l} & i = j, \end{cases} \quad (2.7.6)$$

for $i, j \in \mathcal{N}$. This matrix is found to have a nullspace of dimension two, and hence to find a non-zero determinant it is necessary to remove two rows and columns from the matrix. Then scattering amplitudes in Yang-Mills theory and Einstein gravity in any dimension at tree level for any number of points can be calculated using the following integrands,

$$f_{\text{YM d dimensions}}(s_i, k_i, \epsilon_i) := \frac{1}{\prod_{i \in \mathcal{N}} (s_i - s_{i+1})} (-1)^{a+b} \frac{\text{Pf}(\Psi_{ab}^{ab})}{s_a - s_b} \quad (2.7.7)$$

$$f_{\text{EG d dimensions}}(s_i, k_i, \epsilon_i) := \frac{\det(\Psi_{ab}^{ab})}{(s_a - s_b)^2}$$

where the notation Ψ_{ab}^{ab} corresponds to removing row and column a and b from matrix Ψ , and Pf is the Pfaffian of an antisymmetric matrix, which satisfies $(\text{Pf}M)^2 = \det M$ making manifest double-copy structure of Yang-Mills and Gravity amplitudes [10, 103]. $\frac{1}{\prod_{i \in \mathcal{N}} (s_i - s_{i+1})}$ is referred to as the Parke-Taylor factor in analogy with the Parke-Taylor amplitude from equation (2.4.7), and encodes the cyclic ordering of colour-ordered Yang-Mills amplitudes. It is shown in [10] that these integrands do not depend on the choice of $i, j \in \mathcal{N}$.

These CHY integral formulae for scattering amplitudes in quantum field theory can be calculated from a string model known as ambitwistor string theory, which I introduce and discuss briefly in Section 2.11.

2.8 Refined 4D Scattering Equations

The 4D scattering equations are a refinement of the general d scattering equations which depend on the MHV degree as well as the number of particles [26], and can be used to calculate supersymmetry covariant expressions for the n -point tree level S -matrix of gauge theory and gravity. They are written in terms of the angle and square bracket spinors rather than momentum dot products, which introduces an extra variable t_i into the system for each particle which is related to the little group scaling of the spinor variables. I will think of the t_i as additional worldsheet variables, promoting each worldsheet coordinate from a point on the Riemann sphere to a point $\sigma_i \in \mathbb{C}^2$ defined as $\sigma_i = \frac{1}{t_i} \begin{pmatrix} 1 \\ s_i \end{pmatrix} = \begin{pmatrix} \sigma_i^1 \\ \sigma_i^2 \end{pmatrix}$. It is then natural to combine these variables together into a matrix $\sigma \in \mathbb{C}^{2 \times n}$, and to work with minors of this matrix defined as $(ij) := \det(\sigma_i \sigma_j) = \frac{s_i - s_j}{t_i t_j} = \sigma_i^1 \sigma_j^2 - \sigma_i^2 \sigma_j^1$. There is a natural $\text{GL}(2)$ transformation acting on the left of this matrix, and I discuss symmetries and gauge fixing of the equations in detail in Chapter 3.

In super Yang-Mills and Einstein supergravity, the 4D scattering equations respect the grouping of external states into a set L for negative helicities and a set R of positive helicities, where the MHV degree k of the amplitude is equal to the size of the left set, $k := |L|$, which is equal to the Grassmann degree of the superamplitude, $|L| = k_G$. For the discussion of conformal supergravity in this work it will be necessary to separate the definition of MHV degree and left set of negative helicity superfields, as explained in Section 2.6 and Chapter 7.

The 4D scattering equations are defined as the zeros of the following spinor functions

$$\tilde{E}_l := |l\rangle - \sum_{r \in R} \frac{|r\rangle}{(lr)}, \quad l \in L \quad E_r := |r\rangle - \sum_{l \in L} \frac{|l\rangle}{(rl)} \quad r \in R, \quad (2.8.1)$$

giving the following linear relations between the spinor variables for the external data;

$$|l\rangle = \sum_{r \in R} \frac{|r\rangle}{(lr)}, \quad l \in L \quad |r\rangle = \sum_{l \in L} \frac{|l\rangle}{(rl)} \quad r \in R. \quad (2.8.2)$$

Additionally I define the following set of fermionic functions, specified by an integer n , a left set L and a number of supersymmetries \mathcal{N} , which are used to encode supersymmetry in the 4D scattering equation framework.

$$E_i^{\mathcal{N}} := \delta^{\mathcal{N}} \left(\eta_l - \sum_{r \in R} \frac{\eta_r}{(lr)} \right) \quad (2.8.3)$$

Note that the fermionic functions exist only for the left set which may seem counter intuitive, however it gives a total of $|L|\mathcal{N} = k_G \mathcal{N} = sN_G$ supersymmetries which is the correct number for a given superamplitude. Only the bosonic parts of the scattering equations are localised onto the integral measure for the worldsheet, and so the fermionic equations are not solved in the same way that the bosonic equations are and are instead integrated against when extracting component amplitudes from the superamplitude.

I also define two sets of delta functions as a notational shorthand for the full set of 4D scattering equations. The first is a bosonic set of delta functions

$$\delta^{2 \times n}(\text{SE}_{n,L}) := \prod_{l \in L} \delta^2(\tilde{E}_l) \prod_{r \in R} \delta^2(E_r), \quad (2.8.4)$$

and the second set of delta functions also includes the fermionic variables,

$$\delta^{2 \times n | \mathcal{N} \times |L|}(\text{SE}_{n,L}) = \delta^{(2|\mathcal{N}|) \times |L| + 2 \times |R|}(\text{SE}_{n,L}) := \prod_{l \in L} \delta^{2|\mathcal{N}|}(\tilde{E}_l) \prod_{r \in R} \delta^2(E_r). \quad (2.8.5)$$

I define the mixed bosonic-fermionic delta function $\delta^{2|\mathcal{N}|}(E_l)$ to include the relevant fermionic variables as required from the context; so in this case $\delta^{2|\mathcal{N}|}(E_l) = \delta^2(E_l) \delta^{\mathcal{N}}(E_l^{\mathcal{N}})$. When using the first definition, I will consider the fermionic delta functions as a part of the integrand. With the second definition, the fermionic delta functions are considered as scattering equations for the Grassmann on-shell

superspace variables. I find both approaches to be useful, and hence include both definitions in this thesis.

As in the general d case it is then possible to write tree-level amplitudes for many different theories as integrals of some integrand f over these scattering equation delta functions, either with the fermionic delta functions as a part of the equations;

$$\mathcal{A}_{n,L}^{(0)} = \int \frac{d^{2 \times n} \sigma}{GL(2)} \delta^{2 \times n | \mathcal{N} \times |L|} (\text{SE}_{n,L}) f(\sigma, |i\rangle, |i]),$$

or as a part of the integrand

$$\mathcal{A}_{n,L}^{(0)} = \int \frac{d^{2 \times n} \sigma}{GL(2)} \delta^{2 \times n} (\text{SE}_{n,L}) f^{\mathcal{N}}(\sigma, |i\rangle, |i], \eta_i),$$

Integrands for Einstein gravity and Yang-Mills theory with any number of supersymmetries were derived in [26];

$$\begin{aligned} f_{\text{sYM}}(\sigma, |i\rangle, |i]) &:= \frac{1}{\prod_{i \in \mathcal{N}} (i \ i + 1)} \\ f_{\text{supergravity}}(\sigma, |i\rangle, |i]) &:= \det' \mathcal{H} \det' \tilde{\mathcal{H}} \end{aligned} \quad (2.8.6)$$

where \det' is an instruction to remove one row and column from the matrices before taking the determinant. \mathcal{H} is the Hodges matrix and $\tilde{\mathcal{H}}$ the dual Hodges matrix, defined as

$$\begin{aligned} \mathcal{H}_{ll} &:= - \sum_{l' \in L \setminus \{l\}} \mathcal{H}_{ll'}, & l \in L & & \mathcal{H}_{ll'} &:= \frac{\langle ll' \rangle}{(ll')}, & l \neq l' \in L \\ \tilde{\mathcal{H}}_{rr} &:= - \sum_{r' \in R \setminus \{r\}} \tilde{\mathcal{H}}_{rr'}, & r \in R & & \tilde{\mathcal{H}}_{rr'} &:= \frac{[rr']}{(rr')}, & r \neq r' \in R. \end{aligned} \quad (2.8.7)$$

Both matrices have determinant zero, each a single null vector $(1, 1, \dots, 1)$ and for this reason one row and column is removed before taking the determinant in the scattering equation integrand. The matrices can be shown to be invariant of the choice of row and column removed.

These integrands are valid for the case where the scattering equations include both the bosonic and fermionic variables, and should be integrated against delta functions $\delta^{2 \times n | \mathcal{N} \times |L|} (\text{SE}_{n,L})$. I also define the following integrands which include the fermionic

delta functions

$$\begin{aligned} f_{\text{sYM}}^{\mathcal{N}}(\sigma, |i\rangle, |i], \eta_i) &:= \prod_{l \in L} E_l^{\mathcal{N}} f_{\text{sYM}}(\sigma, |i\rangle, |i], \eta_i) \\ f_{\text{supergravity}}^{\mathcal{N}}(\sigma, |i\rangle, |i], \eta_i) &:= \prod_{l \in L} E_l^{\mathcal{N}} f_{\text{supergravity}}(\sigma, |i\rangle, |i], \eta_i), \end{aligned} \quad (2.8.8)$$

and these integrands should be integrated against $\delta^{2 \times n}(\text{SE}_{n,L})$.

As shown in [56], there are $A(n, k) = \langle \frac{n-3}{k-2} \rangle$ solutions to the n -point N^{k-2} MHV scattering equations, where $\langle \frac{n}{k} \rangle$ are the Eulerian numbers [104], tabulated in Figure 4.1. The inductive proof of the number of solutions finds that $A(n, k)$ can be expanded recursively by taking either a left set particle soft to reduce to an amplitude of the form $A(n-1, k-1)$ or a right set particle soft to reduce to $A(n-1, k)$. Each of these solutions then has a given multiplicity such that

$$A(n, k) = (n - k - 1)A(n - 1, k - 1) + (k - 1)A(n - 1, k), \quad (2.8.9)$$

with one solution in the MHV and $\overline{\text{MHV}}$ sectors for each n , so that $A(n, 2) = A(n, n-2) = 1$.

2.9 On-Shell Diagrams

On-shell diagrams provide an alternative method to calculate amplitudes in a number of different theories, and are based on the computational framework of BCFW (Britto-Cacahazo-Feng-Witten) recursion [8, 9]. In this framework n -point amplitudes are expressed recursively in terms of lower point amplitudes as a sum over factorisation channels. To derive this recursion relation, two of the external momenta of the amplitude are shifted by a complex variable z so that momentum is conserved for all z , and the BCFW shifted amplitude $\mathcal{A}(z)$ is then a meromorphic function of z . The factorisation channels of the original amplitude occur as the poles of the shifted amplitude in the complex z plane, and the residues of these poles are products of two lower point amplitudes. The n -point amplitude can be constructed from $\mathcal{A}(z)$

$$\begin{array}{l}
\begin{array}{c} 3 \\ | \\ \bullet \\ / \quad \backslash \\ 1 \quad 2 \end{array} \\
\begin{array}{c} 3 \\ | \\ \circ \\ / \quad \backslash \\ 1 \quad 2 \end{array} \\
\hline
\end{array}
= \frac{\delta^4(P) \delta^{2\mathcal{N}} (|1\rangle \eta_1 + |2\rangle \eta_2 + |3\rangle \eta_3)}{(\langle 12\rangle \langle 23\rangle \langle 31\rangle)^{\mathcal{N}/4}}
= \frac{\delta^4(P) \delta^{\mathcal{N}} ([12]\eta_3 + [23]\eta_1 + [31]\eta_2)}{([12][23][31])^{\mathcal{N}/4}}
= \int \frac{d^2 |\lambda\rangle d^2 |\tilde{\lambda}\rangle}{GL(2)} d^{\mathcal{N}} \eta$$

Figure 2.1: Vertices and edges for on shell diagrams in $\mathcal{N} = 4$ super Yang-Mills and $\mathcal{N} = 8$ supergravity

as $\oint dz \frac{A(z)}{z}$, where the contour encloses the pole at zero only, and is related to the poles on the factorisation channels using a global residue theorem.

Using this method repeatedly the n -point scattering amplitude can be broken down into 3-point building blocks, and on-shell diagrams are a diagrammatic calculus which encodes this process in four dimensional spacetime, notably in $\mathcal{N} = 4$ super Yang-Mills at all loop orders and $\mathcal{N} = 8$ supergravity at tree level. As the three-point amplitudes in these theories are known simply from the symmetries and some basic physical assumptions as explained in Section 2.2, on-shell diagrams take the minimal possible physical inputs and from this build up the the full S -matrix.

On-shell diagrams are then bipartite graphs constructed from 3-point black and white vertices which correspond to 3-point MHV and $\overline{\text{MHV}}$ superamplitudes respectively, as shown in the upper part of Figure 2.1. Unlike ordinary Feynman diagrams, the internal lines of on-shell diagrams do not contain virtual particles and correspond to integrating over on-shell degrees of freedom, as depicted in the lower part of Figure 2.1.

Scattering amplitudes in planar $\mathcal{N} = 4$ super Yang-Mills can be constructed from on-shell diagrams using the recursion relation in Figure 2.2 [65], which encodes BCFW recursion for loop integrands. Neglecting the second term on the right-hand

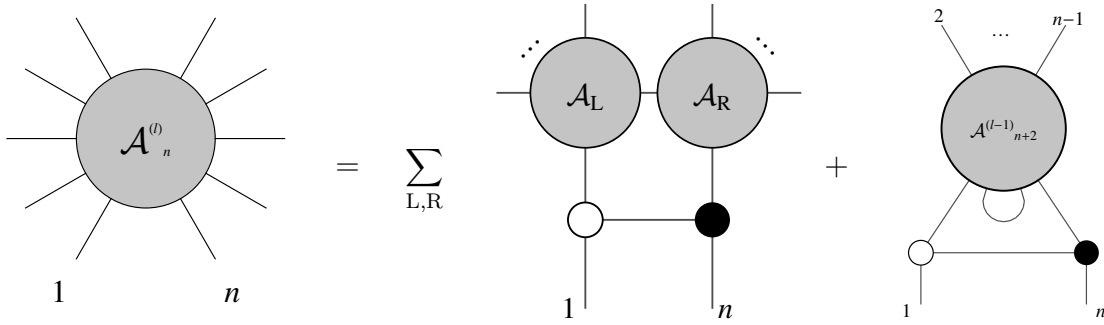


Figure 2.2: Loop-level BCFW recursion for planar $\mathcal{N} = 4$ super Yang-Mills. The loop order of \mathcal{A}_L and \mathcal{A}_R must add up to l , and the total number of legs must add up to $n + 2$.

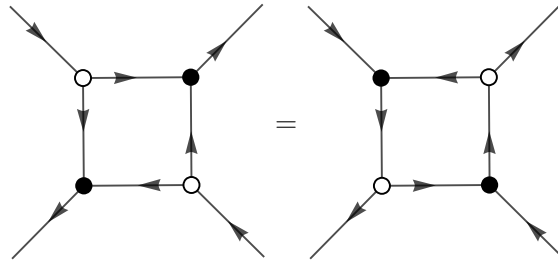


Figure 2.3: Square move equivalence relation super Yang-Mills

side produces the previously described tree-level BCFW recursion. The structure consisting of one white and one black vertex which attaches legs 1 and n to the lower-point on-shell diagrams implements the BCFW shift by complex variable z and is known as a BCFW bridge. In planar $\mathcal{N} = 4$ super Yang-Mills it is possible to extend the recursion relation to the integrand of the loop amplitudes, which is due in part to the fact that it is possible to make a canonical definition for the loop momentum in a planar theory. The loop recursion is taken into account by the second term on the right-hand side in Figure 2.2, which involves connecting two adjacent legs of a lower-loop diagram and attaching a BCFW bridge. This process constrains the momenta on the connected legs to add up to zero in what is known as a ‘forward limit’. The on-shell diagrams of $\mathcal{N} = 4$ super Yang-Mills also respect various equivalence relations such as the square move and mergers depicted in Figures 2.3 and 2.4, which can often be used to simplify calculations.

In $\mathcal{N} = 8$ supergravity it is also possible to define a tree-level recursion relation in terms of on-shell diagrams, as depicted in Figure 2.5 [70]. In this case, the BCFW



Figure 2.4: Merger equivalence relations for $\mathcal{N} = 4$ super Yang-Mills

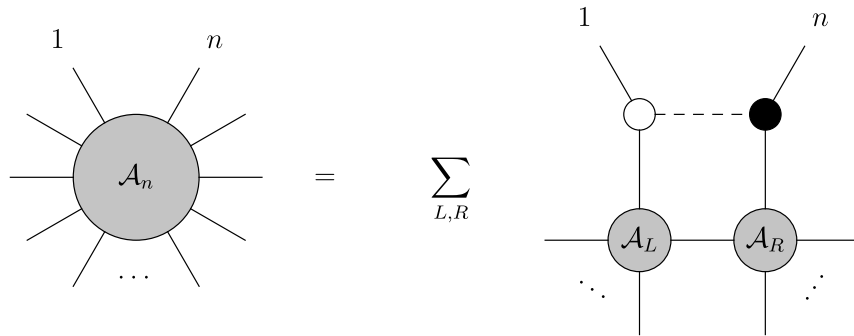


Figure 2.5: Tree-level BCFW recursion relations in $\mathcal{N} = 8$ supergravity

bridge is decorated by a kinematic factor as shown in Figure 2.6, and the expression is summed over all partitions of the external legs of the two subamplitudes which hold legs 1 and n fixed. In general this procedure will yield non-planar on-shell diagrams, but it is possible to restrict the recursion to a planar subset of diagrams by attaching the fixed legs of each subdiagram to the bridge or the other subdiagram at each step in the recursion. The full amplitude can then be obtained by summing over permutations of the unshifted external legs, implying nontrivial identities for non-planar on-shell diagrams. The on-shell diagrams of $\mathcal{N} = 8$ supergravity enjoy equivalence relations similar to those of $\mathcal{N} = 4$ super Yang-Mills, in particular the square move in Figure 2.3 and decorated mergers in Figure 2.7.

A remarkable feature of on-shell diagrams is that they naturally give rise to formulae

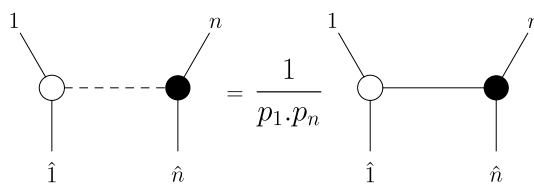


Figure 2.6: Definition of BCFW bridge decoration in $\mathcal{N} = 8$ supergravity

Figure 2.7: Merger equivalence relations in $\mathcal{N} = 8$ supergravity

for N^{k-2} MHV amplitudes in the form of integrals over the Grassmannian $\text{Gr}(k, n)$, which is the space of k planes in n dimensions. Integrals over $\text{Gr}(k, n)$ can be expressed as an integral over a $k \times n$ matrix C modulo a left action of $\text{GL}(k)$ and are supported on delta functions of the form

$$\delta^{k \times (2|\mathcal{N})} (C \cdot \tilde{\lambda} | C \cdot \eta) \delta^{2 \times (n-k)} (\lambda \cdot C^\perp), \quad (2.9.1)$$

where C^\perp is an $n \times (n - k)$ matrix considered to be perpendicular to C . This orthogonality property is expressed by the conditions

$$C^\perp \cdot C = 0, \quad (i_1 \dots i_{n-k})^\perp = \varepsilon_{i_1 \dots i_n} (i_{n-k+1} \dots i_n),$$

where the left and right hand sides denote the minors of C^\perp and C respectively. The dot products appearing in the delta functions are taken with respect to particle number, so that $(C \cdot \tilde{\lambda})_l^\alpha := \sum_{j \in \mathcal{N}} C_{lj} |j]^\alpha$ and $(C \cdot \eta)_l^I := \sum_{j \in \mathcal{N}} C_{lj} \eta_j^I$ for $l \in L$, and $(\lambda \cdot C^\perp)_r^\alpha := \sum_{j \in \mathcal{N}} C_{rj}^\perp \langle j|^\alpha$ for $r \in R$.

It is often convenient to use the $\text{GL}(k)$ symmetry to fix C in such a way that k columns form a $k \times k$ unit matrix, leaving integrals over the remaining $k \times (n - k)$ elements. This form is referred to as the link representation [105] and is closely related to the expressions arising from 4D ambitwistor string theory. In the link representation the delta functions in (2.9.1) take the same form as the 4D scattering equations.

There is a simple algorithm for deriving Grassmannian integral formulae directly from on-shell diagrams, which I now describe schematically, with more details given in Section 6.1. First assign variables α_i to the edges of the diagram, and assign arrows in a ‘perfect orientation’ such that there are two arrows entering and one arrow leaving every black node, and two arrows leaving and one arrow entering every

white node. Then set one edge variable associated with each vertex to unity, leaving $2n - 4$ edge variables. To construct the Grassmannian integral in $\mathcal{N} = 4$ super Yang-Mills, take the measure to be the product of $d\alpha_i/\alpha_i$ for each remaining edge variable, and multiply this by the delta functions in (2.9.1), where the C and C^\perp matrices are computed by summing over paths through the on-shell diagram and taking the product of the edge variables encountered along each path, as described in more detail in Section 6.1. The resulting formula can then be thought of as a gauge fixed Grassmannian integral formula where the gauge symmetry corresponds to $\text{GL}(k)$. Lifting the result to a covariant formula in $\mathcal{N} = 4$ super Yang-Mills gives the following expression or one of its residues,

$$d^{k \times n} \Omega_{\mathcal{N}} := \frac{d^{k \times n} C}{\text{Vol}(\text{GL}(k))} \frac{\delta^{k \times (2|\mathcal{N})}(C \cdot \tilde{\lambda} | C \cdot \eta) \delta^{(n-k) \times 2}(\lambda \cdot C^\perp)}{\prod_{i \in \mathcal{N}} (i \dots i+k-1)}, \quad (2.9.2)$$

which can be considered as a Parke -Taylor expression on $\text{Gr}(k, n)$ due to the cyclic product of minors. A similar factor also appears in Grassmannian integral formulae for $\mathcal{N} = 8$ supergravity amplitudes, so I keep the supersymmetry parameter \mathcal{N} unfixed.

The algorithm for deriving Grassmannian integral formulae in $\mathcal{N} = 8$ supergravity from on-shell diagrams is similar to that of $\mathcal{N} = 4$ super Yang-Mills, except that a factor of $d\alpha/\alpha^2$ must be included for each edge variable leaving a white vertex or entering a black vertex and $d\alpha/\alpha^3$ for each edge variable entering a white vertex or leaving a black vertex. Decorations for the BCFW bridges are also needed as depicted in Figure 2.6, and spinor brackets factor at each vertex. For each black vertex include a factor of $\langle ij \rangle$ where i and j are the two edges with ingoing arrows, and for each white vertex include a factor of $[ij]$ where i and j are the two edges with outgoing arrows. The spinors in these brackets will initially be internal to the diagram, but can be written in terms of the external spinors and edge variables by summing over paths in the on-shell diagram in a similar way to how the C -matrix is computed. In the final step it is necessary to include the delta functions in (2.9.1) and lift the integrand to a covariant expression as in $\mathcal{N} = 4$ super Yang-Mills. More details

and various shortcuts for computing on-shell diagrams in $\mathcal{N} = 8$ supergravity are described in Section 6.1, where I also explain how to incorporate the bonus relations of $\mathcal{N} = 8$ supergravity into the on-shell diagram recursion for MHV amplitudes.

2.10 Twistor Space

Twistor theory provides a mathematical framework for recasting physics from its standard setting in Minkowski spacetime $\mathcal{M}^d(\mathbb{R})$ into twistor space, which parametrises the set of geodesics in spacetime. In this section, I give an introduction to the mathematics of twistor space, discuss some motivations to why it can be a useful alternative to Minkowski spacetime, and provide the mathematical techniques necessary to describe 4D ambitwistor string theory in the next section. Twistor space is most useful for null geodesics, and the parameter space of only null geodesics is referred to as projective twistor space and denoted $\mathbb{P}\mathbb{T}$, I will refer to as simply twistor space in this thesis.

A null ray in flat space can be written as

$$R(x, p) = \{x + \alpha p \mid \alpha \in \mathbb{R}\}, \quad (2.10.1)$$

where $x, p \in \mathcal{M}^4(\mathbb{R})$ with $p^2 = 0$. The moduli space of these curves is

$$\mathbb{P}\mathbb{T}_d = \{x, p \in \mathcal{M}^4(\mathbb{R}) \mid p^2 = 0, x \sim x + \alpha p \text{ for } \alpha \in \mathbb{R}\}, \quad (2.10.2)$$

and twistor space in 4 dimensions is a mapping from this space to a new set of variables which solve the null constraint on p and quotient out by the identification $x \sim x + \alpha p$ automatically. Twistor space in four dimensions of space-time is the most well studied and widely applicable case, and $\mathbb{P}\mathbb{T}_4 = \mathbb{C}\mathbb{P}^3$ in 4D.

A general twistor $\mathcal{Z} = (\mathcal{Z}^A) \in \mathbb{P}\mathbb{T}$ is naturally written in terms of two component

spinors $|\lambda\rangle$ transforming in $SU(2)_R$ and $|\mu\rangle$ transforming in $SU(2)_L$ as

$$\mathcal{Z} = \begin{pmatrix} |\lambda\rangle \\ |\mu\rangle \end{pmatrix}. \quad (2.10.3)$$

The mapping from Minkowski space-time to twistor space is non-local – a single twistor defines a null ray in space-time, and a point in space-time corresponds to a line in twistor space. This non-local mapping is encoded in the twistor incidence relation; a twistor \mathcal{Z} is said to be incident with space-time point x if

$$|\mu\rangle = x |\lambda\rangle, \quad (2.10.4)$$

where x is the 2 by 2 matrix with components $x = (x^{\dot{\alpha}\alpha}) = (x^\mu \sigma_\mu^{\dot{\alpha}\alpha})$. Note that the incidence relation is invariant under a rescaling, respecting the projective nature of \mathbb{CP}^3 .

Now suppose twistor $\mathcal{Z} \in \mathbb{PT}$ is incident to the light ray $R(x, k_i)$, where $k_i = |i\rangle \langle i|$ is the momentum corresponding to the i^{th} external state. The null condition on the direction vector of the geodesic is solved automatically by using the spinor variables, and the quotient by the identification $x \sim x + \alpha |i\rangle \langle i|$ is seen as follows. First let the twistor Z be incident to each point on $R(x, k_i)$, so that $|\mu\rangle = (x + \alpha |i\rangle \langle i|) |\lambda\rangle$, $\forall \alpha \in \mathbb{R}$. This condition implies that $\langle i\lambda\rangle = 0$, from which follows that $|\lambda\rangle = \beta |i\rangle$ for some $\beta \in \mathbb{C}$. This β can be removed using the projective scale on the twistor, giving that the twistor incident to $R(x, k_i)$ is

$$\mathcal{Z} = \begin{pmatrix} |i\rangle \\ x |i\rangle \end{pmatrix}, \quad (2.10.5)$$

which is invariant under $x \mapsto x + \alpha |i\rangle \langle i|$.

Now consider fixing a single twistor $\mathcal{Z} = \begin{pmatrix} |\lambda\rangle \\ |\mu\rangle \end{pmatrix} \in \mathbb{PT}$, and asking what locus of space time points $x \in X \subset M^4(\mathbb{R})$ solve the incidence relation $|\mu\rangle = x(|\lambda\rangle, |\mu\rangle) |\lambda\rangle$. This is equivalent to constructing the inverse mapping to (2.10.5), taking a point in twistor space and giving a null ray in space time. I will then use this to prove that twistor space covers all possible null rays.

There are four possible ways to construct vectors from the spinors $|\lambda\rangle$ and $|\mu\rangle$ and their conjugates, and the set of combinations form a basis for vectors in space-time. Expanding x in this basis gives

$$x = \alpha |\mu\rangle \langle \tilde{\mu}| + \beta |\tilde{\lambda}\rangle \langle \tilde{\mu}| + \gamma |\mu\rangle \langle \lambda| + \delta |\tilde{\lambda}\rangle \langle \lambda| \quad (2.10.6)$$

where $\alpha, \beta, \gamma, \delta \in \mathbb{R}$ are functions of $[\mu\tilde{\lambda}]$ and $\langle \tilde{\mu}\lambda\rangle$, and hence have projective scaling weight 0. To find the functional form of these coefficients, first consider that x must have projective scaling weight 0. Then note that $|\mu\rangle \langle \lambda|$ has weight 2 and $|\tilde{\lambda}\rangle \langle \tilde{\mu}|$ has weight -2 which cannot be balanced by the scaling weight of β or γ , and so it must be true that $\beta = \gamma = 0$. Then it holds that $x = \alpha |\mu\rangle \langle \tilde{\mu}| + \delta |\tilde{\lambda}\rangle \langle \lambda|$, and substituting this form for x into the incidence relation gives that $\alpha = \frac{1}{\langle \tilde{\mu}\lambda\rangle}$. Following from this the locus of spacetime points X incident to twistor $\mathcal{Z} = \begin{pmatrix} |\lambda\rangle \\ |\mu\rangle \end{pmatrix}$ is equal to the following null ray,

$$X = R\left(\frac{|\mu\rangle \langle \tilde{\mu}|}{\langle \tilde{\mu}\lambda\rangle}, |\tilde{\lambda}\rangle \langle \lambda|\right) = \left\{ \frac{|\mu\rangle \langle \tilde{\mu}|}{\langle \tilde{\mu}\lambda\rangle} + \beta |\tilde{\lambda}\rangle \langle \lambda| \mid \beta \in \mathbb{R} \right\}. \quad (2.10.7)$$

The position vector in this expression has norm 0, and this is not generically true for all null rays. To show this expression covers all possible null rays, now prove that the mapping is surjective. First let $x \in \mathcal{M}^d(\mathbb{R})$ be a general spacetime point which need not satisfy $x^2 = 0$, and then check to see whether letting $x \in R\left(\frac{|\mu\rangle \langle \tilde{\mu}|}{\langle \tilde{\mu}\lambda\rangle}, k\right)$ restricts x^2 , noting that the direction along the line $k = |\tilde{\lambda}\rangle \langle \lambda|$ already covers all possible null vectors. Then it follows that $|\mu\rangle = x |\lambda\rangle$, and this form for $|\mu\rangle$ can be inserted into the null ray from equation (2.10.7) to give that

$$\frac{|\mu\rangle \langle \tilde{\mu}|}{\langle \tilde{\mu}\lambda\rangle} + \beta |\tilde{\lambda}\rangle \langle \lambda| = \frac{x |\lambda\rangle [\tilde{\lambda}|x]}{[\tilde{\lambda}|x|\lambda]} + \beta |\tilde{\lambda}\rangle \langle \lambda| = x + \beta' k \quad (2.10.8)$$

where in the third equality the Dirac algebra $x |\lambda\rangle [\tilde{\lambda}| + |\tilde{\lambda}\rangle \langle \lambda| x = [\tilde{\lambda}|x|\lambda]$ has been used and a new parameter $\beta' = \beta - \frac{x^2}{\langle \tilde{\lambda}|x|\lambda\rangle}$ has been defined on the null ray. From this it follows that twistor space covers all possible null rays in spacetime.

It is clear by writing the twistor in the form given in equation (2.10.5) that the little group scaling of the momentum vector acts equally on $|\lambda\rangle$ and $|\mu\rangle$, and so

the projective scale of the twistor corresponds to the action of the little group in space-time. It can also be seen at this point that it is possible for a twistor \mathcal{Z}_i to correspond to the external state i of a scattering process, without being incident to a spacetime point. In this case $\mathcal{Z}_i = \begin{pmatrix} |i\rangle \\ |\mu_i] \end{pmatrix}$, specifying only the first two components $|i\rangle$ in terms of Minkowski space and not the second two $|\mu_i]$. Physically this partially specified twistor can be seen as a consequence of the fact that the state is localised only in momentum space and not in position space due to the quantum uncertainty principle.

Much of the physics of how twistor space is relevant to the study of scattering amplitudes can be seen as a problem of trying to understand how to assign a space-time point x incident to the twistor \mathcal{Z}_i corresponding to each external state i . Three common approaches to this are problem twistor string theory discussed briefly in Section 2.11, 4D ambitwistor string theory discussed in detail in Section 2.11, and momentum twistors [106]. Momentum twistors assign an ordering to the external states, and then construct a position X_i for each twistor in terms of a sum of momentum vectors k_i , and as such is a non-local mapping in particle labels. Momentum twistors are a powerful computational tool in the study of scattering amplitudes and give rise to particularly simple expressions for the amplitudes of $\mathcal{N} = 4$ Super Yang-Mills, although I will not use them in this thesis.

To see how the symmetries of the space-time act on twistor space $\mathbb{P}\mathbb{T}$, let $\mathcal{Z} = \begin{pmatrix} |\lambda\rangle \\ |\mu] \end{pmatrix} \in \mathbb{P}\mathbb{T}$ be incident to the ray $R(x, k_i)$. The Minkowski inner product $x \cdot k_i$ is manifestly Lorentz invariant under $\text{SO}(3,1)$, and is additionally invariant under the conformal group $\text{SO}(4,2)$. This inner product can then be written in two different forms using the twistor incidence relation $|\mu] = x |\lambda\rangle$ and its Hermitian conjugate, so that

$$x \cdot k_i = [i|x|i\rangle = [i\mu] = \langle\mu i\rangle, \quad (2.10.9)$$

where $[i| = |i\rangle^\dagger$ and $\langle\mu| = |\mu]^\dagger$ in real Minkowski spacetime as explained in Section 2.2.

The largest subgroup of the general linear group which acts on \mathcal{Z} as $\mathcal{Z} \mapsto M\mathcal{Z}$,

for $M \in \text{GL}(4)$ and which leaves $[i\mu]$ invariant is the group $\text{SU}(2,2)$, defined by the condition $M\epsilon M^\dagger = \epsilon$ where $\epsilon = \begin{pmatrix} 0 & \mathbb{1}_2 \\ -\mathbb{1}_2 & 0 \end{pmatrix}$. $\text{SU}(2,2)$ is the double cover of the conformal group in $\text{SO}(4,2)$ Minkowski space, and the generators of $\text{SU}(2,2)$ acting on twistor space and $\text{SO}(4,2)$ acting on Minkowski space can be shown to be equivalent [107]. Although the Lorentz group acts linearly on Minkowski space, the conformal group has no linear representation acting directly on Minkowski space, and a key motivation for working in twistor space is the simplified linear action of the conformal group in this setting.

This action of $\text{SU}(2,2)$ motivates an inner product on twistor space with metric ϵ . Twistors \mathcal{W} in the dual space are taken to be hermitian conjugates of those in \mathbb{CP}^3 , so that $\mathcal{W} = \begin{pmatrix} |\rho\rangle & \langle\nu| \end{pmatrix}$. The inner product of a twistor and a dual twistor is then defined as

$$\mathcal{W} \cdot \mathcal{Z} := \mathcal{W}\epsilon\mathcal{Z} = [\rho\mu] - \langle\nu\lambda\rangle. \quad (2.10.10)$$

The dual twistor corresponding to \mathcal{Z} is defined to be

$$\bar{\mathcal{Z}} := \mathcal{Z}^\dagger = \begin{pmatrix} |\lambda\rangle^\dagger & |\mu\rangle^\dagger \end{pmatrix} = \begin{pmatrix} [\tilde{\lambda}] & \langle\tilde{\mu}| \end{pmatrix}, \quad (2.10.11)$$

with norm given by

$$\bar{\mathcal{Z}} \cdot \mathcal{Z} = \mathcal{Z}^\dagger\epsilon\mathcal{Z} = [\tilde{\lambda}\mu] - \langle\lambda\tilde{\mu}\rangle. \quad (2.10.12)$$

Projective twistor space is defined by the condition $\bar{\mathcal{Z}} \cdot \mathcal{Z} = 0$, and hence only the twistors in PT may be incident with a null ray and satisfy equation 2.10.9.

There is also a second $\text{SU}(2,2)$ invariant product defined on twistor space in terms of the totally antisymmetric tensor ϵ_{ABCD} , which is denoted by the angle 4- bracket

$$\langle ijkl \rangle := \epsilon_{ABCD} \mathcal{Z}_i^A \mathcal{Z}_j^B \mathcal{Z}_k^C \mathcal{Z}_l^D, \quad (2.10.13)$$

where $\{i, j, k, l\} \in \mathcal{N}$ label four twistors corresponding to different external states.

The subgroup of $\text{SU}(2,2)$ which corresponds to the Lorentz transformations acting on twistor space is already manifest from the angle and square bracket structure; $|\lambda\rangle$ transforms in $\text{SU}(2)_L$ and $|\mu\rangle$ transforms in $\text{SU}(2)_R$. The conformal group is

reduced to the Lorentz group by introducing a new bi-twistor referred to as the infinity twistor. The infinity twistor is denoted \mathcal{I} , defined as

$$\mathcal{I} := X^{[A} Y^{B]}, \quad X = \begin{pmatrix} 0 \\ 0 \\ 1 \\ 0 \end{pmatrix}, \quad Y = \begin{pmatrix} 0 \\ 0 \\ 0 \\ 1 \end{pmatrix}, \quad (2.10.14)$$

which corresponds to a light ray at null infinity of Minkowski spacetime. \mathcal{I} is invariant under the subgroup $\begin{pmatrix} a & 0 \\ 0 & b \end{pmatrix}$ of $SU(2,2)$, where $a \in SU(2)_L$ and $b \in SU(2)_R$.

Where conformal symmetry is broken a two bracket can then be defined on twistor space as

$$\langle \mathcal{Z}_i \mathcal{Z}_j \rangle := \langle ij \mathcal{I} \rangle = \langle ij \rangle, \quad (2.10.15)$$

which is equal to the angle 2-bracket in momentum space for twistors corresponding to external states i and j . Using this two-bracket allows for expression of all possible momentum dot products in terms of twistor brackets, as $k_i \cdot k_j = \langle \mathcal{Z}_i \mathcal{Z}_j \rangle \langle \bar{\mathcal{Z}}_j \bar{\mathcal{Z}}_i \rangle$. The scattering amplitudes of any conformally invariant theory written in twistor space should have an expression in terms of twistor brackets without using the infinity twistor, and any theory which does not have conformal symmetry will require the infinity twistor in the expression of its scattering amplitudes.

Another key motivation for studying physics in twistor space is that functions on twistor space automatically solve linearized equations of motion in Minkowski spacetime, of the form $\square\phi(x) = 0$ where $\phi(x)$ is a massless spin- s field. Twistor space can then be seen as an extension of complex analysis to 4 dimensions [108], in the sense that any complex analytic function $f(z, \bar{z})$ which satisfies $\bar{\partial}f = 0$ automatically solves $\nabla f = 0$, where the Laplacian is taken in terms of the real and imaginary parts of z . To see that functions on twistor space automatically solve $\square\phi(x) = 0$, note that

$$\frac{\delta}{\delta x^{\dot{\alpha}\alpha}} f \left(\begin{matrix} |\lambda\rangle \\ |\mu\rangle \end{matrix} \right) \Big|_{|\mu\rangle=x|\lambda\rangle} = |\lambda\rangle_{\alpha} \frac{\partial}{\partial (x|\lambda)^{\dot{\alpha}}} f \left(\begin{matrix} |\lambda\rangle \\ x|\lambda\rangle \end{matrix} \right) \quad (2.10.16)$$

Acting again on this formula with $\frac{\delta}{\delta x_{\alpha\dot{\alpha}}}$ to produce $\square f$ contracts together $\langle \lambda |^{\alpha}$ with $|\lambda\rangle_{\alpha}$, giving $\square f = 0$ for all functions $f \left(\begin{matrix} |\lambda\rangle \\ |\mu\rangle \end{matrix} \right)$.

In general a function on twistor space which is homogeneous with degree $2s' - 2$ such

that $f(\alpha\mathcal{Z}) = \alpha^{2s'-2}f(\mathcal{Z})$ will solve the linearized equations of motion for a spin s' field on space-time, and ϕ the explicit mapping from homogeneous functions on twistor space to solutions to massless linearized field equations on Minkowski space-time is known as the Penrose transform. For spin $s' > 0$, each homogenous function on twistor space corresponds to two functions on space-time, one for positive and one for negative helicity, and the Penrose transform in this case is explained in detail in [109]. Spin 0 fields correspond to twistor functions such that $f(\alpha\mathcal{Z}) = \alpha^{-2}f(\mathcal{Z})$, and in this case there is no concept of helicity and hence only one function on space-time. The Penrose transform is given in this case by

$$\phi(x) = \int \langle \lambda d\lambda \rangle f \left(\begin{array}{c} |\lambda\rangle \\ x|\lambda\rangle \end{array} \right). \quad (2.10.17)$$

Note that the scaling weight of f cancels with that of $\langle \lambda d\lambda \rangle$ so that the integral gives a well defined function on Minkowski space-time.

To study the physics of scattering amplitudes in twistor space it is necessary to know which functions on twistor space are momentum eigenstates and hence correspond to plane waves in space-time. The form of a plane wave in twistor space corresponding to a spin s' particle is given by

$$V_i^{(s')}(\mathcal{Z}) = \int \frac{dt}{t^{2s'-1}} \delta^2(|i\rangle - t|\lambda\rangle) e^{it[\mu i]}. \quad (2.10.18)$$

It can be seen that this function satisfies the necessary homogeneity condition $f(\alpha\mathcal{Z}) = \alpha^{2s'-2}f(\mathcal{Z})$ by changing variables to $t' = \alpha t$ in the integral. To see that this function corresponds to a plane wave in space-time for spin $s' = 0$, take the Penrose transform of equation 2.10.18 to give

$$\int \langle \lambda d\lambda \rangle V_i^{(0)} \left(\begin{array}{c} |\lambda\rangle \\ x|\lambda\rangle \end{array} \right) = \int \langle \lambda d\lambda \rangle \int t dt \delta^2(|i\rangle - t|\lambda\rangle) e^{it\langle \lambda|x|i \rangle} \quad (2.10.19)$$

To solve the integrals, expand $|\lambda\rangle$ in a basis $(|i\rangle, |j\rangle)$ so that $|\lambda\rangle = \alpha|i\rangle + \beta|j\rangle$. Then fix $\alpha = 1$ using the projective scale on the twistor to give $\langle \lambda d\lambda \rangle = \langle ij \rangle d\beta$.

Expanding the delta function in this basis gives that

$$\int \langle \lambda d\lambda \rangle V_i^{(0)} \left(\begin{array}{c} |\lambda\rangle \\ x|\lambda\rangle \end{array} \right) = \langle ij \rangle^2 \int d\beta dt t \delta(\beta t \langle ij \rangle) \delta((t-1) \langle ij \rangle) e^{it(\langle i|+\beta\langle j|)x|i\rangle} \quad (2.10.20)$$

The delta functions are then solved by $\beta = 0$ and $t = 1$, and all of the factors $\langle ij \rangle$ cancel to give that

$$\int \langle \lambda d\lambda \rangle V_i^{(0)} \left(\begin{array}{c} |\lambda\rangle \\ x|\lambda\rangle \end{array} \right) = e^{ik_i \cdot x}, \quad (2.10.21)$$

a plane wave in Minkowski space-time with momentum k_i , and hence a momentum eigenstate.

Twistor space has a natural supersymmetric extension with \mathcal{N} supersymmetries known as twistor superspace, which has geometry analogous that of non-supersymmetric twistor space and which I denote and I denote as $\text{PT}^{\mathcal{N}} = \mathbb{CP}^{3|\mathcal{N}}$. A null ray in super Minkowski spacetime is written as

$$R^{\mathcal{N}}(x, |\theta\rangle, p, |q\rangle) = \{(x + \alpha p, |\theta\rangle + \alpha |q\rangle) \mid \alpha \in \mathbb{R}\} \quad (2.10.22)$$

and a supertwistor $\mathcal{Z} \in \text{PT}^{\mathcal{N}}$ is written as

$$\mathcal{Z} = \left(\begin{array}{c} |\lambda\rangle \\ |\mu\rangle \\ \chi \end{array} \right) \quad (2.10.23)$$

where $|\lambda\rangle$ and $|\mu\rangle$ are as before, and $\chi = (\chi^I)$ are Grassmann odd variables transforming in the fundamental representation of the R symmetry group $\text{SU}(\mathcal{N})$.

In twistor superspace there is an incidence relation for both the $|\mu\rangle$ and the χ part of the twistor, so that

$$|\mu\rangle = x |\lambda\rangle, \chi = \langle \theta \lambda \rangle, \quad (2.10.24)$$

and using these relations calculations in twistor superspace follow roughly analogously to those in twistor space.

Setting this twistor incident to the null ray $R^{\mathcal{N}}(x, |\theta\rangle, k_i, |q_i\rangle)$, where $k_i = |i\rangle \langle i|$ and $|q_i\rangle = |i\rangle \eta_i$ gives that

$$\mathcal{Z} = \left(\begin{array}{c} |i\rangle \\ x|i\rangle \\ \langle \theta i \rangle \end{array} \right), \quad (2.10.25)$$

which is invariant under both $x \mapsto x + \alpha |i] \langle i$ and $|\theta\rangle \mapsto |\theta\rangle + \alpha |i\rangle \eta_i$.

It is standard in scattering amplitudes to work in complex Minkowski space $\mathcal{M}^4(\mathbb{C})$, and the corresponding twistor space in this case is referred to as ambitwistor space. Ambitwistor space exists in general dimensions starting from equations 2.10.1 and 2.10.2, and extending all real variables to the complex domain. In this work I will focus on ambitwistor space $\mathbb{P}\mathbb{A}$ in four dimensions, which corresponds to allowing the twistor \mathcal{Z} to become independent of its dual $\tilde{\mathcal{Z}}$. Both the twistor \mathcal{Z} and its ambitwistor conjugate $\tilde{\mathcal{Z}}$ are then treated equally, hence the name ‘ambi’, coming from the Greek for ‘both’.

To form a point in ambitwistor space starting with $\mathcal{Z}, \tilde{\mathcal{Z}} \in \mathbb{C}^4$ it is then necessary to quotient out by the $GL(1)$ scaling

$$\mathcal{Z} \mapsto \alpha \mathcal{Z}, \quad \tilde{\mathcal{Z}} \mapsto \alpha^{-1} \tilde{\mathcal{Z}}, \quad \alpha \in GL(1), \quad (2.10.26)$$

and enforce that

$$\tilde{\mathcal{Z}} \cdot \mathcal{Z} = 0. \quad (2.10.27)$$

Any pair $(\mathcal{Z}, \tilde{\mathcal{Z}})$ satisfying these relations is a point in $\mathbb{P}\mathbb{A}$, which can be expanded in terms of two component spinors as

$$\tilde{\mathcal{Z}} = \left(\langle \tilde{\mu} | \quad [\tilde{\lambda} | \right), \quad \mathcal{Z} = \begin{pmatrix} |\lambda\rangle \\ |\mu\rangle \end{pmatrix}. \quad (2.10.28)$$

The ambitwistor pair corresponding to external state i can be written

$$\tilde{\mathcal{Z}}_i = \left(\langle \tilde{\mu}_i | \quad [i | \right), \quad \mathcal{Z}_i = \begin{pmatrix} |i\rangle \\ |\mu_i\rangle \end{pmatrix}, \quad (2.10.29)$$

and it is natural to define an $SU(2,2)$ invariant square 4-bracket for the dual twistors in ambitwistor space, as well as a corresponding two bracket using the infinity twistor;

$$[ijkl] := \epsilon^{ABCD} \mathcal{W}_{iA} \mathcal{W}_{jB} \mathcal{W}_{kC} \mathcal{W}_{lD} \quad [\mathcal{W}_i \mathcal{W}_j] := [ij\mathcal{I}] = [ij]. \quad (2.10.30)$$

Twistor superspace has a natural extension to ambitwistors, and in this case mo-

momentum eigenstates in supersymmetric ambitwistor space can be written as

$$\tilde{V}_i^{(s)}(\tilde{\mathcal{Z}}) = \int \frac{dt}{t^{2s-1}} \delta^{2|\mathcal{N}}(|i\rangle - t|\tilde{\lambda}\rangle) e^{it\langle\tilde{\mu}i\rangle} \quad (2.10.31)$$

$$V_i^{(s)}(\mathcal{Z}) = \int \frac{dt}{t^{2s-1}} \delta^2(|i\rangle - t|\lambda\rangle) e^{it([\mu i] + \tilde{\chi}\cdot\eta_i)}, \quad (2.10.32)$$

where $\tilde{V}_i^{(s)}(\tilde{\mathcal{Z}})$ corresponds to the negative helicity superfield and $V_i^{(s)}(\mathcal{Z})$ corresponds to the positive helicity. The supersymmetry is encoded differently in the two functions because ambitwistor space is non-chiral and treats the two helicities equally, but the superspace used is chiral. $\tilde{V}_i^{(s)}(\tilde{\mathcal{Z}})$ can be obtained by complex conjugating $V_i^{(s)}(\mathcal{Z})$ and Grassmann Fourier transforming back from $\tilde{\eta}$ superspace back to η superspace.

2.11 4D Ambitwistor String Theory

4D ambitwistor string theory is a worldsheet theory whose target space is ambitwistor space, combining computational techniques from twistor theory as explained in Section 2.10 and string theory [110, 111] to calculate scattering amplitudes in quantum field theory as integrals supported on the 4D scattering equations introduced in Section 2.8. In essence 4D ambitwistor string theory is a modification of the original twistor string theory [12, 13] which expresses scattering amplitudes as integrals over the moduli space of curves in twistor space, and can also be considered as the specialisation to four dimensional spacetime of a general dimensional ambitwistor string model [15] which calculates scattering amplitudes in the CHY formalism reviewed in Section 2.7 from the worldsheet.

Quantum states in the the target space quantum field theory correspond to vertex operators in the ambitwistor string model, and scattering amplitudes are calculated as the correlation functions of vertex operators. Finding the vertex operators requires the worldsheet theory to be quantized, which can be done in the BRST formalism [112, 80], where a Grassmann-odd BRST operator Q is introduced which generates transformations in the space of all possible fixings of the gauge symmetries of the theory. Each gauge symmetry is then assigned a corresponding $b - c$ or $\beta - \gamma$ ghost

system [111] with opposite Grassmann parity to the symmetry, and Q is constructed from the generators of the gauge symmetries of the theory and their associated ghost fields [111]. When all of the gauge symmetries of the theory are anomaly-free at the quantum level the BRST operator is nilpotent so that $Q^2 = 0$, and when this condition holds the string theory is said to be critical. Importantly $Q^2 = 0$ implies that worldsheet conformal transformations are anomaly free, which is necessary for computing loop amplitudes in the theory. As Q is nilpotent it has an associated cohomology in the space of operators of the theory, and the set of vertex operators $\{V\}$ is equivalent to the cohomology of Q . Then all vertex operators of the theory must satisfy $QV = 0$, and are defined up to the identification $V \sim V + QW$ where W is any other operator.

The perturbative loop expansion of the S -matrix in the quantum field theory corresponds to the calculation of this correlation function on worldsheets of increasing genus, with zeroth order calculations on the Riemann sphere and first order calculations on the torus. It is possible to calculate tree-level amplitudes using string theories with anomalous conformal symmetries, but for the theory to be well-defined on the torus it is necessary for the worldsheet conformal symmetry to be anomaly free. In this section I consider two 4D ambitwistor string theories; the first contains both super Yang-Mills and conformal supergravity states and can be made anomaly free at the quantum level due to the existence of a current algebra in the Lagrangian. Loop amplitudes calculated will contain Yang-Mills and conformal gravity states, and there is currently no known way to decouple the states in the loop calculation. The second contains Einstein supergravity states, where there is no known way to cancel the conformal anomaly and define loop amplitudes in the theory. The supersymmetry transformations for a given \mathcal{N} are also anomalous at the quantum level unless $\mathcal{N} = 4$ in the Yang-Mills and conformal supergravity case or $\mathcal{N} = 8$ for the Einstein gravity case.

The worldsheet Lagrangian for ambitwistor string theory in general dimensions can be obtained from the standard string theory action by taking an infinite tension

limit $\alpha' \rightarrow 0$ which is chiral on the worldsheet, in that it treats the two worldsheet directions inhomogeneously. The spectra of ambitwistor string theories contain only states corresponding to a given quantum field theory, which can be understood as the higher string excitations having been damped out by the increasing tension. It is also possible to take a zero tension limit which can be related to ambitwistor string theory in a different way [113, 114, 115].

The Lagrangian is

$$\mathcal{L} = P(\bar{\partial} + e\partial)X - \frac{\alpha}{2}P^2. \quad (2.11.1)$$

I use a complex Euclidean worldsheet in this work which I denote as $s \in \mathbb{C}$ with conjugate \bar{s} , and I denote worldsheet derivatives as $\partial := \frac{\partial}{\partial s}$ and $\bar{\partial} := \frac{\partial}{\partial \bar{s}}$. Then X and P are both worldsheet fields depending on s and \bar{s} , and the theory has two gauge symmetries. The gauge field for the first symmetry is e , which parametrises worldsheet diffeomorphisms in \bar{s} and is the remaining degree of freedom left from the worldsheet metric after taking the chiral infinite tension limit. Note that the Lagrangian is also trivially diffeomorphism invariant in s because it has no kinetic term in ∂ . The second gauge symmetry is a $GL(1)$ with gauge field α , and identifies $X \sim X + \alpha P$. Hence we find that the target space for this theory is the space of null geodesics in Minkowski spacetime in d dimensions, as in equation (2.10.2).

Now consider specialising ambitwistor string theory to four dimensions of spacetime. The worldsheet Lagrangian for 4D ambitwistor string theory [26, 27] can be calculated from the general d ambitwistor Lagrangian in (2.11.1) by specialising to 4D ambitwistor space as explained in Section 2.10. This procedure gives the Lagrangian as

$$\mathcal{L} = \tilde{\mathcal{Z}} \cdot (\bar{\partial} + e\partial)\mathcal{Z} + u \tilde{\mathcal{Z}} \cdot \mathcal{Z}, \quad (2.11.2)$$

so that \mathcal{Z} and $\tilde{\mathcal{Z}}$ are mappings from the worldsheet to $\mathbb{C}^{4|\mathcal{N}}$, both depending on s and \bar{s} . This Lagrangian forms the basis for two 4D ambitwistor string theories; the first contains super Yang-Mills and conformal supergravity states and requires the introduction of a current algebra, and the second contains Einstein supergravity

states with Lagrangian given in equation (2.11.14).

The Lagrangian in equation (2.11.2) has two gauge symmetries. The first has gauge field e describing worldsheet diffeomorphisms as in the general d ambitwistor string, and the second is the $GL(1)$ gauge field u which generates the projective scaling of ambitwistor space in equation (2.10.26). The equations of motion for u enforce that $\tilde{\mathcal{Z}} \cdot \mathcal{Z} = 0$, and together with the projective scaling this reduces the target space of the theory down from $\mathbb{C}^{4|\mathcal{N}} \times \mathbb{C}^{4|\mathcal{N}}$ to 4D ambitwistor space $\mathbb{P}\mathbb{A}$. The equations of motion for the twistors enforce that $\bar{\partial}\mathcal{Z} = \bar{\partial}\tilde{\mathcal{Z}} = 0$, and so the worldsheet fields are holomorphic functions of s .

This is the same action as in twistor string theory [12, 13], and the new feature of 4D ambitwistor strings compared to twistor string theory are that the worldsheet fields \mathcal{Z} and $\tilde{\mathcal{Z}}$ are now on equal footing. In the original twistor string where \mathcal{Z} has weight $(1, 0)$ and $\tilde{\mathcal{Z}}$ has weight $(0, 0)$, and $\tilde{\mathcal{Z}}$ is treated as an auxiliary field which is integrated out directly in the path integral. In 4D ambitwistor string theory \mathcal{Z} and $\tilde{\mathcal{Z}}$ both have conformal weight $(\frac{1}{2}, 0)$, and the two μ fields will be treated as auxiliary fields in the path integral and integrated out directly. This choice of conformal weights puts negative and positive spin external states on equal footing, and based on this there are two types of vertex operators for particles with spin s' , which are based on the momentum eigenstates in ambitwistor space from equation (2.10.31). $\tilde{\mathcal{V}}_l(s)$ is calculated from $\tilde{V}_l^{(s')}(\tilde{\mathcal{Z}}(s))$ and corresponds to a negative helicity superfield, and $\mathcal{V}_r(s)$ is calculated from $V_r^{(s')}(\mathcal{Z}(s))$ and corresponds to a positive helicity superfield.

The twistor fields from the Lagrangian in equation 2.11.2 can be split into components as

$$\mathcal{Z}(s) = \begin{pmatrix} |\lambda(s)\rangle \\ |\mu(s)] \\ \chi(s) \end{pmatrix}, \quad \tilde{\mathcal{Z}}(s) = ([\tilde{\lambda}(s)| \langle \tilde{\mu}(s)| \tilde{\chi}(s)),$$

where χ and $\tilde{\chi}$ transform in the fundamental representation of the R-symmetry group $SU(\mathcal{N})$. In terms of the spinor components of \mathcal{Z} and $\tilde{\mathcal{Z}}$, the 4D ambitwistor Lagrangian can then be written as

$$\mathcal{L} = \langle \tilde{\mu} | \bar{\partial} | \lambda \rangle - [\mu | \bar{\partial} | \tilde{\lambda}] + \chi \cdot \bar{\partial} \tilde{\chi}, \quad (2.11.3)$$

after subtracting the total derivative $\bar{\partial} [\mu \tilde{\lambda}]$ and gauge fixing $e = u = 0$.

The vertex operators for $\mathcal{N} = 4$ super Yang-Mills with supermomentum parametrised by $|i\rangle, |\tilde{i}\rangle$ and η_i are then given by

$$\begin{aligned} \tilde{\mathcal{V}}_l(s) &= \tilde{V}_l^{(1)}(\tilde{\mathcal{Z}}(s))J(s) = \int \frac{dt}{t} \delta^{2|4} (|l\rangle - t |\tilde{\lambda}(s)\rangle) e^{it\langle \tilde{\mu}(s)l \rangle} J(s) \\ \mathcal{V}_r(s) &= V_r^{(1)}(\mathcal{Z}(s))J(s) = \int \frac{dt}{t} \delta^2 (|r\rangle - t |\lambda(s)\rangle) e^{it([\mu(s)r] + \chi(s) \cdot \eta_r)} J(s) \end{aligned} \quad (2.11.4)$$

where J is a Kac-Moody current, described in the context of ambitwistor string theory in [52]. I show that these vertex operators are in the cohomology of the BRST operator in Section 7.7, and the cohomology also contains vertex operators corresponding to the conformal supergravity states which I discuss in Chapter 7.

The superamplitude is then written as a correlation function of these vertex operators, using \mathcal{V} for negative helicity super fields in the left set and \mathcal{V} for positive helicity super fields in the right set

$$\mathcal{A}_{L,n,\mathcal{N}}^{(0)} = \int \frac{d^n s}{SL(2)} \left\langle \prod_{l \in L} \tilde{\mathcal{V}}_l(s_l) \prod_{r \in R} \mathcal{V}_r(s_r) \right\rangle. \quad (2.11.5)$$

Now consider this correlation function for Yang-Mills theory with $\mathcal{N} = 0$ as an example to see how the 4D scattering equation representation for $\mathcal{A}_{L,n}^{(0)}$ arises from the worldsheet. The delta function in each vertex operator will contribute a scattering equation for each external particle in the amplitude, and positive and negative helicity particles have different vertex operators producing left and right set scattering equations. Inserting the expressions for the vertex operators gives

$$\begin{aligned} \mathcal{A}_{L,n}^{(0)} &= \int \frac{\prod_{i \in \mathcal{N}} \frac{ds_i dt_i}{t_i}}{GL(2)} \left\langle \prod_{l \in L} \delta^2 (|l\rangle - t_l |\tilde{\lambda}(s_l)\rangle) e^{it_l \langle \mu(s_l)l \rangle} \times \right. \\ &\quad \left. \prod_{r \in R} \delta^2 (|r\rangle - t_r |\lambda(s_r)\rangle) e^{it_r [\mu(s_r)r]} \prod_{i \in \mathcal{N}} J(s_i) \right\rangle. \end{aligned} \quad (2.11.6)$$

This correlation function is then simplified first by combining the s and t variables into a worldsheet vector $\sigma \in \mathbb{C}^2$ for each particle where $\sigma = \frac{1}{t} \begin{pmatrix} 1 \\ s \end{pmatrix}$, and hence the variables for the 4D scattering equations are two component vectors as discussed in Section 2.8. The worldsheet $\text{SL}(2)$ invariance and the $\text{GL}(1)$ gauge symmetry have been combined together in equation (2.11.6), and the resulting $\text{GL}(2)$ acts as a matrix transformation on the σ variables with inhomogenous transformation law for the left and right sets as described in Section 3.1.

The measure changes as $\frac{ds_i dt_i}{t_i} = t_i^2 d^2 \sigma_i$ under this change of variables, and differences of the worldsheet s variables can be written as $\frac{1}{s_i - s_j} = \frac{(ij)}{t_i t_j}$, where $(ij) = \sigma_i^1 \sigma_j^2 - \sigma_i^2 \sigma_j^1$ are the minors of the 2×2 matrix σ . The current algebra for the J fields decouples from the twistor fields and hence its correlation function can be calculated separately. In general the current algebra correlator has multitrace terms which couple the Yang-Mills states to the conformal supergravity states [20], but taking only the highest order terms in N_c neglects these multitrace terms and produces scattering in Yang-Mills theory. In this case, the correlator evaluates to $\langle \prod_{i \in \mathcal{N}} J(s_i) \rangle = \prod_{i \in \mathcal{N}} \frac{1}{s_i - s_j}$.

The correlation function then simplifies to

$$\mathcal{A}_{L,n}^{(0)} = \int \frac{d^2 \sigma}{\text{GL}(2)} \prod_{i \in \mathcal{N}} \frac{1}{(i \ i+1)} \left\langle \prod_{l \in L} \delta^2(|l\rangle - t_l |\tilde{\lambda}(s_l)\rangle) \times \prod_{r \in R} \delta^2(|r\rangle - t_r |\lambda(s_r)\rangle) e^{i(\sum_{l \in L} \langle \mu(s_l) l \rangle + \sum_{r \in R} [\mu(s_r) r])} \right\rangle.$$

The next step to calculate the correlation function is to write it as a path integral over the worldsheet fields, as

$$\mathcal{A}_{L,n}^{(0)} = \int \frac{d^2 \sigma}{\text{GL}(2)} \prod_{i \in \mathcal{N}} \frac{1}{(i \ i+1)} \int D|\lambda\rangle D|\tilde{\lambda}\rangle D|\mu\rangle D|\tilde{\mu}\rangle e^{i \int d^2 s (\mathcal{L} - \sum_l \delta^2(s-s_l) t_l \langle \tilde{\mu}(s_l) l \rangle - \sum_r \delta^2(s-s_r) t_r [\mu(s_r) r])} \times \prod_{l \in L} \delta^2(|l\rangle - t_l |\tilde{\lambda}(s_l)\rangle) \prod_{r \in R} \delta^2(|r\rangle - t_r |\lambda(s_r)\rangle), \quad (2.11.7)$$

where the exponentials in $|\mu\rangle$ and $|\tilde{\mu}\rangle$ variables from the vertex operators have been combined into the action as an integral over Dirac delta functions.

The calculation differs at this point from a standard string scattering calculation due to the fact that $|\mu\rangle$ and $|\mu\rangle$ appear only in the exponentials and hence can be integrated out directly, which arises from the point of view of the worldsheet due to the fact that the Lagrangian only has kinetic terms in $\bar{\partial}$ and not ∂ . From the point of view of the twistor geometry this can be understood due to the fact that the twistors in each vertex operator are related only to a null vector $|i\rangle\langle i|$, and are not incident with any spacetime position.

The integration in the $|\mu\rangle$ field gives a functional Dirac delta for the $|\tilde{\lambda}\rangle$ field;

$$\Delta_{|\tilde{\lambda}\rangle\mu} := \int D|\mu\rangle e^{i \int d^2s (|\mu\rangle\bar{\partial}|\tilde{\lambda}\rangle - \sum_{l \in L} t_l |\mu\rangle \delta^2(s - s_l))} = \delta \left(\bar{\partial}|\tilde{\lambda}\rangle - \sum_{l \in L} t_l |l\rangle \delta^2(s - s_l) \right). \quad (2.11.8)$$

The argument of the delta function is the equation of motion for the $|\tilde{\lambda}\rangle$ field coming from the Lagrangian with source terms added coming from each vertex operator. The equation of motion can be solved for this delta function to give

$$\Delta_{|\tilde{\lambda}\rangle} = \delta \left(|\tilde{\lambda}(s)\rangle - \frac{1}{t} \sum_{r \in R} \frac{|r\rangle}{(s r)} \right), \quad (2.11.9)$$

where $\sigma_s := \frac{1}{t} \binom{1}{s}$, using that $\bar{\partial}f(s, \bar{s}) = \delta(s - a)$ implies that $f(s, \bar{s}) = f(s) = \frac{1}{s-a}$.

The integration in the $|\tilde{\mu}\rangle$ field is solved similarly to give a functional Dirac delta for the $|\lambda\rangle$ field, and equation of motion for $|\lambda\rangle$ is solved in the same way resulting in the following delta function

$$\Delta_{|\lambda\rangle} = \delta \left(|\lambda(s)\rangle - \frac{1}{t} \sum_{l \in L} \frac{|l\rangle}{(s l)} \right), \quad (2.11.10)$$

The path integrals in $D|\lambda\rangle$ and $D|\tilde{\lambda}\rangle$ are then localised onto these Dirac delta functions and can be integrated out directly. This substitutes the solutions to the equations of motion for $|\lambda\rangle$ and $|\tilde{\lambda}\rangle$ into the delta functions coming from the vertex operators for each external state, giving rise to the 4D scattering equations

$$|l\rangle = \sum_{r \in R} \frac{|r\rangle}{(lr)}, \quad l \in L \quad |r\rangle = \sum_{l \in L} \frac{|l\rangle}{(rl)} \quad r \in R \quad (2.11.11)$$

With all of the path integrals solved, the full tree-level S -matrix for Yang-Mills theory is then obtained from the correlator of the vertex operators as an integral supported on these equations as

$$\mathcal{A}_{n,L}^{(0)} = \int \frac{d^{2 \times n} \sigma}{GL(2)} \frac{1}{\prod_{i \in \mathcal{N}} (i i+1)} \delta^{2 \times n}(\text{SE}_{n,L}). \quad (2.11.12)$$

The cyclic structure in the worldsheet minors can then be seen to arise from the current algebra correlator, and generalises the Parke-Taylor amplitude to all MHV sectors.

For Yang-Mills with \mathcal{N} supersymmetries the calculation follows similar steps, with the addition of the fermionic fields $\chi(s)$ and $\tilde{\chi}(s)$. The $\tilde{\chi}(s)$ field is integrated out in the path integral similarly to the bosonic $|\tilde{\mu}\rangle$ and $|\mu\rangle$ fields, producing a functional delta function localising the $\chi(s)$ field onto the following solution to its equations of motion,

$$t\chi(s) = \sum_{r \in R} \frac{\eta_r}{(sr)}.$$

This relationship gives rise to the fermionic scattering equations in equation (2.8.3), and produces the following supersymmetry covariant expression for the complete tree-level S -matrix

$$\mathcal{A}_{n,L,\mathcal{N}}^{(0)} = \int \frac{d^{2 \times n} \sigma}{GL(2)} \frac{1}{\prod_{i \in \mathcal{N}} (i i+1)} \delta^{2 \times n|\mathcal{N} \times |L|}(\text{SE}_{n,L}). \quad (2.11.13)$$

For Einstein supergravity, the worldsheet theory has \mathcal{Z} and $\tilde{\mathcal{Z}} \in \mathbb{C}^{4|\mathcal{N}}$ as in Yang-Mills, as well as the following additional fields,

$$\mathcal{R} = \begin{pmatrix} |\rho\rangle \\ |\nu\rangle \\ \omega \end{pmatrix} \quad \tilde{\mathcal{R}} = ([\tilde{\rho}], \langle \tilde{\nu} |, \tilde{\omega}),$$

which have the opposite Grassmann degree to \mathcal{Z} , $\tilde{\mathcal{Z}}$, so that for example $\begin{pmatrix} \omega \\ |\rho\rangle \\ |\nu\rangle \end{pmatrix} \in \mathbb{C}^{\mathcal{N}|4}$.

The worldsheet Lagrangian [21] is given in terms of these fields as

$$\mathcal{L} = \tilde{\mathcal{Z}} \cdot \bar{\partial} \mathcal{Z} + \tilde{\rho} \cdot \bar{\partial} \rho + u^B K_B, \quad (2.11.14)$$

where K_B is a vector containing 8 generators for different $GL(1)$ gauge symmetries, and u^B is a vector of corresponding gauge fields. The index B is for notational simplicity only and carries no physical significance. The generators of the 8 gauge symmetries are given by

$$K_B = \left(\tilde{\mathcal{Z}} \cdot \mathcal{Z}, \tilde{\mathcal{R}} \cdot \mathcal{R}, \tilde{\mathcal{Z}} \cdot \mathcal{R}, \tilde{\mathcal{R}} \cdot \mathcal{Z}, \langle \mathcal{Z} \mathcal{R} \rangle, [\tilde{\mathcal{Z}} \tilde{\mathcal{R}}], \langle \mathcal{R} \mathcal{R} \rangle, [\tilde{\mathcal{R}} \tilde{\mathcal{R}}] \right). \quad (2.11.15)$$

The first four symmetries enforce that $\mathcal{Z}, \tilde{\mathcal{Z}}, \mathcal{R}$, and $\tilde{\mathcal{R}}$ form all possible ambitwistor pairs, $\langle \mathcal{Z} \mathcal{R} \rangle$ enforces that $|\rho\rangle \propto |\lambda\rangle$ and similarly for $[\tilde{\mathcal{Z}} \tilde{\mathcal{R}}]$, and $\langle \mathcal{R} \mathcal{R} \rangle$ and $[\tilde{\mathcal{R}} \tilde{\mathcal{R}}]$ are consistency conditions on the spinor two brackets, ensuring for that $\langle \rho \rho \rangle = 0$ as is always the case for bosonic spinors.

The integrated vertex operators are calculated from the plane moves in twistor space as

$$\begin{aligned} \tilde{\mathcal{V}}_l(s) &= \left(\left\langle \mathcal{Z} \frac{\partial}{\partial \tilde{\mathcal{Z}}} \right\rangle + \left\langle \mathcal{R}, \frac{\partial}{\partial \tilde{\mathcal{Z}}} \right\rangle \tilde{\mathcal{R}} \cdot \frac{\partial}{\partial \tilde{\mathcal{Z}}} \right) \tilde{V}_l^{(2)}(\tilde{\mathcal{Z}}(s)) \\ \mathcal{V}_r(s) &= \left(\left[\tilde{\mathcal{Z}} \frac{\partial}{\partial \mathcal{Z}} \right] + \left[\tilde{\mathcal{R}} \frac{\partial}{\partial \mathcal{Z}} \right] \mathcal{R} \cdot \frac{\partial}{\partial \mathcal{Z}} \right) V_r^{(2)}(\mathcal{Z}(s)), \end{aligned} \quad (2.11.16)$$

where I define the square and angle two brackets in terms of the infinity twistor in equation (2.10.30), and $\tilde{V}_r^{(2)}$ and $V_l^{(2)}$ are the momentum eigenstates in ambitwistor space for spin 2 particles from equation (2.10.31). These formulae can be expressed in terms of the spinor components of $\mathcal{Z}, \tilde{\mathcal{Z}}, \mathcal{R}$, and $\tilde{\mathcal{R}}$, and importantly all derivatives of delta functions with respect to spinor variables cancel out after calculating the two brackets with the infinity twistor and the fermionic correlation function in the ρ variables in the path integral. The BRST cohomology also contains unintegrated vertex operators constructed from ghosts associated with the fermionic currents in (2.11.15), which are necessary to give the \det' structure where one row is removed from the Hodges matrices in the worldsheet integral.

This procedure calculates the following supersymmetry covariant expression for

the tree-level S -matrix of Einstein supergravity with \mathcal{N} supersymmetries as

$$\mathcal{M}_{n,L,\mathcal{N}}^{(0)} = \int \frac{d^{2 \times n} \sigma}{GL(2)} \det' \mathcal{H} \det' \tilde{\mathcal{H}} \delta^{2 \times n |\mathcal{N} \times |L|} (SE_{n,L}). \quad (2.11.17)$$

Chapter 3

Analytical Properties of the 4D Scattering Equations

In this chapter I provide a detailed analysis of the 4D scattering equations based on my results from [1]. I cover all aspects necessary for the numerical methods I describe in Chapter 4, building up to my Mathematica implementation `treeamps4dJAF`, which I cover in Section 4.5. In Section 3.1 I give an overview of how to calculate amplitudes from the 4D scattering equation integral, and I then give a detailed proof of various properties of the 4D scattering equations in the following sections. In Section 3.2 I explain how to recover the general d scattering equations for $d = 4$ from the 4D specific equations, and in Section 3.3 I discuss the symmetries of the equations in detail. In Section 3.4 I describe how to 4 of equations imply momentum conservation, in Section 3.5 I discuss how the equations transform under permutations of particle labels, and in finally Section 3.6 I calculate the Jacobian for the equation for different cases.

3.1 Calculating Amplitudes with the 4D Scattering Equations

In this section I describe the analytical results necessary for solving the 4D scattering equations to calculate amplitudes given an integrand for a certain theory. These techniques will then be used explicitly to find amplitudes numerically and analytically in the package `treeamps4dJAF`, which I introduce in Chapter 4. The equations are reviewed in Section 2.8, and are

$$|l\rangle = \sum_{r \in R} \frac{|r\rangle}{(lr)}, \quad l \in L \quad |r\rangle = \sum_{l \in L} \frac{|l\rangle}{(rl)} \quad r \in R. \quad (3.1.1)$$

Scattering amplitudes in this framework can then be expressed as integrals over delta functions enforcing the equations

$$\mathcal{A}_{n,L} = \int \frac{d^{2 \times n} \sigma}{GL(2)} \delta^{2 \times n}(\text{SE}_{n,L}) f^{\mathcal{N}}(\sigma, |i\rangle, |i\rangle),$$

where $f^{\mathcal{N}}$ is a theory-dependent integrand with \mathcal{N} supersymmetries.

As shown in equation (2.8.2), at n points there are $2n$ 4D scattering equations depending on $2n$ worldsheet σ variables. There is a $GL(2)$ symmetry on the worldsheet which acts inhomogeneously on the left and right set of worldsheet coordinates for $G \in GL(2)$ as

$$\sigma_l \mapsto G \sigma_l, \quad l \in L \quad \sigma_r \mapsto \frac{G}{\det G} \sigma_r, \quad r \in R. \quad (3.1.2)$$

Under this $GL(2)$ translation, any minor of the form (lr) remains invariant, and hence the scattering equations are invariant. Fixing this gauge symmetry leaves $2n - 4$ remaining degrees of freedom. Generally in this work I will restrict to gauge transformations specified by two particle labels i, j which fix $\sigma_i = \begin{pmatrix} 1 \\ 0 \end{pmatrix}$ and $\sigma_j = \begin{pmatrix} 0 \\ 1 \end{pmatrix}$, and refer to this operation as ‘gauge-fixing particles i and j ’. As the $GL(2)$ transformations act inhomogeneously on the left and right set, only the two left or the two right particles can be fixed in this way. The details of gauge-fixing and the

symmetries of the equations are explained in Section 3.3.

The system now appears to be over specified and four equations must be removed to match the $2n - 4$ variables. Two spinor equations i and j either from the left set or from the right set can be reduced to a momentum conserving delta function on support of the other scattering equations, as proved in Section 3.4. I refer to this operations as ‘deleting particles i and j ’, and the remaining equations are a well-specified set of $2n - 4$ equations in $2n - 4$ variables.

The number of integrations in equation (3.1) is the same as the number of delta functions, and hence the integrations are an instruction to sum over all of the solutions of the scattering equations. Deleting equations l and $l' \in L$, the Jacobian of the remaining equations can be calculated to solve the delta function integrals as follows

$$\mathcal{A}_{n,L} = \int \frac{d^{2 \times n} \sigma}{GL(2)} \delta^{2 \times n}(\text{SE}_{n,L}) f(\sigma) = \delta^4(P) \sum_{\sigma_{\text{sol}} \in \text{Solutions}} \frac{f(\sigma_{\text{sol}})}{\langle ll' \rangle^{-2} \det(J_L^{n, ll'}(\sigma_{\text{sol}}))}. \quad (3.1.3)$$

where J_L^n is the Jacobian of the scattering equations with respect to the sigma variables, and the superscript l, l' refers to removing four rows and columns corresponding to these two particle labels from the matrix before taking the determinant. The factor $\langle ll' \rangle^2$ comes from the Jacobian for deleting particles l and l' to give $\delta^4(\rho)$. Details of the Jacobian to the scattering equations are explained in Section 3.6. It is now a well-formulated problem to solve the scattering equations and sum a theory dependent integrand f over the full set of solutions to produce an amplitude.

Calculating MHV amplitudes is generally more simple than calculating N^{k-2} MHV amplitudes, and this simplicity is reflected in the structure of the 4D scattering equations. Analytical solutions to the 4D scattering equations are not known for general MHV degree, but can be constructed in the MHV sector. First consider the case where the left set is $L = \{1, 2\}$. Then the MHV equations become

$$\delta^{2 \times n}(\text{SE}_{n,\{1,2\}}) = \delta^2 \left(|1\rangle - \sum_{r \in R} \frac{|r\rangle}{\langle 1r \rangle} \right) \delta^2 \left(|2\rangle - \sum_{r \in R} \frac{|r\rangle}{\langle 2r \rangle} \right) \prod_{r \in R} \delta^2 \left(|r\rangle - \frac{|1\rangle}{\langle 1r \rangle} + \frac{|2\rangle}{\langle 2r \rangle} \right) \quad (3.1.4)$$

The most obvious choice of equations to delete in this case are the two left set equations, which become the overall momentum conservation delta function, along with a Jacobian factor of $\langle 12 \rangle^2$. Similarly, particles 1 and 2 are gauge-fixed to the identity in the Grassmannian, and each delta function of the right-set equations then takes the following form, which can be solved by a Schouten identity,

$$\delta^2 \left(|r\rangle - \frac{|1\rangle}{\sigma_r^2} - \frac{|2\rangle}{\sigma_r^1} \right) = \frac{\langle 12 \rangle^3}{\langle 1r \rangle^2 \langle 2r \rangle^2} \delta \left(\sigma_r^1 - \frac{\langle 12 \rangle}{\langle r1 \rangle} \right) \delta \left(\sigma_r^2 - \frac{\langle 12 \rangle}{\langle r2 \rangle} \right), \quad r \in R. \quad (3.1.5)$$

The full MHV solution along with its minors and the associated expression for the Jacobian of the delta functions is

$$\sigma_{\text{MHV}} = \begin{pmatrix} 1 & 0 & \frac{\langle 12 \rangle}{\langle 31 \rangle} & \cdots & \frac{\langle 12 \rangle}{\langle n1 \rangle} \\ 0 & 1 & \frac{\langle 12 \rangle}{\langle 32 \rangle} & \cdots & \frac{\langle 12 \rangle}{\langle n2 \rangle} \end{pmatrix}$$

$$\delta^{2 \times n}(\text{SE}_{n,\{1,2\}}) = \langle 12 \rangle^2 \prod_{r \in R} \frac{\langle 12 \rangle^3}{\langle 1r \rangle^2 \langle 2r \rangle^2} \delta^4(P) \delta^{2n-4}(\sigma - \sigma_{\text{MHV}})$$

$$(12)_{\text{MHV}} = 1 \quad (rr')_{\text{MHV}} = \frac{\langle 12 \rangle^3 \langle rr' \rangle}{\langle 1r \rangle \langle 1r' \rangle \langle 2r \rangle \langle 2r' \rangle} \quad (1r)_{\text{MHV}} = \frac{\langle 12 \rangle}{\langle r2 \rangle} \quad (2r)_{\text{MHV}} = \frac{\langle 12 \rangle}{\langle 1r \rangle}. \quad (3.1.6)$$

The Jacobian as calculated this way is in agreement with the calculation from Section 3.6, where I also consider the Jacobian for higher MHV degree.

Finding analytical solutions for generic kinematics outside of the MHV sector is currently an unsolved problem, apart from at 6 points NMHV where the scattering equations have four solutions, which are found for the general d equations for $d = 4$ in [101]. Abel's theorem states that there is no algebraic solution in terms of n th roots to a general polynomial equation of degree five or higher with arbitrary coefficients [102]. To find analytical N^{k-2} MHV solutions above 6 points NMHV some underlying

structure would have to exist within the coefficients of the equations, otherwise general analytical solutions are excluded by Abel's theorem. Full sets of solutions can be found analytically for some specific choices of momenta[116].

Due to these difficulties in finding analytical solutions, calculating amplitudes by solving the scattering equations outside of the MHV sector is primarily a numerical problem, which I address in Chapter 4.

One key strength of the scattering equation formalism is that once a full set of solutions is known, amplitudes can be calculated in any theory at relatively small computational cost. The relevant integrand is chosen, and the only necessary operation is to sum over the solutions. Solutions to the scattering equations are graded only by MHV degree and not by a specific choice of left set. This implies that there must exist some transformation on the worldsheet which can map an integrand supported on scattering equations for one left set into an integrand for a different left set of the same degree. For example such a mapping allows for calculation of all 6 point NMHV gluon amplitudes in Yang Mills theory with only one solution to the scattering equations; eg. $\mathcal{A}(+ - + - + -)$ with left set $L = \{2, 4, 6\}$ and $\mathcal{A}(- - - + + +)$ with left set $L = \{1, 2, 3\}$.

The following is an explicit co-ordinate transformation on the worldsheet which swaps two particles, $l_0 \in L$ and $r_0 \in R$, between the left and right sets of the scattering equations.¹

$$\begin{aligned} \sigma_{l_0} \mapsto \sigma'_{l_0} &= \sigma_{l_0} \frac{1}{(l_0 r_0)}, & \sigma_{r_0} \mapsto \sigma'_{r_0} &= \sigma_{r_0} \frac{1}{(r_0 l_0)}, \\ \sigma_l \mapsto \sigma'_l &= \sigma_l \frac{(ll_0)}{(lr_0)} \quad l \neq l_0 \in L, & \sigma_r \mapsto \sigma'_r &= \sigma_r \frac{(rr_0)}{(rl_0)} \quad r \neq r_0 \in R. \end{aligned} \quad (3.1.7)$$

¹I thank Paul Heslop for suggesting this transformation.

Under this transformation the scattering equation integrand transforms as

$$\int \frac{d^{2 \times n} \sigma}{GL(2)} \delta^{2 \times n} (SE_{n,L}) f(\sigma) \mapsto \int \frac{d^{2 \times n} \sigma}{GL(2)} \delta^{2 \times n} (SE_{L'}^n) f'(\sigma) = \int \frac{d^{2 \times n} \sigma}{GL(2)} \delta^{2 \times n} (SE_{L'}^n) \prod_{l \neq l_0 \in L} \frac{(ll_0)^2}{(lr_0)^2} \prod_{r \neq r_0 \in R} \frac{(rr_0)^2}{(rl_0)^2} \frac{f(\sigma')}{(l_0 r_0)^8} \quad (3.1.8)$$

where L' has l_0 swapped with r_0 . This transformation can be used to calculate a new integrand f' for a swap of the choice of left sets for the scattering equations. Details of how the equations vary under this transformation are given in Section 3.5. Repeatedly applying the transformation can be used to reassign any left set.

3.2 Recovering the General d Scattering Equations for $d = 4$

Solutions to the 4D equations are grouped into sets for the different N^{k-2} MHV sectors, whereas the general d equations depend only on n and do not encode this grouping. As the 4D scattering equations contain more information than the general d scattering equations, 4D \Rightarrow general d (for $d = 4$), which I prove in this section; a different argument is given in [74]. The proof also provides an explicit method for finding solutions to the general d equations using those from the 4D specific case. Integrands for the general d equations for $d = 4$ can also be mapped to integrands for the 4D equations [117].

First I prove a lemma which holds for the general d equations. Define world-sheet dependent momentum $P(s) := \sum_{j \in \mathcal{N}} \frac{k_j}{s - s_j}$. Then I prove that $P(s)^2 = 0 \Leftrightarrow$ the general d equations. Note that there are no second order poles in $P(s)^2$ as all of the external momenta k_i are null. Then

$$P(s)^2 = \sum_{\substack{i,j \in \mathcal{N} \\ i \neq j}} \frac{k_i \cdot k_j}{(s - s_i)(s - s_j)} = 2 \sum_{i \in \mathcal{N}} \frac{1}{s - s_i} \left(\sum_{\substack{j \in \mathcal{N} \\ j \neq i}} \frac{k_i \cdot k_j}{s_i - s_j} \right), \quad (3.2.1)$$

where the second equality comes from using partial fractions and relabelling indices.

$P(s)$ is now written explicitly as a sum of its poles, and hence can only be zero if all of its residues are zero. Therefore, $P(s)^2 = 0 \Leftrightarrow \sum_{j \in \mathcal{N}} \frac{k_i \cdot k_j}{s_i - s_j} = 0$.

To relate to the 4D equations, construct a new explicitly null world-sheet dependent momentum in terms of two world-sheet dependent spinors $|\lambda(s)\rangle := \sum_{r \in R} \frac{t_r |r\rangle}{s - s_r}$ and $\langle \lambda(s) | := \sum_{l \in L} \frac{t_l \langle l |}{s - s_l}$. Then the associated momentum vector is

$$\begin{aligned} |\lambda(s)\rangle \langle \lambda(s) | &= \left(\sum_{r \in R} \frac{t_r |r\rangle}{s - s_r} \right) \left(\sum_{l \in L} \frac{t_l \langle l |}{s - s_l} \right) = \sum_{\substack{r \in R \\ l \in L}} \frac{|r\rangle \langle l |}{(rl)} \left(\frac{1}{s - s_l} - \frac{1}{s - s_r} \right) \\ &= \sum_{r \in R} \frac{|r\rangle}{s - s_r} \left(\sum_{l \in L} \frac{\langle l |}{(rl)} \right) + \sum_{l \in L} \left(\sum_{r \in R} \frac{|r\rangle}{(lr)} \right) \frac{\langle l |}{s - s_l} \\ &= \sum_{r \in R} \frac{|r\rangle \langle r |}{s - s_r} + \sum_{l \in L} \frac{|l\rangle \langle l |}{s - s_l} = P(s), \end{aligned} \quad (3.2.2)$$

where the same steps are used as in the previous calculation, and the second-to-last equality uses the 4D scattering equations and $k_i = |i\rangle \langle i|$. Given that $|\lambda(s)\rangle \langle \lambda(s) |$ is explicitly constructed as a null vector, the 4D scattering equations imply that $P(s)^2 = 0$, and hence by the lemma they imply the general d scattering equations.

This proof also provides an explicit mapping from a solution to the 4D scattering equations to a solution to the general d equations. A point in the solution space of the 4D equations is mapped to a point in the n -punctured Riemann sphere by writing each column as $\sigma_i = t_i^{-1} \begin{pmatrix} 1 \\ s_i \end{pmatrix}$, and keeping only the s variables and not the scales t . Suppose there is some solution to the 4D scattering equations which is gauge-fixed such that the first two particles are equal to the identity matrix. Under this mapping the vector $\begin{pmatrix} 1 \\ 0 \end{pmatrix}$ maps to the point at infinity, and the remaining gauge redundancy can be fixed by dividing through by s_3 to arrive at

$$\sigma_{4D} = \begin{pmatrix} 1 & 0 & \sigma_3^1 & \dots & \sigma_n^1 \\ 0 & 1 & \sigma_3^2 & \dots & \sigma_n^2 \end{pmatrix} \mapsto s_{\text{general } d, d=4} = \left(\infty \quad 0 \quad 1 \quad \frac{\sigma_4^1 \sigma_3^2}{\sigma_2^1 \sigma_3^1} \quad \dots \quad \frac{\sigma_n^1 \sigma_3^2}{\sigma_n^2 \sigma_3^1} \right). \quad (3.2.3)$$

It is clear from this analysis that reconstructing a full solution to the 4D equations in terms of the s and t variables is not direct given a $d = 4$ solution to the general

d equations, and it would be interesting to understand how the t variables can be specified in this case.

MHV and $\overline{\text{MHV}}$ solutions to the general d equations for $d = 4$ were derived in [101]. Using the mapping 3.2.3, the map from the MHV solutions to the 4D equations derived in Section 3.1 onto those of the general d equations can be seen explicitly as

$$\sigma_{\text{MHV}} = \begin{pmatrix} 1 & 0 & \frac{\langle 12 \rangle}{\langle 31 \rangle} & \cdots & \frac{\langle 12 \rangle}{\langle n1 \rangle} \\ 0 & 1 & \frac{\langle 12 \rangle}{\langle 32 \rangle} & \cdots & \frac{\langle 12 \rangle}{\langle n2 \rangle} \end{pmatrix} \mapsto s_{\text{MHV}} = \begin{pmatrix} \infty & 0 & 1 & \frac{\langle 41 \rangle \langle 32 \rangle}{\langle 31 \rangle \langle 42 \rangle} & \cdots & \frac{\langle n1 \rangle \langle 32 \rangle}{\langle 31 \rangle \langle n2 \rangle} \end{pmatrix}, \tag{3.2.4}$$

in agreement with equation (49) of [101], up to choice of $\text{SL}(2)$ gauge fixing.

3.3 Symmetries, Little Group Scaling and Grassmanians

The scattering equations have a $\text{GL}(2)$ symmetry which can be realised in different ways in terms of a worldsheet redefinition, or a worldsheet redefinition with a corresponding little group rescaling. The worldsheet $\text{GL}(2)$ symmetry in (3.1.2) is a combination of the standard $\text{SL}(2)$ symmetry of global conformal transformations in the string worldsheet s variables, and a $\text{GL}(1)$ transformation corresponding to a rescaling of the worldsheet t variables. Any function $f(\sigma)$ which is integrated against the scattering equation delta functions must transform as $f(\sigma) \rightarrow f(\sigma)(\det G)^{n-2k}$ under (3.1.2) to balance out the transformation of the measure. All of the integrands for the theories considered in Section 2.8 satisfy this transformation law, as enforced by their underlying 4D ambitwistor string models [26].

Before considering joint worldsheet and little group transformations, I first analyse the little group scaling of amplitudes supported on the scattering equations. Consider a general amplitude $\mathcal{A}_{n,L}$ with some arbitrary integrand $f(\sigma, |i\rangle, |i])$,

$$\mathcal{A}_{n,L} := \int \frac{d^{2 \times n} \sigma}{GL(2)} \delta^{2 \times n}(\text{SE}_{n,L}) f(\sigma, |i\rangle, |i]).$$

Perform a different little group scaling for each particle, such that $|i\rangle \mapsto \alpha_i |i\rangle$ and $|i] \mapsto \alpha_i^{-1} |i]$. Then the amplitude transforms as

$$\begin{aligned} \mathcal{A}_{n,L}(\alpha_i |i\rangle, \alpha_i^{-1} |i]) &= \int \frac{d^{2 \times n} \sigma}{GL(2)} \prod_{l \in L} \delta^2 \left(\frac{|l]}{\alpha_l} - \sum_{r \in R} \frac{|r]}{\alpha_r (lr)} \right) \prod_{r \in R} \delta^2 \left(\alpha_r |r\rangle - \sum_{l \in L} \frac{\alpha_l |l\rangle}{(rl)} \right) \\ &\quad f(\sigma, \alpha_i |i\rangle, \alpha_i^{-1} |i]). \end{aligned} \tag{3.3.1}$$

To relate to the previous expression before the scaling, define new worldsheet coordinates such that $\sigma'_l := \alpha_l^{-1} \sigma_l$ for $l \in L$, and $\sigma'_r := \alpha_r \sigma_r$ for $r \in R$. Then change variables and rename back to σ , picking up factors of the α_i from the delta functions and the measure to arrive at

$$\mathcal{A}_{n,L}(\alpha_i |i\rangle, \alpha_i^{-1} |i]) = \int \frac{d^{2 \times n} \sigma}{GL(2)} \delta^{2 \times n}(\text{SE}_{n,L}) \prod_{l \in L} \alpha_l^4 \prod_{r \in R} \alpha_r^{-4} f(\alpha_l \sigma_l, \alpha_r^{-1} \sigma_r, \alpha_i |i\rangle, \alpha_i^{-1} |i]). \tag{3.3.2}$$

Now consider how the integrand for Yang-Mills theory with \mathcal{N} supersymmetries as defined in Section 2.8 scales under the little group. Under this little group transformation the Grassmann variables transform as $\eta_i \rightarrow \alpha_i^{-1} \eta_i$, and the Grassmann delta functions transform in a similar way to the scattering equation delta functions. The transformation of the Parke-Taylor factor cancels out that of the measure, and the integrand becomes

$$f_{\text{sYM}}(\alpha_l \sigma_l, \alpha_r^{-1} \sigma_r, \alpha_i |i\rangle, \alpha_i^{-1} |i], \alpha_i^{-1} \eta_i) = \prod_{l \in L} \alpha_l^{-2-\mathcal{N}} \prod_{r \in R} \alpha_r^2 f_{\text{sYM}}(\sigma, |i\rangle, |i], \eta_i). \tag{3.3.3}$$

From this the standard little group scaling is found for negative and positive helicity

superfields of a Yang-Mills superamplitude, that

$$\mathcal{A}_{n,L}(\alpha_i |i\rangle, \alpha_i^{-1} |i], \alpha_i^{-1} \eta_i) = \prod_{l \in L} \alpha_l^{2-N} \prod_{r \in R} \alpha_r^{-2} \mathcal{A}_{n,L}(|i\rangle, |i], \eta_i), \quad (3.3.4)$$

and a similar analysis produces the required scaling for gravity amplitudes.

The variables to 4D scattering equations can be considered as $2 \times n$ matrix with a $GL(2)$ gauge freedom, and hence appear at first sight as though sit in the Grassmannian $Gr(2, n)$. This is not directly the case however, due tho the fact that the $GL(2)$ acts differently on the left and right sets of particles. I now show that combining a little group transformation with a worldsheet rescaling can produce a standard $GL(2)$ transformation which acts homogeneously on the left and right sets, and hence the solution space of the equations can indeed be considered as $Gr(2, n)$. Simultaneously performing an inhomogeneous little group scaling such that $|l] \rightarrow \alpha |l], |l\rangle \rightarrow \alpha^{-1} |l\rangle$ for $l \in L$ and $|r] \rightarrow \beta |r], |r\rangle \rightarrow \beta^{-1} |r\rangle$ for $r \in R$, the scattering equations become

$$\begin{aligned} \delta^{2 \times n}(\text{SE}_{n,L}) &= \prod_{l \in L} \alpha^{-2} \delta^2 \left(|l] - \frac{\beta}{\alpha \det G} \sum_{r \in R} \frac{|r]}{(lr)} \right) \prod_{r \in R} \beta^2 \delta^2 \left(|r\rangle - \frac{\beta}{\alpha \det G} \sum_{l \in L} \frac{|l\rangle}{(rl)} \right) \\ &= \alpha^{2n-4k} (\det G)^{2n-2k} \delta^{2 \times n}(\text{SE}_{n,L}), \end{aligned} \quad (3.3.5)$$

where in the last equation $\beta = \alpha \det G$ is chosen to keep the equations invariant.

The measure and delta functions combined transform such that

$$\begin{aligned} \int \frac{d^{2 \times n} \sigma}{GL(2)} \delta^{2 \times n}(\text{SE}_{n,L}) f(\sigma, |i\rangle, |i]) &\mapsto \int \frac{d^{2 \times n} \sigma}{GL(2)} \delta^{2 \times n}(\text{SE}_{n,L}) (\det G)^{3n-2k} \alpha^{2n-4k} \\ &f(G\sigma, \alpha |l\rangle, \alpha^{-1} |l], \alpha \det G |r\rangle, (\alpha \det G)^{-1} |r]). \end{aligned} \quad (3.3.6)$$

As was shown above, the little group transformation of the amplitude \mathcal{A} comes from little group covariance of the integrand f . Any f which integrates to an amplitude must transform covariantly under the little group, and hence f must transform as a

scaling transformation for any combined little group transformation and worldsheet rescaling. It can then be concluded that for any f which describes an amplitude there must exist some x and y real numbers such that

$$f(G\sigma, \alpha |l\rangle, \alpha^{-1} |l\rangle, \alpha \det G |r\rangle, (\alpha \det G)^{-1} |r\rangle) = (\det G)^x \alpha^y f(\sigma, |i\rangle, |i\rangle).$$

Given f which transforms in this way, the little group scaling α can be chosen such that $(\det G)^{3n-2k+x} \alpha^{2n-4k+y} = 1$, and hence this transformation is a symmetry for any amplitude supported on the scattering equations. This $\text{GL}(2)$ invariance is the $\text{GL}(2)$ invariance of the Grassmannian $\text{Gr}(2, n)$, and hence in this sense the solutions to the scattering equations can be thought of as living in $\text{Gr}(2, n)$.

3.4 Deleting Equations and Momentum Conservation

In this section I demonstrate how to remove four equations to give a momentum conserving delta function. There are three possible cases; two particles in the left set, two in the right set, or one particle in each set. First consider the case of two particles in the left set. Without loss of generality, label these particles to be 1 and 2. Defining the delta functions for these particles to be $\Delta_{1,2}$,

$$\begin{aligned} \Delta_{1,2} &:= \delta^2 \left(|1\rangle - \sum_{r \in R} \frac{|r\rangle}{(1r)} \right) \delta^2 \left(|2\rangle - \sum_{r \in R} \frac{|r\rangle}{(2r)} \right) \\ &= \langle 12 \rangle^4 \delta^2 \left(|1\rangle \langle 12\rangle - \sum_{r \in R} \frac{|r\rangle \langle 12\rangle}{(1r)} \right) \delta^2 \left(|2\rangle \langle 21\rangle - \sum_{r \in R} \frac{|r\rangle \langle 21\rangle}{(2r)} \right). \end{aligned} \quad (3.4.1)$$

Now consider a general right set equation and contract with first with $\langle 2|$, and separately with $\langle 1|$, to find that

$$|r\rangle = \sum_{l \in L} \frac{|l\rangle}{(rl)} \implies \begin{cases} \frac{\langle 12\rangle}{(1r)} = -\langle r2\rangle - \sum_{\substack{l \in L \\ l \neq 1,2}} \frac{\langle l2\rangle}{(lr)} \\ \frac{\langle 21\rangle}{(2r)} = -\langle r1\rangle - \sum_{\substack{l \in L \\ l \neq 1,2}} \frac{\langle l1\rangle}{(lr)}. \end{cases} \quad (3.4.2)$$

Substituting into $\Delta_{1,2}$,

$$\begin{aligned} \Delta_{1,2} = \langle 12 \rangle^4 \delta^2 \left(\left(|1\rangle \langle 1| + \sum_{r \in R} |r\rangle \langle r| \right) |2\rangle + \sum_{\substack{r \in R, l \in L \\ l \neq 1,2}} \frac{|r\rangle \langle l2\rangle}{(lr)} \right) \\ \delta^2 \left(\left(|2\rangle \langle 2| + \sum_{r \in R} |r\rangle \langle r| \right) |1\rangle + \sum_{\substack{r \in R, l \in L \\ l \neq 1,2}} \frac{|r\rangle \langle l1\rangle}{(lr)} \right). \end{aligned} \quad (3.4.3)$$

The remaining left set equations are then used to solve the sum over r in the last term in each delta function, arriving at

$$\Delta_{1,2} = \langle 12 \rangle^4 \delta^2 \left(\left(\sum_{n \in \mathcal{N}} |n\rangle \langle n| \right) |2\rangle \right) \delta^2 \left(\left(\sum_{n \in \mathcal{N}} |n\rangle \langle n| \right) |1\rangle \right) = \langle 12 \rangle^2 \delta^4(P). \quad (3.4.4)$$

This is referred to as having ‘deleted equations 1 and 2’, and the remaining $2n - 4$ equations give a well-specified system. Note the Jacobian $\langle 12 \rangle^2$ for this calculation.

The calculation for deleting two equations in the right set goes by the same steps, and labelling the two particles in the right set to be r_1 and r_2 :

$$\delta^2 \left(|r_1\rangle - \sum_{l \in L} \frac{|l\rangle}{(r_1 l)} \right) \delta^2 \left(|r_2\rangle - \sum_{l \in L} \frac{|l\rangle}{(r_2 l)} \right) = [r_1 r_2]^2 \delta^4(P). \quad (3.4.5)$$

There is one remaining choice; deleting one equation from the left set and one equation from the right set. Choosing equations in this way does not produce a momentum-conservation delta function, and hence does not result in a solvable system for spinors satisfying momentum conservation. To see this, label the left set particle as $1 \in L$, and the right set particle as $n \in R$. Then following the same analysis as above,

$$\begin{aligned}
\delta^2 \left(|1\rangle - \sum_{r \in R} \frac{|r\rangle}{(1r)} \right) \delta^2 \left(|n\rangle - \sum_{l \in L} \frac{|l\rangle}{(nl)} \right) \\
= \langle 1n \rangle^2 [1n]^2 \delta^2 \left(|1\rangle \langle 1n| + \sum_{i=2}^{n-1} |i\rangle \langle in| \right) \delta^2 \left(\sum_{i=2}^{n-1} [1i] \langle i| + [1n] \langle n| \right).
\end{aligned} \tag{3.4.6}$$

These equations look deceptively similar to momentum conservation. I prove here that they are in fact not the same, and give a constraint corresponding to non-generic kinematics.

Solving the first equation as $|1\rangle = \frac{1}{\langle n1 \rangle} \sum_{i=2}^{n-1} |i\rangle \langle in|$ and substituting into the second, these delta functions imply that

$$|n\rangle \sum_{i=2}^{n-1} P_n \cdot P_i + \sum_{\substack{i,j=2 \\ j \neq i}}^{n-1} |i\rangle [ij] \langle jn| = |n\rangle \left(\sum_{i=2}^{n-1} P_i \right)^2 = 0, \tag{3.4.7}$$

where between the first two equalities the second sum is split into two terms, and the indices are relabelled using a Schouten identity. Hence to keep consistency with these equations either $|n\rangle$ or the Mandelstam invariant $\left(\sum_{i=2}^{n-1} P_i \right)^2$ must be set to zero, and neither of these choices correspond to generic kinematics. Therefore, it is not possible to delete one equation from each set.

3.5 Permutations and Choice of Left Set

A given n point N^{k-2} MHV amplitude will be supported on scattering equations with a specified left set L . In this section I show how solutions to the scattering equations for one left set can be used to calculate amplitudes with the same MHV degree that are supported on different left set L' . This mapping of different left sets is important computationally as it will allow us to solve the equations only once in each MHV sector and then calculate all amplitudes of this MHV degree for the specified numerical momenta. The explicit worldsheet transformation swapping

particles $l_0 \in L$ and $r_0 \in R$ in between the sets is given in equation (3.1.7). Under this transformation, the scattering equations transform as

$$\begin{aligned} E_l &\longrightarrow E_l - \frac{(l_0 r_0)}{(l r_0)} E_{l_0} & E_{l_0} &\longrightarrow (l_0 r_0) E_{r_0} \\ E_r &\longrightarrow E_r - \frac{(r_0 l_0)}{(r l_0)} E_{r_0} & E_{r_0} &\longrightarrow (l_0 r_0) E_{l_0}, \end{aligned}$$

where a Schouten identity in the worldsheet variables is used in the l and r equations. The second terms in the l and r equations are zero on support of the l_0 and r_0 equations, and hence the scattering equations remain the same up to changing the particles l_0 and r_0 between the left and right set. The delta functions pick up an overall factor of $(l_0 r_0)^{-4}$. Calculating the transformation of the measure, the scattering equation integral transforms as in equation (3.1.8).

Performing a permutation of the external data on the same legs l_0 and r_0 and looking at the transformation properties of the integrands, it can be understood that the amplitude does not depend on a choice of left set for maximally supersymmetric theories and for $\mathcal{N} = 4$ conformal supergravity. This transformation can also be used to understand permutation invariance under swapping between the right and left sets for $\mathcal{N} = 8$ supergravity. Showing permutation invariance of gravity amplitudes under a swapping two legs which carry the same helicity superfield is straightforward, and simply requires renaming the worldsheet variables on the permuted legs.

Now look at the form of the integrand for Yang-Mills theories. Under this transformation,

$$\begin{aligned} \int \frac{d^{2 \times n} \sigma}{GL(2)} \delta^{2 \times n}(\text{SE}_{n,L}) \frac{\prod_{l \in L} \delta^{\mathcal{N}} \left(\eta_l - \sum_{r \in R} \frac{\eta_r}{(lr)} \right)}{\prod_{i \in \mathcal{N}} (i i+1)} \\ \rightarrow \int \frac{d^{2 \times n} \sigma}{GL(2)} \delta^{2 \times n}(\text{SE}_{n,L'}) \frac{\prod_{l \in L'} \delta^{\mathcal{N}} \left(\eta_l - \sum_{r \in R'} \frac{\eta_r}{(lr)} \right)}{\prod_{i \in \mathcal{N}} (i i+1)} (l_0 r_0)^{\mathcal{N}-4}. \end{aligned} \tag{3.5.1}$$

For $\mathcal{N} = 4$ the integrand is unchanged up to a choice of the left set, and hence for $\mathcal{N} = 4$ super Yang-Mills theory the choice of left set does not affect the overall

superamplitude. Now look at the MHV sector for $\mathcal{N} = 0$, fix $L = \{1, 2\}$ and swap the external data for particles 1 and r_0 , as well as performing the integral transformation to swap 1 and r_0 . It is clear that $(1r_0)^4 = \frac{\langle 12 \rangle^4}{\langle 2r_0 \rangle^4}$, which is exactly the factor required to modify the Park-Taylor formula for particles 1 and 2 negative helicity gluons to have particles 2 and r_0 with negative helicities. It is interesting to note that this structure extends outside of the MHV sector at the level of the integrand in the scattering equation formalism.

3.6 The Jacobian of the 4D Scattering Equations

In this section I detail some properties of the Jacobian of the 4D scattering equations. For a general worldsheet integral over the scattering equation delta functions, the integrals can be solved and the expression can be written as a sum over the solutions to the scattering equations. To do this, an explicit expression is needed for the Jacobian $J_L^n(\sigma)$ as follows. I use the notation for matrix A that A^{ij} has rows and columns i and j removed. Let $l, l' \in L$ and delete equations l and l' to arrive at

$$\int \frac{d^{2 \times n} \sigma}{GL(2)} \delta^{2 \times n}(\text{SE}_{n,L}) f(\sigma) = \delta^4(P) \sum_{\sigma_{\text{sol}} \in \text{Solutions}} \frac{f(\sigma_{\text{sol}})}{\langle ll' \rangle^{-2} \det(J_L^{n, ll'}(\sigma_{\text{sol}}))}. \quad (3.6.1)$$

Note that as shown in Section 3.4, the two rows/columns deleted must either both be in the left set or both in the right set, and there is an extra associated factor eg. $\langle ll' \rangle^2$ such that the full determinant of the Jacobian is $\langle ll' \rangle^{-2} \det(J_L^{n, ll'})$ for two left set particles deleted and gauge-fixed.

At n points with left set L the Jacobian is calculated to be

$$J_L^n = \begin{pmatrix} \frac{\partial \tilde{E}_l}{\partial \sigma_{l'}} & \frac{\partial \tilde{E}_l}{\partial \sigma_{r'}} \\ \frac{\partial E_r}{\partial \sigma_{l'}} & \frac{\partial E_r}{\partial \sigma_{r'}} \end{pmatrix} = \begin{pmatrix} -\delta_{ll'} \sum_{r \in R} \frac{|r] \otimes \sigma_r}{(lr)^2} & \frac{|r'] \otimes \sigma_l}{(lr')^2} \\ \frac{\langle l| \otimes \sigma_r}{(lr)^2} & -\delta_{rr'} \sum_{l \in L} \frac{\langle l| \otimes \sigma_l}{(lr)^2} \end{pmatrix}, \quad (3.6.2)$$

where the matrix is written in a block form with blocks of sizes of the left and right set, and each element of these matrices is broken down into a 2×2 matrix which is a

tensor product of a spinor with a worldsheet vector. This matrix has determinant 0, which is simple to check analytically for example in MATHEMATICA. This is insured by the fact that gauge-fixing removes 4 of the sigma variables, and hence four of the rows of the matrix must be removed to produce a well specified system. Similarly, four of the columns of J_L^n must be removed, which is equivalent to deleting two equations as shown in appendix 3.4.

In the MHV sector this matrix is block diagonal and the determinant in terms worldsheet minors can be calculated directly. Taking the left set to the particles 1 and 2 and also gauge-fixing and deleting these particles

$$\det \left(J_{\{1,2\}}^n \right) = \det \left(\frac{\partial E_r}{\partial \sigma_{r'}} \right) = \prod_{r \in R} \det \left(\frac{\langle 1 | \otimes \sigma_1}{(1r)^2} + \frac{\langle 2 | \otimes \sigma_2}{(2r)^2} \right). \quad (3.6.3)$$

A general result for determinants of sums of tensor products of two dimensional vectors is given by

$$\det \left(\sum_{i=1}^m \alpha_i u_i \otimes v_i \right) = \sum_{1 \leq i < j \leq m} \alpha_i \alpha_j \det(u_i u_j) \det(v_i v_j), \quad (3.6.4)$$

for m variables $u_i, v_i \in \mathbb{C}^2$ and $\alpha_i \in \mathbb{C}$. Using this result for the MHV calculation $m = 2$ gives

$$\det \left(J_{\{1,2\}}^n \right) = \prod_{r \in R} \frac{\langle 12 \rangle (12)}{(1r)^2 (2r)^2} = \prod_{r \in R} \frac{\langle 1r \rangle^2 \langle 2r \rangle^2}{\langle 12 \rangle^3}, \quad (3.6.5)$$

where in the last equation the MHV solution from Section 3.1 is substituted in.

It is also possible to analytically evaluate the Jacobian outside of the MHV sector. Assume $1, 2 \in L$ and gauge-fix and delete particles 1 and 2, and use the formula for the determinant of a block matrix to find that

$$\det \left(J_L^n \right) = \det \left(\frac{\partial E_r}{\partial \sigma_{r'}} \right) \det \left(\frac{\partial \tilde{E}_l}{\partial \sigma_{l'}} - \frac{\partial \tilde{E}_l}{\partial \sigma_{r'}} \left(\frac{\partial E_r}{\partial \sigma_{r'}} \right)^{-1} \frac{\partial E_r}{\partial \sigma_{l'}} \right), \quad (3.6.6)$$

where $r, r' \in R$ and $l, l' \in L/\{1, 2\}$.

As $\frac{\partial E_r}{\partial \sigma_{r'}}$ is block diagonal, it is comparatively simple to calculate its determinant and

inverse. Using equation (3.6.4) the determinant becomes

$$\det \left(\frac{\partial E_r}{\partial \sigma_{r'}} \right) = \prod_{r \in R} \sum_{l < l' \in L} \frac{\langle ll' \rangle (ll')}{(rl)^2 (r'l')^2}. \quad (3.6.7)$$

To invert this matrix first notice that in the r, r' indices it is simply $\delta_{rr'}$, leaving the calculation of the inverses of the 2×2 blocks. The general result for a 2×2 matrix M that $M^{-1} = \det(M)^{-1} \begin{pmatrix} 0 & 1 \\ -1 & 0 \end{pmatrix} M \begin{pmatrix} 0 & -1 \\ 1 & 0 \end{pmatrix}$ can be used to invert in the spinor and worldsheet indices. This corresponds to raising and lowering the two indices, and dividing by the determinant as calculated by equation (3.6.4). The result is then that

$$\begin{aligned} & \det \left(\frac{\partial \tilde{E}_l}{\partial \sigma_{l'}} - \frac{\partial \tilde{E}_l}{\partial \sigma_{r'}} \left(\frac{\partial E_r}{\partial \sigma_{r'}} \right)^{-1} \frac{\partial E_r}{\partial \sigma_{l'}} \right) \\ &= \det \left(\sum_{r \in R} \frac{[r] \otimes \sigma_r}{(lr)^2 \sum_{\lambda < \lambda' \in L} \frac{\langle \lambda \lambda' \rangle (\lambda \lambda')}{(r\lambda)^2 (r\lambda')^2}} \left(\sum_{\lambda \in L} \frac{\langle l' \lambda \rangle (l\lambda)}{(\lambda r)^2 (l'r)^2} - \delta_{ll'} \sum_{\lambda < \lambda' \in L} \frac{\langle \lambda \lambda' \rangle (\lambda \lambda')}{(\lambda r)^2 (\lambda' r)^2} \right) \right), \end{aligned} \quad (3.6.8)$$

where the determinant is taken over $l, l' \in L/\{1, 2\}$, combined with the tensor product of spinor and worldsheet indices. In the NMHV sector it is found that $l = l' = 3$ and the determinant of the remaining 2×2 matrix can be calculated using equation (3.6.4). As an example, at 6 points NMHV the determinant is

$$\det(J_{\{1,2,3\}}^6) = \frac{\langle 12 \rangle^2 (12)^2}{\prod_{l,r} (lr)^2} \sum_{\substack{r < r' \in R \\ l < l' \in L}} [rr'] (rr') \langle ll' \rangle (ll') \sum_{\substack{\lambda \in L \\ \rho \in R}} \epsilon_{ll'\lambda} \epsilon_{rr'\rho} (\lambda\rho)^2. \quad (3.6.9)$$

Chapter 4

Monte Carlo Numerical Methods for the 4D Scattering Equations

In this chapter I treat the 4D scattering equations as a numerical system which I solve by Monte Carlo algorithm, based on my work from [1]. I introduce the numerical system in Section 4.1, and discuss why previous algorithms in the literature do not work in this setting in Section 4.2. I present a new Monte Carlo algorithm for solving the equations in any MHV sector in Section 4.3, and discuss the details of an algorithm for extracting component amplitudes from a superamplitude in Section 4.4. I implement the analytical framework from Chapter 3 and the numerical algorithms developed in this chapter in my MATHEMATICA package `treeamps4dJAF` which can be downloaded from the arXiv submission of [1], and which I introduce in Section 4.5.

4.1 The 4D Scattering Equation as a Numerical System

The 4D scattering equations can be thought of as $2n - 4$ equations with variables σ_i^α in the Grassmannian $\text{Gr}(2, n)$, and are parameterised by a set of spinors obeying

momentum conservation, as explained in Section 3.3. A full set of solutions to the scattering equations at n points N^{k-2} MHV will then be a mapping from the external data of the amplitude to $\langle \binom{n-3}{k-2} \rangle$ points in $\text{Gr}(2, n)$. In the MHV case I give this mapping analytically in Section 3.1, but finding analytical solutions for $k > 2$ is complicated due to the combinatorially increasing number of solutions. A well-specified problem is to provide explicit numerical momenta, which will usually be randomly sampled, and to then solve the resulting equations numerically. CHY provide an inverse-soft type algorithm for finding individual numerical solutions to the general d equations [11], but there are difficulties in constructing the full set of solutions in this way which I discuss in Section 4.2. To overcome these problems I provide an explicit algorithm which takes a set of numerical momenta as input and samples random numerical points in $\text{Gr}(2, n)$ to find solutions to the equations stochastically. Algorithms of this type are known as Monte Carlo algorithms, and Monte Carlo methods in high energy physics are well studied [118, 119]. Though not generally applied to solving nonlinear algebraic equations, their application to this type of problem is straightforward.

Random sampling of solution points will eventually cover the whole sample space, and so with enough computing power and time, any non-linear system of equations can be solved by Monte Carlo algorithm. The two key questions to address are when to stop the algorithm, and which distribution to sample the initial points from. The scattering equations are well-suited for solution in this way because the number of solutions is known which gives a clear stopping condition. I address the sampling question in Section 4.3. Finding a set of solutions this way is stochastic and can take a long time, with time complexity now distributed as a random variable which depends on n and k . The expectation of the time complexity increases as n increases and as k moves towards $\lfloor \frac{n}{2} \rfloor$. One advantage of the 4D formalism compared to the general d equations that makes it better suited for solution by Monte Carlo algorithm is that the $(n - 3)!$ solutions are broken down into Eulerian numbers of solutions, tabulated in Figure 4.1. This means that the algorithm can stop after finding a

smaller number of solutions than in general dimensions.

Once a full set of numerical solutions are known for a given number of points and MHV degree, along with the corresponding momenta and left set, they can then be used to calculate amplitudes in different theories for a selection of different external states by substituting different integrands into the sum over solutions.

Tree-level amplitudes are all rational functions of external momenta, and hence for rational numerical external data they will be a rational number. The solutions to the scattering equations are in general not rational numbers, but given a set of rational kinematics they can be calculated to very high precision at relatively low computational cost via deterministic algorithm once all solutions are known. It is then possible to rationalise to the closest rational number to give exact numerical results for the amplitude, and `treeamps4dJAF` provides support for this kind of calculation.

n	$\langle \begin{smallmatrix} n-3 \\ k-2 \end{smallmatrix} \rangle$
4	1
5	1 1
6	1 4 1
7	1 11 11 1
8	1 26 66 26 1
9	1 57 303 302 57 1
10	1 120 1191 2416 1191 120 1

Figure 4.1: Eulerian numbers of solutions to the 4D scattering equations

4.2 Difficulties with CHY's Inverse Soft Algorithm

One proposed algorithm to find numerical solutions to the general d equations is that of CHY [11], which takes one of the momenta soft with parameter ϵ to reduce the equations from n points down to $n - 1$ points. The soft parameter is then reintroduced, and the soft equation at $O(\epsilon)$ is solved for each of the $(n - 4)!$ solutions to the $n - 1$ point equations. The solutions then have a multiplicity of $n - 3$, and

these points are input back into the system with ϵ moving slowly up from 0 to 1. As this algorithm involves slowly bringing the soft parameter back to the full n point system, it is referred to as an inverse soft algorithm. $(n - 3)!$ solutions to the n point equations will be found in this way, but there is no guarantee that all of these solutions will be distinct, and hence they will not necessarily cover the full solution space. It seems to be a generic feature of the algorithm that solutions collide in the inverse soft part of the process, and it is difficult to find kinematics which produce all solutions at n points with this algorithm.

The inverse soft algorithm is based on an inductive argument for counting the total number of solutions, and it can be extended to the 4D case using the analogous 4D solution counting argument, which is reviewed in Section 2.8. Taking one soft parameter ϵ for left set particle $1 \in L$ so that $|1\rangle \mapsto \epsilon|1\rangle$, and a further parameter $\tilde{\epsilon}$ for a right set particle $n \in R$ so that $|n\rangle \mapsto \tilde{\epsilon}|n\rangle$, the 4D scattering equations become

$$\begin{aligned}
 |1\rangle - \sum_{r \in R \setminus \{n\}} \frac{|r\rangle}{(1r)} - \tilde{\epsilon} \frac{|n\rangle}{(1n)} &= 0 & |n\rangle - \epsilon \frac{|1\rangle}{(n1)} - \sum_{l \in L \setminus \{1\}} \frac{|l\rangle}{(nl)} &= 0 \\
 |l\rangle - \sum_{r \in R \setminus \{n\}} \frac{|r\rangle}{(lr)} - \tilde{\epsilon} \frac{|n\rangle}{(ln)} &= 0, \quad l \in L \setminus \{1\} & |r\rangle - \epsilon \frac{|1\rangle}{(r1)} - \sum_{l \in L \setminus \{1\}} \frac{|l\rangle}{(rl)} &= 0, \quad r \in R \setminus \{n\}.
 \end{aligned}
 \tag{4.2.1}$$

It can be seen that the worldsheet variable for the particle in the soft limit decouples, and the equations reduce to $n - 1$ point N^{k-2} MHV equations when $\epsilon = 1, \tilde{\epsilon} \rightarrow 0$ and $n - 1$ point N^{k-3} MHV equations when $\tilde{\epsilon} = 1, \epsilon \rightarrow 0$. Evaluated on the solution to the lower point equations, the remaining equation for the particle that decoupled gives the multiplicity for each solution, as shown in equation (2.8.9).

As detailed in [11] this method is sufficient to produce individual solutions for a specific n and k , but difficulties are found when trying to construct all of the solutions in this way. In four dimensions, two of the different solutions constructed from a lower point amplitude can converge to the same higher point solution, as shown at 6 points NMHV in Figure 4.2. Hence the maximum number of solutions this algorithm

can find is $\langle \binom{n-3}{k-2} \rangle$, and generically it does not find all of the solutions.

MHV and $\overline{\text{MHV}}$ solutions are known analytically, and the first non MHV case is at 6 points NMHV, with four solutions. The ϵ soft limit gives a 5 point $\overline{\text{MHV}}$ amplitude, and the $\tilde{\epsilon}$ soft limit produces a 5 point MHV amplitude. The soft limit equations both have two solutions. Figure 4.2 describes the norm of the MHV solutions as they evolve from $\epsilon = 0$ up to $\epsilon = 1$ in blue, and the $\overline{\text{MHV}}$ solutions from $\tilde{\epsilon} = 0$ up to $\tilde{\epsilon} = 1$ in yellow.

A norm is defined on the solutions by taking the standard norm on \mathbb{C}^n , after flattening the 2×6 worldsheet matrix with gauge-fixed rows deleted down to \mathbb{C}^8 . As depicted in Figure 4.2, the solutions converge when $\epsilon = 1$. Note that where the lines cross for $\epsilon \in [0, 1]$ only the norms of the solutions are equal and not the solutions themselves. Interestingly, when the algorithm is run for ϵ slightly larger than the 1 the solutions separate again.

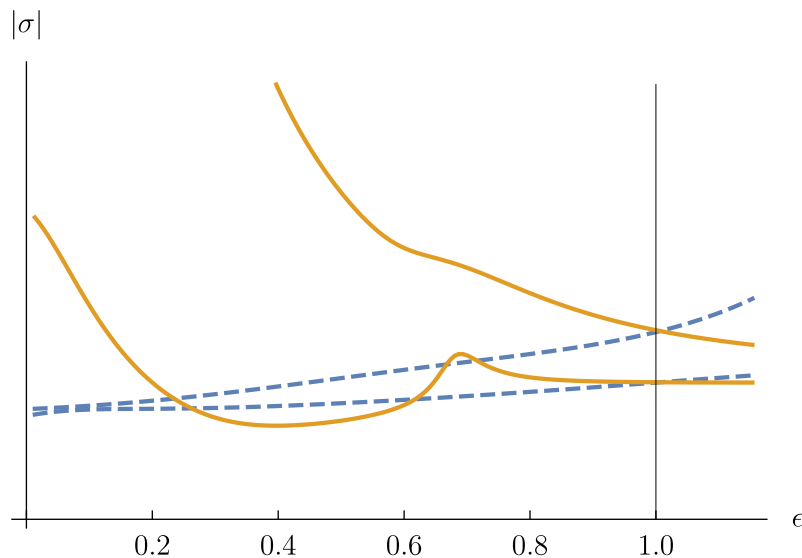


Figure 4.2: Convergent solutions at 6 points NMHV using CHY's inverse soft algorithm. Orange solid lines are solutions coming from 5 points $\overline{\text{MHV}}$ and blue dashed lines are from 5 points MHV.

In the case shown in Figure 4.2, both of the solutions from 5 points MHV collide separately with two individual solutions from 5 points $\overline{\text{MHV}}$. In general for different randomly selected numerical momenta at 6 points NMHV I have found zero, one or

two pairs of solutions converging, and the number of pairs that converge appears to be random based on the selection of random momenta. Solution crashing is a ubiquitous phenomenon; it occurs for nearly all choices and the difficulty is rather to find cases where the solutions do not crash than to find cases where they do.

These difficulties with the inverse soft algorithm inspire developing new methods, and I solve this problem using a Monte Carlo algorithm.

4.3 Monte Carlo Algorithm

The Monte Carlo equation solving algorithm in `treeamps4dJAF` is implemented via `NSolveMonteCarlo`. Many initial random points are sampled from a distribution described below, and chosen as the initial conditions for a `FindRoot` calculation. These initial calls to `FindRoot` run for many iterations, and stop after only one digit of precision is met. Most initial guess points will be far from a solution, and will not converge to 1 digit of precision by the specified number of iterations. Those which do not converge are discarded, and the ones that do converge go back into `FindRoot` up to a higher precision. These points are now solutions, which are compared with a list of all currently found solutions and duplicates are discarded. The algorithm stops when a suitable stopping condition is met, which may be after a specified amount of time or number of iterations, or when some or all solutions are found. A pseudo-code for this algorithm is

```
function NSolveMonteCarlo(equations, variables)
```

```
    Compile equations and Jacobian down to C code for faster evaluation
```

```
    while a stopping condition is not met do
```

```
        Sample 100 initial solution points from a specified distribution
```

```
        Run FindRoot on each point. Stop after 1000 iterations, or when a point
        solves the equations to 1 digit
```

```
        Run FindRoot to higher precision for points that solved the equations
```

```

    Compare solutions to a specified precision and discard any duplicate
    solutions found

end while

end function

```

`NSolveMonteCarlo` is tailored to the 4D scattering equations in the function `NSolveScatteringEquations4D`. This specifies the stopping condition to be when all of the Eulerian numbers of solutions are found, and selects an appropriate distribution to sample the random points from. Figure 4.3 gives a statistical analysis of the time complexity of the algorithm¹ and of the distribution of solution points for all currently accessible n and k . Figure 4.4 expands on this analysis for 6 points NMHV, giving a histogram of the timings. Timings are positively skewed with a similar shape for other n and k . Based on this, the algorithm can currently handle at most around 500 total solutions. Accessing the next cases would require around 1000 solutions, at 10 points N^2 MHV and 13 points NMHV.

I now analyse the sampling of the initial points, and explain which distribution to sample from for most efficient results. Firstly, I solve momentum conservation in terms of the spinors $[1]$ and $[2]$, and delete equations 1 and 2 so that these spinors do not appear in the equations to be solved. This way every random numerical spinor generated is unconstrained, and hence comes from the same uniform distribution. Note that the statistics of the solution points is gauge dependent, and as I always gauge fix particles 1 and 2 it is not possible to make a direct comparison between data points with $k = k'$ and with $k = n - k'$, even though these cases at first glance should be symmetrical.

I perform a statistical analysis at 6 points NMHV, as guided by the analytical understanding in the MHV sector. A solution at 6 points NMHV can be considered as a matrix in $\mathbb{C}^{2 \times 4}$ after removing gauge-fixed columns. I project this down to a

¹All timings were calculated on a Linux desktop computer with 3.30GHz Intel(R) Core(TM) i7-5820K processor, and vary depending on what other processes were running during evaluation of the algorithm.

n	k	$\langle \frac{n-3}{k-2} \rangle$	N_{runs}	N_{σ}	γ_{σ}	MAD_{σ}	\bar{t}	STD_t
6	3	4	7559	483776	0.448	0.462	1.82 s	1.23 s
7	3	11	1047	230340	0.433	0.448	12.5 s	12.2 s
8	3	26	1001	624624	0.443	0.461	1. min	50.1 s
9	3	57	57	90972	0.408	0.427	22.9 min	15.8 min
10	3	120	9	34560	0.423	0.427	4.33 hr	3.65 hr
11	3	247	2	17784	0.508	0.508	10.7 hr	1.57 hr
7	4	11	1001	220220	0.482	0.485	39.8 s	1.49 min
8	4	66	53	83952	0.439	0.447	31. min	29.9 min
9	4	302	2	16912	0.397	0.403	28.7 hr	2.67 hr
8	5	26	328	204672	0.539	0.533	3.45 min	3.02 min
9	6	57	51	81396	0.665	0.642	21.2 min	17.6 min
10	7	120	17	65248	0.698	0.702	59.8 min	34.9 min
11	8	247	2	17784	0.627	0.61	11.5 hr	7.81 hr
12	9	502	1	20080	1.71	1.76	22.3 hr	-

Figure 4.3: Statistical summary of distribution of solutions to 4D scattering equations and timings of NSolveMonteCarlo algorithm. N_{runs} is the number of different set of numerical momenta used, $N_{\sigma} = (4n - 8) \langle \frac{n-3}{k-2} \rangle N_{\text{runs}}$ is the number of solution points checked, γ_{σ} is the scaling parameter of the fitted Cauchy distribution and MAD_{σ} is the median absolute deviation. \bar{t} is the average time and STD_t is the standard deviation. Note that when N_{runs} is small solution point statistics may not be reliable even though N_{σ} is large, as they come from a small number of different choices of numerical momenta.

vector of real numbers in \mathbb{R}^{16} , and hence collect 48 real numbers for each set of numerical momenta which I refer to as ‘solution points’. I then run the algorithm for statistically many sets of random numerical momenta, and collect all of the solution points together into one data set. A histogram of this data is plotted in Figure 4.5. The data are best fitted by a Cauchy distribution, for which the probability density function has the form

$$\mathbb{P}(x; x_0, \gamma) = \frac{1}{\pi\gamma} \left(\frac{\gamma^2}{(x - x_0)^2 + \gamma^2} \right). \tag{4.3.1}$$

The data are symmetrically distributed around 0, and hence the location parameter $x_0 = 0$. This leaves only one remaining parameter γ , which is tabulated for some cases in Figure 4.3. Apriori it would be expected that γ is a function of n, k and

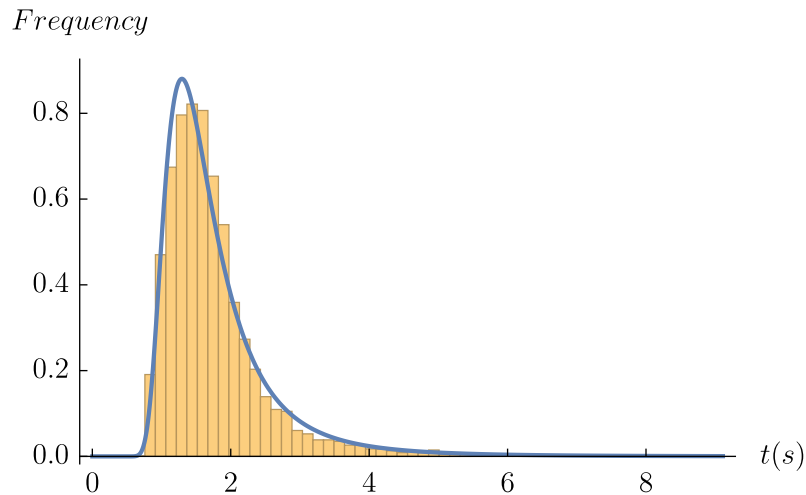


Figure 4.4: Histogram of timings for finding all solutions to the 4D scattering equations for 7559 sets of numerical momenta at 6 pts NMHV using `NSolveScatteringEquations4D`. The blue curve is `FrechetDistribution[3.7, 1.6, -0.2]`, as a best fit by `MATHEMATICA`.

the size of the uniform distribution from which the random momenta are sampled. Some intuition can be used from the analytical result in the MHV sector to reduce this down to just $\gamma = \gamma(n, k)$. Solution points in the MHV sector have a form such as $\text{Re}(\frac{\langle 12 \rangle}{\langle 1r \rangle})$, as shown in Section 3.1. Hence the size of the uniform distribution from which the random events are sampled will divide out statistically, and will not affect the distribution of the solution points. This independence is guaranteed for higher MHV degrees as solutions have mass dimension 0. Performing a statistical analysis of numerical solutions to the scattering equations outside of the MHV sector also verifies these properties, for example as shown in Figure 4.3 where different values for γ are tabulated. The data in Figure 4.3 show that γ is insensitive to k also. I find this independence of γ on n and k to be intriguing and counter-intuitive.

From this analysis, it seems clear that the initial points should be sampled from the relevant Cauchy distribution. However, very many initial points must be sampled for each iteration of the algorithm, and sampling points from Cauchy distribution is significantly slower than sampling from a uniform distribution. I find in practice that it is more efficient to approximate this Cauchy distribution with a uniform

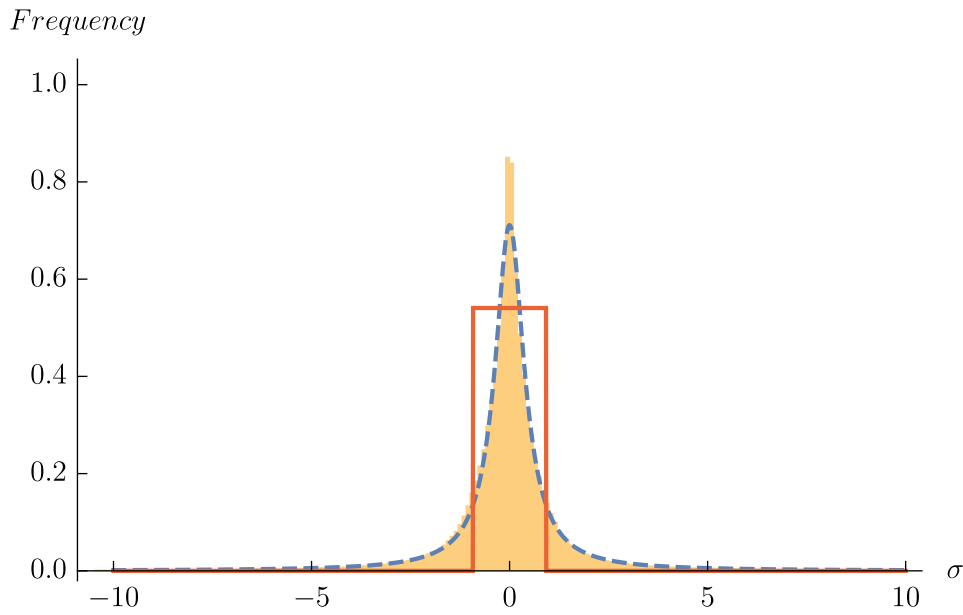


Figure 4.5: Histogram of 43776 solution points at 6 points NMHV taken from 7559 different random momenta. The blue dashed curve is `CauchyDistribution[0,0.447]`, and the red solid curve is an approximation with the uniform distribution $\mathcal{U}([-0.894, 0.894])$.

distribution. To approximate a normal distribution with a uniform distribution, one could choose a symmetric range with a width which is a small multiple of the standard deviation, eg. $\mathcal{U}([-2\sigma, 2\sigma])$. This poses a problem with the Cauchy distribution as it has infinite standard deviation. I use instead the median absolute deviation (MAD), which is roughly equivalent to the γ parameter of the Cauchy distribution, and is tabulated for different n and k in Figure 4.3. To solve the equations for a given n and k , `NSolveScatteringEquations4D` uses the tabulated MAD values from Figure 4.3 to sample initial points from $\mathcal{U}([-2 \text{MAD}, 2 \text{MAD}])$.

When finding solutions by Monte Carlo algorithm, a large percentage ($\sim \frac{3}{4}$) of the solutions tend to be found comparatively quickly, and it can take a long time to find the remaining solutions. It is possible that sampling a certain percentage of the solutions from the approximated uniform distribution and then sampling the remaining solutions from the relevant Cauchy distribution could help to overcome this problem; I leave this for future work.

4.4 Efficient Component Amplitude Extraction

Extracting individual component amplitudes from a super amplitude written as an expansion in Grassmann parameters is a well specified and well understood operation, as explained in Section 2.3. Explicitly evaluating these calculations on the computer is not as simple as the operation itself might suggest. The most naïve application is to expand out the Grassmann super amplitude in terms of each of its factors, and to then throw away any of the terms which are equal to zero either due to $\eta^2 = 0$ or because they do not match the integration measure, but this algorithm is prohibitive in terms of memory usage in the computer. For example a product of $m \in \mathbb{N}$ factors each with a sum of m terms in different Grassmann numbers will result in a total of m^m terms when expanding out naively, nearly all of which are zero. This motivates finding a more efficient algorithm.

In the scattering equation formalism, the Grassmann delta functions are always written in the form $\prod_{l \in L} \delta^{\mathcal{N}} \left(\eta_l - \sum_{r \in R} \frac{\eta_r}{(lr)} \right)$. Integrals of this expression over a subset of the η variables of dimension $k\mathcal{N}$ are a special case of a Grassmann integral of the form $I_G := \int d^m \eta \prod_{i=1}^m \left(\sum_{j=1}^m A_{ij} \eta_j \right)$, where some components of the matrix A are given by worldsheet minors, and the rest are zero. Grassmann integrals of this type can be evaluated in an especially neat analytical form, and it is found that $I_G = \det(A)$. Numerical computation of determinants is generally implemented with an algorithm of time complexity around $O(m^3)$, and hence the Grassmann components can be extracted in a very efficient way using this formula. Grassmann integration of functions of this form then consists simply of assigning the correct values to the matrix A and calculating its determinant. Any product of Grassmann delta functions takes this form, and specifically the fermionic delta functions of the scattering equations, as well as many other standard representations for superamplitudes.

The RAM and time efficiency of this algorithm can be improved further for numerical computations by storing the matrix as a sparse array, where all elements are assumed to be zero unless they are specified (in the case of the 4D scattering equations as

worldsheet minors). The evaluation of the determinant can then be held until explicit numerical values are substituted in for the worldsheet minors, and the determinant of a numerical matrix is all that need be calculated. Calculation in this way is very efficient, saving the need to store large intermediate analytical expressions in the RAM.

4.5 Implementation in Mathematica with `treeamps4dJAF`

`treeamps4dJAF` provides a set of computational tools in MATHEMATICA for analytical and numerical calculation of amplitudes at tree-level. The package's most high-end functions are tailored for calculations in the 4D scattering equation formalism using the techniques derived in Chapters 3 and 4 of this thesis. It is simple within the package to insert new scattering equation integrands and sum them over solutions to the equations, providing a toolbox to explore new theories in which the equations may be relevant. The package also provides functionality for calculating MHV amplitudes analytically with specified external states in the supermultiplets of Yang-Mills and Einstein gravity theories, and graviton multiplets in conformal supergravity. Moving out of the MHV sector the package also provides functionality for solving the scattering equations numerically and using these solutions to calculate amplitudes. At a more low-level analysis of the code, many functions and a framework are provided for analytical computations in general in the spinner helicity formalism for amplitudes, including for example functions for dealing with antisymmetric brackets and the Schouten identity, and for evaluating expressions in terms of momentum twistors numerically.

I include some discussion of the key functions from the package in [1], and in the supporting files of the arXiv submission I provide the MATHEMATICA package along with example code and full documentation, and a lookup table with solutions to

the equations. Numerical solutions to the 4D scattering equations up to 12 points NMHV and 9 points in all MHV sectors are currently accessible to the algorithms of `treeamps4dJAF`, and I tabulate full solution sets with rational external data for these cases in the accompanying data file `SolutionLookupTable.csv` which allows for fast calculation of amplitudes without solving the equations.

Chapter 5

From 4D Scattering Equations to On-Shell Diagrams in $\mathcal{N} = 4$ Super Yang-Mills

In this chapter I develop the theory of scattering amplitudes in $\mathcal{N} = 4$ super Yang-Mills by relating formula derived from on-shell diagrams with those supported on 4D scattering equations, based on my work from [2] and appendix C of [3]. I start with the MHV sector at tree level in Section 5.1, where I first derive a Grassmannian integral formula for the amplitude using on-shell diagrams. I then map the worldsheet expression supported on 4D scattering equations into this Grassmannian integral formula using link variables. I then move to the NMHV sector at tree level in Section 5.2 where I use the same approach, taking into account the fact that this case is more complex as a choice of contour is necessary to specify the Grassmannian integral. I show how to relate the contours arising from the 4D scattering equations and on-shell diagrams by a global residue theorem, and how the three terms arising from on-shell diagrams come from a single top form which can be calculated from a Postnikov diagram. Finally in Section 5.3, I use on-shell diagrams to obtain a new worldsheet formula for the 1-loop four point amplitude via the link variable mapping. This formula is manifestly supersymmetric and supported on new 1-loop scattering

equations refined by MHV degree.

5.1 Tree-level MHV

In this section I derive Grassmannian integral formulae for tree-level MHV amplitudes in $\mathcal{N} = 4$ super Yang-Mills using on-shell diagrams and the 4D scattering equations. The 4D scattering equation formulae can already be thought of as integrals over the Grassmannian $\text{Gr}(2, n)$ if the worldsheet coordinates σ_i are arranged into a $2 \times n$ matrix. For \mathcal{N}^{k-2} MHV amplitudes, this $\text{Gr}(2, n)$ must be mapped into $\text{Gr}(k, n)$ via link variables in order to compare with the expressions obtained from on-shell diagrams, so I will first describe this mapping for MHV amplitudes. I will generalize to non-MHV and 1-loop amplitudes in subsequent sections.

I will first derive the Grassmannian integral formula for MHV amplitudes by mapping the 4D scattering equation formula in (2.11.13) into link variables. This can be accomplished by inserting 1 in the form

$$1 = \int \prod_{l \in L, r \in R} dc_{lr} \delta \left(c_{lr} - \frac{1}{(lr)} \right) \quad (5.1.1)$$

to obtain

$$\begin{aligned} \mathcal{A}_{n,2}^{(0)} = & \int \frac{d^{2 \times n} \sigma}{GL(2)} \prod_{i \in \mathcal{N}} \frac{1}{(i \ i+1)} \prod_{l \in L, r \in R} dc_{lr} \delta \left(c_{lr} - \frac{1}{(lr)} \right) \\ & \times \prod_{l \in L} \delta^{2|4} \left(|l\rangle - \sum_{r \in R} c_{lr} |r\rangle \right) \prod_{r \in R} \delta^2 \left(|r\rangle + \sum_{l \in L} c_{lr} |l\rangle \right) \end{aligned}$$

where the left set is chosen to be $L = \{1, 2\}$. Using $GL(2)$ symmetry to fix $\sigma_1 = \begin{pmatrix} 1 \\ 0 \end{pmatrix}$ and $\sigma_2 = \begin{pmatrix} 0 \\ 1 \end{pmatrix}$, then $(12) = 1$, $(1r) = \sigma_r^2$ and $(2r) = -\sigma_r^1$, the delta functions in the link variables can then be written as

$$\prod_{l \in L, r \in R} \delta \left(c_{lr} - \frac{1}{(lr)} \right) = \prod_{r \in R} \frac{1}{c_{1r}^2 c_{2r}^2} \delta \left(\sigma_r^2 - 1/c_{1r} \right) \delta \left(\sigma_r^1 + 1/c_{2r} \right). \quad (5.1.2)$$

Furthermore, on the support of these delta functions

$$(i \ i+1) = \frac{c_{1i} c_{2i+1} - c_{1i+1} c_{2i}}{c_{1i} c_{2i} c_{1i+1} c_{2i+1}}$$

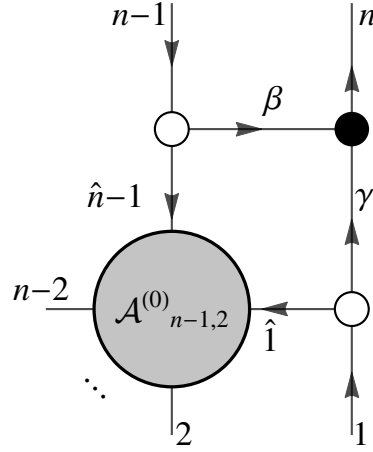


Figure 5.1: On-shell diagram for tree-level n -point MHV amplitude in $\mathcal{N} = 4$ super Yang-Mills in terms of $(n - 1)$ -point MHV amplitude

for $3 \leq i \leq n - 1$. Hence, the worldsheet coordinates are integrated against the delta functions in (5.1.2) the following integrals over link variables are left:

$$\mathcal{A}_{n,2}^{(0)} = \int \frac{d^{2 \times (n-2)} C}{(12) \dots (n1)} \delta^{(2|4) \times 2} (C \cdot \tilde{\lambda}) \delta^{2 \times (n-2)} (\lambda \cdot C^\perp)$$

where the link variables have been arranged into a $2 \times n$ matrix C

$$C = \begin{pmatrix} 1 & 0 & c_{13} & \dots & c_{1n} \\ 0 & 1 & c_{23} & \dots & c_{2n} \end{pmatrix} \quad (5.1.3)$$

and (ij) now refers to a minor of C involving columns i and j rather than an inner product of worldsheet coordinates. If C is thought of as an element of $\text{Gr}(2, n)$, the formula above corresponds to a particular choice of coordinates on this space. The formula for MHV amplitudes can then be written covariantly as follows

$$\mathcal{A}_{n,2}^{(0)} = \int \frac{d^{2 \times n} C}{GL(2) (12) \dots (n1)} \frac{1}{\delta^{2 \times (2|4)}} (C \cdot \tilde{\lambda}) \delta^{(n-2) \times 2} (\lambda \cdot C^\perp). \quad (5.1.4)$$

where the $GL(2)$ allows one to fix four elements of the C -matrix, as done in (5.1.3).

It not difficult to derive this expression directly from on-shell diagrams. Indeed for MHV amplitudes, there is only one on-shell diagram to consider, depicted in Figure 5.1. At n points, it is given by

$$\mathcal{A}_{n,2}^{(0)} = \int \frac{d\beta}{\beta} \frac{d\gamma}{\gamma} \int \frac{d^{2 \times (n-1)} C}{GL(2)} \delta^{2 \times (2|4)} (C \cdot \tilde{\lambda}) \delta^{(n-2) \times 2} (\lambda \cdot C^\perp) \mathcal{I}(\hat{1}, 2, \dots, \hat{n}-1)$$

where \mathcal{I} is the integrand of the $(n-1)$ -point sub-amplitude, without the delta functions. The C matrix can be computed in terms of edge variables following the algorithm in Section 6.1, and is given by

$$C = \begin{pmatrix} 1 & \dots & 0 & \gamma \\ 0 & \dots & 1 & \beta \end{pmatrix},$$

where the rows correspond to legs $(1, n-1)$ and the ellipsis encodes the edge variables of the subdiagram. Noting that $(1\ n-1) = 1$, $(1n) = \beta$, and $(n\ n-1) = \gamma$, the integral over edge variables can be uplifted to the following covariant expression in $\text{Gr}(2, n)$

$$\mathcal{A}_{n,2}^{(0)} = \int \frac{d^{2 \times n} C}{GL(2)} \frac{(1\ n-1)}{(1n)(n\ n-1)} \delta^{2 \times (2|4)} (C \cdot \tilde{\lambda}) \delta^{(n-2) \times 2} (\lambda \cdot C^\perp) \mathcal{I}(\hat{1}, 2, \dots, \hat{n}-1).$$

Using the $GL(2)$ symmetry to set $C = \lambda$, the following recursion relation is obtained for MHV amplitudes

$$\mathcal{A}_{n,2}^{(0)} = \frac{\langle 1\ n-1 \rangle}{\langle 1n \rangle \langle n\ n-1 \rangle} \mathcal{A}_{n-1,2}^{(0)}$$

which is easily solved to give

$$\mathcal{A}_{n,2}^{(0)} = \frac{\delta^{4|8}(P)}{\prod_{i \in \mathcal{N}} \langle i\ i+1 \rangle}.$$

It is easy to see that (5.1.4) is the unique Grassmannian uplift of the above formula, which can be seen by using the $GL(2)$ symmetry to choose $C = \lambda$.

5.2 Tree-level NMHV

In this section I generalize the calculations of Section 5.1 to non-MHV amplitudes, which involves an additional subtlety. Whereas Grassmannian integrals for MHV amplitudes are completely localised by the bosonic delta functions in $C \cdot \tilde{\lambda}$ and $\lambda \cdot C^\perp$, for non-MHV amplitudes there will be more integrals than delta functions so one

must specify a contour in order to make the integrals well-defined. In particular, for an N^{k-2} MHV amplitude there will be $k(n-k)$ integrations and $2n-4$ bosonic delta functions (after subtracting four that impose momentum conservation), so the dimension of the contour will be $(k-2)(n-k-2)$. The precise form of the Grassmannian contour integral will depend on the method one uses to compute the amplitudes. The contour integral implied by BCFW reduces to summing over residues of a single top form in the Grassmannian, each of which corresponds to an on-shell diagram, and can be related to the contour integral arising from the 4D scattering equations using global residue theorems.

To make the discussion as simple as possible I will focus on the example of the 6-point NMHV amplitude, which is the simplest example of a non-MHV amplitude since the contour in the Grassmannian $\text{Gr}(3,6)$ is one-dimensional. I first review how to obtain its Grassmannian integral formula, which was previously derived using various approaches in [28, 78, 72, 120, 73].

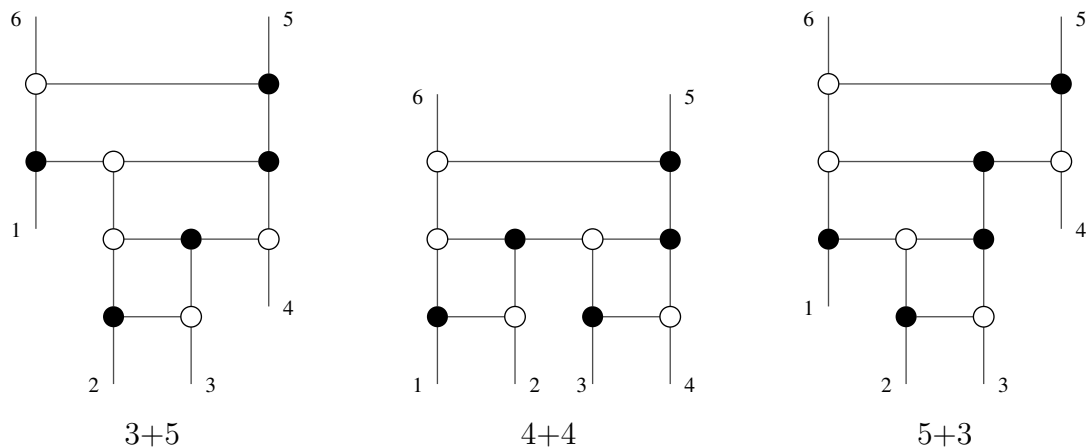


Figure 5.2: On-shell diagrams contributing to the 6-point NMHV amplitude in $\mathcal{N} = 4$ super Yang-Mills

Using the recursion relation defined in Figure 2.2, there are three on-shell diagrams contributing to the 6-point NMHV amplitude, which are shown in Figure 5.2. The first one corresponds to combining a three point $\overline{\text{MHV}}$ diagram with a five point MHV diagram which will be referred to as the 3+5 channel diagram. Secondly two four point diagrams can be pasted together, this channel will be called the 4+4

channel. Finally, a five point $\overline{\text{MHV}}$ can be pasted together with a three point MHV diagram, and this will be referred to as the 5+3 channel.

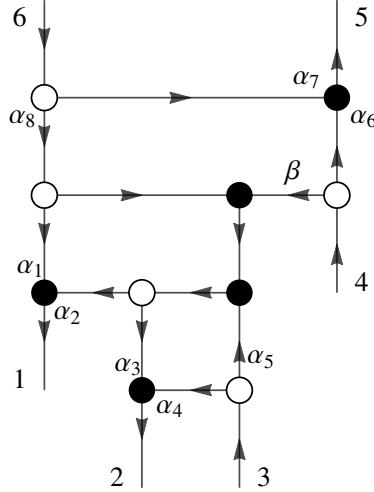


Figure 5.3: The 5+3 channel BCFW diagram contributing to the 6 point NMHV in $\mathcal{N} = 4$ super Yang-Mills. Edge variables are denoted as α_i . The label β is not an edge variable.

On-shell diagrams in $\mathcal{N} = 4$ super Yang-Mills can be evaluated in terms of edge variables using the algorithm defined in Section 2.9. Assigning arrows and variables to the edges of the 5+3 diagram as shown in figure 5.3 gives following formula for the C -matrix by summing over paths between external legs

$$C_{5+3} = \begin{pmatrix} \alpha_2\alpha_5 & \alpha_3\alpha_5 + \alpha_4 & 1 & 0 & 0 & 0 \\ \alpha_2 & \alpha_3 & 0 & 1 & \alpha_6 & 0 \\ \alpha_8(\alpha_1 + \alpha_2) & \alpha_3\alpha_8 & 0 & 0 & \alpha_7 & 1 \end{pmatrix}, \quad (5.2.1)$$

where the rows correspond to legs 3, 4, 6 which have incoming arrows. This matrix has the minor $(456) = 0$, which will ultimately imply a contour in the Grassmannian when writing down a covariant formula for the 5+3 diagram. In order to derive such a formula, first consider the following deformation of the C -matrix,

$$\tilde{C}_{5+3} = \begin{pmatrix} \alpha_2\alpha_5 & \alpha_3\alpha_5 + \alpha_4 & 1 & 0 & \alpha & 0 \\ \alpha_2 & \alpha_3 & 0 & 1 & \alpha_6 & 0 \\ \alpha_8(\alpha_1 + \alpha_2) & \alpha_3\alpha_8 & 0 & 0 & \alpha_7 & 1 \end{pmatrix}. \quad (5.2.2)$$

This deformed matrix now has $(456) = \alpha$ and depends on nine parameters, so it can be used to define an integral over $\text{Gr}(3, 6)$. Using the algorithm in 2.9, the 5+3 diagram is given in terms of edge variables by

$$\mathcal{A}_{6,3}^{(0)}(5+3) = \text{Res}_{\alpha=0} \int \frac{d\alpha}{\alpha} \prod_{i=1}^8 \frac{d\alpha_i}{\alpha_i} \delta^{3 \times (2|4)}(\tilde{C} \cdot \tilde{\lambda}) \delta^{3 \times 2}(\lambda \cdot \tilde{C}^\perp). \quad (5.2.3)$$

Using

$$d^9 \tilde{C} = \alpha_2 \alpha_3 \alpha_8 d\alpha \prod_{i=1}^8 d\alpha_i$$

and

$$(123)(234)(345)(456)(561)(612) = \alpha \alpha_1 \alpha_2 \alpha_3^2 \alpha_4 (\alpha_2 \alpha_5 \alpha_6 - \alpha \alpha_2) \alpha_7 \alpha_8^2,$$

equation (5.2.3) can be uplifted to following covariant formula,

$$\mathcal{A}_{6,3}^{(0)}(5+3) = \text{Res}_{(456)=0} \int d^{3 \times 6} \Omega_4,$$

where $d^{3 \times 6} \Omega_4$ is as defined in (2.9.2).

In summary, I find that the 5+3 diagram arises from a residue of the canonical volume form of $\text{Gr}(3, 6)$. From this, the 3+5 diagram can be calculated immediately by complex conjugating and permuting the external legs. Under this mapping, $[ij] \leftrightarrow \langle ij \rangle$, and $(ijk) \rightarrow \epsilon_{ijkabc}(abc)$ and the permutation $P = \begin{pmatrix} 1 & 2 & 3 & 4 & 5 & 6 \\ 4 & 3 & 2 & 1 & 6 & 5 \end{pmatrix}$ is applied to obtain

$$\mathcal{A}_{6,3}^{(0)}(3+5) = \text{Res}_{(234)=0} \int d^{3 \times 6} \Omega_4 \quad (5.2.4)$$

Finally consider the 4+4 channel diagram, which is oriented and labelled as in figure 5.4. In this case, the (612) minor of the C -matrix vanishes, so the following deformed matrix is considered

$$\tilde{C} = \begin{pmatrix} \alpha_2 & 1 & \alpha_3(\alpha_5 \alpha_6 + \alpha_7) & \alpha_3 \alpha_6 & 0 & 0 \\ \alpha & 0 & \alpha_5 \alpha_6 & \alpha_6 & 1 & 0 \\ \alpha_1 \alpha_4 & 0 & \alpha_4(\alpha_5 \alpha_6 + \alpha_7) + \alpha_5 \alpha_6 \alpha_8 & \alpha_6(\alpha_4 + \alpha_8) & 0 & 1 \end{pmatrix}, \quad (5.2.5)$$

which has been constructed to have the minor $(612) = \alpha$. In terms of edge variables,

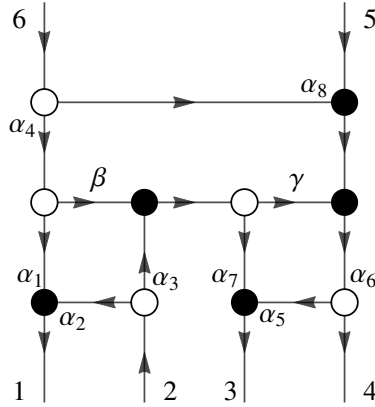


Figure 5.4: The 4+4 channel BCFW diagram contributing to the 6 point NMHV amplitude in $\mathcal{N} = 4$ super Yang-Mills. Edge variables are denoted as α_i . The labels β and γ are not edge variables.

the diagram can be written

$$\mathcal{A}_{6,3}^{(0)}(4+4) = \text{Res}_{\alpha=0} \int \frac{d\alpha}{\alpha} \prod_{i=1}^8 \frac{d\alpha_i}{\alpha_i} \delta^{3 \times (2|4)}(\tilde{C} \cdot \tilde{\lambda}) \delta^{3 \times 2}(\lambda \cdot \tilde{C}^\perp).$$

Noting that

$$d^{3 \times 3} \tilde{C}_{4+4} = \alpha_3 \alpha_4 \alpha_6^3 \alpha_7 d\alpha \prod_{i=1}^8 d\alpha_i$$

and

$$(123)(234)(345)(456)(561)(612) = \alpha \alpha_2 \alpha_3^2 \alpha_4 \alpha_6^3 \alpha_7^2 \alpha_8 (-\alpha_1 \alpha_4 \alpha_5 \alpha_6 + \alpha(\alpha_4(\alpha_5 \alpha_6 + \alpha_7) + \alpha_5 \alpha_6 \alpha_8)), \quad (5.2.6)$$

the 4 + 4 diagram uplifts to the following covariant expression:

$$\mathcal{A}_{6,3}^{(0)}(4+4) = \text{Res}_{(612)=0} \int d^{3 \times 6} \Omega_4. \quad (5.2.7)$$

Note that the 4+4 must be self-conjugate under complex conjugation, and (612) exactly remains invariant under this transformation, paired with the permutation P defined in the 5+3 calculation.

Hence, the full amplitude can be written as a sum of three residues of a single top form

$$\mathcal{A}_{6,3}^{(0)} = \left(\text{Res}_{(234)=0} + \text{Res}_{(456)=0} + \text{Res}_{(612)=0} \right) \int d^{3 \times 6} \Omega_4 \quad (5.2.8)$$

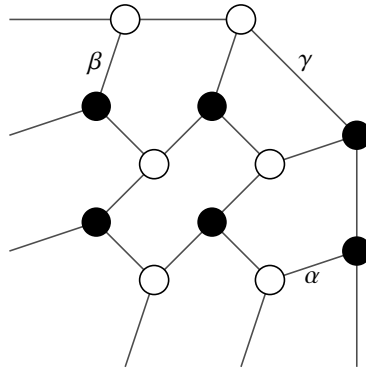


Figure 5.5: Postnikov diagram for the 6 point NMHV amplitude in $\mathcal{N} = 4$ super Yang-Mills

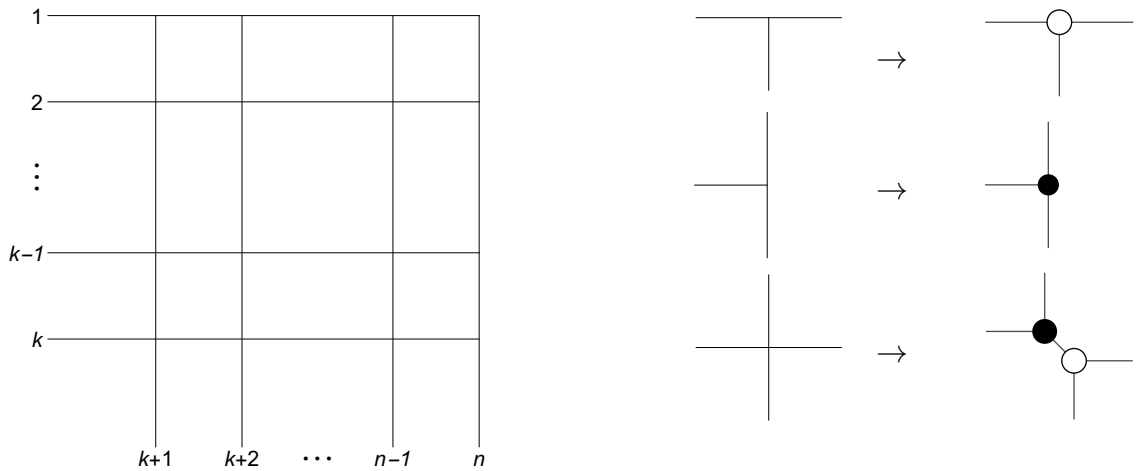


Figure 5.6: Postnikov diagram for n -point N^{k-2} MHV amplitude in $\mathcal{N} = 4$ super Yang-Mills

This can be written as a contour integral if one defines the contour to encircle the three poles in (234), (456), and (612). The existence of such a formula relies on the fact that the three on-shell diagrams in Figure 5.2 can be embedded into a single diagram depicted in Figure 5.5, which is referred to as a Postnikov diagram [121]. In particular, the 3+5, 5+3 and 4+4 diagrams in Figure 5.2 correspond to residues with respect the edge variables α , β and γ respectively, using the square moves and mergers. More generally, the Postnikov diagram for an n -point N^{k-2} MHV amplitude in $\mathcal{N} = 4$ super Yang-Mills can be constructed as in Figure 5.6 [122].

I now derive a Grassmannian contour integral formula for the 6-point NMHV amp-

litude of $\mathcal{N} = 4$ super Yang-Mills using the 4D scattering equation integral formula,

$$\mathcal{A}_{6,3}^{(0)} = \int \frac{d^{2 \times 6} \sigma}{GL(2)} \prod_{i \in \mathcal{N}} \frac{1}{(i \ i+1)} \prod_{l \in L} \delta^{2|4} \left(|l\rangle - \sum_{r \in R} \frac{|r\rangle}{(lr)} \right) \prod_{r \in R} \delta^2 \left(|r\rangle - \sum_{l \in L} \frac{|l\rangle}{(rl)} \right)$$

where I have chosen the left set to be $L = \{1, 3, 5\}$. First multiply by 1 in the form of an integral over link variables

$$1 = \int \prod_{l \in L, r \in R} dc_{lr} \delta \left(c_{lr} - \frac{1}{(lr)} \right)$$

to obtain

$$\begin{aligned} \mathcal{A}_{6,3}^{(0)} &= \int \frac{d^{2 \times 6} \sigma}{GL(2)} \prod_{i \in \mathcal{N}} \frac{1}{(i \ i+1)} \prod_{l \in L, r \in R} dc_{lr} \delta \left(c_{lr} - \frac{1}{(lr)} \right) \\ &\quad \times \prod_{l \in L} \delta^{2|4} \left(|l\rangle - \sum_{r \in R} c_{lr} |r\rangle \right) \prod_{r \in R} \delta^2 \left(|r\rangle + \sum_{l \in L} c_{lr} |l\rangle \right). \end{aligned}$$

Next use the $GL(2)$ symmetry to fix $\sigma_1 = \begin{pmatrix} 1 \\ 0 \end{pmatrix}$ and $\sigma_3 = \begin{pmatrix} 0 \\ 1 \end{pmatrix}$, so that the eight remaining worldsheet coordinates are fixed by eight of the delta functions in the link variables. In particular,

$$\prod_{r \in R} \delta \left(c_{1r} - \frac{1}{(1r)} \right) \delta \left(c_{3r} - \frac{1}{(3r)} \right) = \prod_{r \in R} \frac{1}{c_{1r}^2 c_{3r}^2} \delta \left(\sigma_r^2 - \frac{1}{c_{1r}} \right) \delta \left(\sigma_r^1 + \frac{1}{c_{3r}} \right)$$

and

$$\delta \left(c_{52} - \frac{1}{(52)} \right) \delta \left(c_{54} - \frac{1}{(54)} \right) = \frac{c_{12} c_{34} c_{32} c_{14}}{c_{52}^2 c_{54}^2 (c_{32} c_{14} - c_{12} c_{34})} \delta^2 (\sigma_5 - \sigma_5^*)$$

where

$$\sigma_5^* = \frac{1}{c_{52} c_{54} (c_{32} c_{14} - c_{12} c_{34})} \begin{pmatrix} c_{12} c_{14} (c_{32} c_{54} - c_{34} c_{52}) \\ c_{32} c_{34} (c_{12} c_{54} - c_{14} c_{52}) \end{pmatrix}. \quad (5.2.9)$$

Note that there is one remaining delta function in the link variables which will not be integrated out, and which provides the following constraint on the c_{lr}

$$\delta \left(c_{56} - \frac{1}{(56)} \right) = \frac{c_{52} c_{54} c_{16} c_{36} (c_{32} c_{14} - c_{12} c_{34})}{c_{56}} \delta(S)$$

where

$$S = c_{52}c_{36} (c_{54}c_{16} - c_{56}c_{14}) (c_{12}c_{34} - c_{14}c_{32}) \\ - c_{32}c_{56} (c_{14}c_{36} - c_{16}c_{34}) (c_{52}c_{14} - c_{54}c_{12}).$$

Putting everything together then gives

$$\mathcal{A}_{6,3}^{(0)} = \int d^{3 \times 3} C \frac{(135)\delta(S)}{(123)(345)(561)} \delta^{3(2|4)} (C \cdot \tilde{\lambda}) \delta^{2 \times 3} (\lambda \cdot C^\perp) \quad (5.2.10)$$

where

$$C = \begin{pmatrix} 1 & c_{12} & 0 & c_{14} & 0 & c_{16} \\ 0 & c_{32} & 1 & c_{34} & 0 & c_{36} \\ 0 & c_{52} & 0 & c_{54} & 1 & c_{56} \end{pmatrix}$$

and

$$S = (123)(561)(346)(245) - (125)(136)(456)(234). \quad (5.2.11)$$

Uplifting equation (5.2.10) to a covariant expression in $\text{Gr}(3,6)$ gives a contour integral in the Grassmannian, taking $\delta(S) \rightarrow 1/S$ and defining the contour to encircle the pole at $S = 0$ gives

$$\mathcal{A}_{6,3}^{(0)} = \text{Res}_{S=0} \int \frac{d^{3 \times 6} C}{GL(3)} \frac{1}{S} \frac{(135)}{(123)(345)(561)} \delta^{3 \times (2|4)} (C \cdot \tilde{\lambda}) \delta^{3 \times 2} (\lambda \cdot C^\perp). \quad (5.2.12)$$

A global residue theorem can now be applied to wrap the contour around the other poles of the integrand to obtain

$$\mathcal{A}_{6,3}^{(0)} = \left(\text{Res}_{(123)=0} + \text{Res}_{(345)=0} + \text{Res}_{(561)=0} \right) \int \frac{d^{3 \times 6} C}{GL(3)} \frac{1}{S} \frac{(135)}{(123)(345)(561)} \times \\ \delta^{3 \times (2|4)} (C \cdot \tilde{\lambda}) \delta^{3 \times 2} (\lambda \cdot C^\perp). \quad (5.2.13)$$

Using Plücker identities, S in equation (5.2.11) can be written as

$$S = (135)(234)(456)(612) - (246)(123)(345)(561).$$

Noting that the second term in S can be discarded on support of each of the residues in (5.2.13), it can be seen that (5.2.13) is equivalent to (5.2.8), which was deduced from on-shell diagrams.

In summary, I have obtained two Grassmannian contour integral formulae for the 6-point NMHV amplitude in $\mathcal{N} = 4$ super Yang-Mills using on-shell diagrams and the 4D scattering equations, given by equations (5.2.8) and (5.2.12) respectively. Remarkably, these two contour integrals are related by a global residue theorem.

5.3 One-Loop

In this section I derive a worldsheet formula for the 1-loop four-point integrand in $\mathcal{N} = 4$ super Yang-Mills using on-shell diagrams. The worldsheet formula is manifestly supersymmetric and supported on 4D 1-loop scattering equations refined by MHV degree.

Using the on-shell diagram recursion in Figure 2.2, I find that the 1-loop four-point amplitude can be obtained by applying a forward limit and BCFW bridge to the tree-level 6-point NMHV amplitude, which is described by the three on-shell diagrams in Figure 5.2. After doing so, only the $4 + 4$ channel diagram survives and using square moves and mergers the 1-loop 4-point amplitude can be described by the on-shell diagram in Figure 5.7 (for more details, see [65]), which can be obtained from the diagram in Figure 5.8 by taking the forward limit on legs $-$ and $+$ and attaching a BCFW bridge to legs 1 and 4. The strategy will therefore be to derive a Grassmannian integral formula for Figure 5.8, convert it to a worldsheet formula, and apply a forward limit and BCFW bridge to obtain a worldsheet formula for the 1-loop 4-point amplitude.

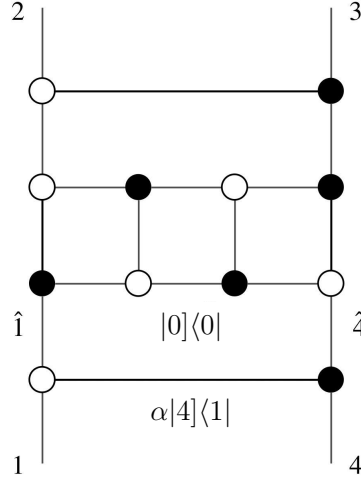


Figure 5.7: On-shell diagram for 1-loop four-point amplitude in $\mathcal{N}=4$ super Yang-Mills

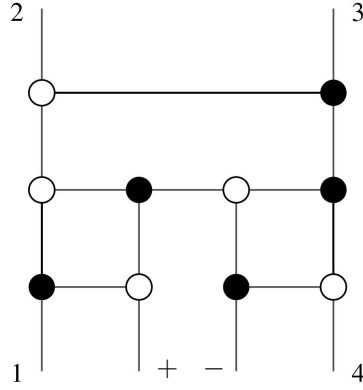


Figure 5.8: On-shell diagram from which Figure 5.7 can be obtained by taking a forward limit and adding a decorated BCFW bridge.

Based on this prescription I define the loop momentum to be the sum of the momenta in these two edges:

$$\ell := |0] \langle 0| + \alpha |4] \langle 1|, \tag{5.3.1}$$

and I define two left and right sets, one for the 4 point amplitude and one for the 6 point diagram before taking the forward limit. Then $L := \{1, 2\}$ and $R := \{3, 4\}$ so that $\mathcal{N} = L \cup R = \{1, 2, 3, 4\}$, and $L' := \{1, 2, -\}$ and $R' := \{3, 4, +\}$, with $\mathcal{N}' = L' \cup R' = \mathcal{N} \cup \{+, -\}$.

The diagram in Figure 5.8 can be obtained from the on in Figure 5.4 by relabelling the external legs according to $P = \begin{pmatrix} 1 & 2 & 3 & 4 & 5 & 6 \\ 1 & + & - & 4 & 3 & 2 \end{pmatrix}$. Applying this relabelling to (5.2.7)

then gives the following Grassmannian integral formula for Figure 5.8:

$$\mathcal{A}_{6,3}^{(0)}{}_{(4+4)'} = \text{Res}_{(012)=0} \int \frac{d^{3 \times 6} C}{GL(3)} \prod_{i \in \mathcal{N}'} \frac{1}{(i \ i+1 \ i+2)} \delta^{3 \times (2|4)}(C \cdot \tilde{\lambda}) \delta^{3 \times 2}(\lambda \cdot C^\perp). \quad (5.3.2)$$

To convert this into a worldsheet formula, it is written in terms of link variables which can then be written in terms of $GL(2)$ covariant minors of the worldsheet σ variables. This can be accomplished by choosing coordinates on the Grassmannian such that

$$C = \begin{pmatrix} c_{1+} & 1 & 0 & c_{13} & c_{14} & 0 \\ c_{2+} & 0 & 1 & c_{23} & c_{24} & 0 \\ 0 & 0 & 0 & c_{-3} & c_{-4} & 1 \end{pmatrix} \quad (5.3.3)$$

where the rows correspond to legs 1, 2, 5. The residue in (5.3.2) sets $c_{-+} = 0$, and hence there are eight link variables which are fixed by eight bosonic delta functions in (5.3.2); recall that the remaining four delta functions enforce momentum conservation. Equation (5.3.2) can then be written as

$$\mathcal{A}_{6,3}^{(0)}{}_{(4+4)'} = \int d^8 C \prod_{i \in \mathcal{N}'} \frac{1}{(i \ i+1 \ i+2)} \delta^{2 \times (2|4)}(C \cdot \tilde{\lambda}) \delta^{3 \times 2}(\lambda \cdot C^\perp)$$

where $d^8 C$ is an integral over the eight link variables in (5.3.3).

The next step is to convert this to a worldsheet integral by introducing six punctures on the 2-sphere with homogeneous coordinates $\sigma_i \in \mathbb{C}^2, i \in \mathcal{N}'$. Setting $\sigma_1 = \begin{pmatrix} 0 \\ 1 \end{pmatrix}$ and $\sigma_2 = \begin{pmatrix} 1 \\ 0 \end{pmatrix}$, the coordinates of the remaining four punctures then provide eight integration variables which match the number of link variables. To map the link variables into worldsheet coordinates, multiply equation (5.3.2) by a factor of 1 in the form

$$1 = \int \prod_{i \in \mathcal{N}'-L} d^2 \sigma_i \left(\prod_{r \in R'} \delta \left(\sigma_r^1 + \frac{1}{c_{1r}} \right) \delta \left(\sigma_r^2 - \frac{1}{c_{2r}} \right) \right) \delta^2(\sigma_- - \sigma_-^*) \quad (5.3.4)$$

where

$$\sigma_-^* = \frac{1}{c_{-3}c_{-4} (c_{14}c_{23} - c_{13}c_{24})} \begin{pmatrix} (c_{14}c_{-3} - c_{13}c_{-4}) c_{23}c_{24} \\ (c_{23}c_{-4} - c_{24}c_{-3}) c_{13}c_{14} \end{pmatrix},$$

which has been chosen so that

$$\delta^2(\sigma_- - \sigma_-^*) = (12)(34) \prod_{r \in R} \frac{1}{(r-)^2} \delta\left(c_{-r} - \frac{1}{(-r)}\right) \quad (5.3.5)$$

in terms of worldsheet minors (ij) . The remaining delta functions in equation (5.3.4) can also be written in terms of worldsheet minors as

$$\prod_{r \in R'} \delta\left(\sigma_r^1 + \frac{1}{c_{1r}}\right) \delta\left(\sigma_r^2 - \frac{1}{c_{2r}}\right) = \prod_{r \in R'} \frac{1}{(1r)^2(2r)^2} \delta\left(c_{1r} - \frac{1}{(1r)}\right) \delta\left(c_{2r} - \frac{1}{(2r)}\right). \quad (5.3.6)$$

Using these expressions it is now straightforward to integrate out the link variables against the delta functions, leaving an integral over worldsheet coordinates. Uplifting the resulting worldsheet integral to a covariant expression in $\text{Gr}(2, n)$ gives,

$$\begin{aligned} \mathcal{A}_{6,3}^{(0)}(4+4)' &= \int \frac{d^{2 \times 6} \sigma}{GL(2)} \prod_{i \in \mathcal{N}'} \frac{1}{(i i+1)} \frac{(14)(+-)}{(1-)(+4)} \delta^{2|4} \left(|-\rangle - \sum_{r \in R} \frac{|r\rangle}{(-r)} \right) \delta^2 \left(|+\rangle - \sum_{l \in L} \frac{|l\rangle}{(+l)} \right) \\ &\quad \times \prod_{l \in L} \delta^{2|4} \left(|l\rangle - \sum_{r \in R} \frac{|r\rangle}{(lr)} - \frac{|+\rangle}{(+)} \right) \prod_{r \in R} \delta^2 \left(|r\rangle - \sum_{l \in L} \frac{|l\rangle}{(rl)} - \frac{|-\rangle}{(-)} \right). \end{aligned}$$

To obtain a worldsheet formula for the 1-loop amplitude from this expression then take a forward limit $|+\rangle \langle +| = -|-\rangle \langle -|$ by setting $(|-\rangle, |-\rangle, \eta_-) = (|+\rangle, -|+\rangle, \eta_+)$, and define a new set of variables for the loop momentum so that $(|0\rangle, |0\rangle, \eta_0) := (|-\rangle, |-\rangle, \eta_-)$, as well as BCFW shifting legs 1 and 4. The loop momentum is then defined as in equation (5.3.1), and the measure in these variables is given by

$$\frac{d^4 \ell}{\ell^2} = \frac{d^2 |0\rangle d^2 |0\rangle d\alpha}{\text{vol GL}(1) \alpha}.$$

Then exchange the definitions of σ_+ and σ_- to give

$$\mathcal{A}_{4,2}^{(1)} = \int \frac{d^4 \ell}{\ell^2} \frac{d^{2 \times 6} \sigma}{GL(2)} \prod_{i \in \mathcal{N}'} \frac{1}{(i i+1)} \frac{(14)(+-)}{(1-)(+4)} \delta^2(\tilde{E}_0^{(1)}) \delta^2(E_0^{(1)}) \prod_{l \in L} \delta^{2|4}(\tilde{E}_l^{(1)}) \prod_{r \in R} \delta^2(E_r^{(1)}), \quad (5.3.7)$$

where the 4 point 1 loop scattering equations refined by MHV degree are given by the zeros of the following functions

$$\tilde{E}_0 := |0\rangle - \sum_r \frac{|r\rangle}{(-r)}, \quad E_0 := |0\rangle - \sum_l \frac{|l\rangle}{(+l)} \quad (5.3.8)$$

$$E_l := |\hat{l}\rangle - \sum_{r \in R} \frac{|r\rangle}{(lr)} + \frac{|0\rangle}{(l+)}, \quad E_r := |\hat{r}\rangle - \sum_{l \in L} \frac{|l\rangle}{(rl)} - \frac{|0\rangle}{(r-)}, \quad (5.3.9)$$

where $|\hat{4}\rangle = |4\rangle - \alpha \langle 1|$, $(|\hat{1}\rangle, \hat{\eta}_1) = (|1\rangle + \alpha |4\rangle, \eta_1 + \alpha \eta_4)$, and the hats act trivially on the other spinors.

The ratio of brackets multiplying the Parke-Taylor factor corresponds to summing over the exchange of σ_+ and σ_- , by the identity

$$\sum_{+\leftrightarrow-} \frac{1}{(-1)(12)(23)(34)(4+)(+-)} = \frac{1}{(-1)(12)(23)(34)(4+)} \frac{(14)}{(+1)(4-)}. \quad (5.3.10)$$

Compared to the tree level equations there are also two auxiliary punctures σ_+ and σ_- which encode the loop momentum. Making the following definition for a 4 point one loop scattering equation delta function

$$\delta^{2 \times 6|4 \times 2}(\text{SE}_{4,L}^{(1)}) := \delta^2(\tilde{E}_0^{(1)}) \delta^2(E_0^{(1)}) \prod_{l \in L} \delta^{2|4}(\tilde{E}_l^{(1)}) \prod_{r \in R} \delta^2(E_r^{(1)}), \quad (5.3.11)$$

the 4 point 1 loop integrand of $\mathcal{N} = 4$ super Yang-Mills can then be written as the following 6 point worldsheet integral supported on 1 loop 4D scattering equations refined by helicity degree

$$\mathcal{A}_{4_2}^{(1)} = \int \frac{d^4 \ell}{\ell^2} \frac{d^{2 \times 6} \sigma}{\text{vol GL}(2)} \left(\frac{1}{(-1) \dots (4+)(+-)} + (+ \leftrightarrow -) \right) \delta^{2 \times 6|4 \times 2}(\text{SE}_{4,L}^{(1)}) \quad (5.3.12)$$

The scattering equations in (5.3.8) have a unique solution on the support of which the worldsheet integral in (5.3.12) gives rise to the standard loop integrand in terms of quadratic Feynman propagators, and I will now solve the equations explicitly to show that the worldsheet integral evaluates to the 4 point 1 loop integrand. After replacing the scattering equations for particles 3 and 4 to give a momentum conservation delta function and gauge fixing the punctures for particles 1 and 2, the

equations form a linear system with solution

$$\sigma_{\text{sol}} = \begin{pmatrix} 1 & 0 & \frac{[34]\langle 12 \rangle}{\langle 1|3+0|4]} & -\frac{[34]\langle 12 \rangle}{\langle 1|4+0|3]} & \frac{\langle 12 \rangle}{\langle 10 \rangle} & \frac{\langle 2|3+0|4]\langle 2|4+0|3]\langle 20 \rangle}{P_{034}^2 \langle 12 \rangle [03][04]} \\ 0 & 1 & \frac{[34]\langle 12 \rangle}{\langle 2|3+0|4]} & -\frac{[34]\langle 12 \rangle}{\langle 2|\hat{4}+0|3]} & \frac{\langle 12 \rangle}{\langle 20 \rangle} & \frac{\langle 1|3+0|4]\langle 1|4+0|3]\langle 0\hat{1}]}{P_{034}^2 \langle 12 \rangle [03][04]} \end{pmatrix},$$

where the columns are labelled 1, 2, 3, 4, +, −, and $P_{034} = |0\rangle \langle 0| + |3\rangle \langle 3| + |4\rangle \langle \hat{4}| = \ell + k_3 + k_4$. The relevant minors of this matrix needed to evaluate the worldsheet integral are given by

$$\begin{aligned} (12) &= 1 & (23) &= -\frac{[34]\langle 12 \rangle}{\langle 1|3+0|4]} \\ (14) &= -\frac{[34]\langle 12 \rangle}{\langle 2|\hat{4}+0|3]} & (34) &= \frac{[34]^3 \langle 12 \rangle^3 P_{034}^2}{\langle 1|3+0|4]\langle 1|4+0|3]\langle 2|3+0|4]\langle 2|\hat{4}+0|3]} \\ (-1) &= -\frac{\langle 1|3+0|4]\langle 1|4+0|3]\langle 0\hat{1}]}{[03][04]\langle 12 \rangle P_{034}^2} & (4+) &= \frac{[34]^2 \langle 12 \rangle^3 \langle 0\hat{4}]}{\langle 2|\hat{4}+0|3]\langle 1|4+0|3]\langle 10 \rangle \langle 20 \rangle} \\ (+1) &= -\frac{\langle 12 \rangle}{\langle 20 \rangle} & (4-) &= \frac{[34]}{[03]}, \end{aligned}$$

and the Jacobian for the system, defined by $\delta^{2 \times 6}(\text{SE}_{4,L}^{(1)}) = J \delta^{(4)}(P) \delta^{(8)}(\sigma - \sigma_{\text{sol}})$, is given by

$$J = \frac{[34]^8 \langle 12 \rangle^8}{P_{034}^2 \langle 1|3+0|4]\langle 1|4+0|3]\langle 2|3+0|4]\langle 2|\hat{4}+0|3]\langle 30 \rangle^2 \langle 40 \rangle^2 \langle 10 \rangle^2 \langle 20 \rangle^2}. \quad (5.3.13)$$

Combining the integrand and Jacobian on support of the solution above, the worldsheet integral can be evaluated to

$$\begin{aligned} \mathcal{A}_{42}^{(1)} &= \int \frac{d^4 \ell}{\ell^2} \int d^{2 \times 6} \sigma \delta^{2 \times 6|4 \times 2}(\text{SE}_{4,L}^{(1)}) \frac{(14)}{(-1)(12)(23)(34)(4+)(+1)(4-)} \\ &= \delta^{4|8}(P) \frac{[34]^2}{\langle 12 \rangle^2} \int \frac{d^4 \ell}{\ell^2 (\ell + k_4)^2 (\ell + k_3 + k_4)^2 (\ell + k_2 + k_3 + k_4)^2}, \end{aligned}$$

noting that $|0\rangle \langle 0| + |4\rangle \langle \hat{4}| = \ell + |4\rangle \langle 4|$, which is the four point amplitude as required.

I now point out some important features of the worldsheet formula for the 1-loop 4-point amplitude in (5.3.7). First note that it contains an integral over the locations of six punctures on a genus-0 worldsheet. Whereas the punctures 1, ..., 4 are associated with the four external particles being scattered, punctures − and + are associated with the two internal particles participating in the forward limit. The

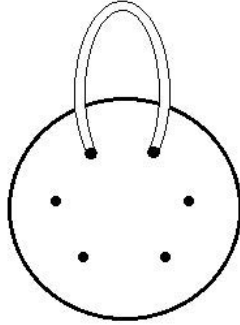


Figure 5.9: The worldsheet configuration describing a 1-loop 4-point amplitude using the 4D scattering equations.

worldsheet can therefore be visualised as Figure 5.9, which corresponds to a non-separating degeneration of a genus-1 worldsheet (similar to the 1-loop amplitudes of 10D ambitwistor string theory [33]). The integral over loop momentum is implemented by decomposing it according to (5.3.1) and integrating over the forward limit momentum $|0\rangle\langle 0|$ and BCFW shift parameter α which appear in the 1-loop scattering equations in (5.3.8). Note that (5.3.7) is manifestly supersymmetric and does not contain Pfaffians, so is simpler than previous worldsheet formulae for 1-loop amplitudes. On the other hand, it must be regulated when integrating over loop momentum since it is intrinsically four-dimensional.

A natural question is then how to extend this formula to higher points, which is currently unclear. At five points, there are three on-shell diagrams, two of which encode the forward limit of a 7-point tree-level amplitude and one of which encodes a one-loop four-point amplitude dressed with a soft factor, as explained in more detail in [3]. Although it is straightforward to map each on-shell diagram into a worldsheet integral, it is unclear how to combine them into a single worldsheet formula because the scattering equations associated with the soft term appear to be incompatible with those encoding the forward limit. The natural generalisation of (5.3.12) to n points is

$$\mathcal{A}_n^{(1),\text{FL}} = \int \frac{d^4\ell}{\ell^2} \frac{d^{2\times(n+2)}}{\text{vol GL}(2)} \left(\prod_{i \in \mathcal{N} \cup \{+, -\}} \frac{1}{(i i + 1)} + (+ \leftrightarrow -) \right) \delta(\text{SE}), \quad (5.3.14)$$

which evaluates to the forward limit contribution to a general n -point one-loop N^k MHV amplitude, rather than evaluating to the full integrand. The intuition coming from these formulae of adding a BCFW shift to a worldsheet expression lead to n -point worldsheet formulae with quadratic propagators in the general dimensional formalism in [3].

Chapter 6

On-Shell Diagrams in $\mathcal{N} = 8$

Supergravity

In this chapter I extend the theory of on-shell diagrams in $\mathcal{N} = 8$ supergravity first considered in [70], based on my work from [4]. I start by describing a streamlined algorithm for computing on-shell diagrams in this setting in Section 6.1. I then derive the Hodges form of the tree level MHV amplitude in Section 6.2, starting with a Grassmannian integral formula for the amplitude using on-shell diagrams, and then mapping the worldsheet expression supported on 4D scattering equations into this Grassmannian integral formula using link variables. In Section 6.3 I derive a simplified version of the BGK formula for the tree level MHV amplitude, using a planar recursion in the on-shell diagram formalism. I then move to the NMHV sector at tree level in Section 6.4 where I derive a Grassmannian expression for the 6 point NMHV amplitude using a planar on-shell diagram recursion. I show that the three terms arising from on-shell diagrams cannot be calculated from a single top form as in $\mathcal{N} = 4$ super Yang-Mills. In Section 5.3, I use on-shell diagrams to obtain a new worldsheet formula for the 1-loop four point amplitude in $\mathcal{N} = 8$ supergravity via the link variable mapping. As with $\mathcal{N} = 4$ super Yang-Mills in Chapter 5, this formula is manifestly supersymmetric and supported on new 1-loop scattering equations refined by MHV degree. In Section 6.6 I explain how to incorporate the bonus relations for

$\mathcal{N} = 8$ supergravity into on-shell diagrams in the MHV sector, and in Section 6.7 I derive identities relating spinor brackets to minors appearing in Grassmannian integral formulae which are necessary for the analysis in other sections.

6.1 Algorithm for Computing On-Shell Diagrams

In this section I provide a streamlined version of the algorithm for calculating on-shell diagrams in $\mathcal{N} = 8$ supergravity in terms of Grassmannian integral formulae which I review in Section 2.9. In particular, given a decorated on-shell diagram computed from the recursion relations described in Section 2.9;

1. Choose a perfect orientation for the diagram by drawing arrows on each edge such that there are two arrows entering and one arrow leaving every black node, and two arrows leaving and one arrow entering every white node.
2. Label every half-edge with an edge variable α so that there are two variables for each internal edge (one associated with each of the two vertices attached to the edge). Then set one of the two edge variables on each internal edge to unity, and set one of the remaining variables associated with each vertex to unity. There will be $2n - 4$ edge variables remaining after this step.
3. To construct the integrand, include a factor of $d\alpha/\alpha^2$ for each edge variable leaving a white vertex or entering a black vertex and $d\alpha/\alpha^3$ for each edge variable entering a white vertex or leaving a black vertex.
4. Now include decorations associated with the BCFW bridges and spinor bracket factors associated with the vertices. The spinor brackets at the bridges cancel with the bridge decoration to leave only edge variables. This step can be summarised as:

- (a) For each BCFW bridge, look at the sub-diagram formed only by this bridge, its two vertices, and the four legs attached to it.
- If there is only one path through the sub diagram which includes the bridge, assign a factor of the edge variable on the bridge, divided by the two edge variables on the legs which are not on that path.
 - If there are four possible paths through the sub diagram, divide through by a factor of each of the edge variables on the external legs, and the edge variable on the bridge squared.

If there is no edge variable in any of the locations described above, then this edge variable was set to unity in step 2.

- (b) For each remaining black vertex not attached to a bridge, add a factor of $\langle ij \rangle$ where i, j are the two edges with ingoing arrows. For each remaining white vertex not associated to a bridge, add a factor of $[ij]$ where i, j are the two edges with outgoing arrows.

5. Now it is necessary to relate all internal spinors to external spinors. This can be done algorithmically by noting that all spinors are related to each other by

$$\begin{aligned} |i\rangle &= \sum_{\text{paths } j \rightarrow i} \left(\prod_{\text{edges in path } e} \alpha_e \right) |j\rangle \\ [i] &= \sum_{\text{paths } i \rightarrow j} \left(\prod_{\text{edges in path } e} \alpha_e \right) [j]. \end{aligned} \quad (6.1.1)$$

In practice however it is often possible obtain simpler expressions using the relations between square and angle brackets at each vertex given in figure 6.1.

6. Calculate the C -matrix in terms of the coordinates assigned to the diagram by associating each column with an external leg and each row with an ingoing external leg. The element C_{ij} can then be computed by summing over all paths from leg i to leg j taking the product of all the edge variables encountered along the path as in the first line of (6.1.1). Similarly, the C^\perp matrix can be computed by summing over the reverse paths as in the second line of (6.1.1).

After doing so, include the following delta functions in the integrand

$$\delta^{k \times (2|8)}(C \cdot \tilde{\lambda} | C \cdot \eta) \delta^{(n-k) \times 2}(\lambda \cdot C^\perp).$$

7. If the diagram contains closed loops, include a factor of $\mathcal{J}^{\mathcal{N}-4}$, where \mathcal{J} is a sum over products of disjoint closed loops [71]:

$$\mathcal{J} = 1 + \sum_i f_i + \sum_{\text{disjoint } i,j} f_i f_j + \sum_{\text{disjoint } i,j,k} f_i f_j f_k + \dots$$

and f_i is minus the product of edge variables around the i 'th closed loop. Note that when there are many closed loops then diagrams become complex to calculate, and a method to work with these cases is given in [123].

8. The above procedure gives an expression for the on-shell diagram as a Grassmannian integral in terms of specific coordinates. This can be uplifted to a covariant expression by expressing the rest of the integrand in terms of minors. This results in an $\text{SL}(k)$ invariant expression, but the overall $\text{GL}(1)$ scaling of the $\text{GL}(k)$ gauge freedom will not be correct in general. There will always be one minor which is gauged fixed to be equal to unity, and the correct number of factors of this minor should be included in the integrand to give an overall $\text{GL}(1)$ weight of zero to the integrand. Note that $d^{k \times n} \Omega_{\mathcal{N}}$ in (2.9.2) has $\text{GL}(1)$ weight $\mathcal{N} - 4$. For on-shell diagrams contributing to non-MHV amplitudes, this lift will specify a nontrivial contour in the Grassmannian. Details of this process for 6 point NMHV amplitudes in $\mathcal{N} = 8$ supergravity are explained in Section 6.4.

6.2 Hodges Formula for Tree-level MHV

In this section, I will derive a new Grassmannian integral formula for the MHV amplitudes of $\mathcal{N} = 8$ supergravity, generalising the results obtained using on-shell diagrams in [70] to n points. As with $\mathcal{N} = 4$ super Yang-Mills in Section 5.1, start

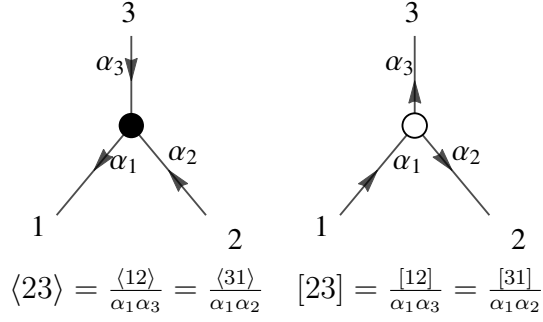


Figure 6.1: Relations between spinor bracket factors at each vertex of an on-shell diagram in $\mathcal{N} = 8$ supergravity

by multiplying 1 in the form of integrals of delta functions as in equation (5.1.1) into the 4D scattering equation formula from Section 2.8 to give

$$\begin{aligned} \mathcal{M}_{n,2}^{(0)} = & \int \frac{d^{2 \times n} \sigma}{GL(2)} \prod_{l \in L, r \in R} dc_{lr} \delta \left(c_{lr} - \frac{1}{(lr)} \right) \det' \mathcal{H} \det' \tilde{\mathcal{H}} \\ & \times \prod_{l \in L} \delta^{2|8} (|l\rangle - c_{lr} |r\rangle) \prod_{r \in R} \delta^2 (|r\rangle + c_{lr} |l\rangle) \end{aligned} \quad (6.2.1)$$

where I have chosen $L = \{1, 2\}$. Using the $GL(2)$ symmetry to fix $\sigma_1 = \begin{pmatrix} 1 \\ 0 \end{pmatrix}$ and $\sigma_2 = \begin{pmatrix} 0 \\ 1 \end{pmatrix}$, the delta functions can be written in the link variables as in (5.1.2), and on the support of these delta functions

$$(ij) = \frac{c_{1j} c_{2i} - c_{1i} c_{2j}}{c_{1i} c_{2i} c_{1j} c_{2j}},$$

where (ij) are the minors of σ , and $i, j \in R$. Next remove row and column 1 from \mathcal{H} , and remove row and column n from $\tilde{\mathcal{H}}$ and additionally rescaling the i 'th row of $\tilde{\mathcal{H}}$ by $c_{1i} c_{2i}$ and the j 'th column by $c_{1j} c_{2j}$. Then $\det' \mathcal{H} = \langle 12 \rangle$, $\tilde{\mathcal{H}}$ reduces to

$$\tilde{\mathcal{H}}_{rr} = - \sum_{r' \neq r} \frac{[rr']}{c_{1r} c_{2r'} - c_{1r'} c_{2r}} \frac{c_{1r'} c_{2r'}}{c_{1r} c_{2r}}, \quad \tilde{\mathcal{H}}_{rr'} = \frac{[rr']}{c_{1r} c_{2r'} - c_{1r'} c_{2r}}, \quad r \neq r',$$

where $r, r' \in \{3, \dots, n-1\}$, and the rescaling of the rows multiplies $\det' \tilde{\mathcal{H}}$ by a factor of $\prod_{r=3}^{n-1} c_{1r}^2 c_{2r}^2$.

Integrating out the worldsheet coordinates in (6.2.1) against the delta functions in (5.1.2) then leaves the following integral over link variables

$$\mathcal{M}_{n,2}^{(0)} = \int \frac{d^{2 \times (n-2)} C \langle 12 \rangle}{GL(2)} \frac{\det \tilde{\mathcal{H}}}{(12)^2 (2n)^2 (n1)^2} \delta^{2 \times (2|8)} (C \cdot \tilde{\lambda}) \delta^{(n-2) \times 2} (\lambda \cdot C^\perp),$$

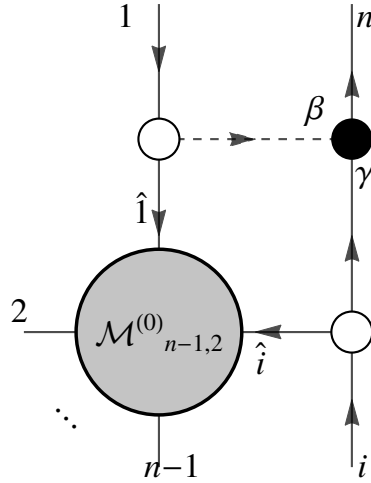


Figure 6.2: On-shell diagram contributing to tree-level n -point MHV tree amplitude in $\mathcal{N} = 8$ supergravity

where (ij) now refers to the minors of C . Note that on the support of the delta functions, $\frac{\langle 12 \rangle}{(12)}$ is invariant under permutations and hence can be replaced with $\frac{\langle pq \rangle}{(pq)}$ for any $p, q \in \mathcal{N}$. For a derivation of this identity relating spinor brackets to minors, as well as a generalisation to higher MHV degree, see Section 6.7.

Uplifting the expression in equation (6.2) to a covariant expression in $\text{Gr}(2, n)$ gives

$$\mathcal{M}_{n,2}^{(0)} = \int \frac{d^{2 \times n} C \langle pq \rangle}{GL(2) (pq) (ab)^2 (bc)^2 (ca)^2} \frac{\det \tilde{\mathcal{H}}}{\delta^{2 \times (2|8)} (C \cdot \tilde{\lambda}) \delta^{(n-2) \times 2} (\lambda \cdot C^\perp)}, \quad (6.2.2)$$

where $a, b, c \in \mathcal{N}$ are distinct, and

$$\tilde{\mathcal{H}}_{ii} = - \sum_{j \in \mathcal{N} \setminus \{a,b,c\}} \frac{[ij] (aj)(bj)}{(ij) (ai)(bi)}, \quad \tilde{\mathcal{H}}_{ij} = \frac{[ij]}{(ij)}, \quad i \neq j$$

where $i, j \in \mathcal{N} \setminus \{a, b, c\}$.

To obtain Hodge’s formula for the MHV amplitude from on-shell diagrams directly, it is necessary to incorporate the bonus relations of $\mathcal{N} = 8$ supergravity, which I explain in detail in Section 6.6. These relations are incorporated into the on-shell diagram recursion for MHV amplitudes by modifying the bridge decoration, and for the diagram in Figure 6.2 the modified bridge decoration is given by

$$B_{12n;i} = \frac{\langle i2 \rangle}{\langle 1i \rangle \langle n2 \rangle [1n]}.$$

Using this modified bridge decoration the full amplitude is obtained by summing the diagram over $i \in \{3, \dots, n-1\}$. In terms of the edge variables on the diagram in figure 6.2, the amplitude is

$$\begin{aligned} \mathcal{M}_{n,2}^{(0)} &= \sum_{i=3}^{n-1} \int \frac{d\beta d\gamma}{\beta^2 \gamma^2} [\beta \hat{1}] [\gamma \hat{i}] \langle \gamma \beta \rangle B_{12n;i} \int \frac{d^{2 \times (n-1)} C}{GL(2)} \delta^{2 \times (2|8)} (C \cdot \tilde{\lambda}) \\ &\quad \times \delta^{(n-2) \times 2} (\lambda \cdot C^\perp) \mathcal{I}_{n-1} (\hat{1}, 2, \dots, \hat{i}, \dots, n-1) \end{aligned} \quad (6.2.3)$$

where \mathcal{I} is the integrand of the $\text{Gr}(2, n-1)$ integral in the $(n-1)$ -point amplitude without the delta functions. Noting that

$$[\beta \hat{1}] [\gamma \hat{i}] \langle \gamma \beta \rangle = \beta \gamma [n1] [ni] \langle i1 \rangle,$$

equation 6.2.3 reduces to

$$\begin{aligned} \mathcal{M}_{n,2}^{(0)} &= \sum_{i=3}^{n-1} \frac{[ni] \langle i2 \rangle}{\langle n2 \rangle} \int \frac{d\beta d\gamma}{\beta \gamma} \int \frac{d^{2 \times (n-1)} C}{GL(2)} \delta^{2 \times (2|8)} (C \cdot \tilde{\lambda}) \times \\ &\quad \delta^{(n-2) \times 2} (\lambda \cdot C^\perp) \mathcal{I}_{n-1} (\hat{1}, 2, \dots, \hat{i}, \dots, n-1). \end{aligned}$$

For the diagram in Figure 6.2, the C -matrix is given by

$$C = \begin{pmatrix} 1 & \dots & 0 & \dots & \beta \\ 0 & \dots & 1 & \dots & \gamma \end{pmatrix}$$

where the rows correspond to particles 1 and i , and the indicated columns correspond to particles 1, i and n . For this C -matrix, $(ni) = \beta$, $(1n) = \gamma$, and $(1i) = 1$, so the amplitude can be written covariantly in $\text{Gr}(2, n)$ as

$$\begin{aligned} \mathcal{M}_{n,2}^{(0)} &= \sum_{i=3}^{n-1} \frac{[ni] \langle i2 \rangle}{\langle n2 \rangle} \int \frac{d^{2 \times n} C}{GL(2)} \frac{(1i)}{(in)(1n)} \delta^{2 \times (2|8)} (C \cdot \tilde{\lambda}) \\ &\quad \times \delta^{(n-2) \times 2} (\lambda \cdot C^\perp) \mathcal{I}_{n-1} (\hat{1}, 2, \dots, \hat{i}, \dots, n-1). \end{aligned}$$

Using the $GL(2)$ symmetry to set $C = \lambda$, the following recursion relation for MHV amplitudes is then obtained

$$\mathcal{M}_{n,2}^{(0)} = \sum_{i=3}^{n-1} \frac{[in] \langle 1i \rangle \langle 2i \rangle}{\langle in \rangle \langle 1n \rangle \langle 2n \rangle} \mathcal{M}_{(n-1),2}^{(0)} (\hat{1}, 2, \dots, \hat{i}, \dots, n-1).$$

This is the recursion relation obtained by Hodges in [124], with solution [22] given by

$$\mathcal{M}_{n,2}^{(0)} = \frac{\delta^{4|16}(P)\det\tilde{\mathcal{H}}}{\langle 12 \rangle^2 \langle 2n \rangle^2 \langle n1 \rangle^2},$$

where the MHV Hodges matrix \mathcal{H} is defined in equation 2.5.8, with $\{a, b, c\} = \{1, 2, n\}$. Equation (6.2.2), as calculated by first mapping the 4D scattering equation expression to a Grassmannian integral, is the unique Grassmannian uplift of (6.2).

6.3 BGK Formula for Tree-level MHV

In this section I solve the planar on-shell diagram recursion relations for MHV amplitudes and obtain the BGK formula [125] in a slightly simplified form, showing that this formula arises naturally from a planar object. The full MHV amplitude can then be obtained by summing this expression over permutations of $(n-3)$ legs, which I verify against the Hodges matrix expression numerically. Although the physical interpretation of this planar object is not clear, it would be interesting to see if it has a geometric interpretation as the volume of some object.

At n points in the MHV sector there is only one planar BCFW diagram to consider as in $\mathcal{N} = 4$ super Yang-Mills in Section 5.1, and the diagram is generated from the $(n-1)$ point planar diagram by adding an inverse soft factor as depicted in Figure 6.2. Two of the legs are fixed in the recursion, and the modified bridge decoration proposed in Section 6.6 can be used to fix an additional leg so that the full amplitude is obtained by summing over permutations of $n-3$ particle labels. The permutation sum is then over a bonus-simplified decorated planar on-shell diagram, which I denote $\mathcal{A}_{n,2}^{(0)*}$. Starting with $\mathcal{A}_{4,2}^{(0)*}$ as the base case of the recursion, with the orientation and labelling in figure 6.3, the 4-point C matrix can be read off as

$$C^4 = \begin{pmatrix} 1 & \alpha_1 & 0 & \alpha_3 \\ 0 & \alpha_2 & 1 & \alpha_4 \end{pmatrix}. \quad (6.3.1)$$

To calculate $\mathcal{A}_{4,2}^{(0)*}$ include a factor $\langle \alpha_2 \alpha_1 \rangle [\alpha_2 \alpha_4] B_{234,1} = \frac{\alpha_2}{\alpha_1} \frac{\langle 23 \rangle \langle 14 \rangle}{\langle 31 \rangle \langle 24 \rangle}$ from the bridge, a

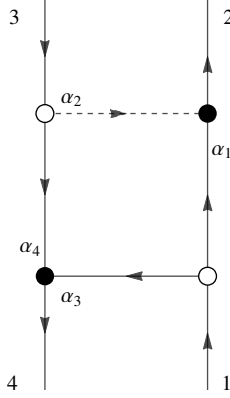


Figure 6.3: Bonus-simplified on-shell diagram for 4-point amplitude

factor of one over each edge variable, and spinor bracket factors of $\langle 13 \rangle$ and $\alpha_1 [12]$ from the two lower vertices not attached to the bridge. The diagram then evaluates to

$$\mathcal{A}_{4,2}^{(0)*} = \int d^{2 \times 4} \Omega_8 \frac{\langle 13 \rangle [12] \langle 23 \rangle \langle 14 \rangle}{\alpha_1 \alpha_3 \alpha_4 \langle 31 \rangle \langle 24 \rangle}, \quad (6.3.2)$$

which can be uplifted to a covariant expression as

$$\mathcal{A}_{4,2}^{(0)*} = \int d^{2 \times 4} \Omega_8 \frac{\langle 13 \rangle [12]}{(\overline{13})^2 (\overline{34}) (\overline{24})}, \quad (6.3.3)$$

where $d^{2 \times 4} \Omega_4$ is defined in (2.9.2). Since this expression has been computed using the bonus relations it needs to be summed over $n-3$ permutations of external states. In this case there are only $4-3 = 1$ permutations, and the diagram is equal to the full 4 point amplitude in $\mathcal{N} = 8$ supergravity,

$$\mathcal{A}_{4,2}^{(0)*} = \mathcal{M}_{4,2}^{(0)} = \int \frac{d^{2 \times 4} C}{\text{Vol}(\text{GL}(2))} \frac{\delta^{2 \times (2|8)}(C \cdot \tilde{\lambda}) \delta^{2 \times 2}(\lambda \cdot C^\perp)}{\prod_{i < j} (ij)} \frac{\langle ab \rangle [cd]}{(\overline{ab}) (\overline{cd})^\perp},$$

where $a \neq b \in \mathcal{N}$ and $c \neq d \in \mathcal{N}$.

Equation (6.3.3) can be rearranged using momentum conservation and by identifying label 5 with label 1 at 4 points to give the following expression,

$$\mathcal{A}_{4,2}^{(0)*} = \int d^{2 \times 4} \Omega_8 \frac{\langle ab \rangle [12] (35) (14)}{(\overline{ab}) (\overline{13})^2 (\overline{34}) (\overline{45}) (\overline{24})}, \quad (6.3.4)$$

which is in a more convenient form to use as the base case for the recursion.

To calculate $\mathcal{A}_{n,2}^{(0)*}$ it is then necessary to choose an orientation and labelling which

can be extended to higher points in a recursive fashion. First use the planar BCFW recursion to add the appropriate inverse soft factor onto legs 1 and 2. Then to produce an n point diagram where the paths remain unchanged compared to the $n-1$ point diagram, apply a cyclic rotation to the labels so that the top inverse soft factor is labelled with legs 1, 2 and 3 and the bottom left black vertex is labelled as leg 4. Performing the recursion in this way and relabelling can be thought of as cutting the orientation of diagram to insert the new inverse soft factor, as shown in Figure 6.4. Note that in this process, BCFW recursion is always carried out in the standard way and the diagram itself is never really cut, it is only the unphysical orientation of the diagram which is cut. Constructing the diagrams in this way allows for a simple recursive calculation of the C matrix, which I denote as C^n at n -points.

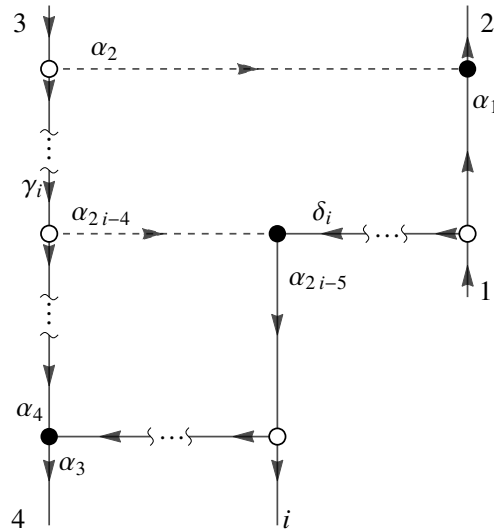


Figure 6.4: On-shell diagram showing how 4-point seed amplitude orientation is cut, and an inverse soft factor is inserted for $i \in \{5, \dots, n\}$

Now consider how to build up C^n from C^{n-1} and the paths through the new inverse soft factor. As the orientation and labelling remain the same on the top inverse soft factor, the first three rows of the C matrix are the same for all n , and it is only necessary to calculate paths through the diagram for the remaining rows of the diagram for $i \in \{4, \dots, n\}$. Each path from 1 to i remains the same except for an extra factor of α_{2n-5} from the new inverse soft factor, and there is now a new path

from 3 to i additional to all of the previous paths. The new path is the same as the longest path from 1 to i in the n point diagram, with an extra factor of $\alpha_{2n-5}\alpha_{2n-4}$ from the new inverse soft factor. Finally, the path from 1 to n picks up only α_{2n-5} and from 3 to n has $\alpha_{2n-5}\alpha_{2n-4}$. Then C^m can be written recursively in terms of C^{m-1} as

$$\begin{aligned}
(C^n)_{ai} &= (C^4)_{ai}, & i \in \{1, 2, 3\}, a \in \{1, 2\} \\
(C^n)_{1i} &= \alpha_{2n-5}(C^{m-1})_{1i}, & i \in \{4, \dots, n-1\} \\
(C^n)_{2i} &= (C^{m-1})_{2i} + \alpha_{2n-5}\alpha_{2n-4}(C^{m-1})_{1i}, & i \in \{4, \dots, n-1\} \\
(C^n)_{1n} &= \alpha_{2n-5} \\
(C^n)_{2n} &= \alpha_{2n-5}\alpha_{2n-4}.
\end{aligned} \tag{6.3.5}$$

Next look at how to relate $\mathcal{A}_{n,2}^{(0)*}$ to $\mathcal{A}_{n-1,2}^{(0)*}$. Because of the way the labelling and orientation have been chosen, the vertex and bridge factors coming from the top inverse soft factor in Figure 6.4 are the same for $\mathcal{A}_{n,2}^{(0)*}$ as for $\mathcal{A}_{n-1,2}^{(0)*}$, apart from an additional factor α_{2n-5} . The algorithm in Section 6.1 shows that it is necessary to multiply by the bridge and vertex factors in the cut inverse soft factor for $i = n$ to complete the recursion. The bridge factor is $B_{\gamma_n\delta_n4;n}$, the left hand white vertex contributes a factor $\frac{\langle\alpha_{2n-4}\gamma_{n-1}\rangle}{\alpha_{2n-4}}$, the black vertex a factor $\frac{\langle\alpha_{2n-4}\delta_n\rangle}{\alpha_{2n-5}^2}$, and the white vertex attached to leg n a factor $\sum_{j=4}^{n-1} \left(\prod_{k=j}^{n-1} \alpha_{2k-5} \right) [ji]$. The recursion relation is then

$$\mathcal{A}_{n,2}^{(0)*} = \mathcal{A}_{n-1,2}^{(0)*} \frac{\langle\alpha_{2n-4}\delta_n\rangle [\alpha_{2n-4}\gamma_{n-1}] B_{\gamma_n\delta_n4;n}}{\alpha_{2n-4}\alpha_{2n-5}} \sum_{j=4}^{n-1} \left(\prod_{k=j}^{n-1} \alpha_{2k-5} \right) [jn]. \tag{6.3.6}$$

The bridge factor and the new spinor bracket factors in this expression are written in terms of internal spinors at each vertex, which must be related to external spinors to evaluate the recursion. These factors simplify to

$$\langle\alpha_{2n-4}\delta_n\rangle [\alpha_{2n-4}\gamma_{n-1}] B_{\gamma_n\delta_n4;n} = \alpha_{2n-4} \frac{\langle\gamma_n\delta_n\rangle \langle n4\rangle}{\langle\delta_n4\rangle \langle\gamma_n n\rangle} = \alpha_{2n-4} \frac{\langle 3\ n+1\rangle \langle 4n\rangle}{\langle 3n\rangle \langle 4\ n+1\rangle},$$

where the first equality substitutes the expression for the bridge factor, and the second uses that $|\gamma_n\rangle = |3\rangle$, and $|\delta_i\rangle = |1\rangle = |n+1\rangle$. Based on this the recursion relation simplifies to

$$\mathcal{A}_{n,2}^{(0)*} = \mathcal{A}_{n-1,2}^{(0)*} \frac{1}{\alpha_{2n-5}} \frac{\langle 3 \ n+1 \rangle \langle 4n \rangle}{\langle 3n \rangle \langle 4 \ n+1 \rangle} \sum_{j=4}^{n-1} \left(\prod_{k=j}^{n-1} \alpha_{2k-5} \right) [jn]. \quad (6.3.7)$$

To uplift to a covariant expression in $\text{Gr}(2, n)$ next calculate the necessary minors of C^n , denoted $(ab)_n$. Recall that for $n = 4$, leg 5 is defined to be leg 1 so for example $(45)_4 := (41)_4 = \alpha_4$, and in general $(45)_n = \alpha_{2n-5}(45)_{n-1}$. The remaining minors needed can be read off from the n point C matrix as

$$\begin{aligned} (13)_n &= 1 \\ (23)_n &= \alpha_1 \\ \frac{(3j)_n}{(3i)_n} &= \prod_{k=j}^{i-1} \alpha_{2k-5}, \quad j < i \in \{4, \dots, n\}. \end{aligned} \quad (6.3.8)$$

Using these results is possible to solve the recursion in equation (6.3.7) and uplift. The factor α_{2n-5}^{-1} is absorbed in changing the $(45)_{n-1}$ in $\mathcal{A}_{n-1,2}^{(0)*}$ to $(45)_n$, and the other edge variables are uplifted using (6.3.8). The final result for the planar MHV diagram is then

$$\begin{aligned} \mathcal{A}_{n,2}^{(0)*} &= \int d^{2 \times n} \Omega_8 \frac{\langle ab \rangle}{(ab)} \frac{[12](35)(14)}{(13)^2(24)(34)(45)} \prod_{i=5}^n \frac{(3 \ i+1)(4i) \sum_{j=4}^{i-1} (3j)[ji]}{(3i)(4 \ i+1) (3i)} \\ &= \int d^{2 \times n} \Omega_8 \frac{\langle ab \rangle}{(ab)} \frac{1}{(23)(34)(42)} \prod_{i=4}^n \frac{\sum_{j=4}^i (3j)[ji+1]}{(3 \ i+1)} \\ &= \frac{\delta^{4|16}(P)}{\prod_{i \in \mathcal{N}} \langle i \ i+1 \rangle} \frac{1}{\langle 23 \rangle \langle 34 \rangle \langle 42 \rangle} \prod_{i=4}^n \frac{\langle 3|P_{4\dots i}|i+1 \rangle}{\langle 3 \ i+1 \rangle}, \end{aligned} \quad (6.3.9)$$

where $a \neq b \in \mathcal{N}$. The full n -point MHV amplitude in $\mathcal{N} = 8$ supergravity can be obtained from the above formula by summing over permutations of the legs $1, 5, \dots, n$, and I have verified numerically up to 10 points that this expression is equal to the Hodges MHV expression in equation (6.2). Equation (6.3.9) can be easily related to the BGK formula for MHV graviton scattering [125], and the similar planar

expression obtained more recently in [126].

6.4 Tree-level NMHV

In this section I generalize the calculations of Sections 6.4 and 6.3 to non-MHV amplitudes, where it is necessary to specify a contour in the Grassmannian in order to make the integrals well-defined as in $\mathcal{N} = 4$ super Yang-Mills in Section 5.2. In that case the contour integral implied by BCFW reduces to summing over residues of a single top form in the Grassmannian, and can be related to the contour integral arising from the 4D scattering equations using global residue theorems. For $\mathcal{N} = 8$ supergravity I show that the decorated planar on-shell diagrams (from which the full amplitude can be deduced by summing over permutations of external legs) do not correspond to residues of a single top form, and so the Grassmannian contour integral has a more complex form. It is also possible to derive such a formula starting from the 4D scattering equations and mapping to $\text{Gr}(k, n)$ using link variables, although it is unclear how to map it into the contour integral arising from on-shell diagrams using global residue theorems in this case.

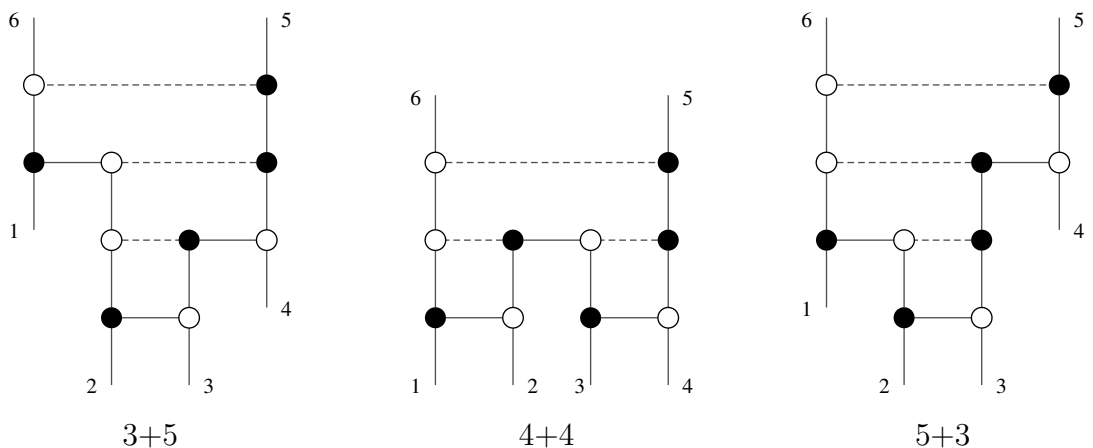


Figure 6.5: Decorated planar on-shell diagrams contributing to the 6 point NMHV amplitude in $\mathcal{N} = 8$ supergravity. The full amplitude can be obtained by summing over permutations of legs 1 to 4.

Since the on-shell diagram recursion can be restricted to a planar sector in $\mathcal{N} = 8$

supergravity, the calculation can be reduced to computing three planar diagrams which are decorated versions of the ones appearing in $\mathcal{N} = 4$ super Yang-Mills, as shown in Figure 6.5. The full 6-point NMHV amplitude can then be obtained by summing over permutations of legs 1 to 4. The same orientation and labelling will be used as the $\mathcal{N} = 4$ super Yang-Mills diagrams, so the C matrices will remain the same.

First compute the 3 + 5 diagram in Figure 6.5. Using the orientation and labelling from figure 5.3 and following the algorithm in Section 6.1,

$$\mathcal{A}_{6,3}^{(0)}(3+5) = \underset{(456)=0}{\text{Res}} \int d^{3 \times 6} \Omega_8 \frac{\alpha_7}{\alpha_6 \alpha_8} \frac{\langle \alpha_1 \alpha_2 \rangle \langle \alpha_3 \alpha_4 \rangle [\alpha_4 \alpha_5] [\beta \alpha_6]}{\prod_{i=1}^8 \alpha_i} \quad (6.4.1)$$

where $d^{3 \times 6} \Omega_8$ is defined in (2.9.2). The internal spinors can then be related to the external spinors by summing over paths connecting them as described in the algorithm, finding

$$\begin{aligned} \langle \alpha_1 \alpha_2 \rangle &= \frac{\alpha_8}{\alpha_2} \langle 16 \rangle \\ \langle \alpha_3 \alpha_4 \rangle &= \frac{1}{\alpha_3} \langle 23 \rangle \\ [\alpha_4 \alpha_5] &= \frac{\alpha_4}{\alpha_5} [23] \\ [\beta \alpha_6] &= \alpha_6 [45]. \end{aligned}$$

Substituting these relations into (6.4.1) and simplifying gives

$$\mathcal{A}_{6,3}^{(0)}(3+5) = \underset{(456)=0}{\text{Res}} \int d^{3 \times 6} \Omega_8 \frac{\langle 16 \rangle [45] \langle 23 \rangle [32]}{\alpha_1 \alpha_2^2 \alpha_3^2 \alpha_5^2 \alpha_6 \alpha_8} \quad (6.4.2)$$

which can be uplifted to the following covariant expression:

$$\mathcal{A}_{6,3}^{(0)}(3+5) = \underset{(456)=0}{\text{Res}} \int d^{3 \times 6} \Omega_8 \frac{\langle 16 \rangle [45] \langle 23 \rangle [32]}{(123)(561)(146)(236)} \quad (6.4.3)$$

where the minors are computed using (5.2.2).

The 5+3 channel in Figure 6.5 can be calculated directly as the complex conjugate of the 3+5 channel, which maps $[ij] \leftrightarrow \langle ij \rangle$, and $(ijk) \rightarrow \epsilon_{ijkabc}(abc)$. To keep the cyclic definition of the legs consistent it is necessary to also apply the permutation

$P = \begin{pmatrix} 1 & 2 & 3 & 4 & 5 & 6 \\ 4 & 3 & 2 & 1 & 6 & 5 \end{pmatrix}$, which gives the non-trivial result that the 3+5 and 5+3 channels both have the same integrand, only with different residues,

$$\mathcal{A}_{6,3}^{(0)}(3+5) = \text{Res}_{(234)=0} \int d^{3 \times 6} \Omega_8 \frac{\langle 16 \rangle [45] \langle 23 \rangle [32]}{(123)(561)(146)(236)}. \quad (6.4.4)$$

Then the 4+4 channel diagram in Figure 6.5 is computed using the orientation and labelling in figure 5.4. Using the algorithm in Section 6.1, the following expression is obtained for the amplitude,

$$\mathcal{A}_{6,3}^{(0)}(4+4) = \text{Res}_{(612)=0} \int d^{3 \times 6} \Omega_8 \frac{\alpha_8 \langle \alpha_1 \alpha_2 \rangle \langle \alpha_5 \alpha_7 \rangle [\alpha_2 \alpha_3] [\alpha_5 \alpha_6]}{\alpha_4 \alpha_6 \prod_{i=1}^8 \alpha_i}. \quad (6.4.5)$$

Writing the internal spinor brackets in terms of external ones then gives

$$\begin{aligned} \langle \alpha_1 \alpha_2 \rangle &= \frac{\alpha_4}{\alpha_2} \langle 16 \rangle \\ \langle \alpha_5 \alpha_7 \rangle &= \frac{1}{\alpha_5 \alpha_6 \alpha_7} (\alpha_3 \alpha_6 \alpha_7 \langle 32 \rangle + \alpha_4 \alpha_6 \alpha_7 \langle 36 \rangle) \\ [\alpha_2 \alpha_3] &= \frac{\alpha_2}{\alpha_3} [12] \\ [4\alpha_5] &= \alpha_5 [43]. \end{aligned}$$

Substituting this into 6.4.5 and uplifting into a covariant expression in $\text{Gr}(3,6)$ then gives

$$\mathcal{A}_{6,3}^{(0)}(4+4) = \text{Res}_{(456)=0} \int d^{3 \times 6} \Omega_8 \frac{\langle 16 \rangle [34] (623) [12] ((346) \langle 32 \rangle + (432) \langle 36 \rangle)}{(123)(561)(346)^2(256)}, \quad (6.4.6)$$

where the minors are computed using (5.2.5). This expression for the integrand can then be simplified further using the relations between spinor brackets and minors derived in Section 6.7. The relevant identities are

$$\begin{aligned} \langle 32 \rangle (346) + \langle 34 \rangle (623) + \langle 36 \rangle (432) &= 0 \\ [43] (145)^\perp - [41] (453)^\perp - [45] (314)^\perp &= 0 \\ [43] (623) + [41] (612) + [45] (256) &= 0. \end{aligned}$$

On the support of residue at $(612) = (453)^\perp = 0$ the terms proportional to $[41]$ in the second two relations can be dropped, and the following simplified expression is

obtained for the 4+4 channel,

$$\mathcal{A}_{6,3}^{(0)}(4+4) = \text{Res}_{(612)=0} \int d^{3 \times 6} \Omega_8 \frac{\langle 16 \rangle [45] \langle 34 \rangle [12]}{(123)(561)(346)^2}. \quad (6.4.7)$$

Adding up the three contributions in (6.4.3) (6.4.4), (6.4.7), the sum of decorated planar on-shell diagrams in Figure 6.5 is found to correspond to the following Grassmannian integral formula:

$$\begin{aligned} \mathcal{A}_{6,3}^{(0)} = & \left(\text{Res}_{(234)=0} + \text{Res}_{(456)=0} \right) \int d^{3 \times 6} \Omega_8 \frac{\langle 16 \rangle [45] \langle 23 \rangle [32]}{(123)(561)(146)(236)} \\ & + \text{Res}_{(612)=0} \int d^{3 \times 6} \Omega_8 \frac{\langle 16 \rangle [45] \langle 34 \rangle [12]}{(123)(561)(346)^2}. \end{aligned} \quad (6.4.8)$$

The full 6-point NMHV amplitude in $\mathcal{N} = 8$ supergravity is then given by summing (6.4.8) over permutations of labels 1 to 4.

From equation (6.4.8) it can be seen that this sum of planar diagrams cannot be written as the sum of three residues of a single top form. To see this, first add and subtract the (612) residue of the first integrand

$$\begin{aligned} \mathcal{A}_{6,3}^{(0)} = & \left(\text{Res}_{(234)=0} + \text{Res}_{(456)=0} + \text{Res}_{(612)=0} \right) \int d^{3 \times 6} \Omega_8 \frac{\langle 16 \rangle [45] \langle 23 \rangle [32]}{(123)(561)(146)(236)} \\ & + \text{Res}_{(612)=0} \int d^{3 \times 6} \Omega_8 \frac{\langle 16 \rangle [45]}{(123)(561)(346)^2 (146)(236)} \left(\langle 34 \rangle [12] (146)(236) - \langle 23 \rangle [32] (346)^2 \right), \end{aligned} \quad (6.4.9)$$

and note that the second line does not vanish on the support of the residue (612) = 0. To see this, choose an appropriate GL(3) gauge so that the solution to the delta functions and residue constraints is

$$C = \begin{pmatrix} |1\rangle & |2\rangle & |3\rangle & |4\rangle & |5\rangle & |6\rangle \\ 0 & [45] & [53] & [34] & 0 & 0 \end{pmatrix}. \quad (6.4.10)$$

Then evaluating the second term on this solution shows that it is not zero for generic momenta.

Hence the decorated planar on-shell diagrams from which the 6-point NMHV amplitude of $\mathcal{N} = 8$ supergravity can be calculated do not correspond to residues of a single top-form, unlike in $\mathcal{N} = 4$ super Yang-Mills. This can be understood dia-

grammatically as follows. Whereas the three planar on-shell diagrams contributing to the 6-point NMHV amplitude in $\mathcal{N} = 4$ super Yang-Mills can be embedded in a single Postnikov diagram in Figure 5.5, it is not possible to decorate this diagram in such a way that it encodes the three decorated on-shell diagrams in Figure 6.5. This is because the merger equivalence relation for $\mathcal{N} = 8$ supergravity described in Section 2.9 is less flexible than the one in $\mathcal{N} = 4$ super Yang-Mills, since it requires opposite edges to be decorated as depicted in Figure 2.7.

It would be interesting to see if a unique top-form can be deduced by solving the on-shell diagram recursion relations in a non-planar sector or incorporating the bonus relations. Note that one can obtain such a formula by uplifting the formulae derived in [127, 128] to covariant expressions in $\text{Gr}(k, n)$, however it is unclear how to relate this to a contour integral arising from on-shell diagrams.

6.5 One-Loop

In this section I derive a worldsheet formula for the 1-loop 4-point amplitude of $\mathcal{N} = 8$ supergravity supported on 4D scattering equations, analogously to the one I derived for $\mathcal{N} = 4$ super Yang-Mills in Section 5.3. Unlike in planar $\mathcal{N} = 4$ super Yang-Mills, a loop-level BCFW recursion relation is not known for $\mathcal{N} = 8$ supergravity, however the 4 point amplitude can still be related to the on-shell diagram formalism by noting that it is equal the on-shell diagram in Figure 6.6 after summing over permutations of the external legs [70].

The diagram in Figure 6.6 can be obtained from the diagram in Figure 6.7 by taking the forward limit of legs $+$ and $-$ and attaching a decorated BCFW bridge to legs 1 and 4. As in the previous section, the loop momentum is defined to be the sum of the momenta in these two edges given by (5.3.1). The necessary steps to obtain a worldsheet formula for the 1-loop 4-point amplitude are to derive a Grassmannian integral formula for Figure 6.7, convert to a worldsheet formula by

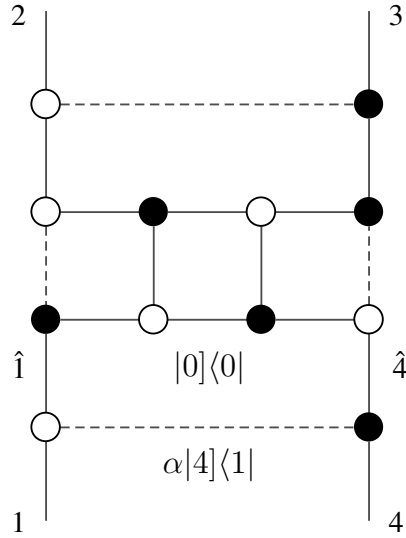


Figure 6.6: On-shell diagram for 1-loop four-point amplitude in $\mathcal{N}=8$ supergravity

using link variables, take a forward limit and add a decorated BCFW bridge, and sum over permutations of the external legs.

Note that the diagram in Figure 6.7 is the same as the $4 + 4$ diagram in Figure 6.5 up to the location of bridge decorations. Hence, it can be computed simply by multiplying the integrand in (6.4.5) by the following ratio of bridge decorations and spinor brackets associated with the vertices,

$$\frac{\text{new decorations}}{\text{old decorations}} \frac{\text{new brackets}}{\text{old brackets}} = \alpha_6^{-2} \alpha_1 \alpha_2^{-1} \frac{\langle \beta \alpha_3 \rangle [\gamma \alpha_7]}{\langle \alpha_1 \alpha_2 \rangle [4 \alpha_5]}.$$

The relabelling $P = \begin{pmatrix} 1 & 2 & 3 & 4 & 5 & 6 \\ 1 & 0 & 5 & 4 & 3 & 2 \end{pmatrix}$ is then applied to match the labelling between Figures 6.7 and 6.5, which gives the following Grassmannian integral formula for the diagram in Figure 6.7,

$$\mathcal{A}_{6,3}^{(0)}(4+4)' = \underset{(+12)=0}{\text{Res}} \int \frac{d^{3 \times 6} C}{GL(3)} \prod_{i \in \mathcal{N}'} \frac{1}{(i \ i+1 \ i+2)} \frac{\langle 12 \rangle \langle 4- \rangle [+1] [34]}{(234)(4-+)(-12)^2} \times \delta^{3 \times (2|8)}(C \cdot \tilde{\lambda}) \delta^{3 \times 2}(\lambda \cdot C^\perp), \quad (6.5.1)$$

where $L := \{1, 2\}$ and $R := \{3, 4\}$ so that $\mathcal{N} = L \cup R = \{1, 2, 3, 4\}$, and $L' := \{1, 2, -\}$ and $R' := \{3, 4, +\}$, with $\mathcal{N}' = L' \cup R' = \mathcal{N} \cup \{+, -\}$ as in Section 5.3.

To map this into a worldsheet formula, it is first written in terms of link variables as

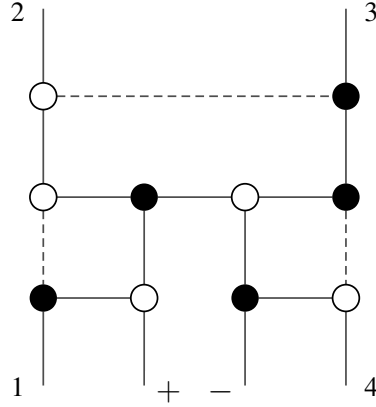


Figure 6.7: On-shell diagram from which Figure 6.6 can be obtained by taking a forward limit and adding a decorated BCFW bridge.

done in the previous section. Choosing coordinates on the Grassmannian according to (5.3.3), (6.5.1) can be written as

$$\mathcal{A}_{6,3}^{(0)}{}_{(4+4)'} = \int d^8 C \prod_{i \in \mathcal{N}'} \frac{1}{(i \ i+1 \ i+2)} \frac{\langle 12 \rangle \langle 4- \rangle [+1] [34]}{(234)(4-+)(-2)^2} \delta^{3 \times (2|8)} (C \cdot \tilde{\lambda}) \delta^{2 \times 3} (\lambda \cdot C^\perp) \quad (6.5.2)$$

where $d^8 C$ is the measure over the eight non-zero link variables in (5.3.3).

The next step is to convert this to a worldsheet integral. Introduce six punctures on the 2-sphere with homogeneous coordinates σ_i for $i \in \mathcal{N}'$, and set $\sigma_1 = \begin{pmatrix} 0 \\ 1 \end{pmatrix}$ and $\sigma_2 = \begin{pmatrix} 1 \\ 0 \end{pmatrix}$. The coordinates of the remaining four punctures then provide eight integration variables which precisely matches the number of link variables. To map the link variables into worldsheet coordinates, multiply a factor of “1” into (6.5.2) in the form given by (5.3.4). Using equations (5.3.6) and (5.3.5) it is then straightforward to integrate out the link variables against these delta functions as in Section 5.3, leaving an integral over worldsheet coordinates. Uplifting the resulting worldsheet integral to a covariant expression in $\text{Gr}(2,6)$ gives

$$\mathcal{A}_{6,3}^{(0)}{}_{(4+4)'} = \langle 12 \rangle \langle 4- \rangle [+1] [34] \int \frac{d^{2 \times 6} \sigma}{GL(2)} \frac{(+2)(13)(14)^3(24)(3-)}{(+4)^2(12)^2(1-)^2(23)(34)^2} \times \delta^{2|8} \left(|- \rangle - \sum_{r \in R} \frac{|r \rangle}{(-r)} \right) \delta^2 \left(|+\rangle - \sum_{l \in L} \frac{|l \rangle}{(+l)} \right)$$

$$\times \prod_{l \in L} \delta^{2|8} \left(|l\rangle - \sum_{r \in R} \frac{|r\rangle}{(lr)} - \frac{|+\rangle}{(l+)} \right) \prod_{r \in R} \delta^2 \left(|r\rangle - \sum_{l \in L} \frac{|l\rangle}{(rl)} - \frac{|-\rangle}{(r-)} \right).$$

To obtain a worldsheet formula for the 1-loop amplitude from this expression then take a forward limit $|+\rangle\langle+| = -|-\rangle\langle-|$ by setting $(|-\rangle, |-\rangle, \eta_-) = (|+\rangle, -|+\rangle, \eta_+)$, and define a new set of variables for the loop momentum so that $(|0\rangle, |0\rangle, \eta_0) := (|-\rangle, |-\rangle, \eta_-)$. Then BCFW shift legs 1 and 4 and sum over permutations, and note that the loop momentum is then defined as in equation (5.3.1), and the measure as in equation (5.3). Exchanging σ_+ with σ_- and simplifying the integrand on the support of the scattering equations gives that

$$\begin{aligned} \mathcal{M}_{4,2}^{(1)} = \sum_{S_4} \langle 12 \rangle^2 [34]^2 \int \frac{d^4 l}{l^2} \frac{d^{2 \times 6} \sigma}{GL(2)} \prod_{i \in \mathcal{N}'} \frac{1}{(i \ i+1)} \frac{(14)(+-)}{(1-)(+4)} \\ \times \delta^2(\tilde{E}_0^{(1)}) \delta^2(E_0^{(1)}) \prod_{l \in L} \delta^{2|8}(\tilde{E}_l^{(1)}) \prod_{r \in R} \delta^2(E_r^{(1)}), \end{aligned}$$

where the scattering equations are defined in (5.3.8) and the sum over S_4 permutations acts on all particle labels in the expression. The hats are defined so that $|\hat{4}\rangle = |4\rangle - \alpha|1\rangle$, $(|\hat{1}\rangle, \hat{\eta}_1) = (|1\rangle + \alpha|4\rangle, \eta_1 + \alpha\eta_4)$, and they act trivially on the other spinors. On the support of the scattering equations the following identity holds

$$\langle 12 \rangle^2 [34]^2 = \frac{\prod_{i \in \mathcal{N}'} (+i)(-i)}{1 - (+-)^2} \det \mathcal{H} \det \tilde{\mathcal{H}},$$

where six point NMHV Hodges matrices defined in Section 2.8 have been taken with rows and columns associated with particles + and - removed to give

$$\mathcal{H} = \begin{pmatrix} -\frac{\langle 10 \rangle}{(1-)} - \frac{\langle 12 \rangle}{(12)} & \frac{\langle 12 \rangle}{(12)} \\ \frac{\langle 12 \rangle}{(12)} & -\frac{\langle 20 \rangle}{(2-)} - \frac{\langle 21 \rangle}{(21)} \end{pmatrix}, \quad \tilde{\mathcal{H}} = \begin{pmatrix} -\frac{[30]}{(3+)} - \frac{[34]}{(34)} & \frac{[34]}{(34)} \\ \frac{[34]}{(34)} & -\frac{[40]}{(4+)} - \frac{[43]}{(43)} \end{pmatrix}.$$

Finally the following worldsheet formula for the 1-loop 4-point amplitude of $\mathcal{N} = 8$

supergravity is obtained

$$\begin{aligned} \mathcal{M}_{4,2}^{(1)} = & \sum_{\text{perms}\{1,2,3,4\}} \int \frac{d^4 l}{l^2} \frac{d^{2 \times 6} \sigma}{GL(2)} \prod_{i \in \mathcal{N}'} \frac{1}{(i \ i+1)} \frac{(14)(+-)}{(1-)(+4)} \\ & \times \frac{\prod_{i \in \mathcal{N}} (+i)(-i)}{1 - (+-)^2} \det \mathcal{H} \det \tilde{\mathcal{H}} \delta^{2 \times 6 | 8 \times 2} (\text{SE}_{4,L}^{(1)}). \end{aligned} \quad (6.5.3)$$

Though it may not be intuitive from the expression above, it can be shown that can be shown that this formula has the expected scaling properties under little group transformations. In particular, the term $1 - (+-)^2$ is invariant because σ_+ and σ_- scale with opposite weight. Little group scaling of worldsheet coordinates is explained in Chapter 3. It should be straightforward to evaluate the worldsheet integrals in the expression explicitly using the solution to the scattering equations calculated in Section 5.3.

The determinants in equation (6.5.3) can be thought of as arising from the forward limit of a tree-level 6-point NMHV amplitude, but the planar Parke-Taylor factor is unusual in a gravity amplitude. It is likely that the factors $\prod_{i \in \mathcal{N}'} \frac{1}{(i \ i+1)}$ and $\prod_{i \in \mathcal{N}} (+i)(-i)$ cancel due to the following relation [33] for sum of the n point worldsheet Parke-Taylor factors over permutations of $n-2$ labels,

$$\sum_{\sigma \in S_{n-2}} \frac{s_+ - s_-}{(s_+ - s_{1\sigma})(s_{1\sigma} - s_{2\sigma}) \dots (s_{n\sigma} - s_-)} = \prod_{i=1}^n \frac{s_+ - s_-}{(s_+ - s_{i\sigma})(s_{i\sigma} - s_-)}, \quad (6.5.4)$$

along with the relations for how the scattering equations transform under permutations of particle labels derived in Section 3.5. The $(1 - (+-)^2)^{-1}$ factor in the integrand is difficult to interpret.

6.6 Bonus Relations in On-Shell Diagrams

In this section I detail how to incorporate the bonus relations of $\mathcal{N} = 8$ supergravity into the on-shell diagram formalism. In general for BCFW recursion to hold for a given theory it is required that the amplitudes behave as $\mathcal{O}(z^{-2})$ as $z \rightarrow \infty$. For $\mathcal{N} = 8$ supergravity, the superamplitudes vanish like $\mathcal{O}(z^{-2})$, which implies that

$$\mathcal{M}_{n,2}^{(0)} = \sum_{i=2}^{n-1} \begin{array}{c} \hat{1} \\ | \\ \textcircled{\mathcal{M}_{n-1,2}^{(0)}} \\ | \\ n-1 \\ \vdots \\ \textcircled{\mathcal{M}_3^{(0)}} \\ | \\ \hat{n} \\ | \\ i \end{array}$$

Figure 6.8: BCFW recursion for tree-level MHV amplitudes in $\mathcal{N} = 8$ supergravity

the sum over factorisation channels weighted by z for each channel should vanish, in addition to the recursion relations themselves. These constraints are known as bonus relations and make it possible to express one factorisation channel as a sum over the others [129, 130]. In the MHV sector the bonus relations will be added by modifying the bridge factor in the on-shell diagrams. For non-MHV amplitudes it is less clear how to incorporate the bonus relations [131], so I restrict my analysis of the bonus relations to the MHV sector in this thesis.

Consider BCFW shifting particles 1 and n of an n -point amplitude, so that

$$|\hat{1}\rangle = |1\rangle + z|n\rangle, \quad |\hat{n}\rangle = |n\rangle - z|1\rangle.$$

The momenta are then shifted as $\hat{p}_1 = p_1 + zq$ and $\hat{p}_n = p_n - zq$, where $q = |n\rangle\langle 1|$. When calculating an MHV amplitude under this shift, each factorisation channel will consist of a 3-point amplitude containing particle n times an $(n-1)$ -point amplitude containing particle 1. The channel can then be labelled by the unshifted external leg appearing on the 3-point amplitude, as depicted in Figure 6.8. The value of z corresponding to the i th factorisation channel is determined by solving $(\hat{p}_n + p_i)^2 = 0$, and is given by

$$z_i = \frac{p_n \cdot p_i}{q \cdot p_i} = \frac{\langle ni \rangle}{\langle 1i \rangle}.$$

In particular for an n -point MHV amplitude BCFW shifted as a described above, the $i = 2$ channel can be expressed as a sum over the other $n-3$ channels as depicted in Figure 6.9. Substituting this into the BCFW recursion relation, the amplitude can

6.7 Relations between spinors and minors

The Grassmannian approach to scattering amplitudes provides a geometrical way to view the λ and $\tilde{\lambda}$ spinors. For an n -point \mathcal{N}^{k-2} MHV amplitude, the λ spinors can be seen to lie inside k -planes in n dimensions and the $\tilde{\lambda}$ spinors lie in the orthogonal $(n-k)$ -planes. Representing the k -planes by an $k \times n$ matrix C and the $(n-k)$ -planes by an $n \times (n-k)$ matrix C^\perp , this is implied by delta functions in the Grassmannian integral formulae for scattering amplitudes enforcing $C \cdot \tilde{\lambda} = \lambda \cdot C^\perp = 0$. I will now show that this gives rise to nontrivial relations between spinor brackets and minors of C and C^\perp .

Let the rows of the $k \times n$ matrix C be denoted $C_{\alpha i}$, $i \in \{1, \dots, n\}$, $\alpha \in \{1, \dots, k\}$. Then Cramer's rule for the linear dependence of the distinct set of rows from 1 to $k+1$ can be written succinctly as follows:

$$\sum_{\sigma \in \mathbb{Z}_{k+1}} (-1)^{1\sigma k} C_{\alpha 1\sigma} (2_\sigma \dots (k+1)_\sigma) = 0,$$

where $(2_\sigma \dots (k+1)_\sigma)$ represents a $k \times k$ minor of the C matrix.

Analogous formulae exist for any distinct set of $k+1$ rows. Taking the product of this vector relation with a $(k-1)$ blade formed of rows of the C matrix generates all possible Plücker identities for $\text{Gr}(k, n)$. As an example, consider $\text{Gr}(3, n)$. Choose four distinct rows a, b, c and d of C . Then Cramer's rule can be written

$$C_{\alpha a}(bcd) - C_{\alpha b}(cda) + C_{\alpha c}(dab) - C_{\alpha d}(abc) = 0,$$

and taking the product with the $(k-1)$ blade $\epsilon^{\alpha\beta\gamma} C_{\beta d} C_{\gamma e}$ gives the Plücker relations

$$(dea)(bcd) - (deb)(cda) + (dec)(dab) = 0$$

The constraints $C \cdot \tilde{\lambda} = \lambda \cdot C^\perp = 0$ imply that the $\text{GL}(k)$ symmetry can be used to set the first two rows of C equal to λ , i.e. $C_{\beta i} = \lambda_{\beta i}$, $\beta \in \{1, 2\}$ and $C_{\alpha i}$, $\alpha \in \{3, \dots, k\}$

are unspecified. Gauge fixing this way gives the mixed Cramer's rule,

$$\sum_{\sigma \in \mathbb{Z}_{k+1}} (-1)^{1_{\sigma k}} |1_{\sigma}\rangle (2_{\sigma} \dots (k+1)_{\sigma}) = 0 \quad (6.7.1)$$

For $k = 2$, this is equivalent to the statement that $\langle ij \rangle / (ij)$ is invariant for all $i \neq j$ [70]. Consider again the same example of $\text{Gr}(3, n)$. Choose four distinct rows a, b, c and d of C . Then the mixed Cramer's rule can be written

$$|a\rangle (bcd) - |b\rangle (cda) + |c\rangle (dab) - |d\rangle (abc) = 0$$

and taking the product with spinor $|d\rangle$ gives the mixed Plücker relations

$$\langle da \rangle (bcd) - \langle db \rangle (cda) + \langle dc \rangle (dab) = 0$$

Deriving these identities relies only on the condition $C \cdot \tilde{\lambda} = 0$. On the support of $\lambda \cdot C^{\perp} = 0$, another mixed Cramer's rule can be derived which relates $\tilde{\lambda}$ spinors and the minors of C^{\perp} ,

$$\sum_{\sigma \in \mathbb{Z}_{n-k+1}} (-1)^{1_{\sigma(n-k)}} |1_{\sigma}] (2_{\sigma} \dots (n-k+1)_{\sigma})^{\perp} = 0. \quad (6.7.2)$$

This identity leads to similar mixed Plücker relations with the square bracket spinors.

Chapter 7

$\mathcal{N} = 4$ Conformal Supergravity Amplitudes in 4D Ambitwistor String Theory

In this chapter I analyse the scattering amplitudes of non-minimal Berkovits-Witten $\mathcal{N} = 4$ conformal supergravity within the framework of 4D ambitwistor string theory, based on my work from [4]. In Section 7.1 I derive worldsheet formulae for scattering amplitudes of graviton multiplets with plane-wave boundary conditions, and in Section 7.2, I show that these formulae reduce to the Berkovits-Witten result in the MHV sector. I then generalise this analysis to non-plane wave states in Section 7.3, working through some examples of amplitudes for non plane wave states in Sections 7.4 and 7.5. The non-plane wave states can be expressed as momentum derivatives of plane wave states using a prescription for taking momentum derivatives of on-shell spinor variables which I develop in Section 7.6, and finally in Section 7.7 I discuss BRST invariance of plane-wave and non-plane wave vertex operators.

7.1 Plane Wave Graviton Multiplet Scattering

In this section I calculate scattering amplitudes for graviton multiplets with plane wave boundary conditions in $\mathcal{N} = 4$ conformal supergravity, first considering the vertex operators for positive and negative helicity superfields of the theory. I review the field content in Section 2.6. The worldsheet Lagrangian of the theory is reviewed in Section 2.11, and after gauge fixing is given by

$$\mathcal{L} = \langle \tilde{\mu} | \bar{\partial} | \lambda \rangle - [\mu | \bar{\partial} | \tilde{\lambda}] + \chi \cdot \tilde{\chi} \quad (7.1.1)$$

in terms of the bosonic spinor fields $|\lambda\rangle$, $|\tilde{\lambda}\rangle$, $|\tilde{\mu}\rangle$ and $|\mu\rangle$, and the fermionic fields χ and $\tilde{\chi}$ which transform in the fundamental representation of the $SU(4)$ R-symmetry group .

$\mathcal{N} = 4$ conformal supergravity amplitudes are computed using four types of vertex operators, in contrast to $\mathcal{N} = 4$ super Yang-Mills and $\mathcal{N} = 8$ supergravity which have only two types of vertex operators. These additional vertex operators reflect the fact that the number of negative helicity superfields scattered \mathcal{N}^- is no longer always equal to the Grassmann degree of the superamplitude, $k_G = \frac{N_G}{\mathcal{N}}$, as discussed in Section 2.6. In this work I choose to define the MHV degree k of the superamplitude to be the Grassmann degree k_G , and so the MHV degree is no longer equal in general to the number of negative helicity superfields scattered. Under this definition the scattering equations are still refined by the MHV degree of the amplitude with the MHV degree corresponding to the size of the left set, and I denote the left set vertex operators by $\tilde{\mathcal{V}}_l$ and right set by \mathcal{V} . Note that this definition is consistent with the standard definition where the MHV degree corresponds to the set of negative helicity particles for all graviton amplitudes, and gives a natural extension to amplitudes with gravitons and scalars such that ϕ^+ states are in the left set and ϕ^- states in the right set.

The vertex operators are

$$\begin{aligned}
\tilde{\mathcal{V}}_l^-(s) &= \int \frac{dt}{t^2} \langle l\lambda(s) \rangle \delta^{2|4} (|l\rangle - t|\tilde{\lambda}(s)\rangle) e^{i\langle\tilde{\mu}(s)l\rangle} \\
\tilde{\mathcal{V}}_l^+(s) &= \int tdt [\tilde{\lambda}(s)\partial\tilde{\lambda}(s)] \delta^{2|4} (|l\rangle - t|\tilde{\lambda}(s)\rangle) e^{i\langle\tilde{\mu}(s)l\rangle} \\
\mathcal{V}_r^-(s) &= \int tdt \langle\lambda(s)\partial\lambda(s)\rangle \delta^2 (|r\rangle - t|\lambda(s)\rangle) e^{i[\tilde{\mu}(s)r] + \chi\tilde{(s)}\cdot\eta_r} \\
\mathcal{V}_r^+(s) &= \int \frac{dt}{t^2} [r\tilde{\lambda}(s)] \delta^2 (|r\rangle - t|\lambda(s)\rangle) e^{i[\tilde{\mu}(s)r] + \chi\tilde{(s)}\cdot\eta_r}.
\end{aligned} \tag{7.1.2}$$

Note that the $\tilde{\mathcal{V}}^\pm$ vertex operators can be obtained by complex conjugating the \mathcal{V}^\mp vertex operators and Grassmann Fourier transforming the on-shell superspace $\tilde{\eta}$ back to the original η space. I verify the BRST invariance of these vertex operators in Section 7.7.

To understand the physics of these vertex operators it can be helpful to consider only the SU(4) singlet states of each multiplet, which are the gravitons h^\pm and the scalars ϕ^\pm . The vertex operators for these states are calculated as superspace integrals of the vertex operators in (7.1.2), and are given by

$$\begin{aligned}
\tilde{\mathcal{V}}_l^{h^-}(s) &= \int \frac{dt}{t^2} \langle l\lambda(s) \rangle \delta^2 (|l\rangle - t|\tilde{\lambda}(s)\rangle) e^{i\langle\tilde{\mu}(s)l\rangle} \\
\tilde{\mathcal{V}}_l^{\phi^+}(s) &= \int tdt [\tilde{\lambda}(s)\partial\tilde{\lambda}(s)] \delta^2 (|l\rangle - t|\tilde{\lambda}(s)\rangle) e^{i\langle\tilde{\mu}(s)l\rangle} \\
\mathcal{V}_r^{\phi^-}(s) &= \int tdt \langle\lambda(s)\partial\lambda(s)\rangle \delta^2 (|r\rangle - t|\lambda(s)\rangle) e^{i[\tilde{\mu}(s)r]} \\
\mathcal{V}_r^{h^+}(s) &= \int \frac{dt}{t^2} [r\tilde{\lambda}(s)] \delta^2 (|r\rangle - t|\lambda(s)\rangle) e^{i[\tilde{\mu}(s)r]},
\end{aligned} \tag{7.1.3}$$

and so the structures $\langle l\lambda(s) \rangle$ and $[\tilde{\lambda}(s)\partial\tilde{\lambda}(s)]$ in the left set vertex operators can be thought of as corresponding to the states h^- and ϕ^+ respectively. In this way the graviton and scalar states contain all of the structure of the scattering for the other states, which can be related to amplitudes for gravitons and scalars by supersymmetry transformations.

To specify an amplitude for plane-wave superfields, it is necessary to give a set of negative helicity superfields and a Grassmann degree k . Then choose a left set with $|L| = k$, and partition the negative helicity superfields into disjoint subsets $\tilde{\Phi}^-$ and Φ^- , depending on whether the superfield is in the left or right set, and similarly for

the positive helicity superfields. Then the left set $L = \tilde{\Phi}^- \sqcup \tilde{\Phi}^+$ and the right set $R = \mathcal{N} - L = \Phi^- \sqcup \Phi^+$ and an n point superamplitude is then obtained by computing a correlator of vertex operators integrated over the worldsheet and quotienting out by the $SL(2)$ gauge freedom in the integral so that

$$\mathcal{M}_{n,\Phi^-,k}^{(0)} = \int \frac{d^n s}{\text{SL}(2)} \left\langle \prod_{l_- \in \tilde{\Phi}^-} \tilde{\mathcal{V}}_{l_-}^- (s_{l_-}) \prod_{l_+ \in \tilde{\Phi}^+} \tilde{\mathcal{V}}_{l_+}^+ (s_{l_+}) \prod_{r_- \in \Phi^-} \mathcal{V}_{r_-}^- (s_{r_-}) \prod_{r_+ \in \Phi^+} \mathcal{V}_{r_+}^+ (s_{r_+}) \right\rangle. \quad (7.1.4)$$

The calculation of this correlation function is straightforward due to the fact that the $|\tilde{\mu}\rangle$ and $|\mu\rangle$ fields in the action are not dynamical, and follows the example given for Yang-Mills in Section 2.11. The $|\tilde{\mu}\rangle$, $|\mu\rangle$ and $\tilde{\chi}$ fields integrate out directly in the path integral, and localise the $|\lambda\rangle$, $|\tilde{\lambda}\rangle$ and χ fields onto the solutions in equations (2.11.9), (2.11) and (2.11). This results in delta functions which localise the worldsheet integral onto solutions of 4D scattering equations.

The n -point N^{k-2}MHV amplitude is then given by the following worldsheet formula

$$\mathcal{M}_{n,\Phi^-,k}^{(0)} = \int \frac{d^{2 \times n} \sigma}{GL(2)} \delta^{2 \times n | 4 \times k} (SE_L^n) \prod_{l_- \in \tilde{\Phi}^-} H_{l_-} \prod_{l_+ \in \tilde{\Phi}^+} \tilde{F}_{l_+} \prod_{r_- \in \Phi^-} F_{r_-} \prod_{r_+ \in \Phi^+} \tilde{H}_{r_+}, \quad (7.1.5)$$

where $k = |L| = |\tilde{\Phi}^-| + |\tilde{\Phi}^+|$, and

$$\begin{aligned} \tilde{F}_l &:= \sum_{r < r' \in R} \frac{[rr'] (rr')}{(lr)^2 (lr')^2}, & H_l &:= \sum_{l' \in L \setminus \{l\}} \frac{\langle ll' \rangle}{(ll')} \\ F_r &:= \sum_{l < l' \in L} \frac{\langle ll' \rangle (ll')}{(rl)^2 (rl')^2}, & \tilde{H}_r &:= \sum_{r' \in R \setminus \{r\}} \frac{[rr']}{(rr')}. \end{aligned}$$

I have checked numerically that the superamplitude is unchanged under replacing Φ^\pm states with $\tilde{\Phi}^\pm$ states as long as the Grassmann degree $k_G = k = |L|$ is preserved, and hence is invariant of the choice of the left set, L . It should be possible to prove this analytically using the results from Section 3.5.

The H factors are the diagonal elements of the Hodges matrices defined in equation (2.8.7), and the F allow for putting the diagonal elements of the Hodges matrix into the set of particles of opposite parity. The factors H , F , \tilde{H} and \tilde{F} can then

be considered as generalisations of the gravitational inverse soft factor from equation (2.5.9) outside of the MHV sector. Component amplitudes can be extracted by integrating out the appropriate η variable; for example, the scalar-graviton amplitudes are obtained by integrating out $(\eta_l)^4$ for $l \in L$, and setting $\eta_r = 0$ for $r \in R$. In a similar way amplitudes with fermions and spin-1 states can also be obtained.

In the MHV sector the scattering equations have only one solution, which is given in Section 3.1. On the support of this solution (7.1.5) reduces to the Berkovits-Witten result [20], and I provide details of this calculation in Section 7.7. The formula is

$$\mathcal{M}_{n,\Phi^-,2}^{(0)} = \delta^{4|8}(P) \prod_{i \in \Phi^+} \sum_{j \in \mathcal{N} \setminus \{i\}} \frac{[ij] \langle jx_i \rangle \langle jy_i \rangle}{\langle ij \rangle \langle ix_i \rangle \langle iy_i \rangle}, \quad (7.1.6)$$

where $|x_i\rangle$ and $|y_i\rangle$ are arbitrary reference spinors.

Evaluating the worldsheet integrals analytically for higher MHV degree is complex because the scattering equations have more than one solution, so the 4D scattering equation formalism is less practical in this setting. I have verified equation (7.1.5) for different component states at higher MHV degrees numerically by matching it against results obtained using Feynman diagrams and colour-kinematics duality in [49] up to eight points with any number of particles¹, using the numerical methods developed in Section 4.3 to evaluate the worldsheet integrals. Some partial analytical results for NMHV amplitudes in $\mathcal{N} = 4$ conformal supergravity are described in [132], and for the special case where the set of negative helicity superfields corresponds to the left set of the amplitude a formula in terms of integrals over curves in twistor space was previously conjectured in [47]. It would be interesting to see how this formula is related to equation (7.1.5).

¹I thank Henrik Johansson for providing numerical results derived from colour-kinematics duality against which to compare my worldsheet formula.

7.2 Derivation of Berkovits-Witten MHV

Formula

In this section I evaluate the worldsheet integral in (7.1.5) for the MHV case with $k = |L| = 2$. This reproduces the formula of Berkovits and Witten from [20], and shows that this amplitude can be considered as the MHV amplitude under my definition in terms of Grassmann degree. In this case, the worldsheet integral can be evaluated analytically using the results from Chapter 3. In this section I take the left set to be $L = \{1, 2\}$ and the right set to be $R = \{3, \dots, n\}$, with $\tilde{\Phi}^- \sqcup \tilde{\Phi}^+ = \{1, 2\}$.

On support of the MHV solution in equation (3.1.6), the amplitude from equation (7.1.5) reduces to

$$\begin{aligned}
 \mathcal{M}_{n, \tilde{\Phi}^-, 2}^{(0)} &= \int \frac{d^{2 \times n} \sigma}{GL(2)} \delta^{2 \times n | 4 \times 2} (SE_{\{1, 2\}}^n) \prod_{l_- \in \tilde{\Phi}^-} H_{l_-} \prod_{l_+ \in \tilde{\Phi}^+} \tilde{F}_{l_+} \prod_{r_- \in \Phi^-} E_{r_-} \prod_{r_+ \in \Phi^+} \tilde{H}_{r_+} \\
 &= \delta^4(P) \frac{\delta^8(Q)}{\langle 12 \rangle^2} \prod_{r \in R} \frac{(1r)^2 (2r)^2}{\langle 12 \rangle (12)} \prod_{l_- \in \tilde{\Phi}^-} \frac{\langle 12 \rangle}{(12)} \prod_{l_+ \in \tilde{\Phi}^+} \sum_{r < r' \in R} \frac{[rr'] (rr')}{(l_+ r)^2 (l_+ r')^2} \\
 &\quad \prod_{r_- \in \Phi^-} \frac{\langle 12 \rangle (12)}{(1r_-)^2 (2r_-)^2} \prod_{r_+ \in \Phi^+} \sum_{r \in R} \frac{[r_+ r]}{(r_+ r)} \Big|_{\sigma = \sigma_{\text{MHV}}} \\
 &= \delta^{4|8}(P) \frac{1}{(12)^2} \prod_{l_+ \in \tilde{\Phi}^+} \sum_{r < r' \in R} \frac{[rr'] (rr') (12)}{(l_+ r)^2 (l_+ r')^2 \langle 12 \rangle} \\
 &\quad \prod_{r_+ \in \Phi^+} \sum_{r \in R} \frac{[r_+ r] (1r_+)^2 (2r_+)^2}{(r_+ r) \langle 12 \rangle (12)} \Big|_{\sigma = \sigma_{\text{MHV}}}, \tag{7.2.1}
 \end{aligned}$$

where in the third line it can be seen explicitly how the factors from the vertex operators of the Φ^- states in the left set cancel the factors from the MHV Jacobian. Now evaluate equation (7.2.1) on the MHV solution. The factor associated with each Φ^+ state in the right set when evaluated on the MHV solution is equal to the gravitational inverse soft factor $\psi_{r_+, n}^{[1]|2\rangle}$ defined in equation (2.5.9),

$$\sum_{r \in R} \frac{[r_+ r] (1r_+)^2 (2r_+)^2}{(r_+ r) \langle 12 \rangle (12)} = \sum_{r \in R} \frac{[r_+ r] \langle 1r \rangle \langle 2r \rangle}{\langle r_+ r \rangle \langle 1r_+ \rangle \langle 2r_+ \rangle} = \psi_{r_+, n}^{[1]|2\rangle}. \tag{7.2.2}$$

Now look at the factor associated with each $\tilde{\Phi}^-$ state in the left set, defining this quantity to be $\psi'_{l_-,n}$. To simplify the notation, define $(l_-)^c$ as the complement of l_- in $L = \{1, 2\}$. Then it can be seen that

$$\psi'_{l_-,n} = \sum_{r < r' \in R} \frac{rr'(12)}{(l_-r)^2(l_-r')^2 \langle 12 \rangle} = \sum_{r < r' \in R} \frac{[rr'] \langle rr' \rangle \langle (l_-)^c r \rangle \langle (l_-)^c r' \rangle}{\langle 12 \rangle^2 \langle l_-r \rangle \langle l_-r' \rangle}. \quad (7.2.3)$$

I find numerically up to high multiplicity that $\psi'_{i,n}$ can be uplifted to an expression $\psi'_{i,n}{}^{|z\rangle}$ in terms of an arbitrary reference spinor $|z\rangle$, and that $\psi'_{i,n}{}^{|z\rangle}$ is equal to the gravitational inverse soft factor $\psi_{i,n}{}^{|x\rangle|y\rangle}$. Then

$$\begin{aligned} \psi'_{i,n}{}^{|z\rangle} &= \sum_{j < k \in \mathcal{N} \setminus \{i\}} \frac{[jk] \langle jk \rangle \langle zj \rangle \langle zk \rangle}{\langle ij \rangle \langle ik \rangle \langle iz \rangle^2} \\ &= \sum_{k \in \mathcal{N} \setminus \{j\}}^n \frac{[jk] \langle kx \rangle \langle ky \rangle}{\langle jk \rangle \langle jx \rangle \langle jy \rangle} = \psi_{i,n}{}^{|x\rangle|y\rangle}, \end{aligned} \quad (7.2.4)$$

where $|x\rangle$ and $|y\rangle$ are arbitrary reference spinors. It is interesting that this expression for the gravitational inverse soft factor depends only on one reference spinor, while the standard expression depends on a choice of two reference spinors.

Finally I find that the general n point plane wave MHV amplitude reduces to the formula of Berkovits and Witten,

$$\mathcal{M}_{n,\Phi^-,2}^{(0)} = \delta^{4|8}(P) \prod_{i \in \Phi^+ \sqcup \tilde{\Phi}^+} \psi_{i,n}.$$

7.3 Scattering Non-Plane Wave States

The fourth order equations of motion for conformal gravity lead to a second set of graviton multiplet states with non-plane wave boundary conditions, and calculating scattering amplitudes for these states using 4D ambitwistor string theory is the subject of this section. I consider scattering only for the $SU(4)$ singlet graviton and scalar states, which as in the plane wave case cover all of the structure of the amplitude up to other states related by supersymmetry transformations.

I review non-plane wave states in Section 2.6. They have functional form $A \cdot x e^{ik \cdot x}$ up to polarisation structure, where A is a vector defined up to the identification $A \sim A + \beta k$ for all $\beta \in \mathbb{R}$. Following from this the vertex operators for non-plane wave states are vectors which will be contracted into a choice of vector A for each state. The vertex operators depend on the worldsheet spinor fields $|\lambda\rangle$, $|\tilde{\lambda}\rangle$, $|\tilde{\mu}\rangle$, $|\mu\rangle$ and the derivatives with respect to the worldsheet variable ∂ as in the plane wave case, and they also depend on derivatives with respect to the spinor vectors defining the momentum eigenstate. I define the following shorthand notation for spinor derivatives

$$|\partial_i\rangle^{\dot{\alpha}} := \frac{\partial}{\partial |i\rangle_{\dot{\alpha}}}, \quad |\partial_i\rangle_{\alpha} := \frac{\partial}{\partial |i\rangle^{\alpha}}, \quad (7.3.1)$$

which allow for spinor contractions with these derivatives to be expressed succinctly, and for example $\langle j |^{\alpha} \frac{\partial}{\partial |i\rangle^{\alpha}} = \langle i \partial_j \rangle$.

I then propose the following vertex operators describing non-plane wave gravitons and scalars,

$$\begin{aligned} \tilde{\mathcal{V}}_l^{h^-}(s) &= \int \frac{dt}{t^2} (|l\rangle |\mu(s)\rangle - |\lambda(s)\rangle |\partial_l\rangle) \delta^2(|l\rangle - t |\tilde{\lambda}(s)\rangle) e^{it\langle \tilde{\mu}(s)l \rangle} \\ \tilde{\mathcal{V}}_l^{\phi^+}(s) &= \int t dt (|\partial \tilde{\mu}(s)\rangle |\tilde{\lambda}(s)\rangle - |\tilde{\mu}(s)\rangle |\partial \tilde{\lambda}(s)\rangle) \delta^2(|l\rangle - t |\tilde{\lambda}(s)\rangle) e^{it\langle \tilde{\mu}(s)l \rangle} \\ \mathcal{V}_r^{\phi^-}(s) &= \int t dt (|\lambda(s)\rangle |\partial \mu(s)\rangle - |\partial \lambda(s)\rangle |\mu(s)\rangle) \delta^2(|r\rangle - t |\lambda(s)\rangle) e^{it\langle \mu(s)r \rangle} \\ \mathcal{V}_r^{h^+}(s) &= \int \frac{dt}{t^2} (|\tilde{\mu}(s)\rangle |r\rangle - |\partial_r\rangle |\tilde{\lambda}(s)\rangle) \delta^2(|r\rangle - t |\lambda(s)\rangle) e^{it\langle \mu(s)r \rangle}, \end{aligned} \quad (7.3.2)$$

where the derivative with respect to the external data $|\partial_r\rangle$ and $|\partial_l\rangle$ act on the delta functions. I verify the BRST invariance of these vertex operators in Section 7.7.

When calculating a correlation function with these vertex operators, it is not possible to integrate out the $|\mu\rangle$ and $|\tilde{\mu}\rangle$ fields directly in the path integral as in the plane wave case because these fields appear additionally outside the exponentials of the vertex operators. This feature makes non-plane wave amplitudes more difficult to calculate from the worldsheet than their plane wave counterparts, and as such it requires a calculation for each combination of non-plane wave states scattered to be able to write down their amplitudes in terms of integrals supported on 4D scattering

equations.

It is possible to remove the dependence of the vertex operators on the $|\mu\rangle$ and $|\tilde{\mu}\rangle$ fields outside of the exponentials by adding source terms for these fields. Then a different correlator can be computed where they only appear in the exponentials, and original correlator obtained by taking functional derivatives with respect to the sources and then setting the sources to zero. Source $|J\rangle$ is introduced to couple to $|\tilde{\mu}\rangle$, and $|\tilde{J}\rangle$ to couple to $|\mu\rangle$, and the modified worldsheet Lagrangian with the sources is then

$$\mathcal{L}_{\text{sources}} = \langle \tilde{\mu} | \bar{\partial} | \lambda \rangle - [\mu | \bar{\partial} | \tilde{\lambda}] + \chi \cdot \tilde{\chi} + [\mu \tilde{J}] - \langle \tilde{\mu} J \rangle.$$

The non-plane wave vertex operators are replaced with

$$\begin{aligned} \tilde{\mathcal{V}}_l^{h^-}(s) &= \int \frac{dt}{t^2} \left(|l\rangle \frac{\delta}{\delta [\tilde{J}(s)]} - |\lambda(s)\rangle \frac{\partial}{\partial |l\rangle} \right) \delta^2(|l\rangle - t |\tilde{\lambda}(s)\rangle) e^{it\langle \tilde{\mu}(s)l \rangle} \\ \tilde{\mathcal{V}}_l^{\phi^+}(s) &= \int t dt \left(\partial \left(\frac{\delta}{\delta |J(s)\rangle} \right) [\tilde{\lambda}(s)| - \frac{\delta}{\delta |J(s)\rangle} [\partial \tilde{\lambda}(s)|] \right) \delta^2(|l\rangle - t |\tilde{\lambda}(s)\rangle) e^{it\langle \tilde{\mu}(s)l \rangle} \\ \mathcal{V}_r^{\phi^-}(s) &= \int t dt \left(|\lambda(s)\rangle \partial \left(\frac{\delta}{\delta [\tilde{J}(s)]} \right) - |\partial \lambda(s)\rangle \frac{\delta}{\delta [\tilde{J}(s)]} \right) \delta^2(|r\rangle - t |\lambda(s)\rangle) e^{it\langle \mu(s)r \rangle} \\ \mathcal{V}_r^{h^+}(s) &= \int \frac{dt}{t^2} \left(\frac{\delta}{\delta |J(s)\rangle} [r| - \frac{\partial}{\partial |r\rangle} [\tilde{\lambda}(s)|] \right) \delta^2(|r\rangle - t |\lambda(s)\rangle) e^{it\langle \mu(s)r \rangle}, \end{aligned} \tag{7.3.3}$$

where from this form it is clear that each term of the vertex operators acts as a derivative, analogously to how the non-plane wave state in momentum space can be written as $A \cdot \frac{\partial e^{ik \cdot x}}{\partial k}$.

Correlators involving these vertex operators can then be evaluated by combining the exponentials in the vertex operators with the action as in the plane wave case, and integrating out $|\mu\rangle$ and $|\tilde{\mu}\rangle$ to give rise to delta functionals which localise the $|\lambda\rangle$ and $|\tilde{\lambda}\rangle$ fields onto their equations of motion. The equations of motion now depend on the sources and are given by

$$\bar{\partial}|\lambda\rangle = \sum_{l \in L} t_l |l\rangle \delta(s - s_l) + |J\rangle, \quad \bar{\partial}|\tilde{\lambda}\rangle = \sum_{r \in R} t_r |r\rangle \delta(s - s_r) + |\tilde{J}\rangle,$$

and are uniquely solved by

$$\begin{aligned} t|\lambda(s)\rangle &= \sum_{l \in L} \frac{|l\rangle}{(sl)} + t \int ds' \frac{|J\rangle(s')}{s-s'} \\ t[\tilde{\lambda}(s)] &= \sum_{r \in R} \frac{|r\rangle}{(sr)} + t \int ds' \frac{|J(s')\rangle}{s-s'}, \end{aligned} \tag{7.3.4}$$

where $\sigma_s^\alpha = \frac{1}{t} \begin{pmatrix} 1 \\ s \end{pmatrix}$.

The functional derivatives with respect to the sources from the vertex operators then act on the functional delta functions enforcing (7.3.4), and using the chain rule for functional differentiation they can be written as

$$\frac{\delta}{\delta[\tilde{J}(s)]} = \int \frac{ds'}{s-s'} \frac{\delta}{\delta[\tilde{\lambda}(s')]} , \quad \frac{\delta}{\delta[J(s)]} = \int \frac{ds'}{s-s'} \frac{\delta}{\delta[\lambda(s')]} , \tag{7.3.5}$$

keeping in mind that they act on the functional delta function enforcing the equations of motion. The sources are then set to zero, which removes the additional terms in equation (7.3.4), and functional integration by parts can be used to move the functional derivatives in the $|\lambda\rangle$ and $[\tilde{\lambda}]$ fields off the delta function enforcing the equations of motion and onto any vertex operators containing these states. The path integral in these fields can then be done by integrating against the delta functions enforcing (7.3.4), which produces the scattering equations from each vertex operator as in the plane wave case. Worked examples for this type of calculation with non-plane wave scalar and graviton states are given in Section 7.4 and 7.5.

The non-plane wave graviton vertex operators in (7.3.2) contain an additional subtlety, in that the two terms in the vertex operator are both singular, and the singularity cancels between the terms. I describe this cancellation in more detail in Section 7.5, where I also present some examples at n points with up to two non-plane wave states, and show that amplitudes with non-plane wave states can be obtained by acting on the plane wave amplitudes with a momentum derivative for each non-plane wave state. That non-plane wave amplitudes can be calculated from plane wave amplitude in this way can be seen schematically from the LSZ reduction formula by noting that a non-plane wave solution can be written as a momentum derivative of

a plane-wave solution, $A \cdot x e^{ik \cdot x} = A \cdot \frac{\partial}{\partial k} e^{ik \cdot x}$, where k is understood to be off-shell prior to taking the derivative.

The non-plane wave functional form $A \cdot x e^{ik \cdot x}$ diverges as $x \rightarrow \infty$, and so at first sight scattering amplitudes of these states appear not to be well defined. The amplitudes do however have a clear definition in a distributional sense when understood as momentum derivatives of plane-wave amplitudes; if a non-plane wave amplitude is multiplied by a test function and integrated over momentum space, it is possible to move the momentum derivative onto the test function using integration by parts, and then only derivatives of the test function multiplied by plane-wave amplitudes remain, which are defined unambiguously.

Since the amplitudes are manifestly 4D and on-shell it is necessary to differentiate on-shell spinor variables with respect to off-shell momentum vectors to make sense of this operation. I define a prescription for taking derivatives of this form in Section 7.6. The key formulae used to differentiate any little group invariant function of spinor brackets with respect to the corresponding off-shell momentum vector are

$$\begin{aligned} \frac{\partial}{\partial p^{\dot{\beta}\beta}} \left(\frac{\langle \lambda |^\alpha}{\langle \lambda \eta \rangle} \right) &= \frac{\langle \eta |^\alpha}{\langle \lambda \eta \rangle^2} \frac{|\lambda\rangle_\beta [\tilde{\xi}]_{\dot{\beta}}} {[\tilde{\xi} \tilde{\lambda}]} \\ \frac{\partial \left(|\tilde{\lambda}\rangle^{\dot{\alpha}} \langle \lambda |^\alpha \right)}{\partial p^{\dot{\beta}\beta}} &= \delta_{\dot{\beta}}^\alpha \delta_{\dot{\beta}}^{\dot{\alpha}} - \frac{[\tilde{\xi}]^{\dot{\alpha}} \langle \xi |^\alpha |\lambda\rangle_\beta [\tilde{\lambda}]_{\dot{\beta}}} {\langle \lambda \xi \rangle [\tilde{\xi} \tilde{\lambda}]}, \end{aligned} \tag{7.3.6}$$

where $|\eta\rangle$ is an arbitrary spinor defining the little group invariant function, and $|\xi\rangle$ is a reference spinor which defines the direction of an off-shell extension to $|\lambda\rangle\langle\lambda|$.

A general plane wave amplitude expressed in terms of on-shell variables has many different possible expressions on support of momentum conservation. Non-plane wave amplitudes are more subtle still, and have more than one possible form even after taking into account momentum conservation. As an example to explain this freedom, consider using momentum conservation to remove the dependence on the momentum of a particular external state. Amplitudes with a single non-plane wave state can then be written with derivatives that act only on the momentum-conserving delta function, but the expressions obtained from worldsheet calculations will generally

not be of this form for amplitudes with more than three legs as seen in Sections 7.4 and 7.5.

7.4 Non-Plane Wave Scalar Amplitudes

In this section I give a worked example of calculating an n -point MHV amplitude with a non-plane wave scalar state using the vertex operators proposed in Section 7.3, and use the method described in Section 7.6 to express them as momentum derivatives of plane wave amplitudes.

I first calculate an amplitude with two plane wave negative helicity gravitons, a negative multiplet scalar with non-plane wave boundary conditions, and $n-3$ plane wave positive helicity gravitons. I define the left set which contains the negative helicity gravitons to be $L = \{1, 2\}$, the right set R to contain the remaining particles, and the set $R' = \{4, \dots, n\}$ to be the set of positive helicity gravitons. The vertex operators for these states can be found in (7.1.3) and (7.3.2). For notational simplicity, I define an antisymmetric bilinear bracket which acts on a pair of functions on the worldsheet as $[f, g](s) := \partial f g - f \partial g$, as well as defining shorthands for the delta functions from the vertex operators as $\delta_{|l]} := \delta^2(|l] - t_l |\tilde{\lambda}(s_l)])$ and $\delta_{|r]} := \delta^2(|r] - t_r |\lambda(s_r)])$.

The amplitude is given by

$$\begin{aligned}
 \mathcal{M}^{(0)}(h^- h^- \phi_x^- h^+ \dots h^+) &= \int \frac{d^n s}{\text{SL}(2)} \left\langle \prod_{l \in L} \tilde{\mathcal{V}}_l^{h^-}(s_l) \mathcal{V}_3^{\phi_x^-}(s_3) \prod_{\rho \in R'} \mathcal{V}_\rho^{h^+}(s_\rho) \right\rangle \\
 &= \int \frac{d^{2 \times n} \sigma}{\text{GL}(2)} \int D|\lambda\rangle D|\mu\rangle D|\tilde{\mu}\rangle D|\tilde{\lambda}\rangle e^{\int d^2 s \mathcal{L}} \prod_{l \in L} \delta_{|l]} e^{i\langle \tilde{\mu}(s_l) | l \rangle} \\
 &\quad \times \prod_{r \in R} \delta_{|r]} e^{i\langle \mu(s_r) | r \rangle} \langle 1\lambda(s_1) \rangle \langle 2\lambda(s_2) \rangle \left[|\mu\rangle, \langle \lambda| \right](s_3) \prod_{\rho \in R'} \left[\rho \tilde{\lambda}(s_\rho) \right].
 \end{aligned} \tag{7.4.1}$$

The $|\tilde{\mu}\rangle$ field in the integrand appears only inside exponentials, and hence the path integral in $|\tilde{\mu}\rangle$ and $|\lambda\rangle$ can be done as in the example for Yang-Mills in Section 2.11. As there are $|\mu\rangle$ fields appearing outside of the exponentials also, I introduce a source $|J\rangle$ for these fields as explained in Section 7.3.2. The Lagrangian with the sources

and exponentials from the vertex operators is then

$$\mathcal{L}' = \langle \tilde{\mu} | \left(\bar{\partial} |\lambda\rangle + i \sum_{l \in L} t_l \delta(s - s_l) |l\rangle \right) + [\mu | \left(\bar{\partial} |\tilde{\lambda}\rangle + i \sum_{r \in R} t_r \delta(s - s_r) |r\rangle + |J\rangle \right), \quad (7.4.2)$$

and the amplitude can be written as

$$\begin{aligned} \mathcal{M}^{(0)}(h^- h^- \phi_x^- h^+ \dots h^+) &= \int \frac{d^{2 \times n} \sigma}{GL(2)} \int D|\lambda\rangle D|\mu\rangle D|\tilde{\mu}\rangle D|\tilde{\lambda}\rangle \prod_{l \in L} \delta_{|l\rangle} \langle l|\lambda(s_l)\rangle \prod_{r \in R} \delta_{|r\rangle} \\ &\quad \times \prod_{\rho \in R'} [\rho \tilde{\lambda}(s_\rho)] \left[\frac{\delta}{\delta |J\rangle}, \langle \lambda | \right] (s_3) e^{\int d^2 s \mathcal{L}'} \Big|_{|J|=0} \\ &= \int \frac{d^{2 \times n} \sigma}{GL(2)} \int D|\lambda\rangle D|\tilde{\lambda}\rangle \prod_{l \in L} \delta_{|l\rangle} \langle l|\lambda(s_l)\rangle \prod_{r \in R} \delta_{|r\rangle} \prod_{\rho \in R'} [\rho \tilde{\lambda}(s_\rho)] \\ &\quad \times \delta \left(\bar{\partial} |\lambda\rangle + i \sum_{l \in L} \delta(s - s_l) |l\rangle \right) \\ &\quad \times \left[\frac{\delta}{\delta |J\rangle}, \langle \lambda | \right] (s_3) \delta \left(\bar{\partial} |\tilde{\lambda}\rangle + i \sum_{r \in R} \delta(s - s_r) |r\rangle + |J\rangle \right) \Big|_{|J|=0} \end{aligned} \quad (7.4.3)$$

Solving the equations of motion for $|\lambda\rangle$ and $|\tilde{\lambda}\rangle$ inside the delta functions gives that

$$\begin{aligned} |\lambda(s)\rangle &= \sum_{l \in L} \frac{t_l |l\rangle}{s - s_l} \\ |\tilde{\lambda}(s)\rangle &= \sum_{r \in R} \frac{t_r |r\rangle}{s - s_r} + \int ds' \frac{|J(s')\rangle}{s - s'} \end{aligned} \quad (7.4.4)$$

Now integrate the delta function enforcing the equations of motion for $|\lambda\rangle$ directly against $D|\lambda\rangle$, and change the functional derivative in $|J\rangle$ to one in $|\tilde{\lambda}\rangle$, and set $|J\rangle = 0$. This introduces an extra integral over s' from the chain rule for functional derivatives.

$$\begin{aligned} \mathcal{M}^{(0)}(h^- h^- \phi_x^- h^+ \dots h^+) &= \int \frac{d^{2 \times n} \sigma}{GL(2)} \int D|\tilde{\lambda}\rangle \prod_{l \in L} \delta_{|l\rangle} \prod_{r \in R} \delta_{|r\rangle} \frac{\langle 12 \rangle^2}{(12)^2} \prod_{\rho \in R'} \sum_{r \in R} \frac{[\rho r]}{(\rho r)} \\ &\quad \times \int ds' \left[\frac{1}{s - s'} \frac{\delta}{\delta |\tilde{\lambda}(s')\rangle}, \sum_{l \in L} \frac{t_l |l\rangle}{s - s_l} \right] (s_3) \delta \left(|\tilde{\lambda}\rangle - \sum_{r \in R} \frac{|r\rangle}{s - s_r} \right) \end{aligned} \quad (7.4.5)$$

Then use functional integration by parts to move the $\frac{\delta}{\delta |\tilde{\lambda}\rangle}$ functional derivative off of the functional delta function, and use the bilinearity of the bracket $[f, g]$ to pull

out $\frac{\delta}{\delta|\tilde{\lambda}|}$ and the $\langle l|$. Then the bracket evaluates to $[\frac{1}{s-s'}, \frac{1}{s-s_l}](s_3) = \frac{s'-s_l}{(s_3-s_l)^2(s'-s_l)^2}$.

Combining these results gives that

$$\begin{aligned} \mathcal{M}^{(0)}(h^- h^- \phi_x^- h^+ \dots h^+) &= \int \frac{d^{2 \times n} \sigma}{GL(2)} \prod_{r \in R} \delta_{|r\rangle} \frac{\langle 12 \rangle^2}{(12)^2} \int D|\tilde{\lambda}| \delta\left(|\tilde{\lambda}| - \sum_{r \in R} \frac{t_r |r\rangle}{s - s_r}\right) \\ &\times \int ds' \sum_{l \in L} \frac{s' - s_l}{(s_3 - s_l)^2 (s' - s_l)^2} \frac{\delta}{\delta|\tilde{\lambda}(s')|} \langle l| \left(\delta_{|1\rangle} \delta_{|2\rangle} \prod_{\rho \in R'} \sum_{r \in R} \frac{[\rho r]}{(\rho r)} \right) \end{aligned} \quad (7.4.6)$$

The derivative structure of the vertex operator with the non-plane wave states acting on the other vertex operators is now clear, showing how the non-plane wave states can be seen as momentum derivatives acting on the corresponding amplitudes with plane-wave states. Expanding out the functional derivative using the chain rule gives normal derivatives with respect to external data acting on the delta functions. There are also delta functions in s' from each action of the functional derivative, localising the s' integral. The final form of the amplitude as a worldsheet integral can then be seen to be

$$\begin{aligned} \mathcal{M}^{(0)}(h^- h^- \phi_x^- h^+ \dots h^+) &= \int \frac{d^{2 \times n} \sigma}{GL(2)} \frac{\langle 12 \rangle^2}{(12)^2} \left(\prod_{\rho \in R'} \sum_{r \in R} \frac{[\rho r]}{(\rho r)} \right) \frac{(12)}{(13)^2 (23)^2} (|\partial_1\rangle \langle 2| - |\partial_2\rangle \langle 1|) \\ &+ \sum_{\rho \in R', l \in L} \frac{|\rho\rangle \langle l| (\rho l)}{(3\rho)^2 (3l)^2} \left(\prod_{\rho' \in R', \rho' \neq \rho} \sum_{r \in R} \frac{[\rho' r]}{(\rho' r)} \right) \delta^{2 \times n}(SE_{n, \{1,2\}}) \end{aligned} \quad (7.4.7)$$

The first term comes from acting with the functional derivatives on the delta functions imposing the scattering equations, and the second term comes from acting on the spinor brackets $[\rho \tilde{\lambda}(s_\rho)]$ in the positive-helicity graviton vertex operators.

The worldsheet integral can be evaluated analytically following the same procedure as in Section 7.2. Using the $GL(2)$ symmetry to fix $\sigma_1 = \begin{pmatrix} 1 \\ 0 \end{pmatrix}$ and $\sigma_2 = \begin{pmatrix} 0 \\ 1 \end{pmatrix}$ and converting the delta functions in the left set into a momentum conserving delta function, it can be seen that the remaining terms do not depend on $|1\rangle$ or $|2\rangle$.

Furthermore, the Jacobian from the scattering equation delta functions only contains angle brackets, so that $|\partial_1]$ and $|\partial_2]$ will act only on the momentum conserving delta function. This part of the amplitude can then be simplified as follows:

$$\begin{aligned} (|\partial_1]^{\dot{\alpha}} \langle 2|^{\alpha} - |\partial_2]^{\dot{\alpha}} \langle 1|^{\alpha}) \delta^4(P) &= \left(\langle 1|_{\beta} \langle 2|^{\alpha} \frac{\partial}{\partial P^{\dot{\alpha}\beta}} - \langle 2|_{\beta} \langle 1|^{\alpha} \frac{\partial}{\partial P^{\dot{\alpha}\beta}} \right) \delta^4(P) \\ &= \langle 12 \rangle \frac{\partial \delta^4(P)}{\partial p_3^{\dot{\alpha}\alpha}}, \end{aligned} \quad (7.4.8)$$

and after some further simplification using the Schouten identity, and writing in terms of the gravitational inverse soft factor, $\psi_{p,n}$ from equation (2.5.9), the explicit form for the amplitude in terms of angle and square brackets is

$$\begin{aligned} \mathcal{M}^{(0)}(h^- h^- \phi_x^- h^+ \dots h^+) &= \langle 12 \rangle^4 \left(\prod_{\rho \in R'} \psi_{\rho,n} \frac{\partial}{\partial p_3} \right. \\ &\quad \left. + \sum_{\rho \in R'} \frac{|\rho| (\langle 12 \rangle \langle \rho 3 \rangle \langle 3| + \langle 23 \rangle \langle 13 \rangle \langle \rho|)}{\langle 3\rho \rangle^2 \langle 1\rho \rangle \langle 2\rho \rangle} \prod_{\rho' \in R', \rho' \neq \rho} \psi_{\rho',n} \right) \delta^4(P) \end{aligned} \quad (7.4.9)$$

I now use this result to show that amplitudes with states with non-plane wave boundary conditions can be calculated as momentum derivatives of those with plane wave boundary conditions. In this case, the statement is that

$$\begin{aligned} \mathcal{M}^{(0)}(h^- h^- \phi_x^- h^+ \dots h^+) &= A_3 \cdot \frac{\partial}{\partial p_3} M(h^- h^- \phi_x^- h^+ \dots h^+) \\ &= \langle 12 \rangle^4 A_3 \cdot \frac{\partial}{\partial p_3} \left(\prod_{\rho \in R'} \psi_{\rho,n} \delta^4(P) \right) \end{aligned} \quad (7.4.10)$$

Clearly for $n = 3$, $|R'| = 0$ and the result holds. To prove for all n , it suffices to prove that

$$A_3 \cdot \frac{|\rho| (\langle 12 \rangle \langle \rho 3 \rangle \langle 3| + \langle 23 \rangle \langle 13 \rangle \langle \rho|)}{\langle 3\rho \rangle^2 \langle 1\rho \rangle \langle 2\rho \rangle} = A_3 \cdot \frac{\partial}{\partial p_3} \psi_{\rho,n}, \quad (7.4.11)$$

given some vector A_3 such that $A_3 \cdot P_3 \neq 0$, which I prove in Section 7.6.

7.5 Non-Plane Wave Graviton Amplitudes

In this section I calculate an n -point MHV amplitude with a non-plane wave graviton state using the vertex operators proposed in Section 7.3, and use the method described in Section 7.6 to express them as momentum derivatives of plane wave amplitudes. There is an additional computational subtlety in the non-plane wave graviton vertex operators which was not present for non-plane wave scalars which must be addressed first. As written the non-plane wave graviton vertex operators contain singular terms, which can be seen for the h_x^- vertex operator as follows. First consider the equation of motion for $|\lambda\rangle$,

$$|\lambda(s)\rangle = \sum_{l \in L} \frac{|l\rangle}{s - s_l}, \quad (7.5.1)$$

where the poles of $|\lambda(s)\rangle$ are located at $s = s_l$. As h^- sits in the left set, $\tilde{\mathcal{V}}_l^{h_x^-}(s_l)$ will be inserted in the correlation function and has a pole at $s = s_l$. Then it appears at first glance that this vertex operator is not well-defined, but there is also a pole of $[\mu(s)]$ which cancels this pole and hence the singularity is removable. The residue at the pole of $|\lambda(s)\rangle$ when $s = s_l$ in the vertex operator is $|l\rangle [\partial_l]$. Given that $[\mu(s)] \sim \frac{1}{s-s'} \frac{\delta}{\delta[\tilde{\lambda}(s')]}$, it can be seen that will also have a pole at $s = s_l$. On support of the delta function, $[\tilde{\lambda}(s_l)] = [l]$ and the residue of this pole will be $-|l\rangle [\partial_l]$, hence the two singularities cancel.

One way to regulate this removable singularity is to insert $\lim_{\alpha \rightarrow s_l} \tilde{\mathcal{V}}_l^{h_x^-}(\alpha)$ into correlation functions instead of $\mathcal{V}_{h^-}(s_l)$, and another is to use the normal-ordered vertex operator $:\tilde{\mathcal{V}}_l^{h_x^-}:$, which is equivalent to inserting $\mathcal{V}_{h_x^-}(s_l)$ directly and dropping singular terms.

I now provide an explicit calculation of the amplitude with one negative non-plane wave graviton, $\mathcal{M}^{(0)}(h_x^- h^- h^+ \dots h^+)$, regulating the removable singularity by writing

the vertex operator as $\tilde{\mathcal{V}}_l^{h_x^-}(s_1) = \lim_{\alpha \rightarrow s_1} \tilde{\mathcal{V}}_l^{h_x^-}(\alpha)$. I define the left set to be $L = \{1, 2\}$, and use the same definitions from the last section for $\delta_{|l]}$ and $\delta_{|r]}$. The amplitude can then be written as

$$\begin{aligned} \mathcal{M}^{(0)}(h_x^- h^- h^+ \dots h^+) &= \int \frac{d^n s}{\text{SL}(2)} \left\langle \tilde{\mathcal{V}}_1^{h_x^-}(s_1) \tilde{\mathcal{V}}_2^{h^-} \prod_{r \in R} \mathcal{V}_r^{h^+}(s_r) \right\rangle \\ &= \int \frac{d^{2 \times n} \sigma}{\text{GL}(2)} \int D|\lambda\rangle D|\mu\rangle D|\tilde{\mu}\rangle D|\tilde{\lambda}\rangle e^{i \int d^2 s \mathcal{L}} e^{i \langle \tilde{\mu}(s_1) | 1 \rangle} \delta_{|2]} e^{i \langle \tilde{\mu}(s_2) | 2 \rangle} \\ &\quad \times \prod_{r \in R} \delta_{|r]} e^{i \langle \mu(s_r) | r \rangle} \langle 2\lambda(s_2) \rangle \prod_{r \in R} [r \tilde{\lambda}(s_r)] \\ &\quad \times \lim_{\alpha \rightarrow s_1} \left(|1\rangle [\mu(\alpha)] - |\lambda(\alpha)\rangle [\partial_1] \right) \delta_{|1]} \end{aligned} \quad (7.5.2)$$

Following the same steps as the calculation with one ϕ_x^- state gives that

$$\begin{aligned} \mathcal{M}^{(0)}(h_x^- h^- h^+ \dots h^+) &= \int \frac{d^{2 \times n} \sigma}{\text{GL}(2)} \prod_{r \in R} \delta_{|r]} \frac{\langle 12 \rangle}{(12)} \int D|\tilde{\lambda}\rangle \delta\left(|\tilde{\lambda}\rangle - \sum_{r \in R} \frac{|r\rangle}{s - s_r}\right) \\ &\quad \times \int d\sigma' \lim_{\alpha \rightarrow s_1} \left(\frac{1}{\alpha - s'} |1\rangle \frac{\delta}{\delta [|\tilde{\lambda}(s')\rangle]} - |\lambda(\alpha)\rangle [\partial_1] \right) \\ &\quad \times \left(\delta_{|1]} \delta_{|2]} \prod_{r \in R} \sum_{r' \in R} [r \tilde{\lambda}(s_r)] \right) \end{aligned} \quad (7.5.3)$$

Calculating the functional derivative and solving the integrals in $|\tilde{\lambda}\rangle$ and s' gives that

$$\begin{aligned} \mathcal{M}^{(0)}(h_x^- h^- h^+ \dots h^+) &= \int \frac{d^{2 \times n} \sigma}{\text{GL}(2)} \frac{\langle 12 \rangle}{(12)} \\ &\quad \times \left(\lim_{\alpha \rightarrow \sigma_1} \left(\frac{|1\rangle [\partial_1]}{\alpha - \sigma_1} + \frac{|1\rangle [\partial_2]}{(12)} - \frac{|1\rangle [\partial_1]}{\alpha - \sigma_1} - \frac{|2\rangle [\partial_2]}{(12)} \right) \prod_{r \in R} \sum_{r' \in R} \frac{[r r']}{(r r')} \right. \\ &\quad \left. + \sum_{r \in R} \frac{|1\rangle [r]}{(1r)} \prod_{r' \neq r \in R} \sum_{r'' \in R} \frac{[r' r'']}{(r' r'')} \right) \delta^{2 \times n}(SE_{n,L}). \end{aligned} \quad (7.5.4)$$

The singular terms cancel, giving an integral expression for the amplitude supported on scattering equations. Solving this integral as in the calculation with one ϕ_x^- state gives

$$\begin{aligned}
 \mathcal{M}^{(0)}(h_x^- h^- h^+ \dots h^+) &= \int \frac{d^{2 \times n} \sigma}{GL(2)} \frac{\langle 12 \rangle}{(12)} \left(\left(\frac{|1\rangle [\partial_2| - |2\rangle [\partial_1|}{(12)} \right) \prod_{r \in R} \sum_{r' \in R} \frac{[rr']}{(rr')} \right. \\
 &\quad \left. + \sum_{r \in R} \frac{|1\rangle [r|}{(1r)} \prod_{r' \neq r \in R} \sum_{r'' \in R} \frac{[r'r'']}{(r'r'')} \right) \delta^{2 \times n}(SE_{n,L}) \\
 &= \langle 12 \rangle^4 \left(\prod_{r \in R} \psi_{r,n} \frac{\partial}{\partial p_1} + \sum_{r \in R} \frac{\langle 12 \rangle |1\rangle [r|}{\langle 1r \rangle^2 \langle 2r \rangle} \prod_{r' \in R, r' \neq r} \psi_{r',n} \right) \delta^4(P),
 \end{aligned} \tag{7.5.5}$$

and using the result for the derivative of a gravitational inverse soft factor from Section 7.6 gives that

$$\mathcal{M}^{(0)}(h_x^- h^- h^+ \dots h^+) = \langle 12 \rangle^4 A_1 \cdot \frac{\partial}{\partial p_1} \left(\prod_{r \in R} \psi_{r,n}^{[1]|2} \delta^4(P) \right). \tag{7.5.6}$$

Following similar steps, the calculation with two non-plane wave gravitons gives that

$$\mathcal{A}(h_x^- h_x^- h^+ \dots h^+) = \langle 12 \rangle^4 \left(A_1 \cdot \frac{\partial}{\partial p_1} \right) \left(A_2 \cdot \frac{\partial}{\partial p_2} \right) \left(\prod_{r \in R} \psi_{r,n}^{[1]|2} \delta^4(P) \right) \tag{7.5.7}$$

where A_1 and A_2 are vectors in the wave functions of particles 1 and 2.

7.6 Momentum Derivatives

In this section I define a prescription to differentiate on-shell spinor variables $|\lambda\rangle$ with respect to a corresponding momentum vector p , as needed to calculate the momentum derivatives of plane wave amplitudes. I work with real momenta, such that $|\tilde{\lambda}\rangle = \langle \lambda |^\dagger$. As written this problem is not well specified, as there are four degrees of freedom in an off shell momentum p and only three degrees of freedom in the spinor variables after the quotient by the $U(1)$ little group. To make the problem well-defined, I add an extra constant reference spinor $|\xi\rangle$ and a variable α proportional to the length of the vector to the system to define a complete co-ordinate transformation from (p^0, p^1, p^2, p^3) to $(|\lambda\rangle, \alpha)$. The direction $\xi = |\xi\rangle \langle \xi|$ then defines a direction which comes off the mass shell, and all other directions $|\tilde{\lambda}\rangle \langle \lambda|$ sit in the

mass-shell. The change of variables is given by

$$p = |\tilde{\lambda}\rangle\langle\lambda| + \alpha|\tilde{\xi}\rangle\langle\xi|. \quad (7.6.1)$$

Inverting this equation to solve for α gives that $\alpha(p) = \frac{p^2}{2p \cdot \xi}$, and it is also possible to solve for $|\lambda(p)\rangle$. To see this, contract equation 7.6.1 with spinor $[\tilde{\xi}]$ to arrive at $[\xi|p = [\tilde{\xi}\tilde{\lambda}]\langle\lambda|$. For real momenta the relationship $|[\tilde{\xi}\tilde{\lambda}]|^2 = \xi \cdot p$ holds, and hence there must exist some phase $\theta(p)$ such that $[\tilde{\xi}\tilde{\lambda}] = e^{-i\theta} \sqrt{\xi \cdot p}$. Given that $|\lambda\rangle$ is defined only up to this arbitrary phase, the inverse coordinate transformation is then given by

$$\langle\lambda(p)| = e^{i\theta(p)} \frac{[\xi|p}{\sqrt{\xi \cdot p}}, \quad \alpha(p) = \frac{p^2}{2p \cdot \xi}. \quad (7.6.2)$$

It may appear strange at first sight that the phase can depend on p but this dependence is actually used regularly, for example when using the little group freedom to fix one of the components of $|\lambda\rangle$. For the choice of reference spinor $\langle\xi| = \begin{pmatrix} 0 \\ 1 \end{pmatrix}$ and $\theta = 0$ the following well-known expression [82]

$$|\lambda(p)\rangle = \frac{1}{\sqrt{p^0 + p^3}} \begin{pmatrix} p^0 + p^3 \\ p^1 - ip^2 \end{pmatrix} \quad (7.6.3)$$

is recovered.

Now consider calculating $\frac{\partial|\lambda\rangle}{\partial p}$ from equation (7.6.2), keeping in mind that the little group phase depends on p . Then

$$\begin{aligned} \frac{\partial\langle\lambda(p)|^\alpha}{\partial p^{\dot{\beta}\beta}} &= \frac{\partial}{\partial p^{\dot{\beta}\beta}} \left(\frac{e^{i\theta(p)} ([\tilde{\xi}|p]^\alpha)}{\sqrt{\xi \cdot p}} \right) \\ &= \frac{\delta_\beta^\alpha e^{i\theta(p)} [\tilde{\xi}|_{\dot{\beta}}]}{\sqrt{\xi \cdot p}} - \frac{1}{2} \frac{e^{i\theta(p)} ([\tilde{\xi}|p]^\alpha)}{\sqrt{\xi \cdot p}} \frac{|\xi\rangle_\beta [\tilde{\xi}|_{\dot{\beta}}]}{\xi \cdot p} + i \frac{\partial\theta(p)}{\partial p^{\dot{\beta}\beta}} \frac{e^{i\theta(p)} ([\tilde{\xi}|p]^\alpha)}{\sqrt{\xi \cdot p}} \\ &= \frac{\delta_\beta^\alpha [\tilde{\xi}|_{\dot{\beta}}]}{[\tilde{\xi}\tilde{\lambda}]} - \frac{1}{2} \frac{\langle\lambda(p)|^\alpha |\xi\rangle_\beta [\tilde{\xi}|_{\dot{\beta}}]}{\langle\lambda\xi\rangle [\tilde{\xi}\tilde{\lambda}]} + i \frac{\partial\theta(p)}{\partial p^{\dot{\beta}\beta}} \langle\lambda(p)|^\alpha, \end{aligned} \quad (7.6.4)$$

and it can be seen that $\frac{\partial|\lambda\rangle}{\partial p}$ transforms as a connection on the U(1) little group.

Now consider taking the momentum derivative of a function of spinor brackets. Due

to the transformation law for $\frac{\partial|\lambda\rangle}{\partial p}$, if the function transforms covariantly in the little group then its derivative will transform as a connection in the little group, and only for little group invariant functions will the derivative transform covariantly. As scattering amplitudes either transform covariantly or are invariant in the little group, it is important to only differentiate little group invariant functions of momenta in the calculation of non-plane wave amplitudes. All acceptably differentiable functions of spinor brackets can then be built up out of two basic little group invariants, $|\tilde{\lambda}\rangle\langle\lambda|$ and $\frac{\langle\lambda|}{\langle\lambda\eta\rangle}$, where $|\eta\rangle$ is any spinor defining the functions.

First consider differentiating $\frac{\langle\lambda|}{\langle\lambda\eta\rangle}$ with respect to p , using equation (7.6.4). Note that while equation (7.6.4) is not little group covariant its contraction with $|\lambda\rangle$ is, resulting in a little group invariant result.

$$\begin{aligned} \frac{\partial}{\partial p^{\dot{\beta}\beta}} \left(\frac{\langle\lambda|^\alpha}{\langle\lambda\eta\rangle} \right) &= \frac{\langle\lambda\eta\rangle \frac{\partial\langle\lambda|^\alpha}{\partial p^{\dot{\beta}\beta}} + \frac{\partial\langle\lambda|^\gamma}{\partial p^{\dot{\beta}\beta}} |\eta\rangle_\gamma \langle\lambda|^\alpha}{\langle\lambda\eta\rangle^2} \\ &= \frac{\langle\eta|^\alpha}{\langle\lambda\eta\rangle^2} |\lambda\rangle_\gamma \frac{\partial\langle\lambda|^\gamma}{\partial p^{\dot{\beta}\beta}} = \frac{\langle\eta|^\alpha |\lambda\rangle_\beta [\tilde{\xi}]_{\dot{\beta}}}{\langle\lambda\eta\rangle^2 [\tilde{\xi}\tilde{\lambda}]}, \end{aligned} \quad (7.6.5)$$

where in the second line the Schouten identity was used, and in the third equality (7.6.4) was used.

Now consider differentiating the on shell momentum vector $|\tilde{\lambda}\rangle\langle\lambda|$. This calculation is more simple using the initial definition of the co-ordinate transformation (7.6.1), which gives that

$$\frac{\partial \left(|\tilde{\lambda}]^{\dot{\alpha}} \langle\lambda|^\alpha \right)}{\partial p^{\dot{\beta}\beta}} = \delta_{\dot{\beta}}^\alpha \delta_{\dot{\beta}}^{\dot{\alpha}} - \frac{|\tilde{\xi}]^{\dot{\alpha}} \langle\xi|^\alpha |\lambda\rangle_\beta [\tilde{\lambda}]_{\dot{\beta}}}{\langle\lambda\xi\rangle [\tilde{\xi}\tilde{\lambda}]}. \quad (7.6.6)$$

The result of this calculation is a projection matrix which satisfies $|\tilde{\xi}]^{\dot{\beta}} \langle\xi|^\beta \frac{\partial(|\tilde{\lambda}]^{\dot{\alpha}} \langle\lambda|^\alpha)}{\partial p^{\dot{\beta}\beta}} = 0$ and $p^{\dot{\beta}\beta} \frac{\partial(|\tilde{\lambda}]^{\dot{\alpha}} \langle\lambda|^\alpha)}{\partial p^{\dot{\beta}\beta}} = |\tilde{\lambda}]^{\dot{\alpha}} \langle\lambda|^\alpha$. Although these formulae depend on a reference spinor, varying with respect to the reference spinor gives terms corresponding to momentum derivatives of functions which vanish on-shell and can therefore be neglected.

Now use these identities to compute two different momentum derivatives of the gravitational inverse-soft factor $\psi_{j,n}^{[a]b)}$ defined in equation (2.5.9), which are used in Sections 7.4 and 7.5. In particular, first differentiate with respect to particle i

where $i \neq j$, and take reference spinors $|a\rangle$ and $|b\rangle$ not to depend on i . Note that the independence of the gravitational inverse soft factor on the two reference spinors is only valid on support of momentum conservation, and when taking derivatives it is necessary to specify what the reference spinors are. Then

$$\begin{aligned}
\frac{\partial}{\partial p_i^{\dot{\beta}\beta}} \psi_{j,n}^{a,b} &= \frac{\partial}{\partial p_i^{\dot{\beta}\beta}} \sum_{k \in \mathcal{N} \setminus \{j\}} \frac{[jk] \langle ka \rangle \langle kb \rangle}{\langle jk \rangle \langle ja \rangle \langle jb \rangle} \\
&= \frac{1}{\langle ja \rangle \langle jb \rangle} \left([j]_{\dot{\alpha}} \frac{\partial}{\partial p_i^{\dot{\beta}\beta}} (|i]^{\dot{\alpha}} \langle i |^{\alpha}) |a\rangle_{\alpha} \frac{\langle ib \rangle}{\langle ji \rangle} + [ji] \langle ia \rangle \frac{\partial}{\partial p_i^{\dot{\beta}\beta}} \left(\frac{\langle i |^{\alpha}}{\langle ji \rangle} \right) |b\rangle_{\alpha} \right) \\
&= \left(|i\rangle_{\beta} \langle ab \rangle \langle ji \rangle + |j\rangle_{\beta} \langle ia \rangle \langle bi \rangle \right) \frac{[j]_{\dot{\beta}}}{\langle ja \rangle \langle jb \rangle \langle ij \rangle^2},
\end{aligned} \tag{7.6.7}$$

where in the second line equations (7.6.6) and (7.6.5) are used, the reference spinor is chosen to be $|\xi\rangle = |j\rangle$, and Schouten identity was also used to rearrange the brackets.

A final example is a different derivative of the gravitational inverse soft factor.

Consider the case where $|a\rangle = |j\rangle$, and $j \neq i$. Then

$$\begin{aligned}
\frac{\partial}{\partial p_j} \psi_{i,n}^{[j]|b)} &= \sum_{k \in \mathcal{N} \setminus \{i,j\}} \frac{[ki] \langle kb \rangle}{\langle ki \rangle \langle ib \rangle} \frac{\partial}{\partial p_j} \left(\frac{\langle kj \rangle}{\langle ij \rangle} \right) \\
&= \sum_{k \in \mathcal{N} \setminus \{i,j\}} \frac{[ki] \langle kb \rangle \langle ik \rangle}{\langle ki \rangle \langle ib \rangle \langle ij \rangle^2} \frac{|\tilde{\xi} \rangle \langle j |}{[\tilde{\xi} j]}
\end{aligned} \tag{7.6.8}$$

Fixing the reference spinor $|\tilde{\xi} \rangle = |i \rangle$ gives that

$$\begin{aligned}
\frac{\partial}{\partial p_j} \psi_{i,n}^{[j]|b)} &= [i] \sum_{k \in \mathcal{N} \setminus \{i,j\}} \left([k] \langle k | \right) |b\rangle \frac{[i] \langle j |}{[ij] \langle bi \rangle \langle ij \rangle^2} \\
&= \frac{\langle bj \rangle [i] \langle j |}{\langle bi \rangle \langle ij \rangle^2}
\end{aligned} \tag{7.6.9}$$

7.7 BRST Quantization

In this section I analyse the BRST quantisation 4D ambitwistor string theory as defined by the worldsheet Lagrangian in equation (2.11.2). This serves as a review of how Yang-Mills states sit in the cohomology of the BRST operator Q , and I also

derive new results showing how the conformal supergravity vertex operators which I provide in Sections 7.1 and 7.3 are also in the cohomology of Q .

The Lagrangian can be written as

$$\mathcal{L} = \mathcal{Z}\bar{\partial}\tilde{\mathcal{Z}} + u\mathcal{Z} \cdot \tilde{\mathcal{Z}} + eT_{matter},$$

where u is a worldsheet gauge field and

$$T_{matter} = \frac{1}{2} (\mathcal{Z} \cdot \partial\tilde{\mathcal{Z}} - \tilde{\mathcal{Z}} \cdot \partial\mathcal{Z}) + T_J,$$

where T_J is the current algebra stress tensor.

Note that this Lagrangian is a (β, γ) ghost system with holomorphic conformal weights $(1/2, 1/2)$. A general (β, γ) system with holomorphic conformal weights $(\lambda, 1 - \lambda)$ has the stress tensor

$$T_{\beta\gamma} = \lambda\beta\partial\gamma - \epsilon(1 - \lambda)\gamma\partial\beta,$$

where $\epsilon = \pm 1$ for bosonic/fermionic statistics. The central charge can then be read off from the OPE of T with itself and is given by

$$c = 2\epsilon(6\lambda^2 - 6\lambda + 1). \quad (7.7.1)$$

The gauge fields can be fixed to $e = u = 0$ using the Fadeev-Popov procedure by introducing ghost systems (b, c) and (\tilde{b}, \tilde{c}) with holomorphic conformal weights $(2, -1)$ and $(1, 0)$, respectively. The stress tensor for the ghosts is then given by $T_{ghost} = T_{bc} + T_{\tilde{b}\tilde{c}}$ where

$$T_{bc} = 2b\partial c - c\partial b, \quad T_{\tilde{b}\tilde{c}} = \tilde{b}\partial\tilde{c}.$$

Using (7.7.1), the contribution of the ghosts to the central charge is $c_{ghost} = -26 - 2 = -28$. The BRST charge Q is then defined as

$$Q = \oint ds \left(c(T_{matter} + T_{ghost}) + \tilde{c}\mathcal{Z} \cdot \tilde{\mathcal{Z}} \right).$$

The key property that Q must satisfy is nilpotency, that $Q^2 = 0$. In order for Q to satisfy this constraint, the total central charge must vanish. The $(\mathcal{Z}, \tilde{\mathcal{Z}})$ system has zero central charge since the bosonic contributions cancel the fermionic ones, so the central charge of the current algebra must be $c_J = +28$.

For vertex operators to be in the cohomology of Q they must satisfy $QV = 0$, which is equivalent to calculating $\{Q, \mathcal{V}\} = 0$ at the level of operators in the 2D conformal field theory. This condition implies that the vertex operators must have holomorphic conformal weight $w_{\mathcal{V}} = 1$ and $GL(1)$ weight $q_{\mathcal{V}} = 0$. The conformal and $GL(1)$ weights may be read off from the OPE of the vertex operator with T and $\mathcal{Z} \cdot \tilde{\mathcal{Z}}$:

$$T(\sigma)\mathcal{V}(s') = \frac{w_{\mathcal{V}}\mathcal{V}(s)}{(s-s')^2} + \dots, \quad \mathcal{Z} \cdot \tilde{\mathcal{Z}}(s)\mathcal{V}(s') = \frac{q_{\mathcal{V}}\mathcal{V}(s)}{s-s'} + \dots$$

where the ellipses denote less singular terms.

Now verify that the vertex operators considered in Sections 7.1 and 7.3 are Q -closed.

A plane-wave vertex operator in the right set is schematically of the form

$$\delta^2(|r\rangle - t|\lambda(s)\rangle) e^{it[\mu(s)r]},$$

where $k_r = |r\rangle\langle r|$ is the on-shell momentum. Let us then consider an ansatz for a plane-wave vertex operator of the form

$$\mathcal{V}(s) = \int \frac{dt}{t^\gamma} \delta^2(|r\rangle - t|\lambda(s)\rangle) e^{it[\mu(s)r]} [\tilde{\lambda}(s)r]^{s'-1} J(s), \quad (7.7.2)$$

where $s' \geq 1$ is the spin. In practice, a long but straightforward OPE calculation can be avoided using the following rules for computing conformal and $GL(1)$ weights;

$$T : [\mathcal{Z}] = [\tilde{\mathcal{Z}}] = -[t] = \frac{1}{2}, \quad [\partial] = 1$$

$$\mathcal{Z} \cdot \tilde{\mathcal{Z}} : [\mathcal{Z}] = -[\tilde{\mathcal{Z}}] = -[t] = 1, \quad [\partial] = 0,$$

where weights of t are fixed by the consistency condition that $[tZ] = 0$. For vertex operators in the left set, t will have opposite weights. External spinors have zero weight, $[|i\rangle] = [i] = 0$. Applying these rules to the vertex operator in (7.7.2), gives that

$$w_{\mathcal{V}} = \frac{1}{2}(\gamma - 1) + \frac{1}{2}(s' - 1) + w_j, \quad q_{\mathcal{V}} = (\gamma - 1) - (s' - 1),$$

where w_j is the conformal weight of the current algebra. Q -closure then implies that $\gamma = s'$ and $w_j = 2 - s'$, which implies that $s' \leq 2$. Note that if the constraint $q_{\mathcal{V}} = 0$ is not imposed then the $GL(1)$ symmetry is not gauged and vertex operators with higher spin appear to be allowed. If $s' = 1$, then the vertex operator reduces to

$$\mathcal{V}(s) = \int \frac{dt}{t} \delta^2(|r\rangle - t|\lambda(s)\rangle) e^{it[\mu(s)r]} J(s) \quad (7.7.3)$$

which describes a gluon in $\mathcal{N} = 4$ super Yang-Mills. For $s = 2$, the vertex operator describes a graviton with plane wave boundary conditions:

$$\mathcal{V}(s) = \int \frac{dt}{t^2} \delta^2(|r\rangle - t|\lambda(s)\rangle) e^{it[\mu(s)r]} [\tilde{\lambda}(s)r],$$

where the current algebra is not present in the vertex operator since $w_j = 0$.

To deduce the vertex operator for a scalar in the right set, consider the ansatz

$$\mathcal{V}(s) = \int \frac{dt}{t^\gamma} \delta^2(|r\rangle - t|\lambda(s)\rangle) e^{it[\mu(s)r]} \langle \lambda(\sigma) \partial \lambda(\sigma) \rangle^{1-s'} J(s) \quad (7.7.4)$$

where $s' \leq 1$. Using the rules described above gives

$$w_{\mathcal{V}} = \frac{1}{2}(\gamma - 1) + 2(1 - s') + w_j, \quad q_{\mathcal{V}} = 2(1 - s') + (\gamma - 1).$$

Imposing $w_{\mathcal{V}} = 1$ and $q_{\mathcal{V}} = 0$ then implies that $\gamma = 2s' - 1$ and $w_j = s'$, from which we deduce that $s' \geq 0$. If $s' = 1$, then the vertex operator reduces to the gluon vertex operator in (7.7.3), but if $s' = 0$ it describes a scalar with plane-wave boundary conditions,

$$\mathcal{V}(s) = \int t dt \delta^2(|r\rangle - t|\lambda(s)\rangle) e^{it[\mu(s)r]} \langle \lambda(s) \cdot \partial \lambda(s) \rangle.$$

Now consider non-plane wave states, using the following ansatz:

$$\mathcal{V}(s) = \int \frac{dt}{t^\gamma} \left(A \cdot (|i\rangle \langle \tilde{\mu}| - |\tilde{\lambda}\rangle \langle \partial_i|) \right)^{s'-1} \delta^2(|r\rangle - t|\lambda(s)\rangle) e^{it[\mu(s)r]}.$$

Following an analysis similar to the one from equation (7.7.2) gives that $s' = \gamma = 2$,

so the vertex operator reduces to that of a non-plane wave graviton. Similarly, the following ansatz

$$\mathcal{V}(s) = \int \frac{dt}{t^\gamma} (A \cdot (|\lambda\rangle \partial[\mu] - \partial|\lambda\rangle [\mu]))^{1-s'} \delta^2(|r\rangle - t|\lambda(s)\rangle) e^{it[\mu(s)r]}$$

must satisfy $s' = 0$ and $\gamma = -1$, and reduces to the vertex operator for a non-plane wave scalar.

Chapter 8

Conclusion

8.1 Summary of Results

In this thesis, I have focused on the framework of the 4D scattering equations, their relationship with 4D ambitwistor string theory and on-shell diagrams, and how they can be used to calculate scattering amplitudes in $\mathcal{N} = 4$ super Yang-Mills, $\mathcal{N} = 8$ supergravity and $\mathcal{N} = 4$ conformal supergravity.

In Chapter 3 I explained in detail the necessary tools for solving the 4D scattering equations analytically in the MHV sector and numerically for higher MHV degree, based on my work from [1], and in Chapter 4 I outlined a Monte Carlo algorithm for solving the scattering equations numerically, and an algorithm for extracting component amplitudes from Grassmann delta functions efficiently. These results allow for computation of tree-level amplitudes in Yang-Mills theory and Einstein gravity with any number of super symmetries, as understood in [26], and sets up the formalism necessary for my later analysis of $\mathcal{N} = 4$ conformal supergravity. Amplitudes in these theories can be calculated explicitly using my accompanying MATHEMATICA package `treeamps4dJAF` which is published alongside [1], and implements the algorithms described in this paper. When integrands are conjectured for new theories it will now be straightforward to test and evaluate them using the package.

In Chapter 5 I then moved on to explore amplitudes in $\mathcal{N} = 4$ super Yang-Mills by understanding the relation between worldsheet integral expressions for the amplitudes of the theory supported on 4D scattering equations, and Grassmannian integral formulae arising from on-shell diagrams, based on my work from [2]. From this analysis I found a deeper understanding of the structure of tree level amplitudes in $\mathcal{N} = 4$ super Yang-Mills, making clear how the two different computational approaches are related by a global residue theorem in the NMHV sector, and understanding how the different terms in the amplitude can be seen to arise from taking residues of a single top form in the Grassmannian in this case. I also derived new worldsheet formulae for the 1-loop 4 point integrand of the theory which is manifestly supersymmetric and supported on scattering equations refined by MHV degree. I then solved the scattering equations to evaluate this worldsheet integral, based on my work from appendix C of [3]

I went on in Chapter 6 to extend the theory of on-shell diagrams for $\mathcal{N} = 8$ supergravity, and to extend my analysis of the mapping between 4D scattering equations and on-shell diagrams to this setting, also based on my work from [2]. This allowed me to compute the n -point tree level MHV amplitude in supergravity using on-shell diagrams, matching against known expressions in terms of both the inherently non-planar Hodges matrix and the planar BGK formula. For NMHV amplitudes, I find that the decorated planar on-shell diagrams of $\mathcal{N} = 8$ supergravity do not arise from the residues of a single top form in the Grassmannian, in contrast to the planar on-shell diagrams of $\mathcal{N} = 4$ super Yang-Mills. I also derived new worldsheet formulae for the 1-loop 4 point integrand in $\mathcal{N} = 8$ supergravity, equivalent to the one I found in $\mathcal{N} = 4$ super Yang-Mills in Chapter 5.

Finally, in Chapter 7 I investigated tree-level scattering amplitudes of graviton multiplets in $\mathcal{N} = 4$ conformal supergravity using 4D ambitwistor string theory, based on my work from [4]. In contrast to the 4D ambitwistor string formulae for $\mathcal{N} = 4$ super Yang-Mills and $\mathcal{N} = 8$ supergravity, I find that the number of negative helicity superfields is not equal to the Grassmann degree of the amplitude, and that

the scattering equations for conformal supergravity are defined by the Grassmann degree. I found simple expressions for the vertex operators for plane wave graviton multiplets of the theory, and by calculating correlation functions of these vertex operators I obtained simple formulae for scattering amplitudes of graviton multiplets which generalize previous results of Berkovits and Witten for Grassmann degree 2. For Grassmann degree 3 and higher I evaluated the worldsheet integrals numerically using my methods from Chapters 3 and 4, and I matched the results against those obtained using Feynman diagrams and the double copy approach developed in [49] up to 8 points.

I went on in Chapter 7 to analyse graviton multiplets with non-plane wave boundary conditions of the form $A \cdot x e^{ik \cdot x}$. I found that amplitudes with such states were subtle to compute, requiring the introduction of sources in the worldsheet path integral which lead to deformed scattering equations as an intermediate step in the calculation. Using this formalism I derived worldsheet formulae for some amplitudes with non-plane wave graviton states at n -points. I then developed a prescription for differentiating spinor variables with respect to their corresponding off-shell momenta, which I used to show that non-plane wave amplitudes of the theory can be obtained by acting on plane wave amplitudes with momentum derivatives.

8.2 Directions for Future Work

I now give a brief description of directions for future research based on my work in this thesis.

Firstly building on the work analysing numerical and analytical aspects of the 4D scattering equations from Chapters 3 and 4, the following are possible areas for future research:

- A natural question to ask is whether my numerical methods for solving the 4D scattering equations are applicable to the general d scattering equations.

It should be simple to map a full set of solutions at n points from the 4D scattering equations to the general d scattering equations for $d = 4$, which would allow calculating amplitudes for the wider variety of theories supported by these equations in four dimensions. Solving the general d equations directly using this algorithm is more difficult as they are not refined by helicity degree and all $(n - 3)!$ solutions must be found. MATHEMATICA's inbuilt algorithms can already solve the general d equations numerically up to 9 points with a deterministic algorithm, so it would be necessary to improve on the efficiency of the Monte Carlo algorithm if it is to become a viable method for this problem.

- The explicit implementation of the algorithms in my Mathematica package `treeamps4dJAF` which is published alongside this work provide only a basic implementation of the Monte Carlo equation solving algorithm, and there are a number of different ways that it could be improved. `NSolveMonteCarlo` does not support parallel computation of different calls to `FindRoot`, and does not use an optimal algorithm for deciding whether solutions are duplicate. The sampling method used where all initial points are taken from an approximated uniform distribution could be improved on. An updated algorithm with these changes in MATHEMATICA should have significantly better behaved time complexity. Re-writing the core solution finding algorithm in a different programming language better suited to low-level numerical computation such as C++ could also increase efficiency dramatically. These changes should allow solution finding in the 4D case for higher n and k , and it is possible that they could allow solving the general d equations by Monte Carlo algorithm to become viable.
- It is intriguing to find that the Cauchy distribution arises in the statistical analysis of the solutions to the 4D scattering equations, and especially to find that the parameter of the distribution is insensitive to changing n and k . It would be interesting to explore how the functional form of this distribution is

related to the physics of the equations.

- A clear limitation of the 4D scattering equations is that they currently only support tree-level calculations, and the forward limit part of one loop integrands as explained in Chapter 5. Although loop-level scattering equations exist in general dimensions [133, 134], and work has been done with the general d scattering equations in 4 dimensions [3] at one loop, there is as yet no n -point formula for loop integrands in terms of helicity refined 4D scattering equations. A natural future direction is to investigate the existence of n -point loop level 4D scattering equations, and another direction for future work could implement numerical algorithms to evaluate loop-level integrands as sums over solutions to the general d equations. It would also be interesting to extend the work from [3] to two loops.
- The 4D scattering equations are not restricted only to calculating amplitudes, they also cover form factors [135] and possibly further structures in quantum field theory. They can also be used to calculate more physically relevant standard model amplitudes [136]. The tools I have provided in this paper should be directly relevant to calculation of form factors, and could play a role in finding new types of structures that can be supported on scattering equations.
- Recent work in [137, 138] proposes a set of 6D scattering equations, and [139] extends the general d scattering equations from the Riemann sphere to $\mathbb{C}P^k$. It would be interesting to see if the algorithms I provide in this thesis are useful in finding solutions to these new extended scattering equations.

Based on my work understanding how the 4D scattering equations are related to on-shell diagrams in $\mathcal{N} = 4$ super Yang-Mills in Chapter 5, I pose the following questions for future research:

- In Section 6.6, I use the bonus relations to solve the on-shell diagram recursion

relations in the planar sector for MHV amplitudes in $\mathcal{N} = 8$ and obtain a compact expression for any number of legs. It would be interesting to see if this expression has a geometric interpretation, analogous to the amplituhedron for planar $\mathcal{N} = 4$ super Yang-Mills. Beyond MHV, I find that the decorated planar on-shell diagrams from which the full amplitudes can be deduced do not correspond to residues of a single top-form, so it would be interesting to see if a unique top-form can be deduced by solving the recursion relations in a non-planar sector or incorporating the bonus relations, possibly using the work on non-planar on-shell diagrams in [140]. Interesting progress has been made recently towards finding a geometrical object to describe gravity amplitudes in [123, 141].

- Since integrability is usually restricted to two-dimensional models, one would expect that reformulating perturbative scattering amplitudes as worldsheet integrals should provide new insight into the origin of such properties in a 4D theory like $\mathcal{N} = 4$ super Yang-Mills. It would therefore be interesting to investigate how Yangian symmetry is realised for the worldsheet formulae of $\mathcal{N} = 4$ super Yang-Mills arising from 4D ambitwistor string theory, compared with that of the original twistor string [142]. Moreover, if it is possible to generalize my worldsheet formulae for $\mathcal{N} = 8$ supergravity to higher loops, it would be interesting to investigate if they provide hints into the origin of unexpected UV cancellations, or if they provide a simple prescription for regulating IR divergences.
- There has been a great deal of progress in computing tree-level form factors in $\mathcal{N} = 4$ super Yang-Mills using on-shell diagrams [143] and 4D ambitwistor string theory [136, 144, 135, 145], so it would be interesting to see if my one-loop worldsheet formula for $\mathcal{N} = 4$ super Yang-Mills can be generalised to form-factors.

And finally based on my work understanding the structure of $\mathcal{N} = 4$ conformal

supergravity amplitudes, and how they can be described as integrals over the 4D scattering equations arising from 4D ambitwistor string theory, I suggest the following directions for future research:

- Although $\mathcal{N} = 4$ conformal supergravity is invariant under the conformal group, this symmetry is not manifest in my worldsheet formulae. As explained in [48], this may be expected since choosing plane wave external states singles out 2-derivative solutions to the 4-derivative equations of motion, breaking conformal invariance. On the other hand, the underlying theory has conformal symmetry so it would be interesting to understand how it is realised at the level of amplitudes. Hidden conformal symmetry of gravitational amplitudes was recently explored in [146], so it would be interesting to see if the ideas developed in that paper can be applied to conformal gravity.
- As I show in Chapters 5 and 6, the 4D scattering equation formulae for $\mathcal{N} = 4$ super Yang-Mills and $\mathcal{N} = 8$ supergravity can be mapped into Grassmannian integral formulae which can be derived from a completely different approach involving on-shell diagrams. For $\mathcal{N} = 4$ super Yang-Mills, these formulae suggest a new interpretation of the amplitudes as the volume of a geometric object known as the Amplituhedron [68]. It would be interesting to carry out an analogous mapping for conformal supergravity amplitudes and see if they have a similar geometric interpretation.
- A double copy construction has recently been proposed for conformal supergravity [49], which involves combining super-Yang-Mills with a certain non-supersymmetric $(DF)^2$ gauge theory, and an ambitwistor string theory describing the latter in general dimensions was proposed in [50]. It would be interesting to try to formulate the $(DF)^2$ theory using 4D ambitwistor string theory and obtain worldsheet formulae for the scattering amplitudes supported on refined scattering equations.
- One major open problem is to derive perturbative loop amplitudes directly from

the worldsheet theories for $\mathcal{N} = 4$ super Yang-Mills and $\mathcal{N} = 8$ supergravity. This may be challenging using the worldsheet models developed so far since the worldsheet theory for $\mathcal{N} = 4$ super Yang-Mills contains conformal supergravity in its spectrum [20] and the worldsheet theory for $\mathcal{N} = 8$ supergravity is not critical if one gauges the Virasoro symmetry [21]. The work I have done in understanding tree-level conformal supergravity amplitudes in this thesis may be relevant to solving this problem.

8.3 Concluding Remarks

In summary, I have given a thorough analysis of the computational frameworks of the 4D scattering equations, on-shell diagrams and 4D ambitwistor string theory, and have developed new approaches to understanding the structure of the scattering amplitudes of $\mathcal{N} = 4$ super Yang-Mills, $\mathcal{N} = 8$ supergravity and $\mathcal{N} = 4$ conformal supergravity using these techniques. I have derived a number of results in these settings which are new in the literature, and which I hope will provide a small contribution towards answering some of the deep questions of theoretical physics. My results for amplitudes in $\mathcal{N} = 4$ super Yang-Mills could give provide insights towards new computational techniques in the physical Yang-Mills theory without supersymmetries which may ultimately lead to more efficient computational techniques allowing a wider range of scattering amplitudes to become accessible to experimental physics. My work on the amplitudes of $\mathcal{N} = 8$ supergravity and $\mathcal{N} = 4$ conformal supergravity may lead to a deeper understanding of gravitational amplitudes, which could ultimately be applied to more realistic models and hopefully provide a small piece in the puzzle of the problem of quantum gravity.

Bibliography

- [1] Joseph A. Farrow. A Monte Carlo Approach to the 4D Scattering Equations. *JHEP*, 08:085, 2018.
- [2] Joseph A. Farrow and Arthur E. Lipstein. From 4d Ambitwistor Strings to On Shell Diagrams and Back. *JHEP*, 07:114, 2017.
- [3] Joseph A. Farrow, Yvonne Geyer, Arthur E. Lipstein, Ricardo Monteiro, and Ricardo Stark-Muchão. Propagators, BCFW recursion and new scattering equations at one loop. *JHEP*, 10:074, 2020.
- [4] Joseph A. Farrow and Arthur E. Lipstein. New Worldsheet Formulae for Conformal Supergravity Amplitudes. *JHEP*, 07:074, 2018.
- [5] Zhan Xu, Da-Hua Zhang, and Lee Chang. Helicity Amplitudes for Multiple Bremsstrahlung in Massless Nonabelian Gauge Theories. *Nucl. Phys.*, B291:392–428, 1987.
- [6] R. Kleiss and W. James Stirling. Spinor Techniques for Calculating p anti- $p \rightarrow W^{+-} / Z^0 + \text{Jets}$. *Nucl. Phys.*, B262:235–262, 1985.
- [7] Stephen J. Parke and T. R. Taylor. An Amplitude for n Gluon Scattering. *Phys. Rev. Lett.*, 56:2459, 1986.
- [8] Ruth Britto, Freddy Cachazo, and Bo Feng. New recursion relations for tree amplitudes of gluons. *Nucl. Phys.*, B715:499–522, 2005.

-
- [9] Ruth Britto, Freddy Cachazo, Bo Feng, and Edward Witten. Direct proof of tree-level recursion relation in Yang-Mills theory. *Phys. Rev. Lett.*, 94:181602, 2005.
- [10] Freddy Cachazo, Song He, and Ellis Ye Yuan. Scattering of Massless Particles in Arbitrary Dimensions. *Phys. Rev. Lett.*, 113(17):171601, 2014.
- [11] Freddy Cachazo, Song He, and Ellis Ye Yuan. Scattering equations and Kawai-Lewellen-Tye orthogonality. *Phys. Rev.*, D90(6):065001, 2014.
- [12] Edward Witten. Perturbative gauge theory as a string theory in twistor space. *Commun. Math. Phys.*, 252:189–258, 2004.
- [13] Nathan Berkovits. An Alternative string theory in twistor space for $N=4$ superYang-Mills. *Phys. Rev. Lett.*, 93:011601, 2004.
- [14] Radu Roiban, Marcus Spradlin, and Anastasia Volovich. On the tree level S matrix of Yang-Mills theory. *Phys. Rev.*, D70:026009, 2004.
- [15] Lionel Mason and David Skinner. Ambitwistor strings and the scattering equations. *JHEP*, 07:048, 2014.
- [16] Eduardo Casali, Yvonne Geyer, Lionel Mason, Ricardo Monteiro, and Kai A. Roehrig. New Ambitwistor String Theories. *JHEP*, 11:038, 2015.
- [17] James M. Drummond, Johannes M. Henn, and Jan Plefka. Yangian symmetry of scattering amplitudes in $N=4$ super Yang-Mills theory. *JHEP*, 05:046, 2009.
- [18] Zvi Bern, Lance J. Dixon, and Radu Roiban. Is $N = 8$ supergravity ultraviolet finite? *Phys. Lett.*, B644:265–271, 2007.
- [19] V. P. Nair. A Current Algebra for Some Gauge Theory Amplitudes. *Phys. Lett.*, B214:215–218, 1988.
- [20] Nathan Berkovits and Edward Witten. Conformal supergravity in twistor-string theory. *JHEP*, 08:009, 2004.

-
- [21] David Skinner. Twistor Strings for N=8 Supergravity. 2013.
- [22] Andrew Hodges. A simple formula for gravitational MHV amplitudes. 2012.
- [23] Freddy Cachazo, Song He, and Ellis Ye Yuan. Scattering Equations and Matrices: From Einstein To Yang-Mills, DBI and NLSM. *JHEP*, 07:149, 2015.
- [24] David J. Gross and Paul F. Mende. The High-Energy Behavior of String Scattering Amplitudes. *Phys. Lett.*, B197:129–134, 1987.
- [25] D. B. Fairlie and D. E. Roberts. DUAL MODELS WITHOUT TACHYONS - A NEW APPROACH. 1972.
- [26] Yvonne Geyer, Arthur E. Lipstein, and Lionel J. Mason. Ambitwistor Strings in Four Dimensions. *Phys. Rev. Lett.*, 113(8):081602, 2014.
- [27] Igor Bandos. Twistor/ambitwistor strings and null-superstrings in spacetime of D=4, 10 and 11 dimensions. *JHEP*, 09:086, 2014.
- [28] Marcus Spradlin and Anastasia Volovich. From Twistor String Theory To Recursion Relations. *Phys. Rev.*, D80:085022, 2009.
- [29] Tim Adamo, Eduardo Casali, and David Skinner. Ambitwistor strings and the scattering equations at one loop. *JHEP*, 04:104, 2014.
- [30] Yvonne Geyer, Lionel Mason, Ricardo Monteiro, and Piotr Tourkine. Loop Integrands for Scattering Amplitudes from the Riemann Sphere. *Phys. Rev. Lett.*, 115(12):121603, 2015.
- [31] Freddy Cachazo, Song He, and Ellis Ye Yuan. One-Loop Corrections from Higher Dimensional Tree Amplitudes. *JHEP*, 08:008, 2016.
- [32] Christian Baadsgaard, N. E. J. Bjerrum-Bohr, Jacob L. Bourjaily, Simon Caron-Huot, Poul H. Damgaard, and Bo Feng. New Representations of the Perturbative S-Matrix. *Phys. Rev. Lett.*, 116(6):061601, 2016.

-
- [33] Yvonne Geyer, Lionel Mason, Ricardo Monteiro, and Piotr Tourkine. One-loop amplitudes on the Riemann sphere. *JHEP*, 03:114, 2016.
- [34] Yvonne Geyer, Lionel Mason, Ricardo Monteiro, and Piotr Tourkine. Two-Loop Scattering Amplitudes from the Riemann Sphere. *Phys. Rev.*, D94(12):125029, 2016.
- [35] Henrik Johansson, Gustav Mogull, and Fei Teng. Unraveling conformal gravity amplitudes. *JHEP*, 09:080, 2018.
- [36] Eric Bergshoeff, M De Roo, and B De Wit. Extended conformal supergravity. *Nuclear Physics B*, 182(1-2):173–204, 1981.
- [37] ES Fradkin and AA Tseytlin. Instanton zero modes and β -functions in conformal supergravity. *Physics Letters B*, 134(5):307–312, 1984.
- [38] E. S. Fradkin and Arkady A. Tseytlin. CONFORMAL SUPERGRAVITY. *Phys. Rept.*, 119:233–362, 1985.
- [39] Juan Maldacena. Einstein Gravity from Conformal Gravity. 5 2011.
- [40] Michael T Anderson. L^2 curvature and volume renormalization of the metrics on 4-manifolds. *arXiv preprint math/0011051*, 2000.
- [41] Giorgos Anastasiou and Rodrigo Olea. From conformal to Einstein Gravity. *Phys. Rev. D*, 94(8):086008, 2016.
- [42] Tim Adamo and Lionel Mason. Einstein supergravity amplitudes from twistor-string theory. *Class. Quant. Grav.*, 29:145010, 2012.
- [43] Tim Adamo and Lionel Mason. Conformal and Einstein gravity from twistor actions. *Class. Quant. Grav.*, 31(4):045014, 2014.
- [44] Chang-hyun Ahn. Comments on MHV tree amplitudes for conformal supergravitons from topological B-model. *JHEP*, 07:004, 2005.

- [45] Louise Dolan and Jay N. Ihry. Conformal Supergravity Tree Amplitudes from Open Twistor String Theory. *Nucl. Phys. B*, 819:375–399, 2009.
- [46] Johannes Broedel and Bernhard Wurm. New Twistor String Theories revisited. *Phys. Lett. B*, 675:463–468, 2009.
- [47] Tim Adamo and Lionel Mason. Twistor-strings and gravity tree amplitudes. *Class. Quant. Grav.*, 30:075020, 2013.
- [48] Tim Adamo, Simon Nakach, and Arkady A. Tseytlin. Scattering of conformal higher spin fields. *JHEP*, 07:016, 2018.
- [49] Henrik Johansson and Josh Nohle. Conformal Gravity from Gauge Theory. 2017.
- [50] Thales Azevedo and Oluf Tang Engelund. Ambitwistor formulations of R^2 gravity and $(DF)^2$ gauge theories. *JHEP*, 11:052, 2017.
- [51] Lorenz Eberhardt, Shota Komatsu, and Sebastian Mizera. Scattering equations in AdS: scalar correlators in arbitrary dimensions. *JHEP*, 11:158, 2020.
- [52] Kai Roehrig and David Skinner. Ambitwistor Strings and the Scattering Equations on $AdS_3 \times S^3$. 7 2020.
- [53] Joseph A. Farrow, Arthur E. Lipstein, and Paul McFadden. Double copy structure of CFT correlators. *JHEP*, 02:130, 2019.
- [54] Arthur E. Lipstein and Paul McFadden. Double copy structure and the flat space limit of conformal correlators in even dimensions. *Phys. Rev. D*, 101(12):125006, 2020.
- [55] Connor Armstrong, Arthur E. Lipstein, and Jiajie Mei. Color/kinematics duality in AdS_4 . *JHEP*, 02:194, 2021.
- [56] Arthur E. Lipstein. Soft Theorems from Conformal Field Theory. *JHEP*, 06:166, 2015.

-
- [57] Burkhard U. W. Schwab and Anastasia Volovich. Subleading Soft Theorem in Arbitrary Dimensions from Scattering Equations. *Phys. Rev. Lett.*, 113(10):101601, 2014.
- [58] Freddy Cachazo, Song He, and Ellis Ye Yuan. New Double Soft Emission Theorems. *Phys. Rev.*, D92(6):065030, 2015.
- [59] Tim Adamo, Eduardo Casali, and David Skinner. Perturbative gravity at null infinity. *Class. Quant. Grav.*, 31(22):225008, 2014.
- [60] Yvonne Geyer, Arthur E. Lipstein, and Lionel Mason. Ambitwistor strings at null infinity and (subleading) soft limits. *Class. Quant. Grav.*, 32(5):055003, 2015.
- [61] Dhritiman Nandan, Jan Plefka, and Wadim Wormsbecher. Collinear limits beyond the leading order from the scattering equations. *JHEP*, 02:038, 2017.
- [62] Dhritiman Nandan, Jan Plefka, Oliver Schlotterer, and Congkao Wen. Einstein-Yang-Mills from pure Yang-Mills amplitudes. *JHEP*, 10:070, 2016.
- [63] Christian Baadsgaard, N. E. J. Bjerrum-Bohr, Jacob L. Bourjaily, and Poul H. Damgaard. Integration Rules for Scattering Equations. *JHEP*, 09:129, 2015.
- [64] Christian Baadsgaard, N. E. J. Bjerrum-Bohr, Jacob L. Bourjaily, Poul H. Damgaard, and Bo Feng. Integration Rules for Loop Scattering Equations. *JHEP*, 11:080, 2015.
- [65] Nima Arkani-Hamed, Jacob L. Bourjaily, Freddy Cachazo, Alexander B. Goncharov, Alexander Postnikov, and Jaroslav Trnka. *Grassmannian Geometry of Scattering Amplitudes*. Cambridge University Press, 4 2016.
- [66] Nima Arkani-Hamed, Jacob L. Bourjaily, Freddy Cachazo, Simon Caron-Huot, and Jaroslav Trnka. The All-Loop Integrand For Scattering Amplitudes in Planar N=4 SYM. *JHEP*, 01:041, 2011.

-
- [67] Nima Arkani-Hamed, Freddy Cachazo, Clifford Cheung, and Jared Kaplan. A Duality For The S Matrix. *JHEP*, 03:020, 2010.
- [68] Nima Arkani-Hamed and Jaroslav Trnka. The Amplituhedron. *JHEP*, 10:030, 2014.
- [69] Paolo Benincasa. On-shell diagrammatics and the perturbative structure of planar gauge theories. 10 2015.
- [70] Paul Heslop and Arthur E. Lipstein. On-shell diagrams for $\mathcal{N} = 8$ supergravity amplitudes. *JHEP*, 06:069, 2016.
- [71] Enrico Herrmann and Jaroslav Trnka. Gravity On-shell Diagrams. *JHEP*, 11:136, 2016.
- [72] Dhritiman Nandan, Anastasia Volovich, and Congkao Wen. A Grassmannian Etude in NMHV Minors. *JHEP*, 07:061, 2010.
- [73] Nima Arkani-Hamed, Jacob Bourjaily, Freddy Cachazo, and Jaroslav Trnka. Unification of Residues and Grassmannian Dualities. *JHEP*, 01:049, 2011.
- [74] Louise Dolan and Peter Goddard. The Polynomial Form of the Scattering Equations. *JHEP*, 07:029, 2014.
- [75] Lance J. Dixon, Johannes M. Henn, Jan Plefka, and Theodor Schuster. All tree-level amplitudes in massless QCD. *JHEP*, 01:035, 2011.
- [76] Jacob L. Bourjaily. Efficient Tree-Amplitudes in N=4: Automatic BCFW Recursion in Mathematica. 2010.
- [77] Mads Søgaard and Yang Zhang. Scattering Equations and Global Duality of Residues. *Phys. Rev.*, D93(10):105009, 2016.
- [78] Louise Dolan and Peter Goddard. Gluon Tree Amplitudes in Open Twistor String Theory. *JHEP*, 12:032, 2009.

-
- [79] Frits A Berends, WT Giele, and H Kuijf. On relations between multi-gluon and multi-graviton scattering. *Physics Letters B*, 211(1-2):91–94, 1988.
- [80] Michael Peskin. *An introduction to quantum field theory*. CRC press, 2018.
- [81] Giulia Pancheri and Y. N. Srivastava. Introduction to the physics of the total cross-section at LHC: A Review of Data and Models. *Eur. Phys. J. C*, 77(3):150, 2017.
- [82] Mark Srednicki. *Quantum field theory*. Cambridge University Press, 2007.
- [83] Henriette Elvang and Yu-tin Huang. *Scattering Amplitudes in Gauge Theory and Gravity*. Cambridge University Press, 2015.
- [84] Marcel Froissart. Asymptotic behavior and subtractions in the mandelstam representation. *Physical Review*, 123(3):1053, 1961.
- [85] Johannes M. Henn and Jan C. Plefka. Scattering Amplitudes in Gauge Theories. *Lect. Notes Phys.*, 883:pp.1–195, 2014.
- [86] Andrea Marzolla. The 4D on-shell 3-point amplitude in spinor-helicity formalism and BCFW recursion relations. *PoS*, Modave2016:002, 2017.
- [87] J. Wess and B. Zumino. Supergauge Transformations in Four-Dimensions. *Nucl. Phys. B*, 70:39–50, 1974.
- [88] Gordon L Kane. *The supersymmetric world: The beginnings of the theory*. World Scientific, 2000.
- [89] Werner Porod. Supersymmetric models in view of recent LHC data. In *52nd Rencontres de Moriond on QCD and High Energy Interactions*, pages 145–148, 2017.
- [90] Julius Wess and Jonathan Bagger. *Supersymmetry and Supergravity: Revised Edition*. Princeton university press, 2020.

-
- [91] Henriette Elvang, Yu-tin Huang, and Cheng Peng. On-shell superamplitudes in $N < 4$ SYM. *JHEP*, 09:031, 2011.
- [92] Juan Maldacena. The large- n limit of superconformal field theories and supergravity. *International journal of theoretical physics*, 38(4):1113–1133, 1999.
- [93] J. M. Drummond and J. M. Henn. All tree-level amplitudes in $N=4$ SYM. *JHEP*, 04:018, 2009.
- [94] J. M. Drummond. Hidden Simplicity of Gauge Theory Amplitudes. *Class. Quant. Grav.*, 27:214001, 2010.
- [95] Charles W Misner, Kip S Thorne, and John Archibald Wheeler. *Gravitation*. Macmillan, 1973.
- [96] James Bedford, Andreas Brandhuber, Bill J. Spence, and Gabriele Travaglini. A Recursion relation for gravity amplitudes. *Nucl. Phys.*, B721:98–110, 2005.
- [97] Philippe Francesco, Pierre Mathieu, and David Sénéchal. *Conformal field theory*. Springer Science & Business Media, 2012.
- [98] Paul H. Ginsparg. APPLIED CONFORMAL FIELD THEORY. In *Les Houches Summer School in Theoretical Physics: Fields, Strings, Critical Phenomena*, 9 1988.
- [99] Philip D. Mannheim. Making the Case for Conformal Gravity. *Found. Phys.*, 42:388–420, 2012.
- [100] M. Beccaria, S. Nakach, and A. A. Tseytlin. On triviality of S-matrix in conformal higher spin theory. *JHEP*, 09:034, 2016.
- [101] Stefan Weinzierl. On the solutions of the scattering equations. *JHEP*, 04:092, 2014.
- [102] V.B. Alekseev. *Abel's Theorem in Problems and Solutions*. Springer Netherlands, 2004.

-
- [103] Zvi Bern, John Joseph Carrasco, Marco Chiodaroli, Henrik Johansson, and Radu Roiban. The Duality Between Color and Kinematics and its Applications. 9 2019.
- [104] N. J. A. Sloane. Triangle of Eulerian numbers $T(n,k)$. <https://oeis.org/A008292>.
- [105] Nima Arkani-Hamed, Freddy Cachazo, Clifford Cheung, and Jared Kaplan. The S-Matrix in Twistor Space. *JHEP*, 03:110, 2010.
- [106] Andrew Hodges. Eliminating spurious poles from gauge-theoretic amplitudes. *JHEP*, 05:135, 2013.
- [107] Stephen A Huggett, Kenneth P Tod, et al. *An introduction to twistor theory*. Number 4. Cambridge University Press, 1994.
- [108] Michael Atiyah, Maciej Dunajski, and Lionel Mason. Twistor theory at fifty: from contour integrals to twistor strings. *Proc. Roy. Soc. Lond. A*, 473(2206):20170530, 2017.
- [109] Tim Adamo, Mathew Bullimore, Lionel Mason, and David Skinner. Scattering Amplitudes and Wilson Loops in Twistor Space. *J. Phys. A*, 44:454008, 2011.
- [110] Gabriele Veneziano. Construction of a crossing-symmetric, regge-behaved amplitude for linearly rising trajectories. *Il Nuovo Cimento A (1965-1970)*, 57(1):190–197, 1968.
- [111] Joseph Polchinski. *String theory: Volume 1, an introduction to the bosonic string*. Cambridge university press, 1998.
- [112] Carlo Becchi, Alain Rouet, and Raymond Stora. Renormalization of gauge theories. *Annals of Physics*, 98(2):287–321, 1976.
- [113] W. Siegel. Amplitudes for left-handed strings. 12 2015.

-
- [114] Nikhil Kalyanapuram. Ambitwistor Integrands from Tensionless Chiral Superstring Integrands. 3 2021.
- [115] Eduardo Casali and Piotr Tourkine. On the null origin of the ambitwistor string. *JHEP*, 11:036, 2016.
- [116] Chrysostomos Kalousios. Massless scattering at special kinematics as Jacobi polynomials. *J. Phys.*, A47:215402, 2014.
- [117] Kai A. Roehrig. Chiral splitting and $\mathcal{N} = 4$ Einstein-Yang-Mills tree amplitudes in 4d. *JHEP*, 08:033, 2017.
- [118] G. Peter Lepage. A New Algorithm for Adaptive Multidimensional Integration. *J. Comput. Phys.*, 27:192, 1978.
- [119] J. Alwall, R. Frederix, S. Frixione, V. Hirschi, F. Maltoni, O. Mattelaer, H. S. Shao, T. Stelzer, P. Torrielli, and M. Zaro. The automated computation of tree-level and next-to-leading order differential cross sections, and their matching to parton shower simulations. *JHEP*, 07:079, 2014.
- [120] Mathew Bullimore, L. J. Mason, and David Skinner. Twistor-Strings, Grassmannians and Leading Singularities. *JHEP*, 03:070, 2010.
- [121] Alexander Postnikov. Total positivity, Grassmannians, and networks. 2006.
- [122] Livia Ferro, Tomasz Łukowski, Carlo Meneghelli, Jan Plefka, and Matthias Staudacher. Spectral Parameters for Scattering Amplitudes in $N=4$ Super Yang-Mills Theory. *JHEP*, 01:094, 2014.
- [123] Connor Armstrong, Joseph A. Farrow, and Arthur E. Lipstein. $\mathcal{N} = 7$ On-shell diagrams and supergravity amplitudes in momentum twistor space. *JHEP*, 01:181, 2021.
- [124] Andrew Hodges. New expressions for gravitational scattering amplitudes. *JHEP*, 07:075, 2013.

-
- [125] Frits A. Berends, W. T. Giele, and H. Kuijf. On relations between multi - gluon and multigraviton scattering. *Phys. Lett.*, B211:91–94, 1988.
- [126] L. J. Mason and David Skinner. Gravity, Twistors and the MHV Formalism. *Commun. Math. Phys.*, 294:827–862, 2010.
- [127] Freddy Cachazo, Lionel Mason, and David Skinner. Gravity in Twistor Space and its Grassmannian Formulation. *SIGMA*, 10:051, 2014.
- [128] Song He. A Link Representation for Gravity Amplitudes. *JHEP*, 10:139, 2013.
- [129] Nima Arkani-Hamed, Freddy Cachazo, and Jared Kaplan. What is the Simplest Quantum Field Theory? *JHEP*, 09:016, 2010.
- [130] Marcus Spradlin, Anastasia Volovich, and Congkao Wen. Three Applications of a Bonus Relation for Gravity Amplitudes. *Phys. Lett.*, B674:69–72, 2009.
- [131] Song He, Dhritiman Nandan, and Congkao Wen. Note on Bonus Relations for N=8 Supergravity Tree Amplitudes. *JHEP*, 02:005, 2011.
- [132] Giuseppe De Laurentis. Analytical amplitudes from numerical solutions of the scattering equations. *JHEP*, 02:194, 2020.
- [133] Yvonne Geyer and Ricardo Monteiro. Gluons and gravitons at one loop from ambitwistor strings. *JHEP*, 03:068, 2018.
- [134] Yvonne Geyer and Ricardo Monteiro. Two-Loop Scattering Amplitudes from Ambitwistor Strings: from Genus Two to the Nodal Riemann Sphere. *JHEP*, 11:008, 2018.
- [135] Andreas Brandhuber, Edward Hughes, Rodolfo Panerai, Bill Spence, and Gabriele Travaglini. The connected prescription for form factors in twistor space. *JHEP*, 11:143, 2016.
- [136] Song He and Yong Zhang. Connected formulas for amplitudes in standard model. *JHEP*, 03:093, 2017.

-
- [137] Yvonne Geyer and Lionel Mason. The M-theory S-matrix. 2019.
- [138] Yvonne Geyer and Lionel Mason. The polarized scattering equations for 6d superamplitudes. *Phys. Rev. Lett.*, 122(10):101601, 2019.
- [139] Freddy Cachazo, Nick Early, Alfredo Guevara, and Sebastian Mizera. Scattering Equations: From Projective Spaces to Tropical Grassmannians. 2019.
- [140] Freddy Cachazo, Nick Early, Alfredo Guevara, and Sebastian Mizera. Δ -algebra and scattering amplitudes. *JHEP*, 02:005, 2019.
- [141] Jaroslav Trnka. Towards the Gravituhedron: New Expressions for NMHV Gravity Amplitudes. 12 2020.
- [142] John Corn, Thomas Creutzig, and Louise Dolan. Yangian in the Twistor String. *JHEP*, 10:076, 2010.
- [143] Rouven Frassek, David Meidinger, Dhritiman Nandan, and Matthias Wilhelm. On-shell diagrams, Grassmannians and integrability for form factors. *JHEP*, 01:182, 2016.
- [144] Song He and Zhengwen Liu. A note on connected formula for form factors. *JHEP*, 12:006, 2016.
- [145] L. V. Bork and A. I. Onishchenko. Four dimensional ambitwistor strings and form factors of local and Wilson line operators. 2017.
- [146] Florian Loebbert, Matin Mojaza, and Jan Plefka. Hidden Conformal Symmetry in Tree-Level Graviton Scattering. *JHEP*, 05:208, 2018.
- [147] Nima Arkani-Hamed, Yuntao Bai, Song He, and Gongwang Yan. Scattering Forms and the Positive Geometry of Kinematics, Color and the Worldsheet. *JHEP*, 05:096, 2018.

-
- [148] Nima Arkani-Hamed, Jacob L. Bourjaily, Freddy Cachazo, Alexander B. Goncharov, Alexander Postnikov, and Jaroslav Trnka. *Scattering Amplitudes and the Positive Grassmannian*. Cambridge University Press, 2016.
- [149] Nima Arkani-Hamed and Jared Kaplan. On Tree Amplitudes in Gauge Theory and Gravity. *JHEP*, 04:076, 2008.
- [150] Thales Azevedo, Marco Chiodaroli, Henrik Johansson, and Oliver Schlotterer. Heterotic and bosonic string amplitudes via field theory. *JHEP*, 10:012, 2018.
- [151] Z. Bern and A. G. Morgan. Massive loop amplitudes from unitarity. *Nucl. Phys.*, B467:479–509, 1996.
- [152] Andreas Brandhuber, Simon McNamara, Bill Spence, and Gabriele Travaglini. Recursion relations for one-loop gravity amplitudes. *JHEP*, 03:029, 2007.
- [153] L. Brink, Schwarz J. H., and J. Scherk. Supersymmetric Yang-Mills Theories. *Nucl. Phys. B*, 1977.
- [154] Freddy Cachazo and Yvonne Geyer. A 'Twistor String' Inspired Formula For Tree-Level Scattering Amplitudes in N=8 SUGRA. 2012.
- [155] Freddy Cachazo, Alfredo Guevara, Matthew Heydeman, Sebastian Mizera, John H. Schwarz, and Congkao Wen. The S Matrix of 6D Super Yang-Mills and Maximal Supergravity from Rational Maps. *JHEP*, 09:125, 2018.
- [156] Freddy Cachazo, Song He, and Ellis Ye Yuan. One-Loop Corrections from Higher Dimensional Tree Amplitudes. *JHEP*, 08:008, 2016.
- [157] Freddy Cachazo, Song He, and Ellis Ye Yuan. Einstein-Yang-Mills Scattering Amplitudes From Scattering Equations. *JHEP*, 01:121, 2015.
- [158] Freddy Cachazo, Song He, and Ellis Ye Yuan. Scattering of Massless Particles: Scalars, Gluons and Gravitons. *JHEP*, 07:033, 2014.

-
- [159] Freddy Cachazo, Song He, and Ellis Ye Yuan. Scattering in Three Dimensions from Rational Maps. *JHEP*, 10:141, 2013.
- [160] Freddy Cachazo and Peter Svrcek. Tree level recursion relations in general relativity. 2005.
- [161] Eduardo Casali and Piotr Tourkine. Infrared behaviour of the one-loop scattering equations and supergravity integrands. *JHEP*, 04:013, 2015.
- [162] Louise Dolan and Peter Goddard. General Solution of the Scattering Equations. *JHEP*, 10:149, 2016.
- [163] Louise Dolan and Peter Goddard. Proof of the Formula of Cachazo, He and Yuan for Yang-Mills Tree Amplitudes in Arbitrary Dimension. *JHEP*, 05:010, 2014.
- [164] J. M. Drummond, M. Spradlin, A. Volovich, and C. Wen. Tree-Level Amplitudes in N=8 Supergravity. *Phys. Rev.*, D79:105018, 2009.
- [165] Nick Early. Generalized Permutohedra, Scattering Amplitudes, and a Cubic Three-Fold. 2017.
- [166] Michael B. Green, John H. Schwarz, and Lars Brink. N=4 Yang-Mills and N=8 Supergravity as Limits of String Theories. *Nucl. Phys.*, B198:474–492, 1982.
- [167] Song He and Ellis Ye Yuan. One-loop Scattering Equations and Amplitudes from Forward Limit. *Phys. Rev.*, D92(10):105004, 2015.
- [168] Matthew Heydeman, John H. Schwarz, and Congkao Wen. M5-Brane and D-Brane Scattering Amplitudes. *JHEP*, 12:003, 2017.
- [169] Matthew Heydeman, John H. Schwarz, Congkao Wen, and Shun-Qing Zhang. All Tree Amplitudes of 6D (2, 0) Supergravity: Interacting Tensor Multiplets and the $K3$ Moduli Space. 2018.

-
- [170] Rijun Huang, Junjie Rao, Bo Feng, and Yang-Hui He. An Algebraic Approach to the Scattering Equations. *JHEP*, 12:056, 2015.
- [171] Arthur E. Lipstein and Lionel Mason. From d logs to dilogs the super Yang-Mills MHV amplitude revisited. *JHEP*, 01:169, 2014.
- [172] Zhengwen Liu and Xiaoran Zhao. Bootstrapping the Solutions of Scattering Equations. 2018.
- [173] Stephen G. Naculich. CHY representations for gauge theory and gravity amplitudes with up to three massive particles. *JHEP*, 05:050, 2015.
- [174] Stephen G. Naculich. Scattering equations and BCJ relations for gauge and gravitational amplitudes with massive scalar particles. *JHEP*, 09:029, 2014.
- [175] Kai A. Roehrig and David Skinner. A Gluing Operator for the Ambitwistor String. *JHEP*, 01:069, 2018.
- [176] N. J. A. Sloane. The On-Line Encyclopedia of Integer Sequences. <http://www.oeis.org>.